Design, Syntheses and Functional Studies of Porous Materials for Remediation of Environmental Pollutants

A Thesis

Submitted in Partial Fulfillment of the Requirements for the

Degree of

Doctor of Philosophy

by

Partha Samanta

Reg. ID: 20133264

Indian Institute of Science Education and Research (IISER), Pune

2019

Dedicated to

Maa, Baba and Puja

Indian Institute of Science Education and Research (IISER), Pune

Certificate

It is hereby certified that the work described in this thesis entitled *"Design, Syntheses and Functional Studies of Porous Materials for Remediation of Environmental Pollutants"* submitted by *Mr. Partha Samanta* was carried out by the candidate, under my supervision. The work presented here or any part of it has not been included in any other thesis submitted previously for the award of any degree or diploma from any other university or institution.

Date:

Dr. Sujit K. Ghosh
Research Supervisor
Email: sghosh@iiserpune.ac.in
Contact No.:+91(20)25908076

Declaration

I declare that this written submission represents my ideas in my own words and wherever other's ideas have been included; I have adequately cited and referenced the original sources. I also declare that I have adhered to all principles of academic honesty and integrity and have not misrepresented or fabricated or falsified any idea/ data/ fact/ source in my submission. I understand that violation of the above will cause for disciplinary action by the Institute and can also evoke penal action from the sources which have thus not been properly cited or from whom proper permission has not been taken when needed.

Date:

Partha Samanta

Reg. Id: 20133264

Acknowledgement

At the very outset, I would like to take the opportunity to convey my deepest gratitude to my research supervisor Dr. Sujit K. Ghosh for his continuous support and motivation throughout my PhD tenure. I feel his illimitable encouragement has propelled my research in forward direction. It has been an immense privilege for me to work under his supervision. I believe that his inspiring guidance has helped me to design and execute different research projects successfully. Thank you very much Sir for all your diligent efforts, trust in me and most importantly for being such a wonderful guide.

I sincerely acknowledge the former director of Indian Institute of Science Education and Research (IISER) Pune Prof. K. N. Ganesh and the current director Prof. J. B. Udgaonkar for providing world class facilities and having a vibrant research environment. I am also extremely thankful to my research advisory committee (RAC) members, Prof. Amitava Das (CSIR-CSMCRI, Bhavnagar), Dr. Sakya Sen (NCL, Pune) and Dr. Partha Hazra (IISER, Pune) for their valuable suggestions, advices and support during the annual RAC meetings. I am also grateful to Prof. M. Jayakannan (Chair, Chemistry department) and all other faculty members of the department of chemistry for being approachable for any help and maintaining such research friendly healthy environment in the department. I sincerely thank all the collaborators - especially Dr. Sreekumar Kurungot (National Chemical Laboratory, Pune), Dr. Mandar M. Shirolkar (University of Technology of China), who assisted me in completion of different projects.

It has been a great privilege for me to be a part of the 'Microporous Materials Lab' and I am extremely grateful to all the past and present members of the team. I would like to thank all of them (Dr. Sanjog Nagarkar, Dr. Biplab Joarder, Dr. Abhijeet K. Chaudhari, Dr. Biplab Manna, Dr. Soumya Mukherjee, Dr. Avishek Karmakar, Dr. Partha Chowdhury, Dr. Tarak Nath Mandal, Dr. Sreenu Bhanoth, Dinesh Mullangi, Arif Inamdar, Shilpa Sonar, Dr. Aamod V. Desai, Shivani Sharma, Samraj Mollick, Yogeshwar More, Prateek Agrawal, Arunabha Sen, Subhajit Dutta, Sumanta Let, Writakshi Mandal, Sahel Fajal, Debanjan Mahato, Amrit Kumar, Shweta Singh, Naveen Kumar, Priyanshu Chandra, Govind, Kriti Gupta). Thank you very much all for your significant contribution, help and providing friendly environment in the lab. My sincere thanks go out for all my seniors: Sanjog, Biplab da, Manna da, Soumya da and Avishek da for your guidance, support and

valuable suggestions. I would to mention that it was an immense pleasure to work with all of you and I feel I have learnt a lot of things from you guys. Of them, I have worked most of the time with Biplab da, Avishek da and Soumya da; thank you all for teaching me a lot of lessons. Apart from my seniors, I would like to express my special appreciation to all my current lab members, because without them this journey would not have been as exciting and memorable as it has been. I would consider myself lucky to have a batch-mate and friend like Aamod, with whom I had maximum overlap in time and spent most of the time in lab. I really admire his depth of understanding in different subjects (which has helped a lot during this tenure) and mesmerizing skills. I am grateful to him for his wonderful friendship and contributions in my researches. I would like to acknowledge the prompt and unconditional assistance from Samraj, Shivani, Arunabha, Subhajit, Sumanta, Sahel, Writakshi and Debanjan whenever required. I am thankful to Tarak da and Sreenuji for providing a timely advice and perspective. I would like to specially mention about two undergraduate students who worked with me over a long period - Priyanshu and Govind, for their enthusiastic involvement and optimistic ideas. I am especially thankful to Aamod, Subhajit, Sumanta and Shivani for their invaluable support during the last phase of my PhD. I express my sincere gratitude to Ma'am (Dr. Sudarshana Mukherjee) for her friendly advices; and I wish Suvan all the best for his future.

I would like to convey my deepest regards towards my old school and university teachers who have encouraged me throughout different stages of life. I am grateful to Pradyut Sir (first school teacher of my life) and all teachers of Vidyanagar Multi Purpose School (VMPS) (especially, Arun Sir, Anindya Sir, Harisadhan Sir, Malay Sir, Tapan Sir, Chittaranjan Sir, Rajashri Madam, Swadha Madam, Mrityunjay Sir, Aman Sir). I am also very much thankful to Dr. Ratan Kumar Kar (Vivekananda College) who has inspired me to pursue a PhD degree. I would like to express my sincere regards towards all the faculty members of Indian Institute of Technology (IIT), Kharagpur for their lessons and support during my Masters study. I thank Prof. Sudip Malik (IACS, Kolkata) for providing me the first opportunity to be familiar with the field of research. I am also thankful to Prof. Tanmaya Pathak (IIT Kharagpur) for providing me the opportunity to carry out my Masters project for one year in his lab. I would like to express my gratitude to Chanchal da and Santu da who have mentored my research works at IACS and IIT Kharagpur

respectively.

I acknowledge University Grant Commission (UGC), India for providing me fellowship. I would also like to thank American Chemical Society (ACS), Royal Society of Chemistry (RSC), John Wiley & Sons (Wiley-VCH), Cell Press, Nature Publishing Group (NPG), Elsevier for the various research. review articles and book chapter that I managed to publish in my PhD tenure. For the smooth progress in a long course, the support of technical and administrative staff is equally important. I thank Dr. Umeshareddy Kacherki and Anuradha for library support, technical staff of the institute - Parveen Nasa, Archana, Mahesh Jadhav, Nilesh Dumbre, Swati, Anil, Yatish, Ganesh Dimbar, Suresh Prajapat, Sandeep, Nitin, Megha, Deepali and administrative staff - Mayuresh, Nayana, Tushar, Vrushali, Suresh, Prabhas, Priyadarshani for their prompt assistance at multiple occasions. During my PhD tenure, I had the opportunity to attend several national (CRSI-2015; IUCr-2017; MTIC-2017) and international conferences (EuroMOF-2017), for which I thank Infosys Foundation, UGC and IISER-Pune for funding.

I wish to thank all my friends for their support and help at different stages of my life, especially, Sagar, Soumyabrata, Arnab, Arijit, Sudip, Kaushik, Subhajit, Rabi, Debayan, Tapo, Sayari, Rituparna, Sritama, Santi, Annesha, Arghya, Vasu, Kartik, Rupam, Pappu da. I thank all my batch-mates (August-2013) and Chemphilic team-2016-17. Especially, I'm thankful to Tanuka and her family for all their support. I would like to acknowledge Abhigyan da, Tanmay da, Sohini di, Arundhati di, Abhik da, Arindam da, Chandramouli, Amit, Soumendu da, Reja da, Sudeb da, Shyama da, Rajkumar da, Konoya, Supratik, Barun da, Maidul da, Rahi, Bijoy da, Projjwal, Kingshuk. I apologize in advance for not being able to take all of your names, but am sure, it would not offend you to a great extent. Also, I would like to mention about our Bengali football and cricket team, of which I was a part for the last five years and I wish the members all the success in the forthcoming years. Lastly, I am really grateful to my whole family (my parents, Puja, mejomama, mejomamima, chhotomama, chhotomamima, mejokaku, mejokakima, Jhilik, chhotokaku, chhotokakima, Riya). I would like to thank my parents and my sister Puja, who stood beside me at every moment of my life so far. Without their scarifies, motivation and support, I would not have reached here.

- Partha Samanta

Contents

Synopsis

The primary motivation of all the works included in this thesis is to design and synthesize of functional porous materials for the remediation of water pollutants. In the domain of porous materials, metal-organic frameworks (MOFs) and lately evolved covalently linked porous organic materials have seen immense progress in recent years. Owing to high surface area, tuneable pore surface etc. MOFs and porous organic materials have become one of the frontrunner in the domain of material science. These kind of porous materials have already been employed for wide range of applications such as gas storage, separation of gasses and industrially relevant iquid hydrocarbons, heterogeneous catalysis, drug delivery etc. But MOFs and porous organic materials have rarely been explored for the capture of environmentally hazardous and toxic species from water. In this context, sensing of toxic Hg^{2+} ion has been demonstrated with functionalized luminescent MOF (LMOF) in water medium. Further, capture of cationic and anionic hazardous water pollutants have been studied with strategically designed and synthesized porous organic materials.

Chapter 1. Introduction

In this section, a brief discussion about porous materials (MOFs and porous organic materials) and their applications is included. Different classification of MOFs and target specific synthesis of such porous materials has been discussed further. The scope of MOFs and porous organic materials for the environmental applications have been demonstrated. In addition, another discussion regarding the water pollution is also included in the later part of this section. Various types of water pollution and moreover, water pollutions by hazardous and toxic chemicals have been discussed thoroughly. Furthermore, scope of strategically designed and synthesized functionalized MOFs and porous organic materials for the remediation of water pollutants has been covered in this chapter.

Chapter 2. Selective Recognition of Hg(II) ion in Water by a Functionalized Metal-Organic Framework (MOF) Based Chemodosimeter

In this chapter, a functionalized metal-organic framework (MOF) has been synthesized for detection of toxic Hg^{2+} ion. To sense mercury ion in water medium water stable UiO-66@Butyne MOF has been synthesized and further has been characterized. Butyne functionality has been appended strategically to the MOF as Hg^{2+} ion known to react with alkyne moiety in water medium. As a consequence of the oxymercuration reaction mercury ion and butyne groups MOF-66@Butyne has produced signal via

luminescence quenching. In addition to check the selectivity of the probe, MOF-66@Butyne has been treated with various other metal ions like Cd^{2+}, Ba^{2+}, Zn^{2+}, Sr^{2+}, Cu^{2+}, Co^{2+}, Ni^{2+}, Mg^{2+} etc. MOF-66@Butyne has been found to be selective for Hg^{2+} ion in this regard. Furthermore, this probe has effectively shown response for the Hg^{2+} ion even in presence of aforementioned concurrent cations. The limit of detection for the probe has been calculated to be 2.18 ppb which is in the regime of the permitted level declared by World Health Organization (WHO).

Inorg. Chem., 2018, **57**, 2360-2364.

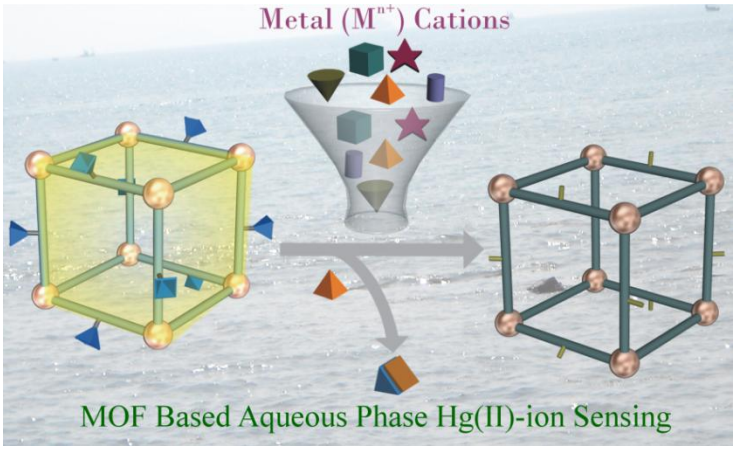

Chapter 3. Chemically Stable Porous Organic Material: An Efficient Selective Cationic Dye Scavenger from Aqueous Medium

In this chapter, a chemically stable and cost-effective microporous hyper-cross-linked polymer (HCP) has been synthesized. By using lewis acid catalyzed Friedel-Craft reaction hydroxy-functionalized HCP-91 has been synthesized via knitting strategy. Owing to the high chemical stability of the compound, HCP-91 has been further modified with aqueous NaOH to incorporate free exchangeable Na^{+} ion inside the network of the HCP. This HCP-91@Na has been utilized for the removal of organic cationic dyes (methylene blue, crystal violet and rhodamine B) from via cation exchange. This capture study has been found to be selective for the cationic dyes over anionic dye. In this regard, an anionic dye (methyl orange) has been employed, but HCP-91@Na has shown negligible uptake for the anionic dye. Further, selective capture of cationic dyes has been performed with HCP-91@Na from binary mixture of cationic and anionic dyes (methylene blue-methyl orange and rhodamine B-methyl orange).

Mater. Chem. Front., 2017, **1**, 1384-1388.

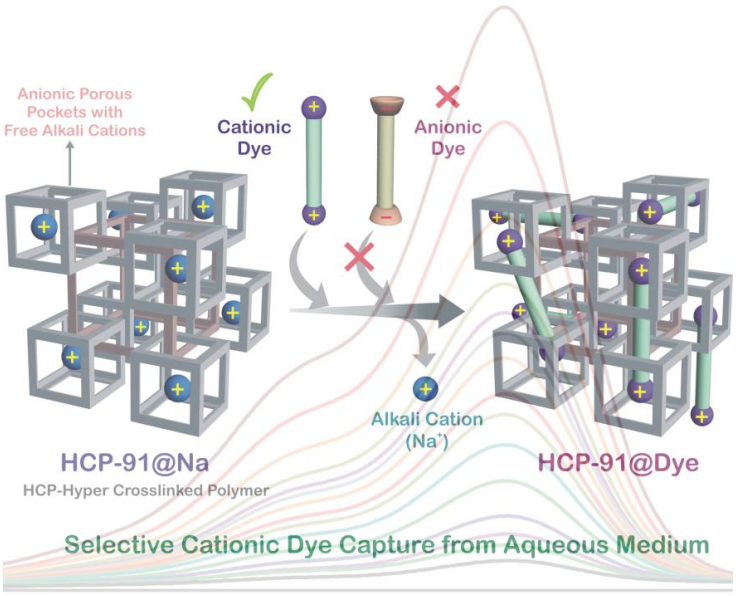

Chapter 4. Hydroxy Functionalized Porous Organic Material: A Cost Effective Route to Remove Iodine from Vapor and Water Medium

Moving apart from the cationic pollutants, porous organic materials further has been used for the capture of anionic pollutants. Radioactive iodine (mostly, ^{129}I, ^{131}I) is known to present in the water medium in various forms and among them I_3^- ion is one. In this chapter, capture of iodine from water has been demonstrated with hydroxy functionalized HCPs (HCP-91 and HCP-92) by using aqueous solution of I_3^- ion solution. Furthermore, I_3^- ion capture study in presence of concurrent anions like Cl^-, NO_3^- and SO_4^{2-} has revealed the efficiency of HCP-91 and HCP-92 to capture iodine in waste water too. Capacity for the HCPs has been found to be very high for I_3^- ion. In addition, both the compounds have been reused for several by treating the iodine encapsulated phases with methanol.

Manuscript submitted.

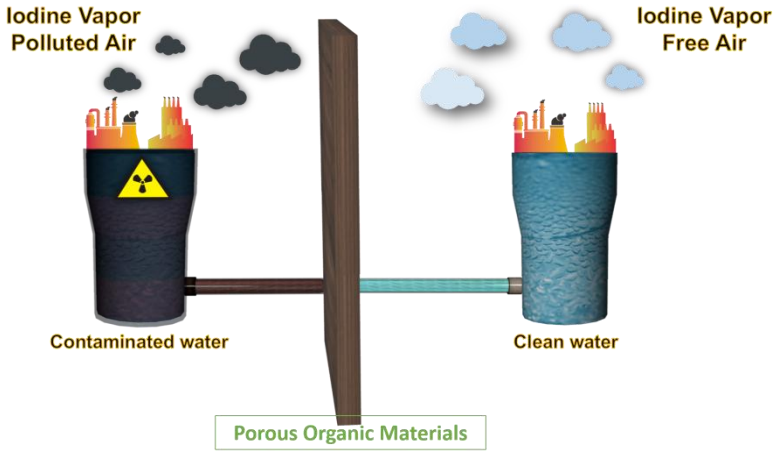

Chapter 5. Chemically Stable Viologen-based Organic Network for Efficient Removal of Hazardous Oxo-anions from Water

Water pollution due to oxo-anions of different heavy metal pollutants has become a global concern. Removal of Cr(VI)-based oxo-anions (viz., chromate and dichromate anions) has gained paramount interests since chromium has been found to be very much toxic, carcinogenic and mutagenic in nature. In this regard, a chemically stable viologen based extended organic network (compound-1) has been synthesized via Zincke's reaction. Compound-1 has been used for the capture of CrO_4^{2-} ion from water and further it has been observed compound-1 can capture chromate anions even in presence of concurrent anions such as Cl^-, NO_3^- and SO_4^{2-} ions. Moreover,

Chem. Sci., 2018, **9**, 7874-7881.

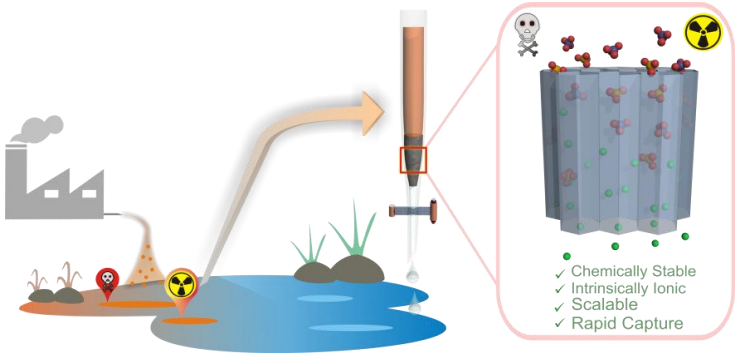

Abbreviations

Anal.	Analysis
Calc.	Calculated
DMF	N,N'-dimethylformamide
DCM	Dichloromethane
EtOH	Ethanol
FT-IR	Fourier transform infra-red spectroscopy
g	Gram
HCP	Hyper-cross-linked polymer
MeOH	Methanol
mg	Milligram
min	Minutes
mL	Milliliter
mM	Millimolar
mmol	Milli moles
MOF	Metal-Organic Framework
PCP	Porous Coordination Polymer
PXRD	Powder X-Ray Diffraction
RT	Room Temperature
TGA	Thermo-gravimetric Analysis
UV	Ultraviolet
FE-SEM	Field Emission Scanning Electron Microscopy
MeCN	Acetonitrile
NMR	Nuclear Magnetic Resonance
EDX	Energy Dispersive X-ray Analysis
ICP-AES	Inductively Coupled Plasma Atomic Emission Spectroscopy

Rights and Permissions

Chapter 2:

Chapter 3:

Chapter 5:

Research Publications

([†] - indicates equal contribution)

Included in Thesis:

1. Selective Recognition of Hg(II) ion in Water by a Functionalized Metal-Organic Framework (MOF) Based Chemodosimeter.
   Partha Samanta, Aamod V. Desai, Shivani Sharma, Priyanshu Chandra and Sujit K. Ghosh.
   Inorg. Chem. 2018, **57**, 2360-2364.
2. Microporous Hyper-cross-linked Polymer (HCP): An Efficient Selective Cationic Dye Scavenger from Aqueous Medium.
   Partha Samanta, Priyanshu Chandra, Aamod V. Desai and Sujit K. Ghosh.
   Mater. Chem. Front. 2017, **1**, 1384-1388.
3. Hydroxy Functionalized Porous Organic Material: A Cost Effective Scavenger of Iodine from Vapor and Water Medium.
   Partha Samanta,[†] Subhajit Dutta[†] and Sujit K. Ghosh.
   Manuscript submitted, 2018.
4. Chemically stable ionic viologen-organic network: an efficient scavenger of toxic oxo-anions from water.
   Partha Samanta, Priyanshu Chandra,[†] Subhajit Dutta,[†] Aamod V. Desai and Sujit K. Ghosh.
   Chem. Sci., 2018, **9**, 7874-7881.

Not Included in Thesis:

5. Enhanced Proton Conduction by Post-Synthetic Covalent Modification in a Porous Coordination Framework.
   Partha Samanta,[†] Aamod V. Desai,[†] Bihag Anothumakkool, Mandar M. Shirolkar, Avishek Karmakar, Sreekumar Kurungot and Sujit K. Ghosh.
   J. Mater. Chem. A, 2017, **5**, 13659-13664.
6. Aqueous Phase Nitric Oxide Detection by an Amine Decorated Metal-Organic Framework.
   Aamod V. Desai,[†] **Partha Samanta,**[†] Biplab Manna and Sujit K. Ghosh.
   Chem. Commun., 2015, **51**, 6111-6114.
7. Metal-organic Frameworks (MOFs) for Detection and Desensitization of Environmentally Hazardous Nitro-explosives and Related High Energy Materials (HEMs).
   Partha Samanta, Subhajit Dutta and Sujit K. Ghosh.
   Elsevier, Book chapter (Manuscript under revision), **2018**, Edited by: Dr. Sujit K. Ghosh.
   Book Title: Metal-Organic Frameworks (MOFs) for Environmental Applications.
8. Hydroxy-functionalized hyper-cross-linked ultra-microporous organic polymers for selective CO_2 capture at room temperature.
   Partha Samanta, Priyanshu Chandra and Sujit K. Ghosh.
   Beilstein J. Org. Chem., 2016, **12**, 1981-1986.

9. Size selective dual sensing of toxic amine with a dye encapsulated metal-organic framework.
   Partha Samanta, Shivani Sharma,[†] Priyanshu Chandra[†] and Sujit K. Ghosh.
   Manuscript submitted, **2018**.
10. Fluorescent Turn-on Sensors Based on Metal-organic Frameworks (MOFs).
    Avishek Karmakar,[†] **Partha Samanta**[†] and Sujit K. Ghosh.
    Dalton Trans. **2018**, Manuscript under preparation. (Invited frontier article)
11. Guest Responsive Metal-Organic Frameworks as Scaffolds for Separation and Sensing Applications.
    Avishek Karmakar, **Partha Samanta**, Aamod V. Desai and Sujit K. Ghosh.
    Acc. Chem. Res., 2017, **50**, 2457-2469.
12. Hydrogen-Bonded Organic Frameworks: A New Class of Porous Crystalline Proton Conducting Materials.
    Avishek Karmakar, Rajith Illathvalappil, Bihag Anothumakkool, Arunabha Sen, **Partha Samanta**, Aamod V. Desai, SreekumarKurungot and Sujit K. Ghosh.
    Angew. Chem. Int. Ed., 2016, **55**, 10667-10671.
13. Multifunctional Behavior of Sulfonate-based Hydrolytically Stable Microporous Metal-Organic Frameworks.
    Aamod V. Desai, Biplab Joarder, Arkendu Roy, **Partha Samanta**, Ravichandar Babarao and Sujit K. Ghosh.
    ACS Appl. Mater. Interfaces, 2018 (Just accepted) .
14. Base-Resistant Ionic Metal-Organic Framework as a Porous Ion-Exchange Sorbent.
    Aamod V. Desai, Arkendu Roy, **Partha Samanta**, Biplab Manna and Sujit K. Ghosh.
    iScience, 2018, **3**, 21-30.
15. Advanced porous materials: A promising candidate for sequestration of industrial hazardous dye effluents.
    Arunabha Sen, **Partha Samanta** and Sujit K. Ghosh.
    Central West Publishing, Book chapter (Manuscript under revision), 2018, Edited by: Dr. Vikas Mittal.
    Book Title: Porous Polymer Networks.
16. Self-assembled, Fluorine-rich Porous Organic Polymers: A Class of Mechanically Stiff and Hydrophobic Materials.
    Soumya Mukherjee, Zhixin Zeng, Mandar M. Shirolkar, **Partha Samanta**, Abhijeet K. Chaudhari, Jin-Chong Tan and Sujit K. Ghosh.
    Chem. Eur. J., 2018, **24**, 11771-11778.
17. Aqueous Phase Sensing of Cyanide Ion Using a Hydrolytically Stable Metal-Organic Framework.
    Avishek Karmakar, Biplab Joarder, Abhik Mallick, **Partha Samanta**, Aamod V. Desai, Sudipta Basu and Sujit K. Ghosh.
    Chem. Commun., 2017, **53**, 1253-1256.
18. Post-synthetically modified metal-organic framework as a scaffold for selective bisulphite recognition in water.
    Arunabha Sen, Aamod V. Desai, **Partha Samanta**, Subhajit Dutta, Sumanta Let and Sujit K. Ghosh.
    Polyhedron, 2018, DOI: 10.1016/j.poly.2018.08.069.
19. Syntheses and structural elucidation of neutral N-donor linker based bi-porous isostructural cationic metal-organic frameworks.

Subhajit Dutta, Aamod V. Desai, **Partha Samanta** and Sujit K. Ghosh.

Inorganica Chimica Acta, 2018, Just accepted.

20. Bimodal Functionality in a Porous Covalent Triazine Framework by Rational Integration of Electron Rich and Deficient Pore Surface.

    Avishek Karmakar, Amrit Kumar, Abhijeet K. Chaudhari, **Partha Samanta**, Aamod V. Desai, Rajamani Krishna and Sujit K. Ghosh.

    Chem. Eur. J., 2016, **22**, 4931-4937.

21. A Post-Synthetically Modified MOF for Selective and Sensitive Aqueous Phase Detection of Highly Toxic Cyanide Ion.

    Avishek Karmakar, Naveen Kumar, **Partha Samanta**, Aamod V. Desai and Sujit K. Ghosh.

    Chem. Eur. J., 2016, **22**, 864-868.

22. Coherent Fusion of Water Array and Protonated Amine in a Metal-Sulphate Based Coordination Polymer for Proton Conduction.

    Biplab Manna, Bihag Anothumakkool, Aamod V. Desai, **Partha Samanta**, Sreekumar Kurungot and Sujit K. Ghosh.

    Inorg. Chem., 2015, **54**, 5366-5371.

23. Aqueous Phase Selective Detection of 2,4,6-trinitrophenol using a Fluorescent Metal-Organic Framework with a Pendant Recognition Site.

    Sanjog S. Nagarkar, Aamod V. Desai, **Partha Samanta** and Sujit K. Ghosh.

    Dalton Trans., 2015, **44**, 15175-15180.

24. Selective and Sensitive Aqueous Phase Detection of TNP (2,4,6-trinitrophenol) by an Amine Functionalized Metal-Organic Framework.

    Biplab Joarder, Aamod V. Desai, **Partha Samanta**, Soumya Mukherjee and Sujit K. Ghosh.

    Chem. Eur. J., 2015, **21**, 965-969.

25. Selective Detection of Cyanide by a Polyfluorene-based Organoboron Fluorescent Chemodosimeter.

    Chanchal Chakraborty, Manas Kumar Bera, **Partha Samanta** and Sudip Malik.

    New J. Chem., 2013, **37**, 3222-3228.

Chapter 1

Introduction

1.1 Porous Materials

Design and creation of porosity in porous architectures by mimicking nature have taken an important position in science. Last few decades have witnessed the evolution of various types of porous material. Construction of porosity from meso- to nano-scale range in varieties of material have gained huge attention due to their various types of application (Fig. 1.1).[1] Till date different types of porous material have been reported in the literature. Among them zeolites, activated carbons, porous silica, mesoporous clay materials etc. are well known.[2] In the domain of porous materials, metal-organic frameworks (MOFs) have evolved in last two decades as one of the important class of material. MOFs are crystalline ordered networks constructed from organic linkers and metal nodes via coordination bonds.[3] Further, MOFs have been generally classified on the basis of its generation or charge on the framework. In this regard, MOFs have been classified in different generations, namely, 1st generation, 2nd generation and 3rd generation etc.[4] In case of 1st generation MOFs, upon removal of the occluded guest molecules from the networks, the frameworks have been found to collapse completely. Moving apart from 1st generation to the 2nd generation MOFs, upon removal of the guest molecules the respective framework of 2nd generation MOFs have been found to be stable and rigid. On the other hand, MOFs with flexible frameworks which undergo structural changes upon occluded guest removal are known as 3rd generation MOFs. Further, on the basis of charge on the framework, MOFs can be classified as neutral MOFs and ionic MOFs, i.e., i-MOFs.[5] MOFs with neutral frameworks have majorly been reported in literature and most of them are constructed from carboxylic acid. Whereas, i-MOFs can be further divided into cationic MOFs and anionic MOFs based on the nature of the charge on the frameworks. Apart from structural versatility, it is noteworthy to mention that MOFs have become one of the frontrunner in this regime due to its highly tuneable architecture, structure property correlation, high surface area etc. Although MOFs have several advantages over other congener porous materials and have found great interests of research, but often poor physiochemical stability, difficulties in bulk scale synthesis etc. have hindered their applications.[6] In this regard, porous organic materials have attracted much attentions of researchers in recent years. Advantages like amenability in the design and synthesis, high surface area, tuneable pore surface etc. have made such covalently linked porous organic materials one of the important material in the domain of porous materials.[7] Being constructed from light weight elements (such as C, N, H, O, B etc.), these compounds are found to be light weight nature which is another advantage for practical applications. This type of porous organic materials can be synthesized from both covalent and noncovalent interactions. In terms of stability covalently linked porous organic materials are more suitable. In this thesis, all the porous organic materials have been fabricated via covalent linkage. In the area of covalently linked porous organic materials there are different types of compounds which includes covalent organic

frameworks (COFs), porous organic frameworks (POFs), porous organic polymers (POPs), porous aromatic frameworks (PAFs), covalent triazine frameworks (CTFs), porous polymer networks (PPNs), hyper-cross-linked polymers (HCPs), conjugated microporous polymers (CMPs) etc. Such extended organic materials have attracted much attention since it has advantages of both porous materials and polymers. Moreover, COFs and few CTFs have been found to be crystalline nature and most of the remaining porous organic materials are found to be amorphous. Whereas, CMPs are covalently linked π-conjugated extended polymeric organic networks with higher dimension. Again, HCPs are the microporous hyper-cross-linked organic polymers. One step Lewis acid catalysed Friedel-Craft reaction has been found to be one of the effective tool for the synthesis of microporous HCPs. Depending on the versatility in organic building blocks, various types of HCPs can be fabricated with different types of functional moieties. On the other hand, different types of chemical reactions have been explored to design and synthesis of various porous organic compounds. Among these Schiff base condensation, acid catalysed trimerisation, Suzuki cross-coupling reaction, Friedel-Crafts reaction, Sonogashira–Hagihara reaction, Yamamoto reaction etc. are well known reactions. Again, being constructed from stronger covalent bonds, such porous organic materials are found to be highly physiochemical stable over congener MOFs. In addition, it has been observed that high physiochemical stability often score over structure property correlation, since for real time applications high chemical stability is one of the prerequisite.[8] Among these porous organic materials, CMPs are Apart from neutral networks in such organic materials, charged network with free counter ions can also be designed and synthesized via judicious selection of synthetic routes and building blocks. In this regard, imparting functionality or charge over the extended networks of MOFs or porous organic materials can be achieved by two routes, namely, pre-synthetic route and post-synthetic modification. In pre-synthetic route, suitable choice of the molecular building units have been found to play the crucial role in imparting the functionality inside the network. On the other hand, post-synthetic modification has been found to be one of the important tool, since pre-synthetic functionalization of the porous materials is not easy and straight forward always.[9] Post-synthetic modification has earned paramount interest as desired functionality can be incorporated to the pores for targeted applications. Porous organic materials have also found wide range of applications as similar to the MOFs due to its feasibility in functionalization, tuneable pore surface etc.

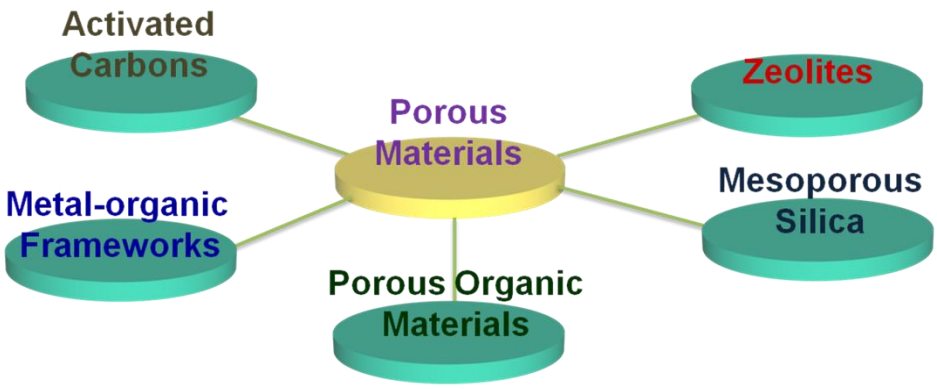

Figure 1.1: Schematic representation for the classification of porous materials.

1.2 Applications of MOFs and Porous Organic Materials

Both metal-organic frameworks and porous organic materials have been explored in diverse fields of application (Fig. 1.2), such as,[3,7]

- gas storage
- separation of gases and industrially important liquids
- carbon capture and conversion
- drug delivery
- heterogeneous catalysis
- sensing of various hazardous and toxic species
- fuel cell applications
- electrochemical applications

Although these materials have extensively been used in such aforementioned applications, but have rarely been explored for the capture of toxic and hazardous pollutants from waste water. In this regard, both MOFs and porous organic materials have been found to be suitable candidate for such environmental applications. Luminescent metal-organic frameworks (LMOFs) have shown huge promise for the sensing of environmentally hazardous and toxic species. But often poor chemical stability and even relatively low hydrolytic stability of MOFs have hindered their applications related to the remediation of water pollutants. As stated earlier, owing to the high physiochemical stability porous organic materials can be well suited candidate for the sequestration of the environmentally hazardous water pollutants.

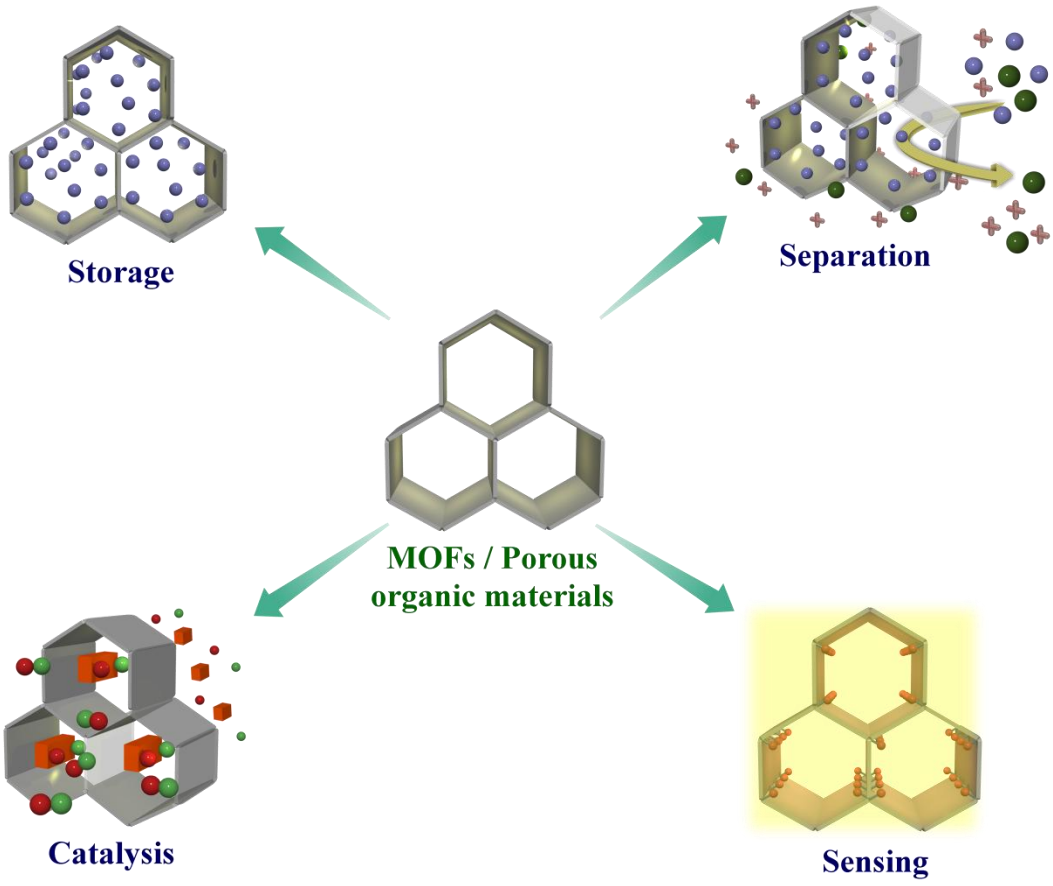

Figure 1.2: Schematic representation of different types of application of MOFs and porous organic materials.

1.3 Water Pollutions and Remediation

Gradual increase in environmental pollution has become a global concern and for the remediation of the pollutants a huge attention is being paid worldwide. Enhanced civilizations and worldwide industrializations have made huge negative impact on the environment by causing such pollutions.[10] Among all kinds of pollution, water pollution is one of the major concern in recent days. It has been observed that extensive use of fresh water and increasing water pollutions have affected the water system of Earth in a greater extent (Fig. 1.3).[11] Consequently, approximately half of the total world's population have been found to be living in the areas which are marked as water stressed zone. Recent statistics revealed that near about 1 billion of people do not have access of clean water. This situation is expected to be turned into even worst condition in near future. In a recent report, United Nations (UN) has estimated that in coming ~ 15 years there will be approximately 40% shortage of clean water.[12] Further, it has been observed that almost 2 million of people die each year from waterborne diseases, such as diarrhea, poor

hygiene etc., which are caused due to extensive water pollutions. Water pollutants or contaminants are broadly defined as physical, chemical or biological matters or substances present in water by the Safe Drinking Water Act (SDWA).[13] Again, there are different types of water pollution that are known till date. Among them surface water pollution, groundwater pollution, ocean pollution, point source, nonpoint source etc. are well known. On the other hand, water pollution can be categorized into different forms such as chemical water pollution, pollution by various pathogens, physical water pollution etc. Pathogens are disease causing microorganisms. Water pollution due to various pathogens can lead to several health problems which includes fever, diarrhea, abdominal discomfort etc. Such water pollutions due to pathogens can occur from on-site sanitation systems or untreated sewage discharges to the water effluents. Furthermore, physical water pollution can be caused by the discharge of different physical substances to the sewages or any other water effluents. Again, Water pollution by various types of toxic and hazardous chemicals has been accounted as one of the highly dangerous and threatening towards the living systems. Water pollution due to chemicals has been found to be increased gradually as polluted waste waters from different sources directly getting discharged to the effluents. Further, chemical water

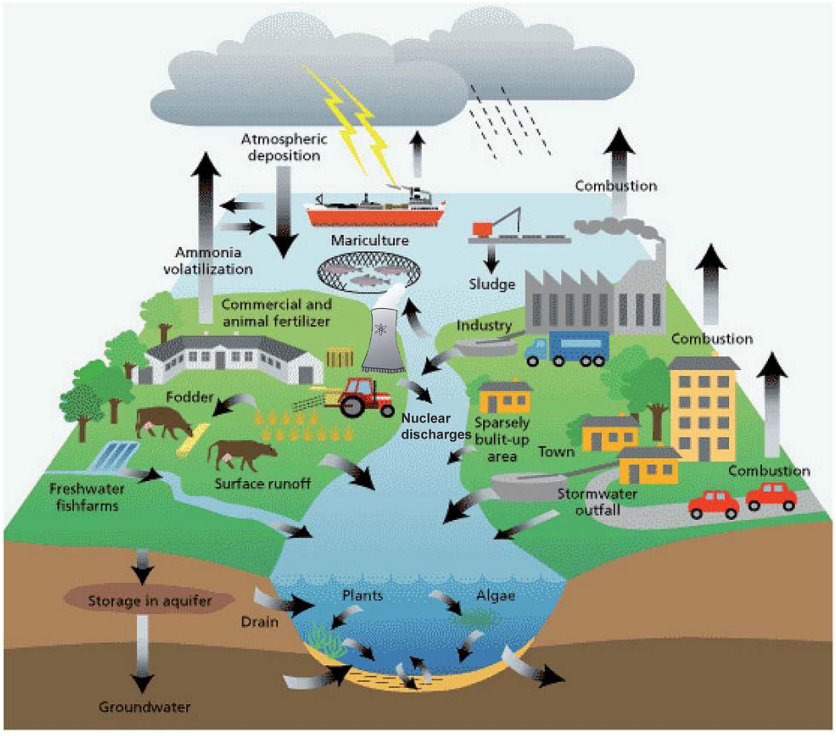

Figure 1.3: Schematic representation of sources of water pollution. Reproduced with permission from reference 11a.

pollutants have been broadly classified into organic and inorganic pollutants (Fig. 1.4).[11a, 13] In case of organic pollutants, diverse and wide range of organic compounds belong to this subgroup of water pollutants. Most common and well known organic pollutants are different types of dye molecules, herbicides/pesticides, oils, pharmaceutical products, personal care products, polyaromatic hydrocarbons, detergents etc.[14] Organic pollutants have been found to be discharged from various domestic activities, different industries, agriculture fields etc. On the other hand, inorganic pollutants include different types of heavy metal (e.g., Hg^{2+}, Pb^{2+}, Cd^{2+} etc.), oxo-anion (e.g., CrO_4^{2-}, $Cr_2O_7^{2-}$, AsO_4^{3-}, SeO_3^{2-}, SeO_4^{2-} etc.), radionuclides (e.g., ^{99}Tc, ^{131}I, ^{129}I, ^{137}Cs, ^{89}Sr, ^{235}U etc.) etc.[15] The range of variety and number of inorganic pollutants are not as wide as organic pollutants. But inorganic pollutants persist in the environment for much longer time as compare to the organic pollutants. In addition, inorganic pollutants are very much difficult to degrade or convert into some eco-friendly species. On the other hand, organic pollutants are relatively less persistent to the environment and relatively easy to degrade. Furthermore, organic pollutants have been known as pseudo-persistent pollutants to our environment since huge amount of organic materials have been found to be discharged to the different water effluents. All these inorganic and organic pollutants are mostly toxic, hazardous and carcinogenic in nature. Because of this chemical water pollution leads to several lethal diseases.

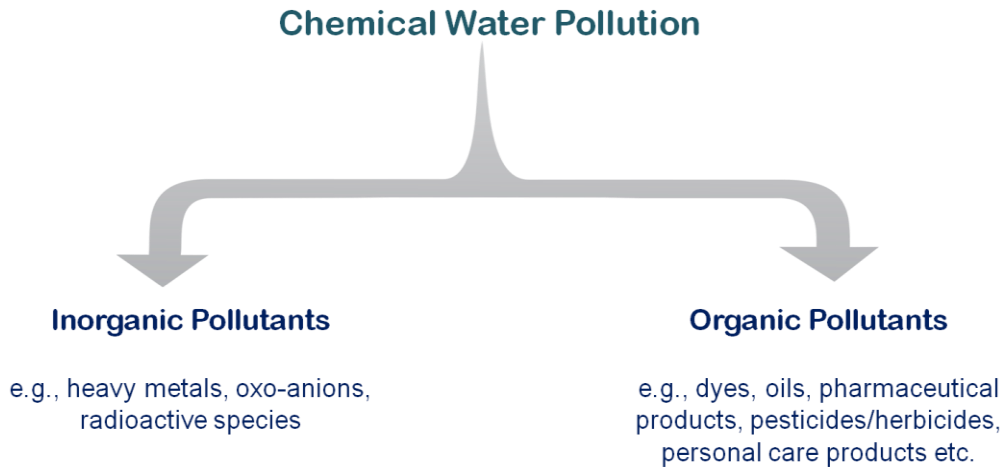

Figure 1.4: Schematic representation for classification of the chemical water pollution.

Understating the threat of water pollution, United Nations adopted Sustainable Development Agenda to provide universal access to clean water. In this regard, desalination of the seawater for freshwater or clean water harvesting from groundwater has become one of the priority option. But this techniques have to be

efficient and also the cost should be affordable worldwide for real time uses. Further, extensive use of such techniques can lead to crisis in the groundwater levels as well desalination plants for the treatment of the seawater can lead to the contamination in the coastal areas.[11a, 14d] In this regard, other than purification of groundwater and seawater, reuse of water has become one of the greater prospect to reduce such water crisis. Reuse of water is gaining paramount interests and different types of technology are being employed for this purpose. Currently employed techniques for treatment of water pollutions include precipitation, flocculation/coagulation, membrane technology, sedimentation, biological process, filtration, advanced oxidation process etc. Although these techniques are working, but several drawbacks like high operation cost, complicated operation, generation of secondary pollutants, unable to remove wastes completely from water etc. have led researchers to find alternative solution. In this regard, adsorption based technique has come up as an alternate of the aforementioned processes. Owing to low operation cost, simplicity in operation, easy regeneration for uses in multiple cycles, relatively less generation of the secondary pollutants, higher waste removal efficiency etc., adsorption based processes have scored over other conventional techniques. To perform removal of toxic and hazardous chemical waste from water via adsorption method several materials, such as polymer resins, zeolites, activated carbons, mesoporous silica, mesoporous clay materials etc., have been explored till date. But often slow kinetics, low capacity, relatively complicated synthesis of adsorbates, poor selectivity etc. of those aforementioned materials have found to create problem for real time applications with higher efficiency. In recent years, MOF-based materials have been started to be explored for the environmental applications. Sensing and sequestration of environmentally hazardous species with MOFs has gained paramount interest. But often MOFs fail to fulfill all the criteria required for capture study because of its poor chemical stability. Further, owing to high physiochemical stability, facile design and synthesis, tuneable architecture have led porous organic materials one of the well suited candidate for the remediation of water pollution. Such environmental applications with porous organic materials have been explored rarely. Since, such extended organic materials have advantages of both porous materials and polymers, this type materials have been found to be a suitable platform for the desired applications. Since scavenging of chemical water pollutants from wastewater requires extensive chemical stability over wide pH-range, porous organic materials have been accounted as potential candidate owing to its robust nature. Further, high porosity of this type of materials can lead to high capacity of the targeted pollutants which is another advantageous feature. On the other hand, easy bulk scale synthesis of such porous materials is another leverage. From these aforementioned points, it can be stated that covalently linked porous organic materials can be a worthy candidate for tackling chemical water pollution.

1.4 Thesis Overview

Here in this thesis, all the works have majorly focused on the design and synthesis of functional MOFs and porous organic materials for the environmental applications. Sensing and sequestration environmentally toxic and hazardous water pollutants have been less explored with MOFs and porous organic materials (Fig. 1.5). In this regard, sensing of toxic pollutants have been carried out with functionalized MOF, but due to lack of desired and sufficient chemical stability of most of the MOFs, capture of pollutants have not been explored with MOFs here. To carry out sequestration of toxic water pollutants, functionalized porous organic materials have been employed further. Task specific porous materials have been utilized toward remediation of water pollutants in each work included in this thesis.

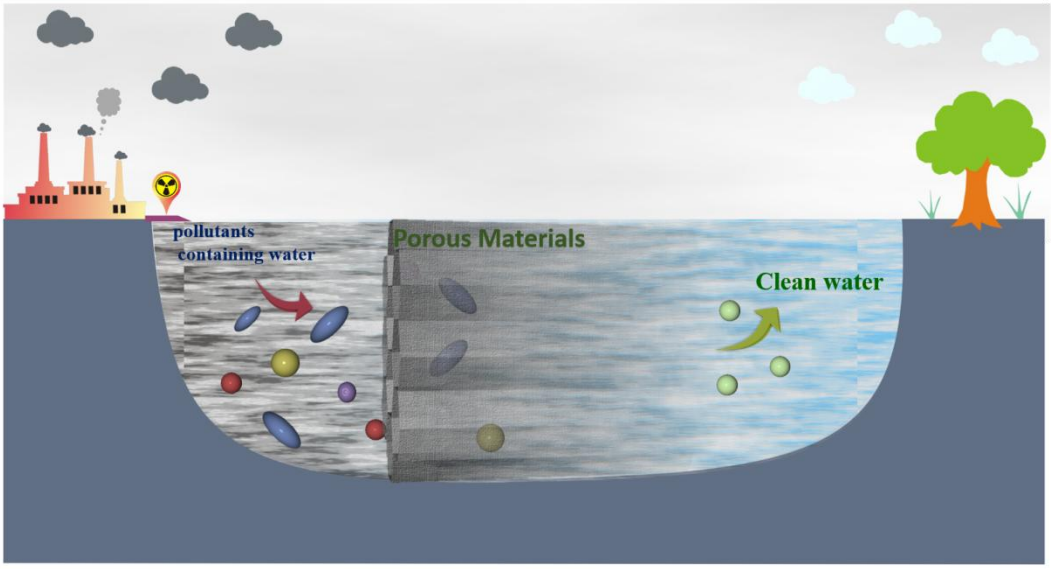

Figure 1.5: Schematic representation of remediation of the water pollutants with porous materials.

In the second chapter (**chapter-2**), sensing of toxic and lethal heavy metal, i.e., Hg^{2+} ion, was performed with a functionalized MOF. To carry out detection of mercury ion in water medium, UiO-series MOF was used as these are found to be stable in water. Target specific butyne groups (UiO-66@Butyn MOF) were appended in the MOF since alkyne moiety found to react selectively with Hg^{2+} ion via oxymercuration reaction. Thus reaction based cleavage of the butyne functionality in the UiO-66@Butyne led to the change in the luminescence property of the MOF to produce the signal. Further the probe was tested against other concurrent metal ions to check the selectivity of the probe. Selectivity test affirmed that the probe highly selective for Hg^{2+} ion and further sensing can be carried out even in presence of interfering metal analytes.

Although MOF based sensing was carried in the previous chapter, but only sensing of pollutants not enough for the remediation purpose. To carry out the capture study of such environmentally toxic and hazardous contaminants from water covalently linked porous organic materials were used further for their high chemical stability. Apart from inorganic cationic pollutants, organic cationic compounds (such as cationic dyes etc.) are one of the major water pollutants. Capture of cationic dyes with cost-effective, chemically stable hyper-cross-linked polymer was performed in the next work (**chapter-3**). Owing to easy one pot synthesis, hydroxy functionalized HCP-91 was synthesized via knitting strategy with the help of Friedel-Craft reaction. Further HCP-91 was post-synthetically modified by aqueous NaOH treatment to incorporate free exchangeable Na^+ ions inside the networks (HCP-91@Na). This HCP-91@Na was used for the selective capture of cationic organic dyes (methylene blue, crystal violet and rhodamine B) from water via cation exchange. The ion-exchange process followed order of size of the respective dye molecules, i.e., larger dye molecules took longer time for complete removal. Selectivity was further confirmed with an anion organic dye, namely methyl orange (MO), where MO showed almost negligible uptake with HCP-91@Na. Furthermore, HCP-91@Na demonstrated selective capture of cationic dyes from binary mixture of cationic and anionic dyes (binary mixture of methylene blue and methyl orange; rhodamine B and methyl orange) in water medium.

Apart from cationic pollutants, anionic water pollutants removal from water gained paramount interest of research because of its high water solubility, toxicity and hazardous nature towards the environment. Radioactive iodine found to present in water in different forms, I_3^- ion is one of them. Previous and recent nuclear disasters has contaminated seawater as well as groundwater in many countries with radioactive pollutants and iodine is one of them. Consequently, capture of iodine from water with porous materials have become one of the recent topic of research worldwide. Hydroxy functionalized hyper-cross-linked polymers (viz. HCP-91 and HCP-92) were utilized for the capture of iodine from water in the next chapter (**chapter-4**). Both the compounds showed efficient removal of iodine from water medium as well as vapor phase. Capture of iodine from water with both HCP-91 and HCP-92 was found to be pseudo-second order. Further, since waste water contains other anions like Cl^-, NO_3^- and SO_4^{2-} along with targeted pollutants, capture study of I_3^- ion was studied in presence those aforementioned anions. Both the HCPs were found to be efficient scavenger of iodine even in presence interfering anions. Capacity of both the compounds for iodine were calculated (2.9 g g^{-1} and 2.49 g g^{-1}) and found be one of the highest in the domain of porous materials. Further, both the compounds were found to be reusable and recyclability was checked up to three cycles.

Apart from simple anionic species, another class of anionic water pollutants are oxo-anions of different heavy metals or radioactive metals. Since chromium is hazardous, carcinogenic and mutagenic in nature,

pollution due to Cr(VI)-based oxo-anions have attracted much concern globally. In the **chapter-5**, a viologen based extended organic network (compound-1) was designed and synthesized for the capture of chromate ion (CrO_4^{2-}). Compound-1 captured CrO_4^{2-} ion from water efficiently and further anion dependent capture study was also performed. Compound-1 showed effective removal of CrO_4^{2-} ion even in presence of concurrent anions like Cl^-, NO_3^- and SO_4^{2-}. Water pollution due to another oxo-anion, viz. TcO_4^- ion, has also become a concern as one of the isotope of technetium (^{99}Tc) is radioactive in nature. As handing of radioactive species is not convenient for laboratory condition, capture of TcO_4^- ion was performed with compound-1 by using surrogating MnO_4^- and ReO_4^- ion. Compound-1 was further reused for several cycles with 3 M HCl solution.

In conclusion, MOFs and porous organic materials have been employed for the sensing and sequestration of hazardous pollutants from water. In this regard, a comparison table has been included which has demonstrated the advantages and disadvantages of each materials (Table 1.1).

	Properties			Advantages for Environmental Applications	Disadvantages for Environmental Applications	General Remarks
	Porosity	Crystallinity	Chemical Stability			
Metal-organic Frameworks (MOFs)	Micro-, meso-, and macropores	High	Moderate (Poor to good)	(i) Suitable structure property correlation (ii) Structural diversity	Comparatively less chemical stability	Owing to structure property correlation and luminescent nature, MOFs provide excellent platform for the sensing of toxic species
Hyper-cross-linked Polymers (HCPs)	Micro-, meso-, and macropores	Amorphous	Typically high	(i) High chemical stability (ii) Wide range of diversity in building blocks (iii) Easy bulk scale synthesis at low cost	Poor structure property correlation due to amorphous nature	(i) Owing to high chemical stability and easy large scale synthesis at low cost, HCPs have been considered as suitable candidate for target specific capture studies. (ii) Hydrophobic cavities of HCPs often offers selectivity to some specific pollutants (e.g., organic dyes, iodine etc.).
Ionic viologen-based organic networks	Micro-, mesopores	Both (Amorphous to crystalline)	Typically high	(i) High chemical stability (ii) Owing to ionic in nature, excellent for ionic pollutants capture (iii) Easy bulk scale synthesis	Poor structure property correlation in case of amorphous compounds	Owing to free exchangeable anions inside the networks and high chemical stability, these materials are suitable candidate for toxic anion capture from waste water.

Table 1.1: Comparison table of MOFs, HCPs and ionic viologen-based networks toward environmental applications.

1.5 References

1. (a) D. Wu, F. Xu, B. Sun, R. Fu, H. He, and K. Matyjaszewski, *Chem. Rev.*, 2012, **112**, 3959−4015.

2. (a) A. G. Slater, A. I. Cooper, *Science*, 2015, **348**, aaa8075.

3. (a) R. E. Morris and J. Čejka, *Nat. Chem.*, 2015, DOI: 10.1038/NCHEM.2222. (b) H. M. El-Kaderi, J. R. Hunt, J. L. Mendoza-Cortés, A. P. Côté, R. E. Taylor, M. O'Keeffe and O. M. Yaghi, *Science*, 2007, **316**, 268–272. (c) S. Furukawa, J. Reboul, S. Diring, K. Sumida and S. Kitagawa, *Chem. Soc. Rev.*, 2014, **43**, 5700–5734. (d) A. J. Howarth, M. J. Katz, T. C. Wang, A. E. Platero-Prats, K. W. Chapman, J. T. Hupp and O. K. Farha, *J. Am. Chem. Soc.*, 2015, **137**, 7488−7494. (e) T. Kitao, Y. Zhang, S. Kitagawa, B. Wang and T. Uemura, *Chem. Soc. Rev.*, 2017, **46**, 3108–3133. (f) Z. Hu, B. J. Deibert and J. Li, *Chem. Soc. Rev.*, 2014, **43**, 5815–5840. (g) Z. Chang , D. -H. Yang , J. Xu , T. -L. Hu and X. -H. Bu, *Adv. Mater.*, 2015, **27**, 5432–5441. (h) W. Xia, A. Mahmood, R. Zou and Q. Xu, *Energy Environ. Sci.*, 2015, DOI: 10.1039/C5EE00762C. (i) M. Sindoro, N. Yanai, A. -Y. Jee and S. Granick, *Acc. Chem. Res.*, 2014, **47**, 459-469. (j) J. Aguilera-Sigalat and D. Bradshaw, *Coord. Chem. Rev.*, 2016, **307**, 267-291. (k) L. Zhu, X. -Q. Liu, H. -L. Jiang and L. -B. Sun, *Chem. Rev.*, 2017, **117**, 8129−8176. (l) C. R. Kim, T. Uemura and S. Kitagawa, *Chem. Soc. Rev.*, 2016,**45**, 3828-3845. (m) J. Canivet, A. Fateeva, Y. Guo, B. Coasne and D. Farrusseng, *Chem. Soc. Rev.*, 2014, **43**, 5594-5617. (n) J. -P. Zhang, Y. -B. Zhang, J. -B. Lin, and X. -M. Chen, *Chem. Rev.*, 2012, **112**, 1001–1033. (o) J. Rocha, L. D. Carlos, F. A. A. Paza and D. Ananias, *Chem. Soc. Rev.*, 2011, **40**, 926–940. (p) O. Shekhah, J. Liu, R. A. Fischer and C. Wöll, *Chem. Soc. Rev.*, 2011, **40**, 1081–1106.

4. S. Horike, S. Shimomura and S. Kitagawa, *Nat. Chem.*, 2009, **1**, 695-704.

5. A. Karmakar, A. V. Desai and S. K. Ghosh, *Coord. Chem. Rev.*, 2016, **307**, 313–341.

6. (a) W. Lu, D. Yuan, J. Sculley, D. Zhao, R. Krishna and H. –C. Zhou, *J. Am. Chem. Soc.*, 2011, **133**, 18126–18129. (b) S. Keskin, T. M. van Heest and D. S. Sholl, *ChemSusChem*, 2010, **3**, 879–891.

7. (a) X. Feng, X. Ding and D. Jiang, *Chem. Soc. Rev.*, 2012, **41**, 6010–6022. (b) S. Das, P. Heasman, T. Ben and S. Qiu, *Chem. Rev.*, 2017, **117**, 1515−1563. (c) P. J. Waller, F. Gándara and O. M. Yaghi, *Acc. Chem. Res.*, 2015, **48**, 3053−3063. (d) L. Zou, Y. Sun, S. Che, X. Yang, X. Wang, M. Bosch,

Q. Wang, H. Li, M. Smith, S. Yuan, Z. Perry and H. -C. Zhou, *Adv. Mater.*, 2017, **29**, 1700229. (e) Y. Xu, S. Jin, H. Xu, A. Nagai and D. Jiang, *Chem. Soc. Rev.*, 2013, **42**, 8012–8031. (f) R. P. Bisbey and W. R. Dichtel, *ACS Cent. Sci.*, 2017, **3**, 533−543. (g) B. Aguila, Q. Sun, J. A. Perman, L. D. Earl, C. W. Abney, R. Elzein, R. Schlaf and S. Ma, *Adv. Mater.*, 2017, **29**, DOI: 10.1002/adma.201700665. (h) U. Diaza and A. Corma, *Coord. Chem. Rev.*, 2016, **311**, 85–124. (i) D. D. Medina, T. Sick and T. Bein, *Adv. Energy Mater*., 2017, DOI: 10.1002/aenm.201700387. (j) J. Wu, F. Xu, S. Li, P. Ma, X. Zhang, Q. Liu, R. Fu and D. Wu, *Adv. Mater.*, 2018, DOI: 10.1002/adma.201802922. (k) F. Beuerle and B. Gole, *Angew. Chem. Int. Ed.*, 2018, **57**, 4850– 4878. (l) M. S. Lohse and T. Bein, *Adv. Funct. Mater.*, 2018, **28**, DOI: 10.1002/adfm.201705553. (l) S. M. J. Rogge, A. Bavykina, J. Hajek, H. Garcia, A. I. Olivos-Suarez, A. Sepúlveda-Escribano, A. Vimont, G. Clet, P. Bazin, F. Kapteijn, M. Daturi, E. V. Ramos-Fernandez, F. X. Llabrés i Xamena, V. Van Speybroeck and J. Gascon, *Chem. Soc. Rev.*, 2017,**46**, 3134-3184.

8. (a) W. Lu, D. Yuan, D. Zhao, C. I. Schilling, O. Plietzsch, T. Muller, S. Bräse, J. Guenther, J. Blümel, R. Krishna, Z. Li and H. -C. Zhou, *Chem. Mater.*, 2010, **22**, 5964–5972. (b) M. G. Rabbani and H. M. El-Kaderi, *Chem. Mater.*, 2011, **23**, 1650–1653.

9. (a) S. M. Cohen, *Chem. Rev.*, 2012, **112**, 970–1000. (b) Z. Yin, S. Wan, J. Yang, M. Kurmoo and M. -H. Zeng, *Coord. Chem. Rev.*, 2019, DOI: 10.1016/j.ccr.2017.11.015. (c) T. Islamoglu, S. Goswami, Z. Li, A. J. Howarth, O. K. Farha and J. T. Hupp, *Acc. Chem. Res.*, 2017, **50**, 805−813.

10. A. J. Howarth, Y. Liu, J. T. Hupp and O. K. Farha, *CrystEngComm*, 2015, **17**, 7245–7253.

11. (a) M. Mon, R. Bruno, J. Ferrando-Soria, D. Armentano and E. Pardo, *J. Mater. Chem. A*, 2018, **6**, 4912–4947. (b) J. Murria, *Nat. Hazards Rev.*, 2003, **4**, 166.

12. (a) D. T. Sun, L. Peng, W. S. Reeder, S. M. Moosavi, D. Tiana, D. K. Britt, E. Oveisi and W. L. Queen, *ACS Central Science*, **2018**, *4*, 349-356. (b) WWAP (United Nations World Water Assessment Programme). Water for a Sustainable World; The United Nations World Water Development Report: UNESCO:Paris, 2015; pp 1−67.

13. https://www.epa.gov/dwstandardsregulations.

14. (a) Organic Pollutants in Water, ed. I. H. Suffet and M. Malaiyandi, American Chemical Society, Washington, DC, 1986, vol. 214. (b) I. Ali, M. Asim and T. A. Khan, *J. Environ. Manage.*, 2012, **113**,

170–183. (c) M. Yang, *J. Environ. Sci. Health, Part C: Environ. Carcinog. Ecotoxicol. Rev.*, 2011, **29**, 223–249. (d) E. M. Dias and C. Petit, *J. Mater. Chem. A*, 2015, **3**, 22484–22506.

15. (a) P. B. Tchounwou, C. G. Yedjou, A. K. Patlolla and D. J. Sutton, *EXS*, 2012, 133–164. (b) J. Li, X. Wang, G. Zhao, C. Chen, Z. Chai, A. Alsaedi, T. Hayat and X. Wang, *Chem. Soc. Rev.*, 2018, **47**, 2322-2356. (c) S. N. Groudev, S. G. Bratcova and K. Komnitsas, *Miner. Eng.*, 1999, **12**, 261–270. (d) Q. Gao, J. Xu and X. -H. Bu, *Coord. Chem. Rev.*, 2019, DOI:10.1016/j.ccr.2018.03.015.

Chapter 2

Selective Recognition of Hg(II) ion in Water by a Functionalized Metal-Organic Framework (MOF) Based Chemodosimeter

2.1 Introduction

Water Environmental pollution due to heavy metal (Hg, Pb, As and Cd) ions is becoming a huge threat to the human life and other biological species, because of their high toxicity and carcinogenicity.[1] Among these heavy metals, mercury ion (Hg^{2+}) accounts as one of the most poisonous and widespread environment pollutant as it easily reacts with various biomolecules causing several deadly diseases like acrodynia (pink disease), minamata and Hunter-Russell syndrome, even at very low concentration.[2] Extensive use of Hg^{2+} across different fields (batteries, dental amalgam, electrical apparatus etc.) has led to remarkable disposal and contamination of the environment. According to U.S. Environmental Protection Agency (EPA), the estimated release of Hg^{2+} into the environment has reached ~7500 tons per year.[3] Contamination of Hg^{2+} in the natural water resources, especially in the drinking water is one of the most threatening issues. Considering the deleterious consequences of mercury, it has become imperative to urgently design efficient sensors which can detect Hg^{2+} ion at very low concentration in aqueous medium.

Till date numerous efforts have been made to develop efficient sensors for Hg^{2+} ion. Different kind of techniques such as liquid chromatography, chemiluminescence, colorimetric detection, inductively coupled plasma mass spectrometry (ICPMS), X-ray absorption spectroscopy and anodic stripping voltammetry have been employed for the detection of toxic mercury ion.[4] Among these techniques, chemiluminescence has attracted considerable attention over others, because of its operational simplicity, instant response, cost effectiveness and high sensitivity.[5] Prompted by the efficacy of this technique various type of fluorescent probes have been developed based on organic small molecules, DNAs, quantum dots (QDs), inorganic-organic hybrid materials, organic polymers etc.[6] But low water solubility of organic molecules based sensors and low water stability of the organic-inorganic hybrid materials hinder their suitability for the real time application. These shortcomings have necessitated urgent development of new efficient Hg^{2+} sensors.

In recent years, metal-organic frameworks (MOFs) have emerged as a promising and unique class of materials with extended crystalline and porous architecture.[7] MOFs have been synthesised from metal nodes and organic struts, wherein the organic linker can be functionalized in accordance with the targeted applications. Owing to the large surface area, tuneable porosity and functionality, MOFs have emerged as front-runners as target-specific guest accessible host systems. Based on such host-guest chemistry, MOFs have been employed in the field of gas and solvent separation, drug delivery, catalysis, sensing application etc.[8] Detection of Hg^{2+} ion using MOFs has been recently investigated with plenty of room for improvement; both in terms of control over selectivity/sensitivity and applicability under real-time

conditions.[9] Most of the MOFs for Hg^{2+} sensing and trapping have been reported till date are based on chemosensors and they can be classified in two types: (1) having nitrogen centres or amine groups, which can coordinate to Hg^{2+} and (2) sulfur rich probes where Hg^{2+} can bind strongly to the sulfur centre due to soft-soft interaction between them (Hg···S interaction) to produce the signal. Despite having reasonable sensitivity, aforementioned probes have certain inherent drawbacks such as, (1) both amines and sulfides can undergo aerial oxidation during long time storage, (2) on the other hand sulfur based probes cannot provide suitable response in sulfur rich environment due to the presence of mercury in great quantity.[10] To overcome these difficulties, we have adopted the chemodosimeter based approach, which is devoid of the presence of any amine or sulfur functionality. In case of chemodosimeter, the target analyte reacts with dosimeter molecules (probes) in an irreversible fashion (unlike chemosensors) to provide the permanent signals.[11] As a consequence it has been observed that both sensitivity and selectivity of chemodosimeters towards analyte are high in comparison to chemosensors. Consequently, we sought to develop alkyne functionalised MOF based chemodosimeter for detection of Hg^{2+} ion (Scheme 2.1), based on the knowledge that Hg^{2+} ions react with alkyne groups via oxymercuration reaction in presence of H_2O.[10,12] To the best of our knowledge, reaction-based detection of Hg(II) in aqueous medium has not been reported in the regime of MOF till date.

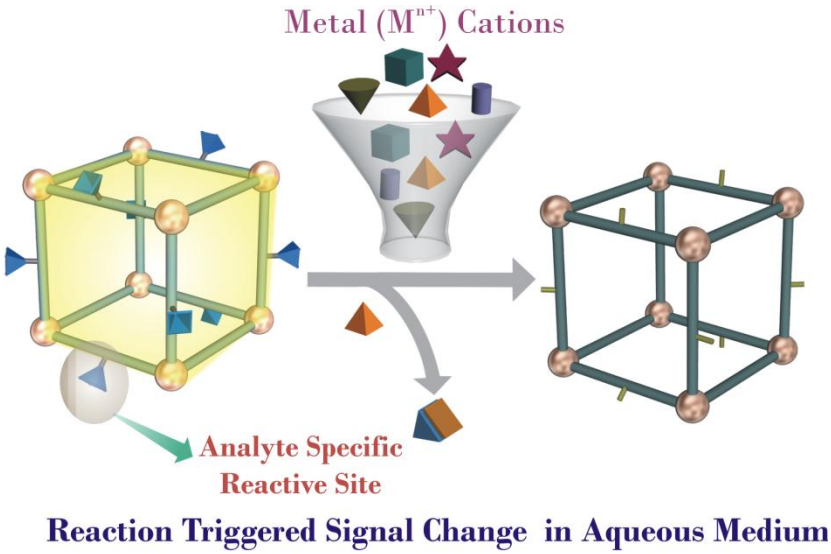

Scheme 2.1: Detection of Hg(II) ion in water medium with a functionalized metal-organic framework (MOF).

2.2 Experimental

2.2.1 Materials:

2,5-dihydroxy terephthalic acid was purchased from TCI chemicals, 3-butyn-1-ol, $Hg(NO_3)_2$ and NaOD in D_2O were purchased from Sigma-Aldrich, $ZrCl_4$ and all other metal salts were purchased from Merck, solvents and other chemicals were obtained locally. These chemicals were used without further purification.

2.2.2 Physical Measurements:

All fluorescence measurements were done on Jobin Yvon Fluoromax-4 spectrofluorometer. Powder X-ray diffraction patterns were recorded on Bruker D8 Advanced X-Ray diffractometer using Cu Kα radiation (λ= 1.5406 Å) in 5° to 40° 2θ range. The IR Spectra were acquired by using NICOLET 6700 FT-IR spectrophotometer using KBr pellet in 400-4000 cm^{-1} range. Gas adsorption measurements were studied using BelSorp-max instrument from Bel Japan. ^1H & ^{13}C NMR spectra were recorded on a JEOL 400 MHz or Bruker 400 MHz spectrometer. The EDX data were obtained using FEI Quanta 3D dual beam ESEM at 30 KV.

2.2.3 Synthesis:

Synthesis of Dimethyl 2,5-dihydroxyterephthalate: 2,5-dihydroxy terephthalic acid (500 mg, 2.52 mmol) was taken in 100 ml of round bottom flask and to that 30 ml of methanol and 1 ml of concentrated H_2SO_4 were added (Scheme 2.2). This reaction mixture was allowed to reflux at 80 ^oC for 12 hours. After 12 hours solvent was evaporated under reduced pressure. Water was added to the reaction mixture and then neutralised with saturated solution of $NaHCO_3$. Later compound was obtained from water with dichloromethane (DCM) by extracting two times. Both the organic layers combined together and dried over anhydrous Na_2SO_4. Then DCM was evaporated to obtain yellow coloured solid compound. Yield: 560 mg

Synthesis of 2,5-bis(but-3-yn-1-yloxy)terephthalic acid (L1): Thus prepared Dimethyl 2,5-dihydroxyterephthalate (200 mg, 0.885 mmol) was dissolved 25 ml acetonitrile and to that 560 mg K_2CO_3 (4 mmol) was added at inert condition. After 15 mins to the reaction mixture 596 mg of 3-Butynyl *p*-toluenesulfonate (5 mmol) was added and it was allowed to stir for overnight at refluxing condition (Scheme 2.2). On completion of the reaction acetonitrile was evaporated under reduced pressure and the solid mass was extracted with chloroform and water for two times. Organic layers were combined and dried over anhydrous Na_2SO_4.Solid yellow mass was obtained on evaporation of organic layer under reduced pressure. Compound (100 mg) thus obtained was further dissolved in 30 ml of tetrahydrofuran (THF) and to that 200 mg KOH was added (dissolved in water) (Scheme 2.2). The reaction mixture was

allowed to stir for 6 hours. On completion THF was evaporated and water was added to the reaction mixture. Then aqueous phase was neutralised to get the solid compound which was filtered off. Yield: 75 mg

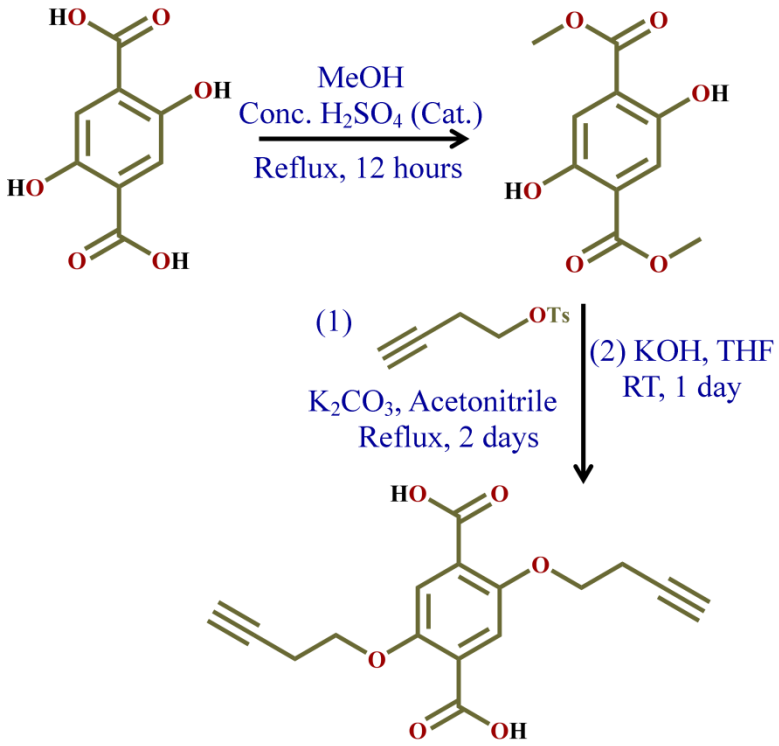

Scheme 2.2: Synthesis scheme of ligand.

Synthesis of UiO-66@Butyne (1-Butyne): A mixture of $ZrCl_4$ (83mg, 0.35mmol), ligand (L1) (105 mg, 0.35mmol) and benzoic acid (1.28gm, 10.5mmol) were dissolved in 4mL of N,N-dimethylformamide (DMF), the resulting solution was placed in a Teflon lined Parr stainless steel vessel (17 mL) and sealed. The sealed vessel was then placed in an oven and allowed to heat at 120 °C for 24 hours. After slow cooling to room temperature yellow crystalline powder of UiO-66@Butyne (**1′-Butyne**) was isolated by filtration and washed with DMF three times. Obtained MOF (**1′-Butyne**) was dipped in MeOH for 4 days to exchange occluded solvent molecules with MeOH and solvent was exchanged with fresh MeOH in every 12 hours. The MeOH exchanged MOF was filtered and heated at 100 °C under vacuum for 12 hours to get guest free UiO-66@Butyne (**1-Butyne**). Thus obtained (**1-Butyne**) was used for all measurements. UiO-66@OH has also been synthesized by adopting the similar protocol with 2,5-dihydroxyterephthalic acid as ligand.

2.2.4 Analyte prepration:

First, Stock solutions of metal salts were prepared from their respective nitrate and choride salts in water of concentration 0.05 mM. Hg(II)-ion solution then diluted 10 times to prepare 0.005 mM stock solution in water.

2.2.5 Luminescence studies with UiO-66@Butyne:

1 mg desolvated UiO-66@Butyne has been taken in a cuvette and 2 mL water has been added to that. Initial luminescence spectra of UiO-66@Butyne in water has been recorded by exciting at 340 nm (spectra recorded in the range of 355-650 nm). Then to the dispersed MOF in water we have added stock solution of Hg(II) ion in water (20 µL to 200 µL) and spectra were for each addition. With each addition of Hg(II) ion, we found quenching in the fluorescence emission of UiO-66@Butyne.

For competing studies we have taken Ba^{2+}, Cd^{2+}, Co^{2+}, Cu^{2+}, Zn^{2+}, Cr^{3+}, Fe^{3+}, Mg^{2+}, Mn^{2+}, Ni^{2+} and Sr^{2+} ions in water. In a typical way, for initial study we have taken 1 mg of UiO-66@Butyne in 2 mL of water. To the dispersed MOF we have added 200 µL of the competing cation from the stock solution and recorded the corresponding spectra to check the response of MOF towards other metal ions (which we have provided in a bar diagram profile).

Later, in a similar way to the dispersed MOF (1 mg) in water medium (2 mL) we have added 200 µL of competing cation and followed by the addition of 200 µL Hg(II) ion solution from the stock as prepared earlier. We have recorded both responses of MOF in presence of competing metal ions and in presence of both competing metal ion and Hg(II) ion. By combining two responses we got the sensitivity of UiO-66@Butyne towards Hg(II) ion in presence of other competing ions.

2.2.6 NMR study of Hg(II)-treated UiO-66@Butyne:

We have studied the ^{13}C-NMR of Hg(II) treated UiO-66@Butyne after digesting the corresponding MOF in NaOD and D_2O medium. First, we have taken UiO-66@Butyne in a small round bottom flask and to the MOF 40% NaOD in D_2O was added to break the MOF. Later, to the solution D_2O has been added to dilute it and ^{13}C-NMR was carried out with the supernatant solution (Appendix 2.7).

2.3 Results and discussion

For practical applications of any compound as chemical sensory materials, water stability is the primary criteria as in most of the cases detection of the targeted analytes has been carried out from waste water or any other water sources. UiO-series MOFs are well known for high chemical stability arising from its secondary building unit $Zr_6O_4(OH)_4(CO_2)_{12}$.[13] On account of the high chemical stability of UiO-66, we have chosen butyne functionalized UiO-66@Butyne as a potential Hg(II) sensor, which can provide

signal through irreversible Oxymercuration reaction (Fig. 2.1). UiO-66@Butyne is an isoreticular MOF to terephthalic acid derived UiO-66. To synthesize UiO-66@Butyne, we first synthesized terephthalic acid having two side chains ended up with butyne functionalization (BDC@Butyne) and then MOF-formation was carried out in solvothermal method with $ZrCl_4$ in DMF as the solvent. To check the framework integrity of thus prepared UiO-66@Butyne, characterization was carried out with powder X-ray diffraction (PXRD), infra-red (IR) spectroscopy, thermo-gravimetric analysis (TGA), N_2 gas adsorption measurement at 77 K and field emission scanning electron microscope (FE-SEM). PXRD pattern of UiO-66@Butyne was found to be crystalline and matched with UiO-66, which indicated both the compounds were iso-structural (Appendix 2.8).[14] Peak around 2950 cm^{-1} corresponded to the stretching frequency of C-H (in -CH_2- group) present in the alkyl chain and thus confirmed the presence of butyne groups in the framework (Appendix 2.9).[15] In TGA, there was initial loss of ~ 20% in the as-synthesized compound because of occluded solvent molecules as guest; upon activation of the compound we found very negligible loss upto ~250 °C (Appendix 2.10). So, we have synthesized water stable Zr-based MOF bearing butyne groups as active sites for Hg(II)-detection, instead of conventionally adopted functionality like amine groups or sulfur groups. To check the activity of UiO-66@Butyne towards Hg(II) ion, we have dispersed desolvated MOF in water and excited at 340 nm to obtain fluorescence spectra in the range of 355-650 nm. Upon excitation at 340 nm, compound showed smooth emission spectra with maxima at 537 nm which got quenched upon addition of aqueous Hg(II) ion solution (Fig. 2.2). This fluorescence change occurs due to the formation of UiO-66@OH, which is relatively less-fluorescent, as a result of the oxymercuration reaction between UiO-66@Butyne and Hg(II) ion in water.

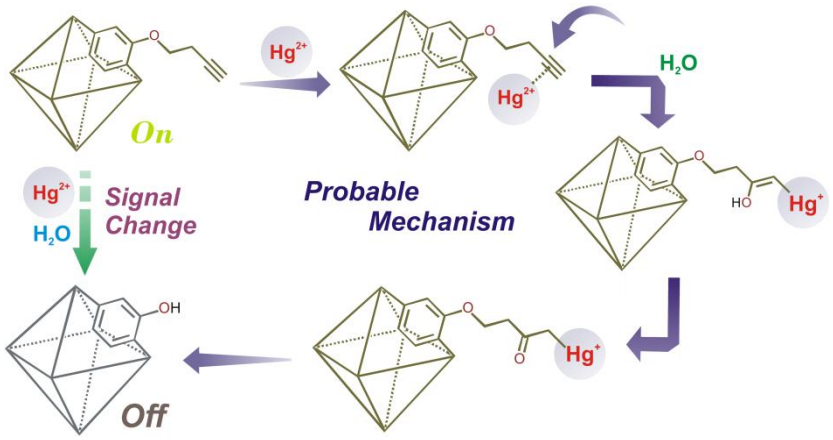

Figure 2.1: Schematic representation of probable mechanism of Hg(II) sensing in UiO-66@Butyne.

To examine the structural stability of Hg(II) ion treated phase of UiO-66@Butyne we did thorough characterization using the aforementioned techniques. PXRD pattern of the Hg(II) ion treated phase showed that the compound remained crystalline and maintained its framework as parent compound (Appendix 2.12). Similar thermal stability of this compound was obtained from TGA profiles, which validated the retention of the framework integrity (Appendix 2.13). Diminishing peak at ~2950 cm^{-1} in IR spectroscopy indicated to the loss of alkyne functionality on treatment with Hg(II) ion (Fig. 2.3a). In addition to IR spectra, we have performed ^{13}C-NMR of Hg(II) ion treated UiO-66@Butyne to substantiate the reaction (Appendix 2.7). Furthermore, we performed FE-SEM to check the morphological stability of UiO-66@Butyne. Both the compounds were found to be having similar morphology affirming the similar framework integrity and stability of UiO-66@Butyne even after oxymercuration reaction in aqueous medium (Appendix 2.14). With the desolvated phase of both compounds low temperature gas adsorption measurements (N_2 at 77 K) were carried out. Due to the presence of bulky substituent in UiO-66@Butyne, very low uptake of N_2 gas was observed. In case of Hg(II) ion treated phase, because of the removal of the butyne groups, N_2 uptake was enhanced by 10 times as compare to UiO-66@Butyne (Appendix 2.15). In addition, BET (Brunauer–Emmett–Teller) surface area of UiO-66@Butyne was found to be very negligible, whereas upon reaction with Hg(II) ion, the surface area increased to 174 m^2g^{-1}. This result also confirmed that oxymercuration reaction occurred inside the pores and framework integrity was maintained after reaction.

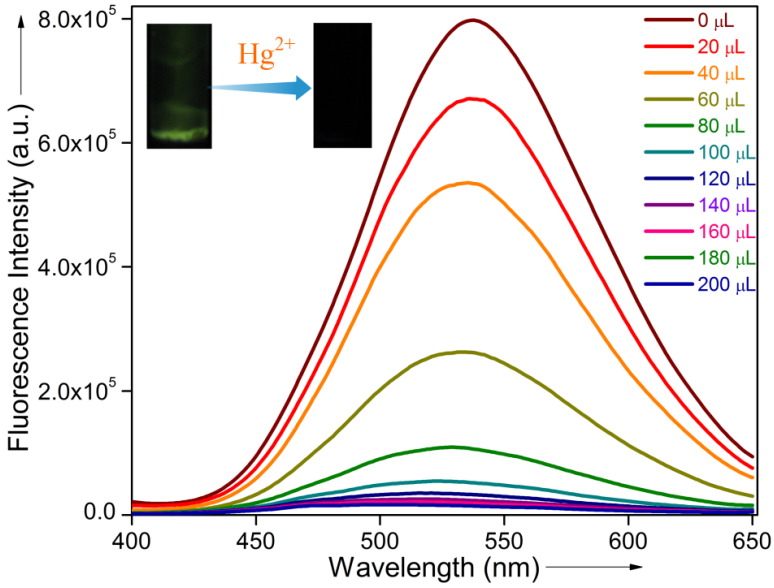

Figure 2.2: Change in the fluorescence spectra of UiO-66@Butyne upon incremental addition of Hg(II)-ion solution in water medium.

Enthused from the above results, we sought to carry out further experiments regarding the detection of Hg(II) ion in aqueous medium. Here, all the fluorescence measurements were carried out in dispersed phase, where 1 mg of MOF has been dispersed in 2 ml of water. At first we have recorded the fluorescence response of UiO-66@Butyne on incremental addition of Hg(II) ion solution in aqueous medium with 3 minutes equilibration time. It has been found that on increasing concentration of Hg(II) ion in the solution, the intensity of photoluminescence profile got quenched (Appendix 2.17). Also in kinetic study of UiO-66@Butyne in presence Hg(II) ion instant change in the intensity of the compound was observed (Appendix 2.18). This kind of rapid and high quenching ability of our MOF observed due to fast and strong interaction of it with the analyte molecules. Limit of detection (LOD) for the probe was calculated according to the previous reports and found to be 10.9 nM (Appendix 2.19 and Appendix Table 2).[16] According to the U.S. EPA, the toxicity level of Hg^{2+} ion is 10 nM in drinking water. So, detection limit of UiO-66@Butyne lies close to the permitted range by EPA and is one of the best in the MOF regime reported till date.[17] Finally, we have recorded photoluminescence spectra of UiO-66@OH (analogous of UiO-66@Butyne) before and after addition Hg(II) ion to check the effect of butyne groups. We did not found any response of UiO-66@OH towards Hg^{2+} ion indicating the role of butyne group here (Appendix 2.20). Similarly, only ligand did not show any noticeable response towards Hg(II) ion, which clearly explains the importance of the ordered framework in this case (Appendix 2.20). Here the restriction of C-O bond rotation due to the presence of bulky butyne groups can be attributed to origin of fluorescence in UiO-66@Butyne; thus on removal of butyne groups via oxymercuration reaction results into the signal change.[18]

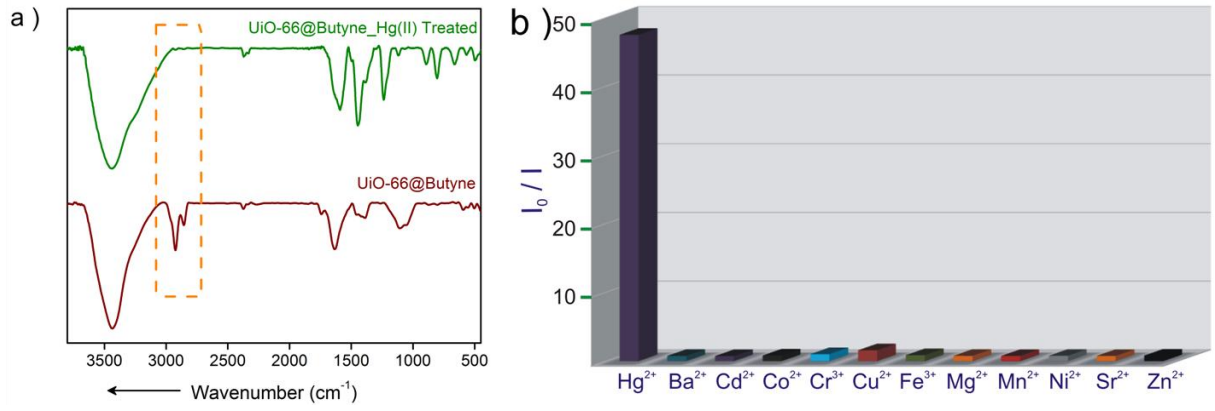

Figure 2.3: a) IR spectra of UiO-66@Butyne (wine red) and after Hg(II) ion treatment (green); b) Extent of fluorescence response of UiO-66@Butyne towards various metal ions.

Apart from sensitivity high selectivity is also a very important criterion for a good sensory material to be used. Keeping this point in mind we recorded the response of UiO-66@Butyne towards other metal ions (Ba^{2+}, Cd^{2+}, Co^{2+}, Cu^{2+}, Zn^{2+}, Cr^{3+}, Fe^{3+}, Mg^{2+}, Mn^{2+}, Ni^{2+} and Sr^{2+}) having similar concentration as Hg^{2+} ion in similar way. No such response in the fluorescence spectra was observed in presence of other cations in aqueous medium (Fig. 2.3b). So the reaction based approach to detect Hg^{2+} ion, made the probe highly selective and sensitive over other approaches like coordination of the targeted metal ion to the active sites of MOFs. Encouraged from this result we thought to examine the efficacy of the probe to sense Hg^{2+} ion in presence of other metal ions. In a typical experiment MOF was dispersed in water and to that particular metal ion was added, followed by fluorescence spectra was recorded after 3 minutes equilibration time. Later Hg^{2+} ion was added to the solution and again fluorescence of the solution was measured. As expected, respective metal ions did not show much change, but fluorescence intensity of the solution quenched upon addition of Hg^{2+} ion (Appendix 2.22). So, this experiment proves that our MOF based system can sense Hg(II) ion with high sensitivity and selectivity even in presence of concurrent metal ions. Further, EDX analysis was carried for UiO-66@Butyne and Hg(II)-ion treated phase of UiO-66@Butyne which revealed the presence of carbon, oxygen and zirconuim in both compounds, also ruled out the presence of mercury (Appendix 2.23-2.26).

2.4 Conclusions

In conclusion, we have synthesized a stable and butyne functionalized MOF via ligand modulation, which is analogous to UiO-66. Rendering the butyne functionality we have achieved selective detection of Hg(II) ion in aqueous medium via oxymercuration reaction. Although few MOF based Hg(II) ion sensing have been reported in recent days, but reaction based sensor not reported till date in the MOF regime. Irreversible reaction between Hg(II) ion and butyne group provides selectivity as well as high sensitivity with detection limit of 10.9 nM. We believe that this work will stimulate the research in the field of MOF based Hg(II) ion sensing in a chemodosimeter approach and will also motivate to fabricate MOF based probes for other toxic heavy metals.

2.5 Appendix Section

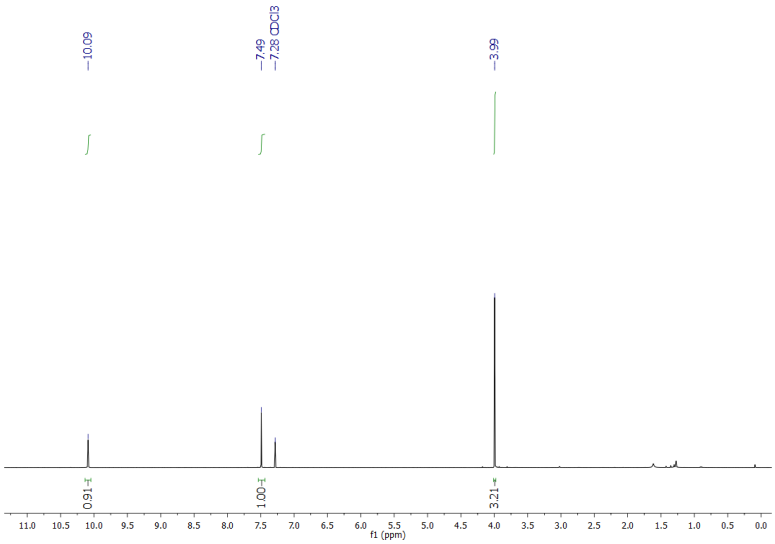

Appendix 2.1: ^{1}H-NMR spectrum of dimethyl 2,5-dihydroxyterephthalate in $CDCl_3$ solvent.

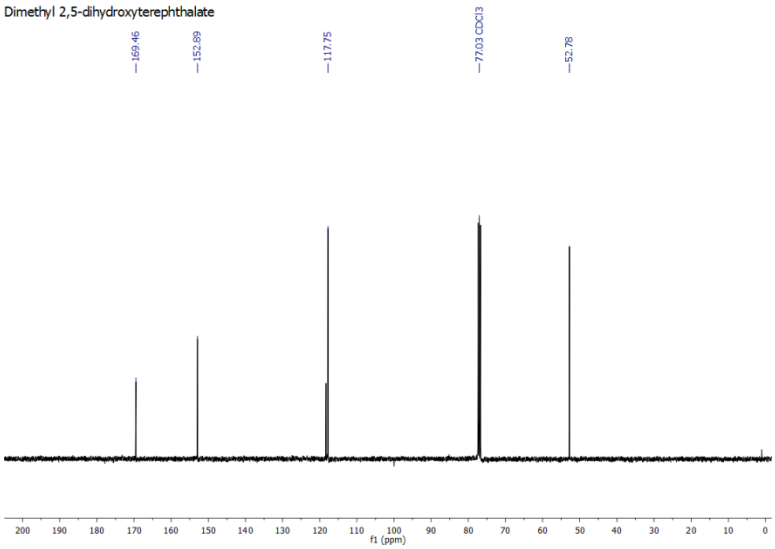

Appendix 2.2: ^{13}C-NMR spectrum of dimethyl 2,5-dihydroxyterephthalate in $CDCl_3$ solvent.

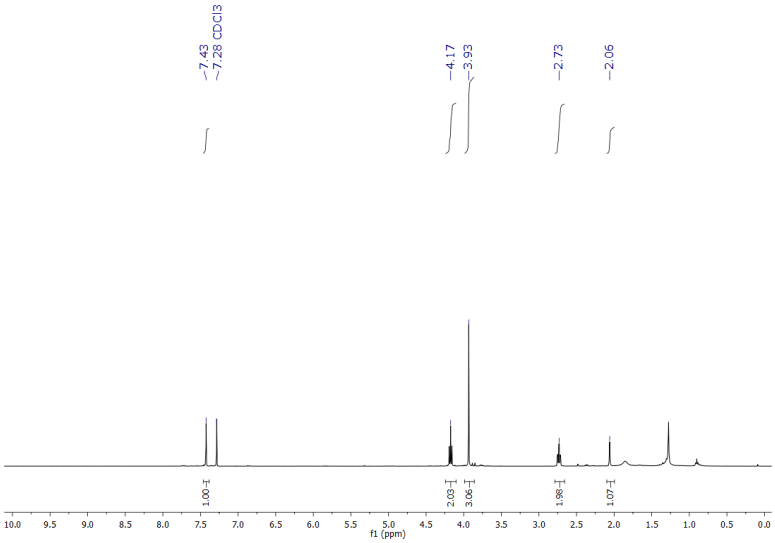

Appendix 2.3: ^{1}H-NMR spectrum of dimethyl 2,5-bis(but-3-yn-1-yloxy)terephthalate in $CDCl_3$ solvent.

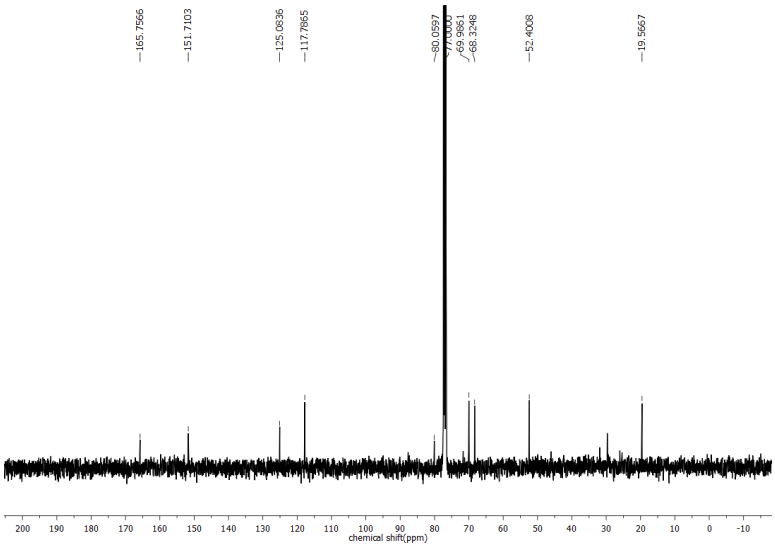

Appendix 2.4: ^{13}C-NMR spectrum of dimethyl 2,5-bis(but-3-yn-1-yloxy)terephthalate in $CDCl_3$ solvent.

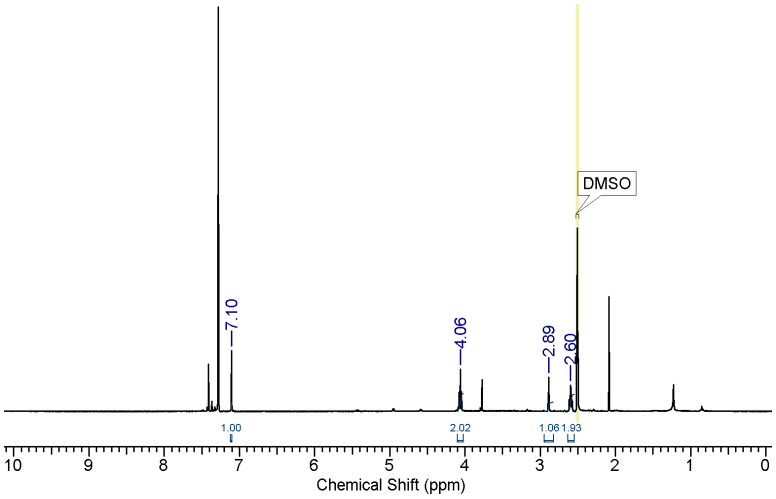

Appendix 2.5: ^{1}H-NMR spectrum of ligand (L1) in $(CD_3)_2SO$ solvent.

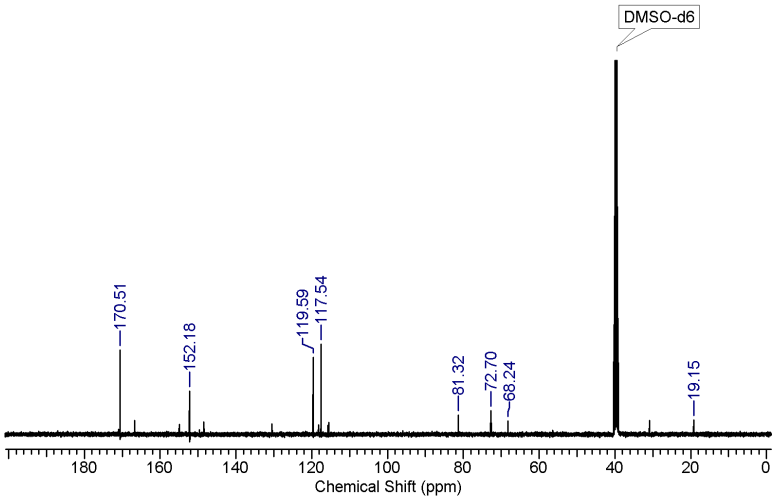

Appendix 2.6: ^{13}C-NMR spectrum of ligand (L1) in $(CD_3)_2SO$ solvent.

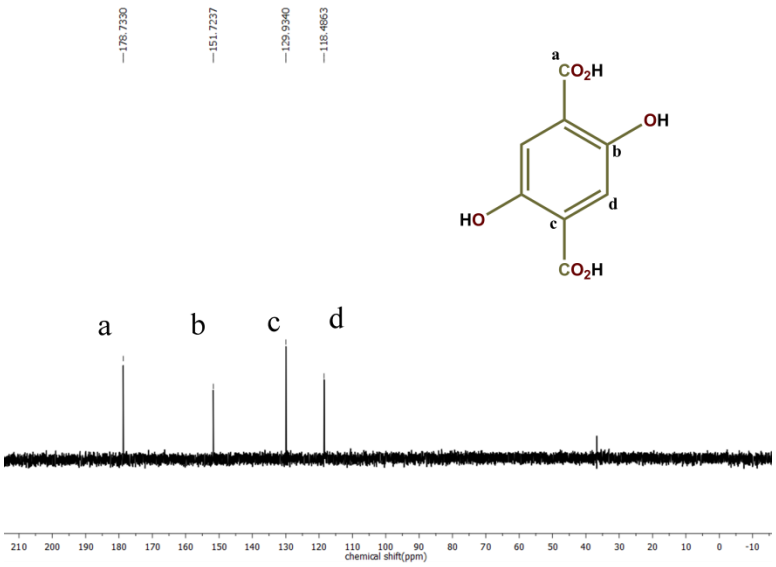

Appendix 2.7: ^{13}C-NMR spectrum of UiO-66@Butyne after Hg(II) ion treatment in D_2O as solvent.

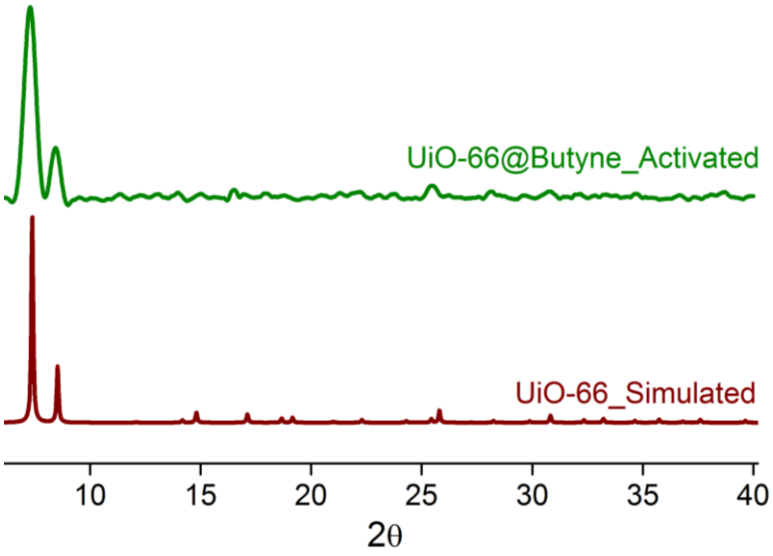

Appendix 2.8: Powder X-ray diffraction patterns of simulated UiO-66 (wine red) and activated phase of UiO-66@Butyne (green).

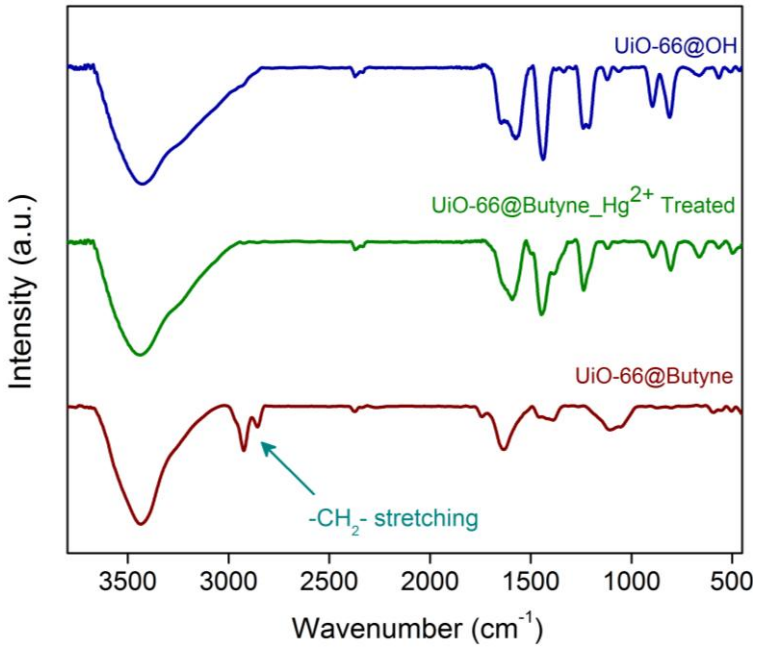

Appendix 2.9: IR spectra of UiO-66@Butyne (wine red), UiO-66@Butyne after Hg^{2+} treatment (green) and UiO-66@OH (Blue).

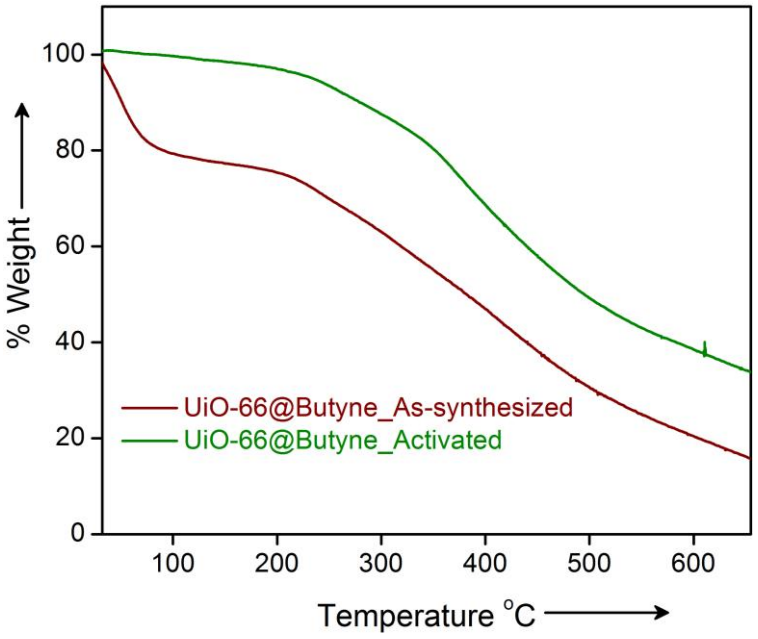

Appendix 2.10: Thermo-gravimetric analysis profiles of as-synthesized UiO-66@Butyne (wine red) and desolvated UiO-66@Butyne (green).

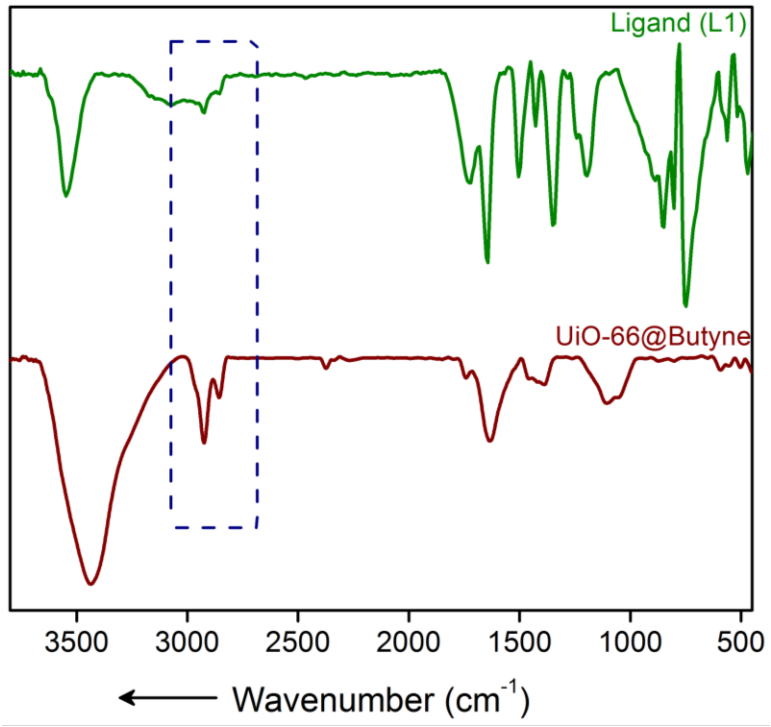

Appendix 2.11: IR spectra of UiO-66@Butyne (wine red) and ligand (green).

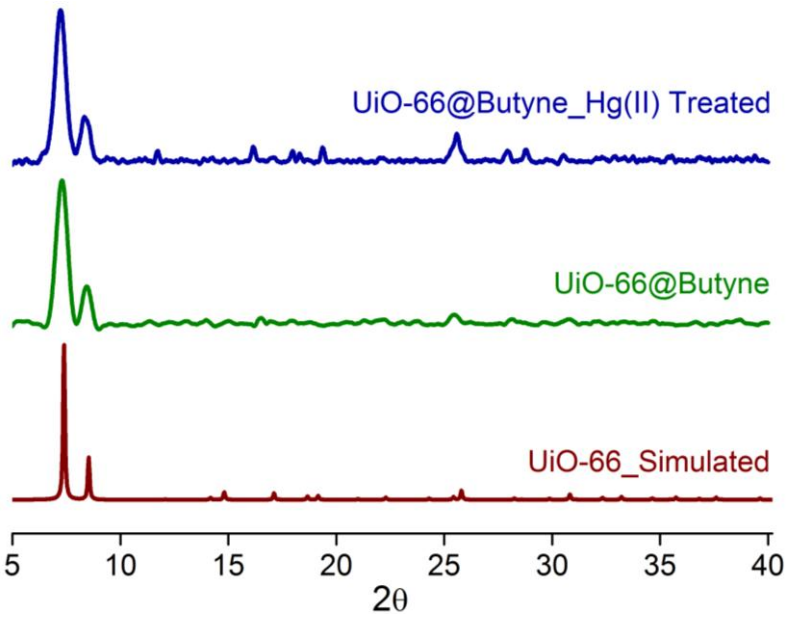

Appendix 2.12: Powder X-ray diffraction patterns of simulated UiO-66 (wine red), UiO-66@Butyne (green) and Hg(II) treated UiO-66@Butyne in aqueous medium (blue).

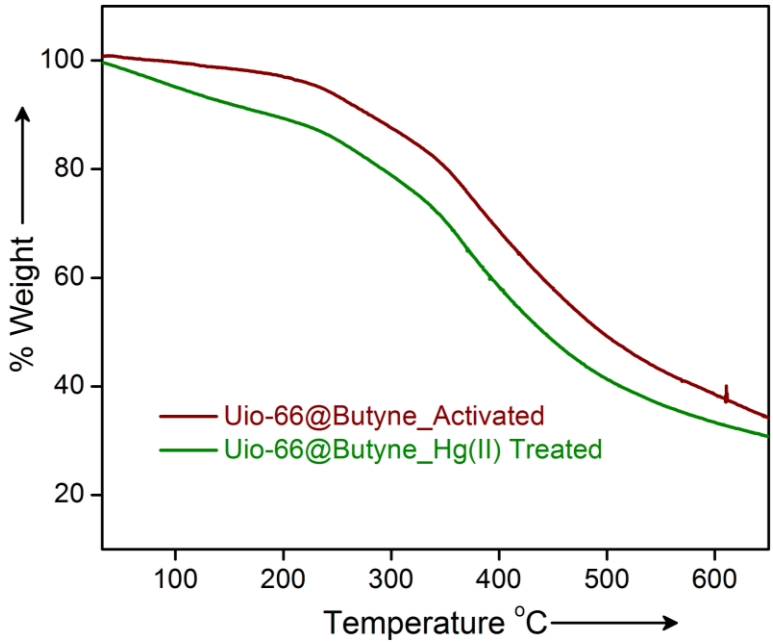

Appendix 2.13: Thermo-gravimetric analysis profiles of desolvated phase of UiO-66@Butyne and Hg(II) ion treated phase of UiO-66@Butyne.

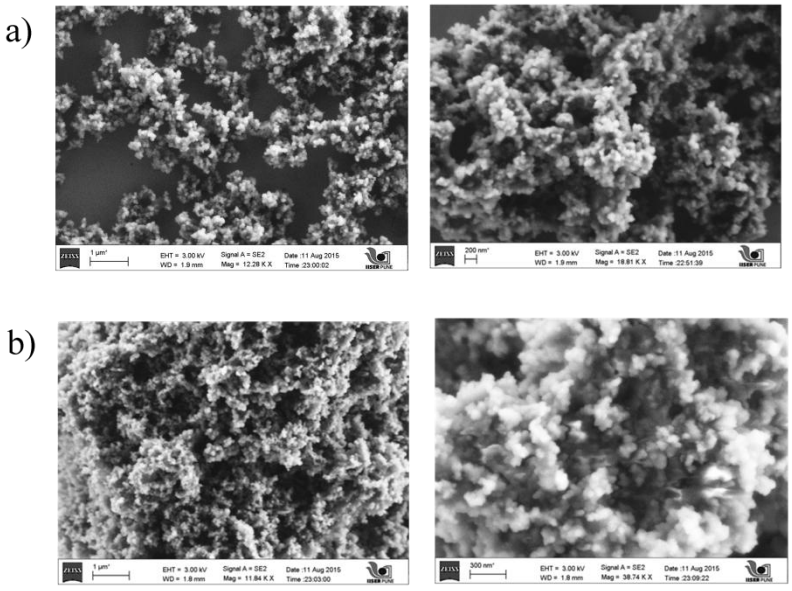

Appendix 2.14: SEM images of a) UiO-66@Butyne and b) UiO-66@Butyne after Hg(II) treatment.

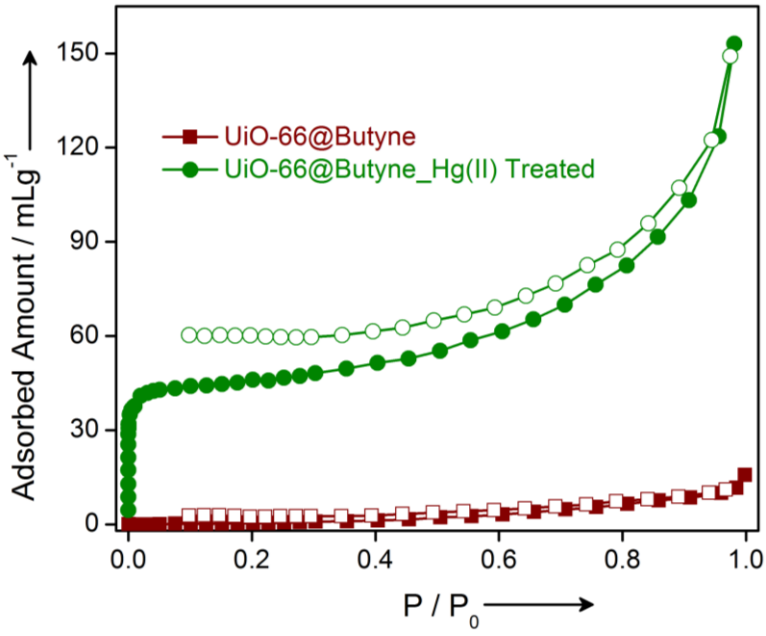

Appendix 2.15: N_2 adsorption (at 77 K) profiles of UiO-66@Butyne (wine red) and UiO-66@Butyne after Hg(II) treatment (green).

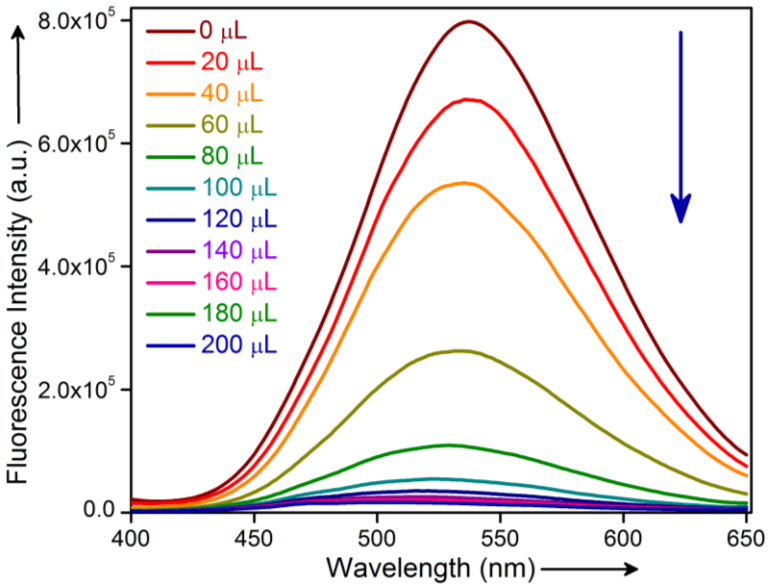

Appendix 2.16: Emission spectra of UiO-66@Butyne at 537 nm dispersed in water medium on incremental addition of Hg^{2+} solution.

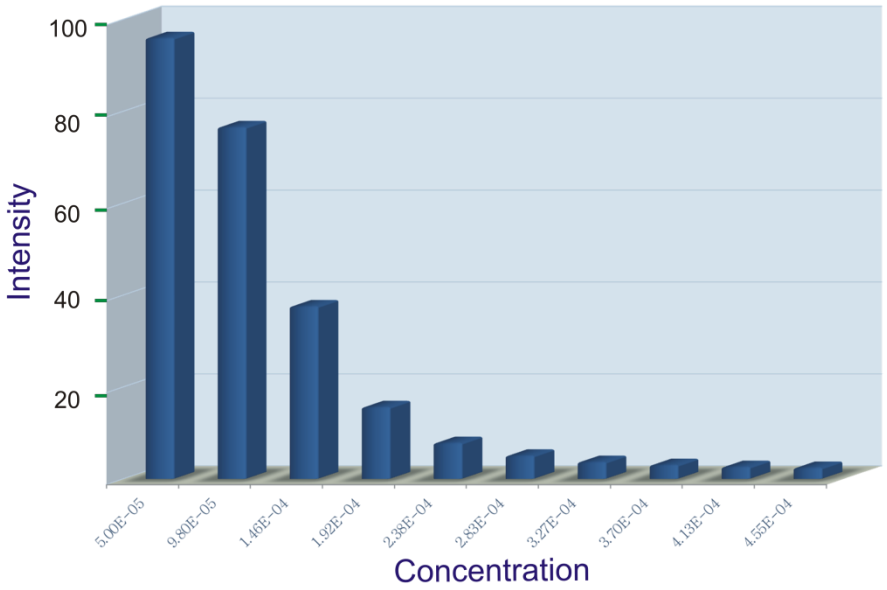

Appendix 2.17: Change in the fluorescence intensity of UiO-66@Butyne in water medium with increasing concentration of the Hg^{2+} at 537 nm.

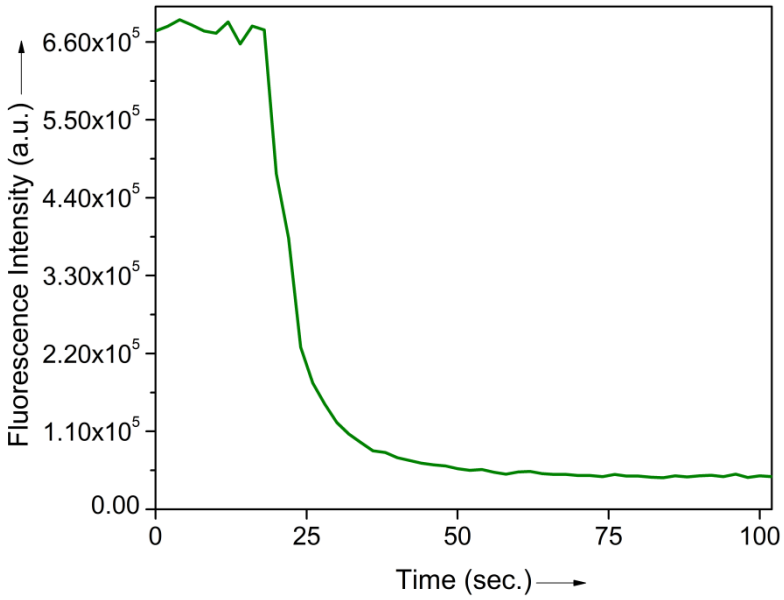

Appendix 2.18: Kinetic of UiO-66@Butyne with aqueous solution of Hg^{2+} at 537 nm.

Detection Limit Calculation:

For calculating detection limit, Hg^{2+} (20 – 200 µL, 0.005 mM stock solution) was added to probe (desolvated UiO-66@Butyne) (1mg, in 2 mL water) and fluorescent intensity was recorded. By plotting fluorescence intensity with increasing concentration of Hg^{2+}, slope (m) of graph was found to be 4.14 x 10^9 (R^2= 0.97506). Standard deviation (σ) was calculated from five blank measurements of probe. Detection limit is calculated according to the formula:

$$\text{Detection limit: } (3\sigma/m)$$

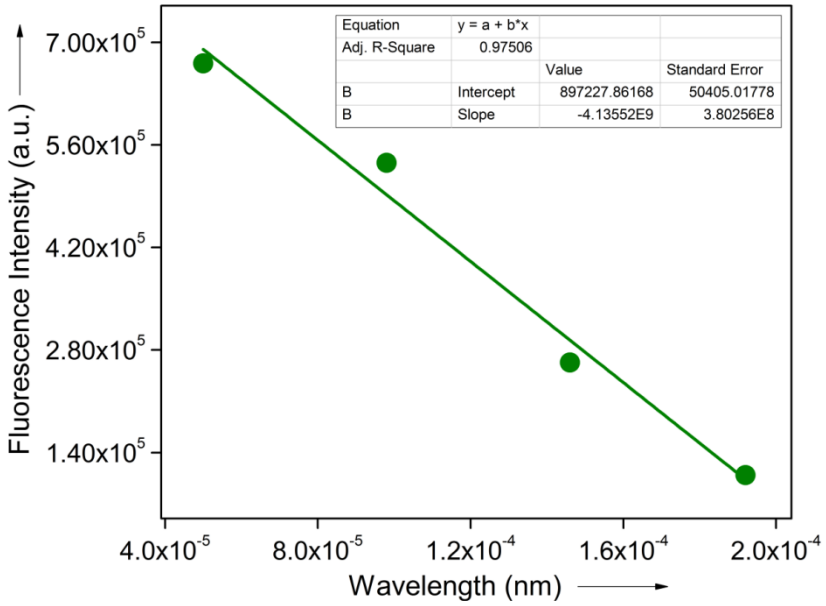

Appendix 2.19: Linear region of fluorescence intensity of probe upon addition of Hg^{2+} (20 – 200 µL, 0.005 mM stock solution) at λ_{em} = 537 nm (upon λ_{ex} = 340 nm) (R^2= 0.97506).

Calculation of standard deviation:

Appendix Table 1: Standard deviation for probe

Blank Readings (only probe)	**FL Intensity**
Reading 1	3.50E+05
Reading 2	3.53E+05
Reading 3	3.65E+05
Reading 4	3.28E+05
Reading 5	3.64E+05
Standard Deviation (σ)	15065.70729

Calculation of Detection Limit:

Appendix Table 2: Detection limit calculation for probe

Slope from Graph (m)	4.14E+09	mM^{-1}
Detection limit ($3\sigma/m$)	1.09E-05 i.e., 10.9	mM nM

LOD of UiO-66@Butyne: 2.18 ppb

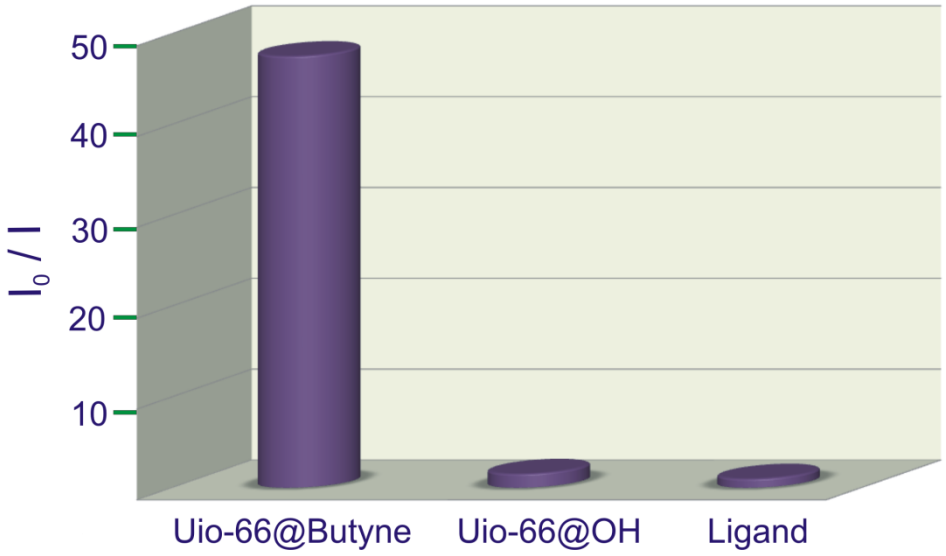

Appendix 2.20: Change in the fluorescence intensity of UiO-66@Butyne, UiO-66@OH and ligand with increasing concentration of the Hg^{2+} at 537 nm.

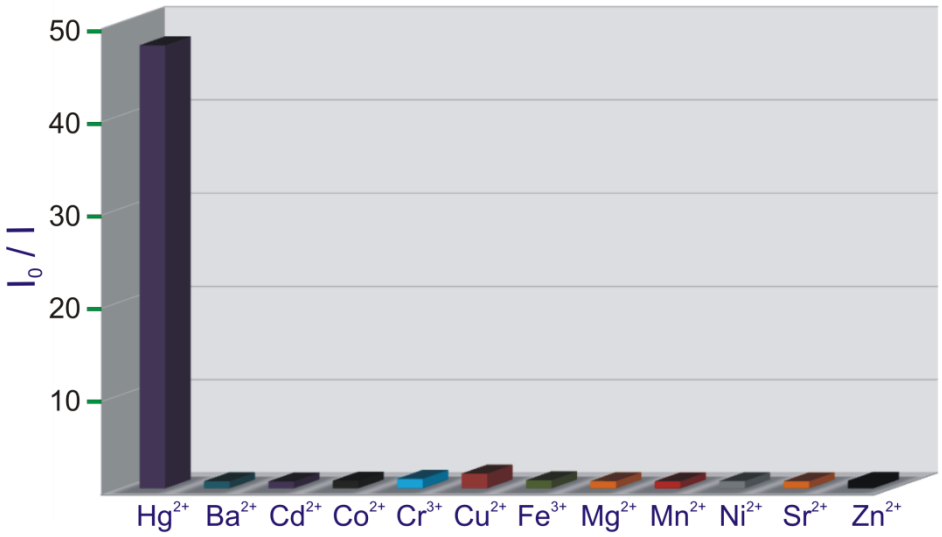

Appendix 2.21: Quenching efficiency of UiO-66@Butyne at 537 nm in presence of Hg^{2+} and other metal ions (Ba^{2+}, Cd^{2+}, Co^{2+}, Cr^{3+}, Cu^{2+}, Fe^{3+}, Mg^{2+}, Mn^{2+}, Ni^{2+}, Sr^{2+} and Zn^{2+}) in water medium.

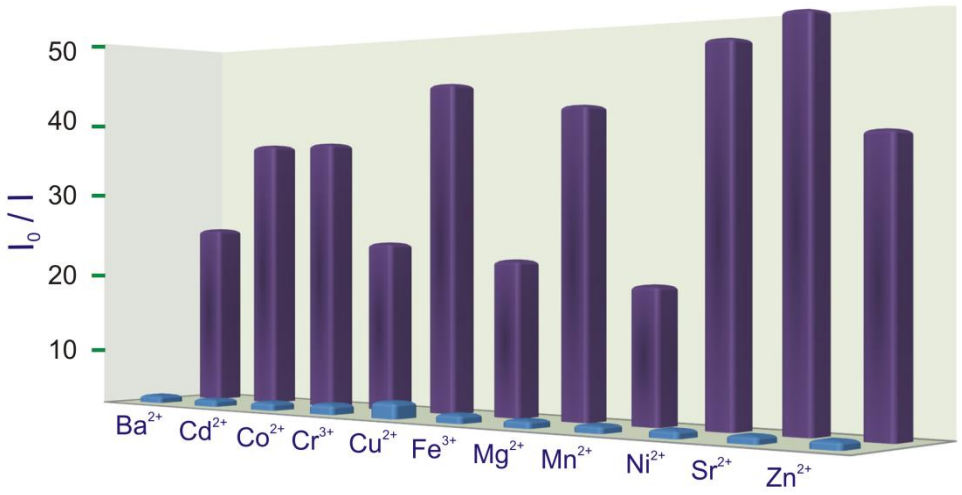

Appendix 2.22: Quenching efficiency of UiO-66@Butyne at 537 nm with Hg^{2+} in presence of other metal ions (Ba^{2+}, Cd^{2+}, Co^{2+}, Cr^{3+}, Cu^{2+}, Fe^{3+}, Mg^{2+}, Mn^{2+}, Ni^{2+}, Sr^{2+} and Zn^{2+}) in water medium.

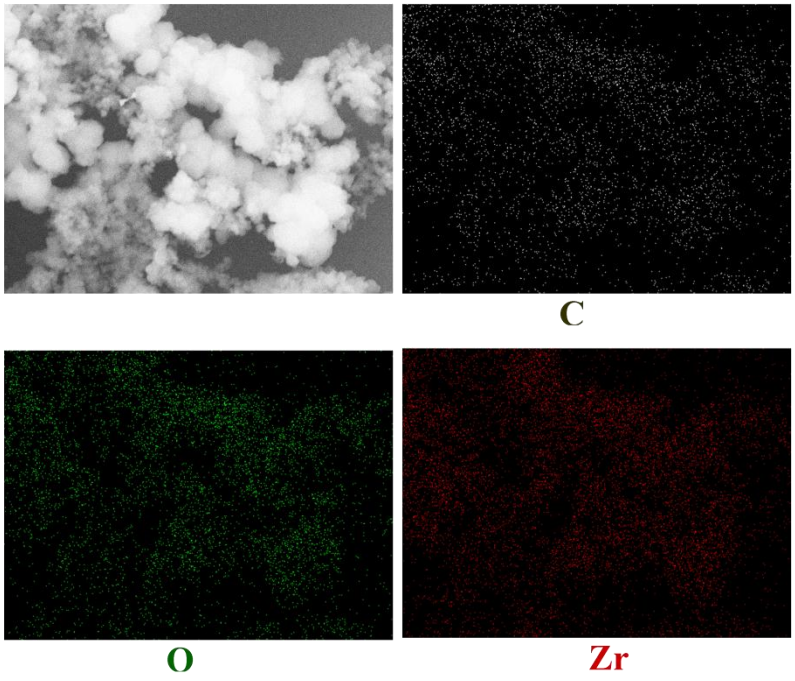

Appendix 2.23: Elemental mapping of UiO-66@Butyne (reveals the presence of carbon, oxygen and zirconium).

Element	Weight %
C	40.30
O	39.48
Zr	20.22
Total	100

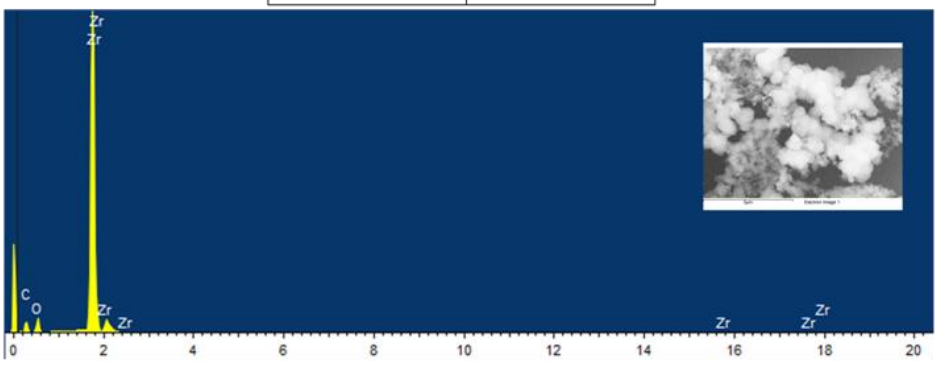

Appendix 2.24: EDX analysis of UiO-66@Butyne.

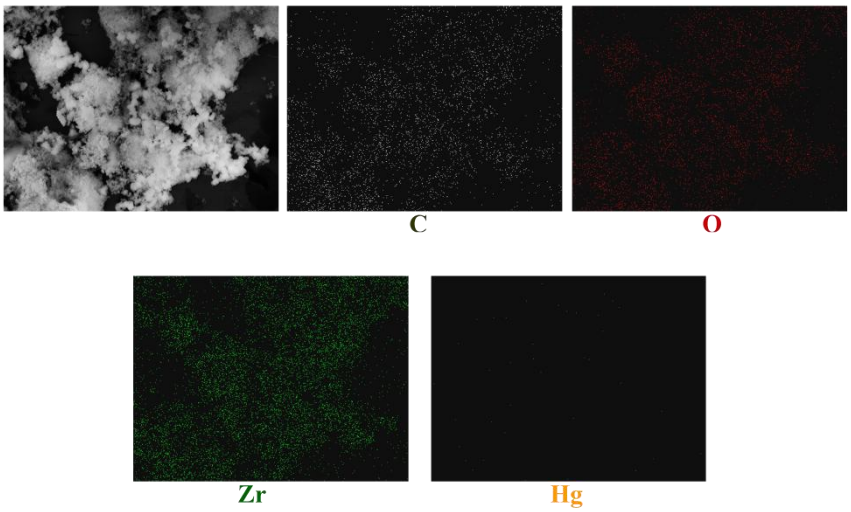

Appendix 2.25: Elemental mapping of UiO-66@Butyne after Hg(II) treatment in water (reveals the presence of carbon, oxygen, zirconium and absence of mercury).

Element	Weight %
C	42.01
O	38.13
Zr	19.86
Total	100

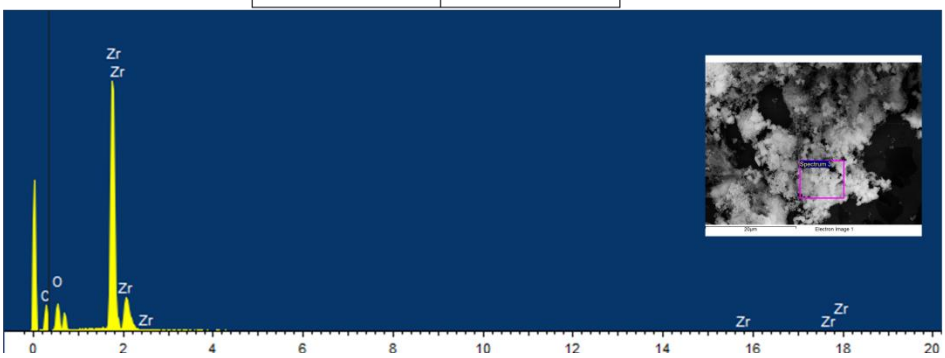

Appendix 2.26: EDX analysis of UiO-66@Butyne after Hg(II) treatment in water.

2.6 References

1. (a) G. Aragay, J. Pons and A. Merkoçi, *Chem. Rev.*, 2011, **111**, 3433-3458. (b) M. Li, H. Gou, I. Al-Ogaidi and N. Wu, *ACS Sustainable Chem. Eng.*, 2013, **1**, 713-723.

2. (a) ATSDR, Toxicological Profile for Mercury, U.S. Department of Health and Human Services, *Atlanta, GA*, 1999, 1-696. (b) Fluorescent Chemosensors for Ion and Molecule Recognition; A. W. Czarnik, Ed.; *American Chemical Society: Washington*, DC, 1992.

3. Regulatory Impact Analysis of the Clean Air Mercury Rule: EPA- 452/R-05-003; U.S. Environmental Protection Agency: Research Triangle Park, NC, 2005.

4. (a) X. Chen, C. Han, H. Cheng, Y. Wang, J. Liu, Z. Xu and L. Hu, *J. Chromatogr. A*, 2013, **1314**, 86-93. (b) A. Bernaus, X. Gaona, J. M. Esbri, P. Higueras, G. Falkenberg and M. Valiente, *Environ. Sci. Technol.*, 2006, **40,** 4090-4095. (c) N. Kanayama, T. Takarada and M. Maeda, *Chem. Commun.*, 2011, **47**, 2077-2079. (d) M. -Y. Chae and A. W. Czarnik, *J. Am. Chem. Soc.*, 1992, **114**, 9704-9705.

5. (a) A. Gupta, A. Chaudhary, P. Mehta, C. Dwivedi, S. Khan, N. C. Verma and C. K Nandi, *Chem. Commun.*, 2015, **51**, 10750-10753. (b) S. Ando and K. Koide, *J. Am. Chem. Soc.*, 2011, **133**, 2556–2566. (c) S. Venkateswarlu and M. Yoon, *Dalton Trans.*, 2015, **44**, 18427–18437.

6. (a) H. N. Kim, W. X. Ren, J. S. Kim and J. Yoon, *Chem. Soc. Rev.*, 2012, **41**, 3210-3244. (b) E.M. Nolan and S. J. Lippard, *Chem. Rev.*, 2008, **108**, 3443-3480. (c) E. M. Nolan and S. J. Lippard, *J. Am. Chem. Soc.*, 2007, **129**, 5910-5918.

7. (a) M. O'Keeffe and O. M. Yaghi, *Chem. Rev.*, 2012, **112**, 675-702. (b) A. Schneemann, V. Bon, I. Schwedler, I. Senkovska, S. Kaskel and R. A. Fischer, *Chem. Soc. Rev.*, 2014, **43**, 6062-6096. (c) C. R. Kim, T. Uemura and S. Kitagawa, *Chem. Soc. Rev.*, 2016, **45**, 3828-3845. (d) G. Peng, L. Ma, J. Cai, L. Liang, H. Deng and G. E. Kostakis, *Cryst. Growth Des.*, 2011, **11**, 2485–2492. (e) M. Sindoro, N. Yanai, A. -Y. Jee and S. Granick, *Acc. Chem. Res.*, 2014, **47**, 459-469.

8. (a) C. He, D. Liu and W. Lin, *Chem. Rev.*, 2015, **115**, 11079-11108. (b) S. T. Meek, J. A. Greathouse and M. D. Allendorf, *Adv. Mater.*, 2011, **23**, 249-267. (c) P. Horcajada, R. Gref, T. Baati, P. K. Allan, G. Maurin, P. Couvreur, G. Férey, R. E. Morrisa and C. Serre, *Chem. Rev.*, 2012, **112**, 1232-1268. (d) Y. Cui, Y. Yue, G. Qian and B. Chen, *Chem. Rev.*, 2012, **112**, 1126-1162. (e) S. Sen, N. N. Nair, T. Yamada, H. Kitagawa and P. K. Bharadwaj, *J. Am. Chem. Soc.*, 2012, **134**, 19432-19437. (f) Z. Hu, B. J. Deibert and J. Li, *Chem. Soc. Rev.*, 2014, **43**, 5815-5840; (g) J. Aguilera-Sigalat and D. Bradshaw, *Coord. Chem. Rev.*, 2016, **307**, 267-291. (h) H. Yang, S. J. Bradley, A. Chan, G. I. N. Waterhouse, T. Nann, P. E. Kruger and S. G. Telfer, *J. Am. Chem. Soc.*, 2016, **138**, 11872-11881. (i) K. -K. Yee, N. Reimer, J. Liu, S. -Y. Cheng, S. -M. Yiu, J. Weber, N. Stock and Z. Xu, *J. Am. Chem. Soc.*, 2013, **135**, 7795−7798. (j) Y. Zheng, H. Sato, P. Wu, H. J. Jeon, R. Matsuda and S. Kitagawa, *Nat. Commun.*, 2017**, 8**, DOI: 10.1038/s41467-017-00122-5.

9. (a) Y. -M. Zhu, C. -H. Zeng, T. -S. Chu, H. -M. Wang, Y. -Y. Yang, Y. -X. Tong, C. -Y. Su, W. -T. Wong, *J. Mater. Chem. A*, 2013, **1**, 11312-11319. (b) L. -L. Wu, Z. Wang, S. -N. Zhao, X. Meng, X. -Z. Song, J. Feng, S. -Y. Song, H. -J. Zhang, *Chem. Eur. J.*, 2016, **22**, 477-480. (c) P. Wu, Y. Liu, Y. Liu, J. Wang, Y. Li, W. Liu and J. Wang, *Inorg. Chem.*, 2015, **54**, 11046-11048. (d) H. -M. Wang, Y. -Y. Yang, C. -H. Zeng, T. -S. Chu, Y. -M. Zhu and S. W. Ng, *Photochem. Photobiol. Sci.*, 2013, **12**, 1700-1706. (e) L. Wen, X. Zheng, K. Lv, C. Wang and X. Xu, *Inorg. Chem.*, 2015, **54**, 7133-7135. (f) N. D. Rudd, H. Wang, E. M. A. Fuentes-Fernandez, S. J. Teat, F. Chen, G. S. Hall, Y. J. Chabal, J. Li, *ACS Appl. Mater. Interfaces*, 2016, **8**, 30294–30303. (g) A. Shahat, S. A. Elsalam, J. M. Herrero-Martínez, E.

F. Simó-Alfonso and G. Ramis-Ramos, *Sensors and Actuators B: Chemical,* 2017, **253**, 164-172. (h) S. A. A. Razavi, M. Y. Masoomi and A. Morsali, *Inorg. Chem.*, 2017, **56**, 9646−9652. (i) T. Liu, J. -X. Che, Y. -Z. Hu, X. -W. Dong, X. -Y. Liu and C. -M. Che, *Chem. Eur. J.*, 2014, **20**, 14090 – 14095.

10. (a) M. Dong, Y. -W. Wang and Y. Peng, *Org. Lett.*, 2010**, 12**, 5310-5313. (b) F. Song, S. Watanabe, P. E. Floreancig and K. Koide, *J. Am. Chem. Soc.*, 2008, **130**, 16460-16461.

11. M. E. Jun, B. Roy and K. H. Ahn, *Chem. Commun.*, 2011, **47**, 7583-7601.

12. M. Santra, D. Ryu, A. Chatterjee, S. -K. Ko, I. Shin and K. H. Ahn, *Chem. Commun.*, 2009, 2115-2117.

13. J. H. Cavka, S. Jakobsen, U. Olsbye, N. Guillou, C. Lamberti, S. Bordiga, K. P. Lillerud, *J. Am. Chem. Soc.*, 2008, **130**, 13850-13851.

14. S. J. Garibay and S. M. Cohen, *Chem. Commun.*, 2010, **46**, 7700-7702.

15. Y. Sun, Q. Sun, H. Huang, B. Aguila, Z. Niu, J. A. Perman and S. Ma, *J. Mater. Chem. A*, 2017, **5**, 18770–18776.

16. A. V. Desai, P. Samanta, B. Manna and S. K. Ghosh, *Chem. Commun.*, 2015, **51**, 6111-6114.

17. J. Yang, Z. Wang, Y. Li, Q. Zhuang, W. Zhao and J. Gu, *RSC Adv.*, 2016, **6**, 69807-69814.

18. P. Mahato, S. Saha, P. Das, H. Agarwalla and A. Das, *RSC Adv.*, 2014, **4**, 36140-36174.

Chapter 3

Chemically Stable Porous Organic Material: An Efficient Selective Cationic Dye Scavenger from Aqueous Medium

3.1 Introduction

Last decade has witnessed the evolution of microporous organic polymers (MOPs) in the domain of material chemistry. High surface area, tuneable porosity and high physiochemical stability of such materials has grown paramount interest among the researchers.[1] Wide range of microporous organic materials have been explored in recent times, such as covalent organic frameworks (COFs), porous organic frameworks (POFs), porous aromatic frameworks (PAFs), covalent triazine frameworks (CTFs), porous organic polymer (POPs), porous polymer networks (PPNs) etc.[2] Hyper-cross-linked polymers (HCPs) have emerged as relatively new subclass in the field of MOPs.[3] Single step Friedel-Crafts reaction provides key tool to build the network of aromatic molecules via extensive hyper-cross-linked polymerization in presence of anhydrous $FeCl_3$ and formaldehyde dimethyl acetal (FDA) as external cross-linking agents.[4] In such cases small organic aromatic building units have been connected and held together by methylene (-CH_2-) groups.Such extensive cross-linking among several organic building blocks results into permanent porosity and high stability of such materials. In addition to the simple one-step easy synthesis of HCPs and high physiochemical stability, tunable porosity by varying the organic unit and low cost synthesis have attracted huge attention of researchers.[5] It is noteworthy to mention, HCPs are the much less-explored class of materials in the regime of microporous organic materials. Till date, microporous HCPs have often been used for deriving carbon capture and catalysis applications; but to the best of our knowledge, pollutant removal from aqueous medium has not been investigated yet.[6]

Dye molecules are widely used in many industries including pharmaceuticals, paper, printing, ceramics, paints, textile, cosmetics, plastics etc. Removal of such pollutant dye molecules from colored wastewater has emerged as a big challenge to the researchers, as a consequence of heavy usage of dyes in the growing industries. It has been found that there are over 1,00,000 dyes available in the market with a production rate over 7 x 10^5 tons per year; among which 2% dyes are released into different water bodies.[7] Water pollution because of dye molecules hinders growth of bacteria which are responsible for degradation of water impurities and also affects photosynthesis of aquatic plants.[8] Apart from this, few dyes can result into aesthetic problem as well as chronic effects on exposure to organisms.[9] Furthermore, organic dye molecules are very much chemically stable (even stable to oxidation and light); so chances of biodegradation for such water pollutants are very less.[10] Several techniques based on physical, chemical and biological methods have been introduced to remove dye pollutants from wastewater. Among them adsorption based dye removal has attracted much attention, because it can produce high quality water, function at ambient temperature, cost-effective and feasible to remove multiple dyes simultaneously.[11] Although several adsorbents have been reported in literature for dye molecules removal; but materials with high capacity and separation by virtue of both size and ionic selectivity is still a challenge to be

addressed. With advantages like tunable porosity and separation based on ionic selectivity, metal-organic frameworks (MOFs) have set up a new avenue in the domain of pollutant removal like dye molecules from wastewater.[12] Ionic framework of MOFs imparts the selectivity in adsorption based on charge over respective dye molecules in addition to size factor. Despite of the impactful contribution of MOFs in the field of pollutant trapping, they have few drawbacks like poor water stability because of weaker coordination bonds and difficulties with bulk scale synthesis.[13]

To overcome aforementioned problems, researchers have come up with replacement of coordination bonds with stronger covalent bonds in the form of porous covalent organic materials. Porous organic frameworks based pollutant trapping from wastewater is in very early stage. Especially, dye molecules capture from colored wastewater based on such material is very rare and to the best of our knowledge cationic dye capture is not yet reported in this domain.[14] In this report, we have strategically synthesized alkoxide based microporous HCP through base (aqueous NaOH) treatment of free –OH groups to get free cations inside the network. Thus obtained exchangable cations can easily be replaced by cationic dye molecules in water medium. Based on this concept, we have performed adsorption of cationic dyes, viz., methylene blue (MB), crystal violet (CV) and rhodamine B (RB) from water solution (Scheme 3.1).

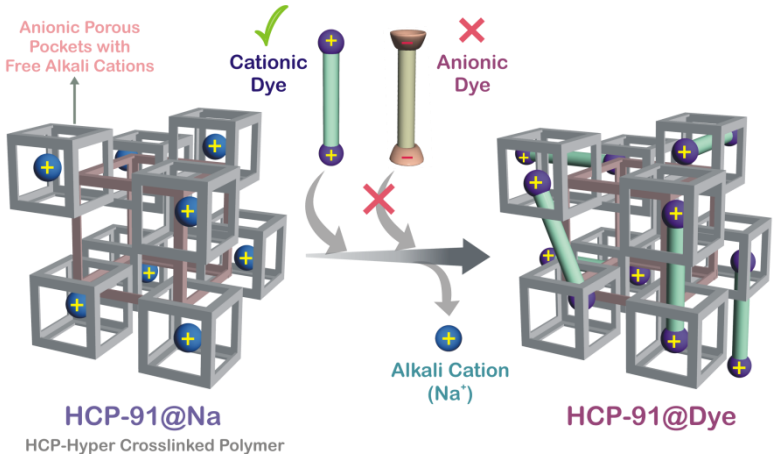

Scheme 3.1: Schematic representation of selective cationic dye capture in hyper-cross-linked polymer (HCP).

3.2 Experimental

3.2.1 Materials:

4-phenylphenol, $FeCl_3$, formaldehyde dimethyl acetal (FDA), methylene blue, crystal violet and rhodamine B were purchased from Sigma-Aldrich. Methyl orange andremaining solvents were obtained locally. These chemicals were used without further purification.

3.2.2 Physical measurements

All Infra-red Spectra were acquired by using NICOLET 6700 FT-IR spectrophotometer using KBr pellet in 400-4000 cm^{-1} range. Gas adsorption measurements were studied using BelSorp-max instrument from Bel Japan. FE-SEM was done by using FEI Quanta 3D dual beam ESEM at 30KV. UV-Visible spectra were recorded on Shimadzu UV 2600 Spectrophotometer. Powder X-ray diffraction data was recorded at room temperature with a Bruker D8 Advance diffractometer by using $Cu_{K\alpha}$ radiation (λ = 1.5406 Å). Solid-state ^{13}C CP-MAS NMR spectra was recorded with a Bruker Advance-III Ultrashield500WB spectrometer (probe: MAS BB 4MM, spinning rate: 5KHz).

3.2.3 Synthesis:

Synthesis of HCP-91: The HCP-91 has been synthesized from cross-coupling of 4-phenylphenol (Scheme 3.2) by following our previous report.[5b] To a round bottom flask 4-phenylphenol (300 mg, 1.7625 mmol) has been taken and to that 20 ml of dichloroethane ($C_2H_4Cl_2$) was added. Then to the reaction mixture formaldehyde dimethyl acetal (470 µl, 5.288 mmol) and $FeCl_3$ (860 mg, 5.288 mmol) were added respectively. The reaction mixture was heated at 50 °C for 5 hours and then was allowed to reflux at 80 °C for 20 hours (Scheme 3.2). On completion of the reaction brown colored precipitate was filtered off and washed with DMF, methanol, water, chloroform, dichloromethane and tetrahydrofuran (THF) repeatedly. Thus obtained brown colored solid material was then kept in 1:1 $CHCl_3$-THF mixture (25 ml) for 3 days to remove the high boiling solvents from the porous network of HCP-91. Then the solvent exchanged phase of HCP-91 was heated at 100 ^oC under vacuum to obtain the guest free activated material and with this phase further works have been carried out. Yield: 335 mg

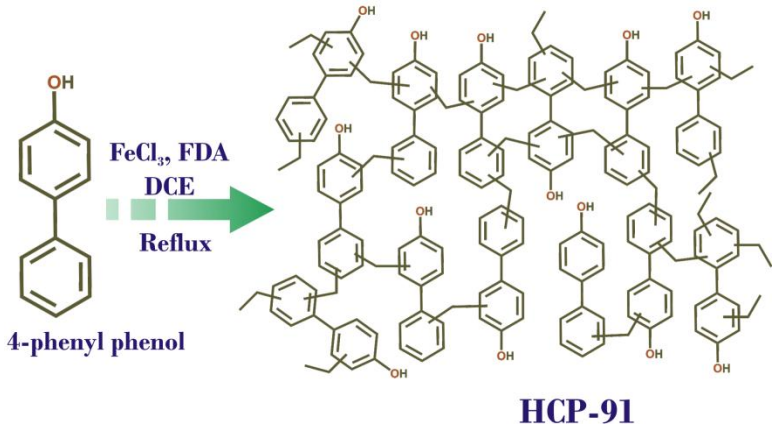

Scheme 3.2: Synthesis of HCP-91 from 4-phenylphenol.

Synthesis of HCP-91@Na: Desolvated HCP-91 (100 mg) was taken in a conical flask and to that 10 ml of distilled water has been added. Then to the reaction mixture NaOH (40 mg, 1 mmol) was added and allowed stir overnight at room temperature (Scheme 3.3). On completion of the kept in MeOH (25 ml) for 3 days and MeOH was changed two times in a day to remove the high boiling solvents from the porous network of HCP-91@Na. Then the solvent exchanged phase of HCP-91@Na was heated at 100 ^{o}C under vacuum to obtain the guest free activated material and with this phase further works have been carried out. Yield: 115 mg

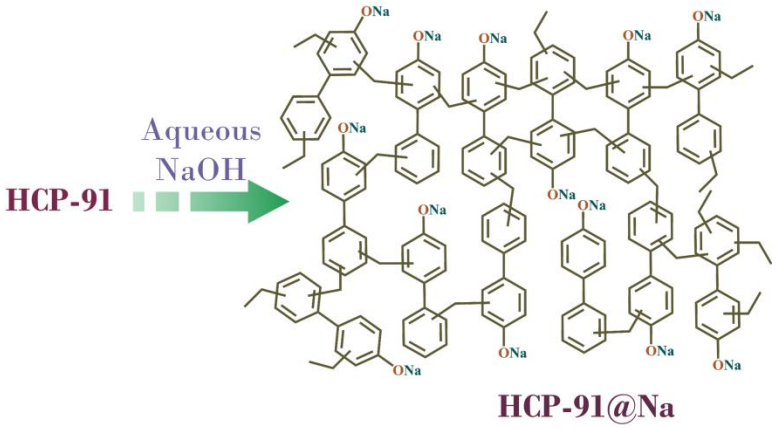

Scheme 3.3: Synthesis of HCP-91@Na from HCP-91 via post-synthetic modification.

3.2.3 Ion-exchange Studies

Dye capture study: Dye capture experiments were performed with 0.02 mM aqueous solutions of respective dye molecules. In a typical experiment, first UV-Visible spectrum was recorded of 2 mL of 0.02 mM dye solution and then to the solution 1 mg of HCP-91@Na was added. Thus UV-Vis spectra of the supernatant solution of each dyes were recorded with certain time intervals.

Kinetics study: From the titration plot of the respective dyes, capacity for HCP-91@Na for the corresponding dyes were plotted with time. Further, best fit model for all the dyes were found to be pseudo second order kinetics. The equation for the pseudo second order model as follows,

$$Q_t = \frac{k_2 Q_e^{\,2} t}{1 + k_2 Q_e t}$$

where, t is the time in minute, Q_t and Q_e are the amount of adsorbate (mg gm^{-1}) onto adsorbent at the different time intervals and equilibrium respectively.

3.3 Results and discussion

Herein, we report highly efficient cationic dye adsorbent HCP-91@Na, synthesized from –OH groups containing HCP-91 via reaction with aqueous NaOH. HCP-91 has been synthesized by following our previous report through C-C cross coupling reaction (Friedel-Crafts reaction) of 4-phenylphenol in presence of $FeCl_3$ and FDA (Scheme 3.2).[5b] Thus synthesized HCP-91 was poured into $CHCl_3$-THF mixture to remove high boiling solvent molecules and later desolvated under vacuum at 100 ^oC. Desolvated HCP-91 was treated with NaOH in water medium to convert hydroxyl groups to $–O^-Na^+$ (HCP-91@Na). In a similar way, solvent exchange of HCP-91@Na has been carried out in methanol and later desolvation was carried out. Both HCP-91 and HCP-91@Na have been characterized with infra-red (IR) spectroscopy, thermo-gravimetric analysis (TGA), low temperature N_2 adsorption and field emission scanning electron microscope (FE-SEM).

In FT-IR spectroscopy peaks at 1465 cm^{-1} and 1635 cm^{-1} in case of HCP-91 and 1388 cm^{-1} and 1639 cm^{-1} for HCP-91@Na corresponding to the C=C double bond stretching frequencies respectively are observed (Appendix 3.1). TGA profiles of desolvated phases of both compounds revealed that negligible loss upto ~350 ^oC and after that sharp decay were observed (Appendix 3.3). As a consequence of incorporation sodium cation pore size of HCP-91@Na decreased as compare to HCP-91 and that is clearly reflected in the N_2 adsorption isotherm at 77 K (Appendix 3.4 and 3.5). From Horvath–Kawazoe plot pore size distribution was found to be 0.46 nm for HCP-91@Na (Appendix 3.6). Solid state ^{13}C-NMR revealed the presence of aromatic building block used, i.e., 4-phenylphenol, along with bridging $-CH_2-$ linkage (Appendix 3.7). FE-SEM images confirmed retention of agglomerated morphology of HCP-91 in HCP-

91@Na too (Appendix 3.8). EDAX analysis of HCP-91@Na confirmed the presence of sodium ion (Appendix 3.9). To check the reversibility between HCP-91 and HCP-91@Na, we have treated HCP-91@Na with 1M HCl to get back HCP-91. Thus obtained material was characterized with FT-IR spectroscopy, FE-SEM and N_2 adsorption at 77 K. FT-IR spectra of HCP-91 and HCl treated HCP-91@Na matched properly, whereas morphology was found to be similar from FE-SEM in both cases (Appendix 3.11 and 3.8). N_2 adsorption (at 77 K) substantiated the claim where we found similar adsorption of N_2 for both HCP-91 and HCl treated HCP-91@Na (Appendix 3.5).

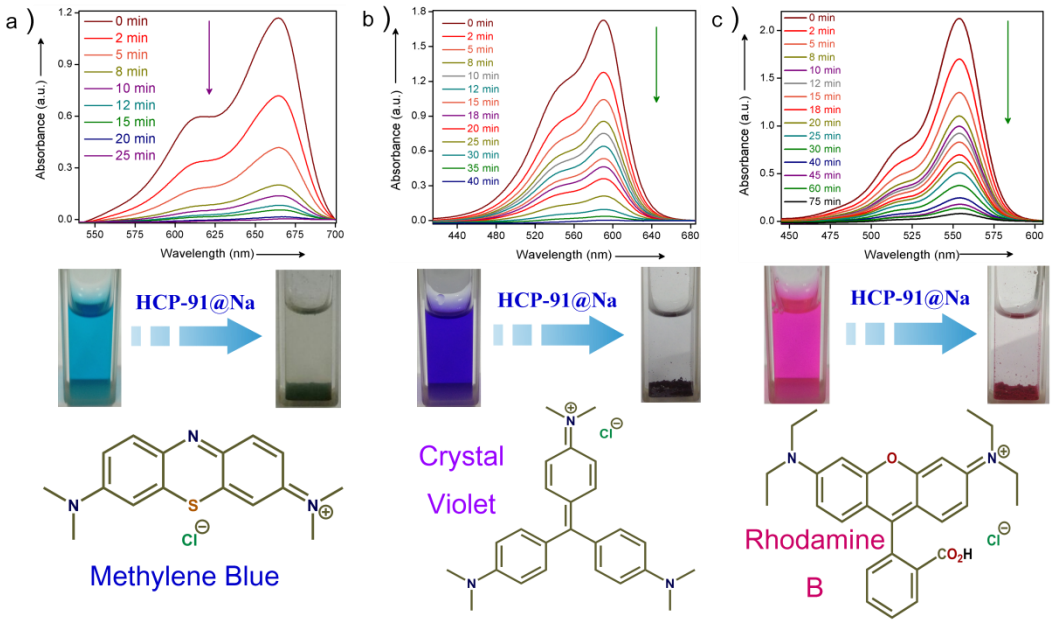

Figure 3.1: a) Adsorption profile of methylene blue at different time intervals by HCP-91@Na and corresponding decolorisation of blue solution (below), b) UV-Vis spectra of adsorption profile of crystal violet at different time intervals by HCP-91@Na and corresponding decolorisation of violet solution (below), c) UV-Vis spectra of adsorption profile of methylene blue at different time intervals by HCP-91@Na and corresponding decolorisation of pink solution (below).

To check the activity of HCP-91@Na towards the cationic dye molecules, we dispersed 1 mg of compound in 0.02 mM of methylene blue (MB). Blue colored water solution transformed to colorless solution after 20 minutes as a consequence of ion exchange. Enthused from this result, we sought to record UV-Visible spectra of dye solution at different time to monitor adsorption of methylene blue in HCP-91@Na (Appendix 3.12). To record UV-Vis data, 2 mL of 0.02 mM MB solution was taken and 1 mg of HCP-91@Na was poured into the solution. Then spectrum was recorded at different set of time to get the respective absorbance which was directly correlated to the concentration of the dye solution. As a

consequence of adsorption of dye molecules inside the network of HCP, we found continuous decrease in UV-Vis profile with time (Fig. 3.1a). From this data we found the concentration of the MB solution at different time intervals and also found percent (%) of dye uptake by HCP-91@Na with time (Appendix 3.13 and 3.14). In concentration decay profile with time, we observed sharp decrease with time which trend to almost zero concentration (~ 99.7% of dye was removed) of the respective dye solution with saturation (Appendix 3.14). As a result of methylene blue adsorption, brown colored HCP-91@Na converted to green colored material (Appendix 3.12). To validate our speculation regarding cationic dye capture, we have taken another two cationic dyes with different sizes, namely, crystal violet (CV) and rhodamine B (RB). In a similar way, we performed dye adsorption study with 1 mg of HCP-91@Na and 2 mL of 0.02 mM respective dye solutions (Appendix 3.15 and 3.16). UV-Vis spectra revealed adsorption of both cationic dyes inside the porous network of HCP-91@Na (Fig. 3.1b and 3.1c). Since, calculation of pore diameter in this case was found to be difficult, we checked the pore size distribution of HCP-91@Na from N_2 adsorption at 77K (0.46 Å as per HK plot). Due to the presence of flexible methylene (-CH_2-) linkages inside the network (swelling effect), HCP-91@Na could accommodate cationic dyes even with bigger sizes. But size restriction of HCP-91@Na affected the kinetics of dye capture when sizes of respective dyes varied. Consequently, smaller methylene blue (4.97 Å x 14.24 Å) took lesser time as compare to crystal violet (13.92 Å) and rhodamine B (15.04 Å x 8.2 Å x 6.52 Å) (Appendix 3.17 and 3.18). On the other hand, because of larger size of rhodamine B, it took much more time for the complete removal as compare to the remaining dyes (Fig. 3.2a). Further, capture of all the aforementioned dye with HCP-91@Na followed the pseudo second order kinetics (Appendix 3.19-3.21). After capture studies, all the dye encapsulated phases were characterized with solid state UV-Vis spectroscopy, FE-SEM analysis, EDX elemental mapping, CHNS analysis (Appendix 3.22-3.29). Solid state UV-Vis spectra of dye encapsulated phases revealed the presence of respective dyes entrapped inside the network of HCP-91@Na (Appendix 3.22). Further, elemental mapping and CHNS affirmed the presence of nitrogen and sulphur elements in the dye entrapped phases for corresponding dye molecules (Appendix 3.26-3.29).

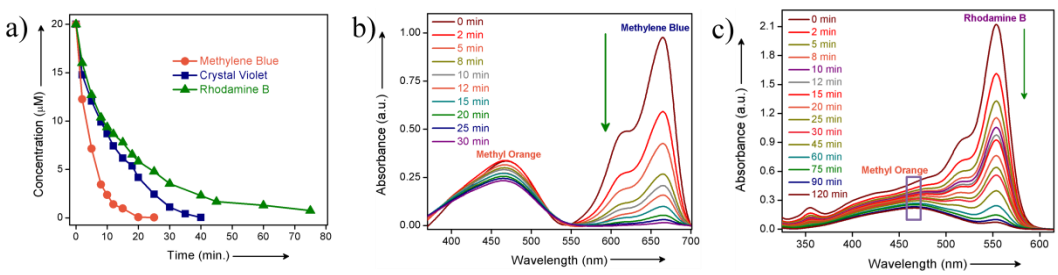

Figure 3.2: a) Decrease in concentration of cationic dyes (methylene blue, crystal violet and rhodamine B) with time, b) Time dependent adsorption study of a mixture of methylene blue and methyl orange solution with UV-Vis spectroscopy, c) Time dependent adsorption study of a mixture of rhodamine B and methyl orange solution with UV-Vis spectroscopy.

In addition to the size factor, our synthesized HCP-91@Na showed selectivity in adsorption on the basis of charge over the adsorbates. To check ionic selectivity, we performed adsorption study of a well known anionic dye, namely methyl orange (MO) with HCP-91@Na. Similar to case for cationic dyes, 2 mL of 0.02 mM aqueous solution of methyl orange poured into a cuvette having 1 mg of HCP-91@Na and with different time intervals UV-Vis spectra were recorded. We found negligible change in the UV-Vis spectra of MO solution in comparison to the huge change in case of cationic dyes solutions (Appendix 3.30). This data affirmed our speculation over selectivity of HCP-91@Na based on the ionic charge of dye molecules. Furthermore, selective dye trapping from a mixture of solution of cationic and anionic dyes is much more challenging and important as an ion-adsorbent. We sought to perform such experiment with our material to check the efficiency of charge selective dye capture from a mixture of dyes. In a typical experiment, we have taken 1:1 mixture of 0.02 mM of methylene blue and methyl orange dye solution. To the mixture of dye solution we have added 1 mg of HCP-91@Na and monitored with UV-Vis spectroscopy. As anticipated, with time the peak corresponding to MB (λ_{max} = 670 nm) decreased sharply, whereas peak for MO (λ_{max} = 460nm) remained almost unaltered (Fig. 3.2b). In addition to UV-Vis spectra, we observed the visual change as well. Color of the mixture solution was green initially (color of MB is blue and MO is orange), with time intervals color of solution turned orange as only methyl orange left in solution (Appendix 3.32). For further validation, we have performed the same with mixture of methyl orange and largest dye used, i.e., rhodamine B. As per our expectation, here also we have found similar result as in case of MB and MO mixture. Both UV-Vis spectra and visual change validated our speculation as only RB got selectively adsorbed by HCP-91@Na and MO left in the solution (Fig. 3.2c and Appendix 3.33). Conclusively, our adsorbent material adsorbed selectively cationic dye molecules, on the other hand depending on the size of cationic dyes time of adsorption changed from lower to higher.

3.4 Conclusions

In conclusion, we have synthesized a robust and cost-effective microporous hyper-cross-linked polymer (HCPs) and later done post-synthetic incorporation of cations inside the network (HCP-91). On the basis of cation exchange, efficient cationic dye capture has been performed with HCP-91@Na. Furthermore, we have shown selectively cationic dye (methylene blue, crystal violet and rhodamine B) capture over anionic dye (methyl orange) by virtue of the ionic charge selectivity. To the best our knowledge, selective cationic dye capture in the regime of microporous organic framework is not reported till date. We believe

that this work will propel the research in the area of pollutant trapping with such robust and cost-effective materials.

3.5 Appendix Section

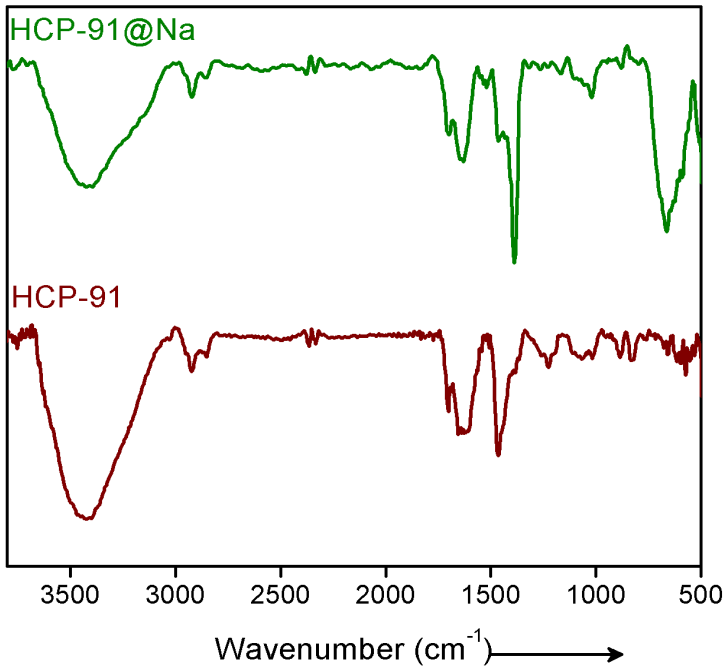

Appendix 3.1: FT-IR spectra of HCP-91 and HCP-91@Na.

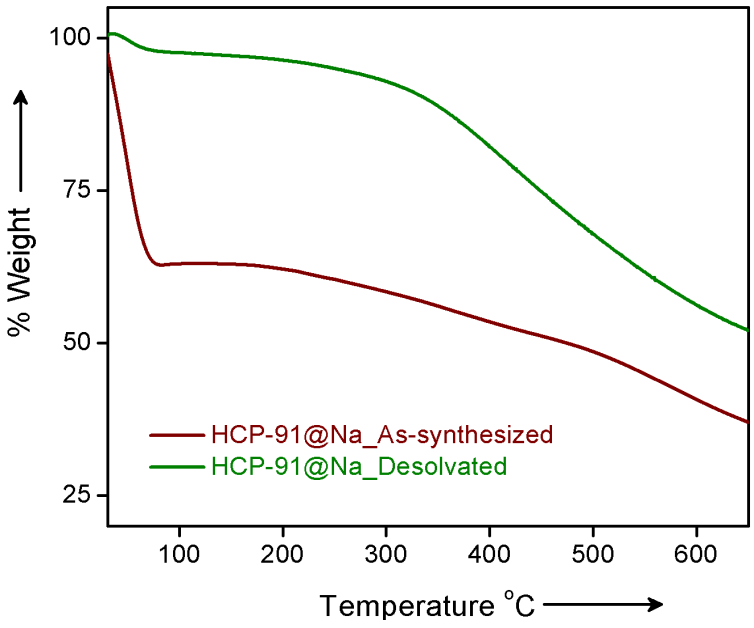

Appendix 3.2: Thermo-gravimetric analysis (TGA) profiles of as-synthesized HCP-91@Na (wine red) and desolvated phase of HCP-91@Na (green).

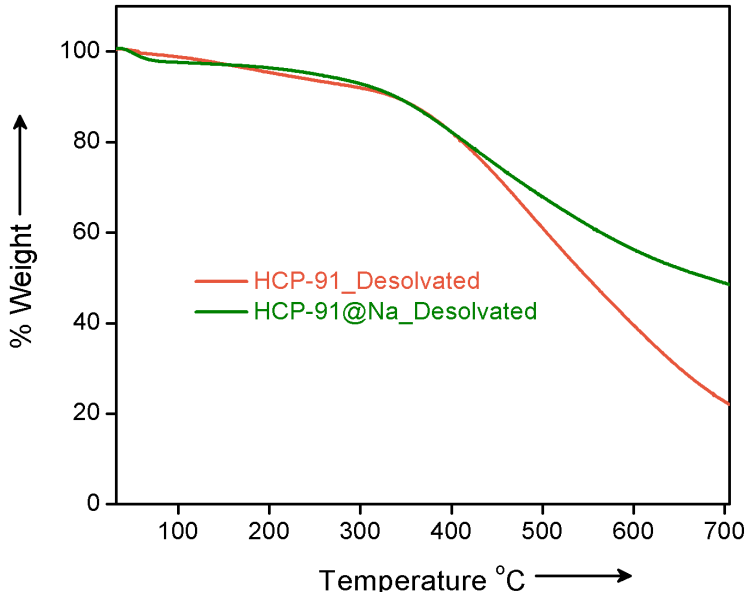

Appendix 3.3: Thermo-gravimetric analysis (TGA) profiles of desolvated phases of HCP-91 (orange) and HCP-91@Na (green).

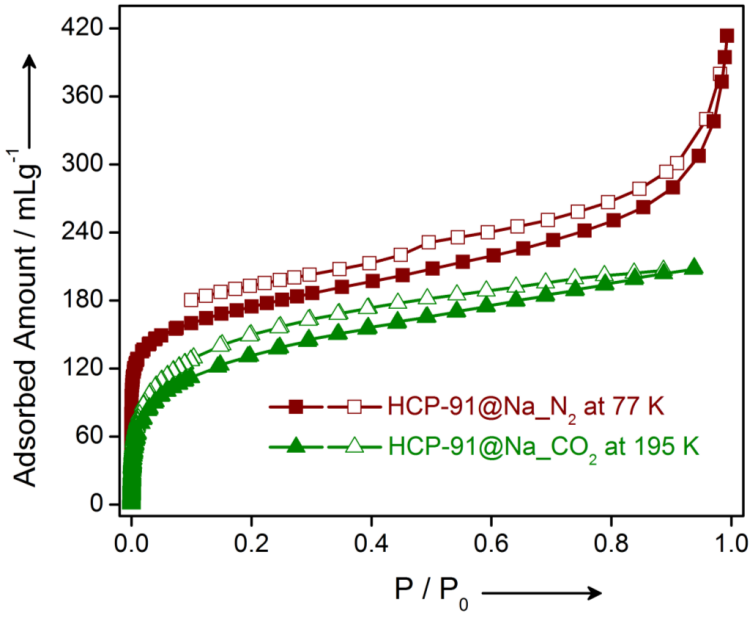

Appendix 3.4: N_2 adsorption profile at 77 K (wine red) and CO2 adsorption profile at 195 K (green) of HCP-91@Na.

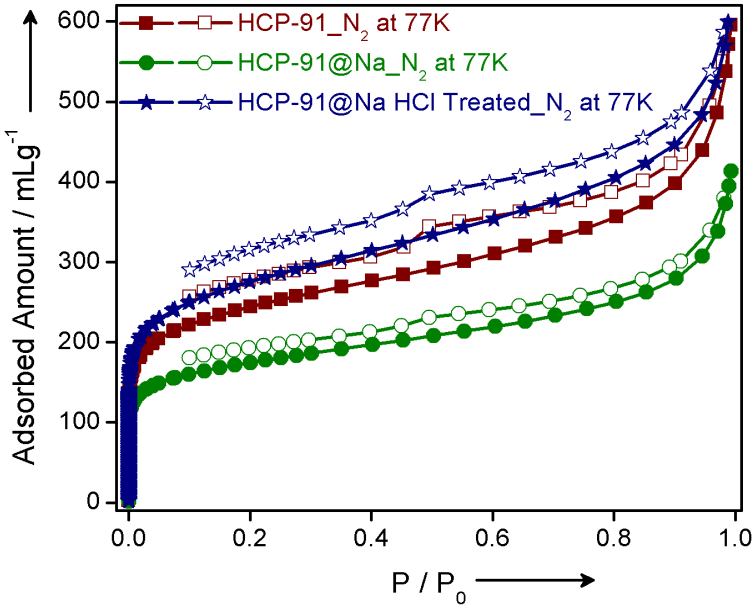

Appendix 3.5: N_2 adsorption profile at 77 K of HCP-91 (wine red), HCP-91@Na (green) and HCl treated phase of HCP-91@Na (blue).

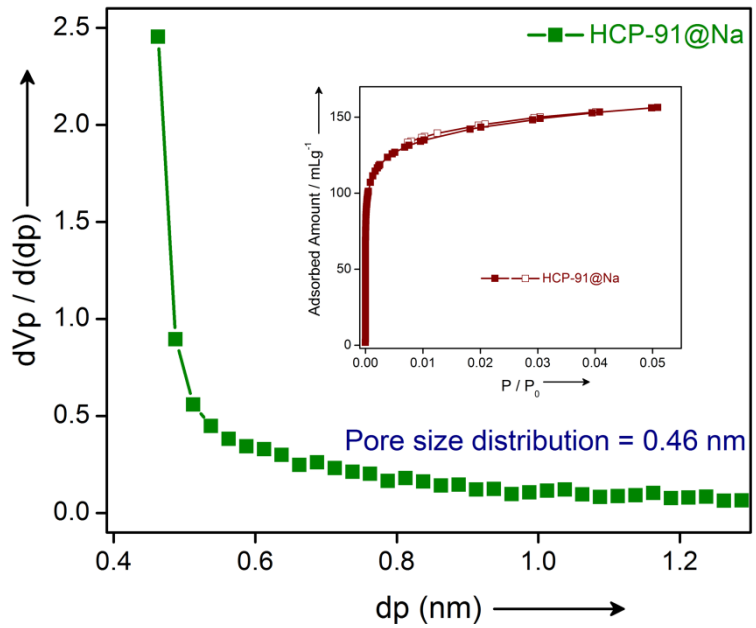

Appendix 3.6: HK plot of HCP-91@Na from N_2 adsorption (at 77 K) at low pressure region.

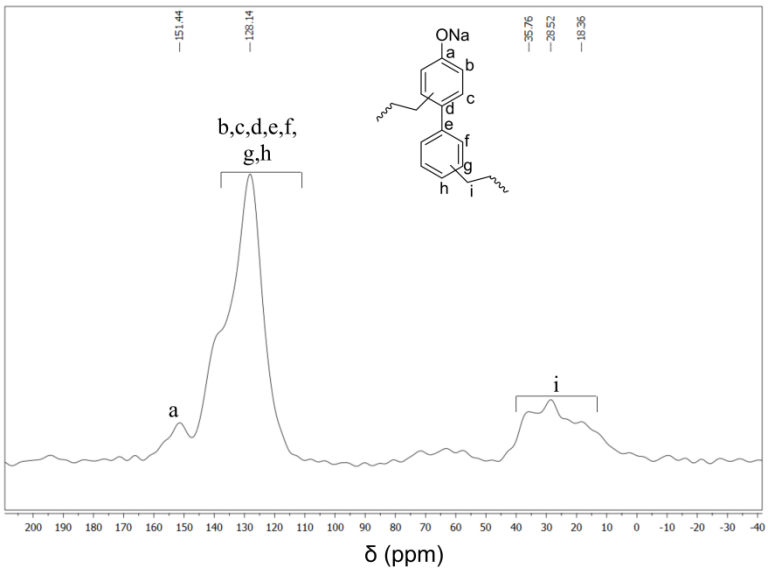

Appendix 3.7: Solid state ^{13}C-NMR of HCP-91@Na.

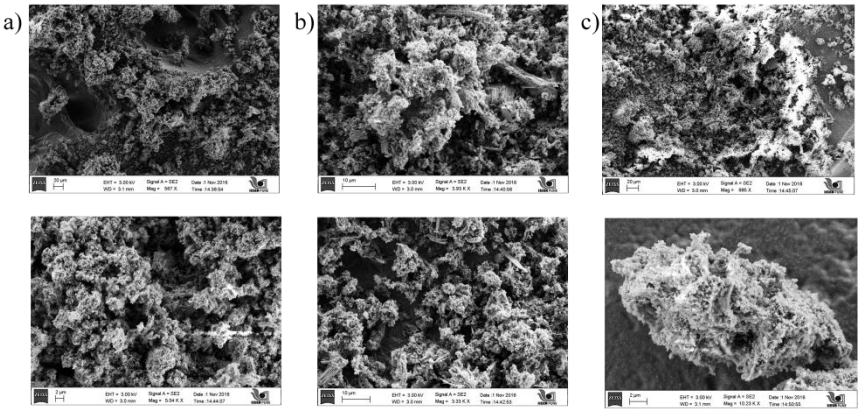

Appendix 3.8: FE-SEM images of a) HCP-91, b) HCP-91@Na and c) HCl treated HCP-91@Na respectively

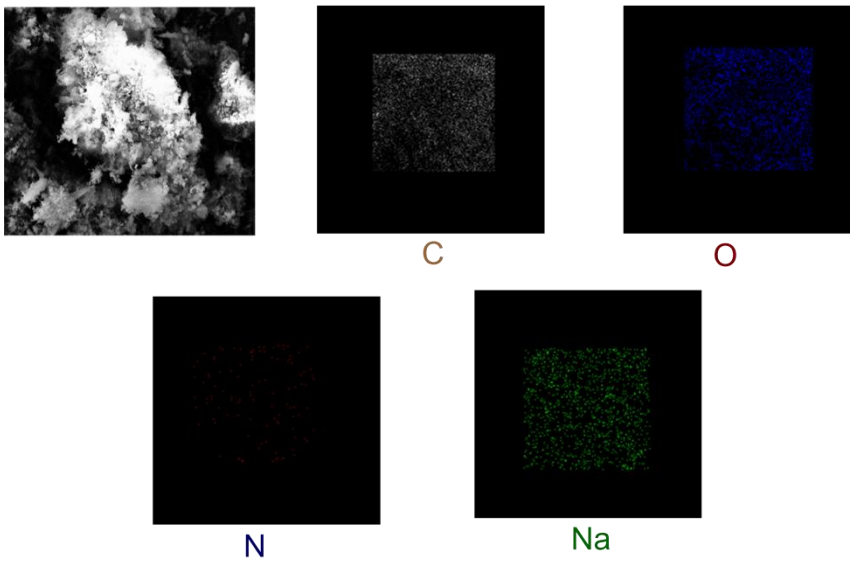

Appendix 3.9: EDX elemental imaging of HCP-91@Na.

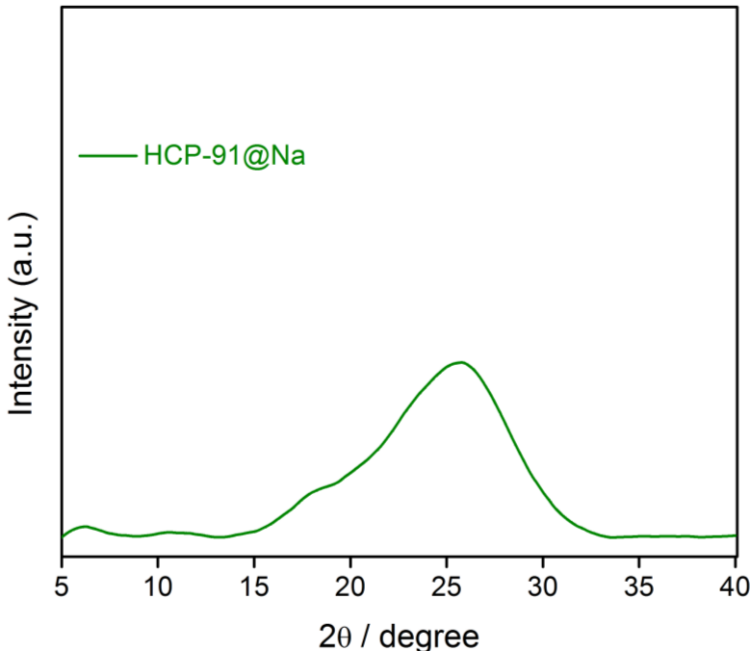

Appendix 3.10: Powder X-ray diffraction patterns of HCP-91@Na.

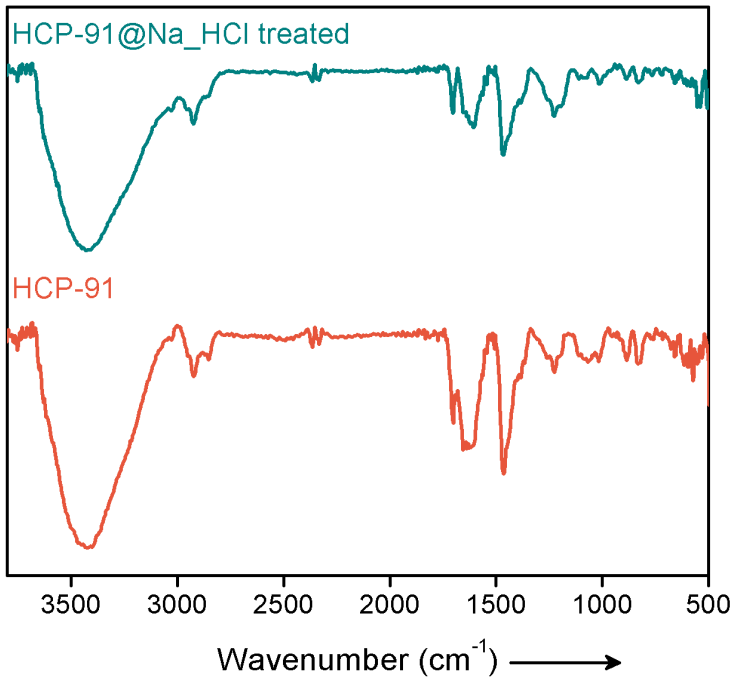

Appendix 3.11: FT-IR spectra of HCP-91 (red) and HCP-91@Na (cyan) after HCl treatment.

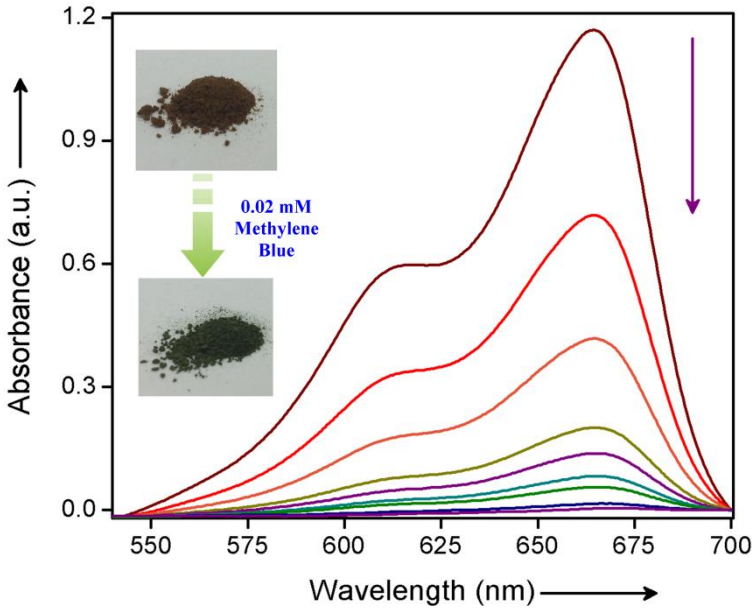

Appendix 3.12: UV-Vis spectra of 0.02 mM methylene blue solution in presence of HCP-91@Na at different time.

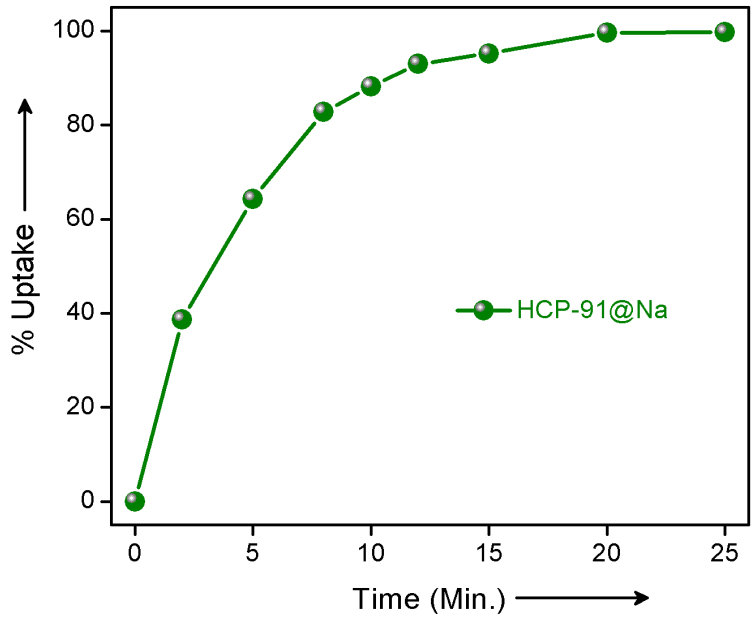

Appendix 3.13: Uptake (in %) of methylene blue by HCP-91@Na with time.

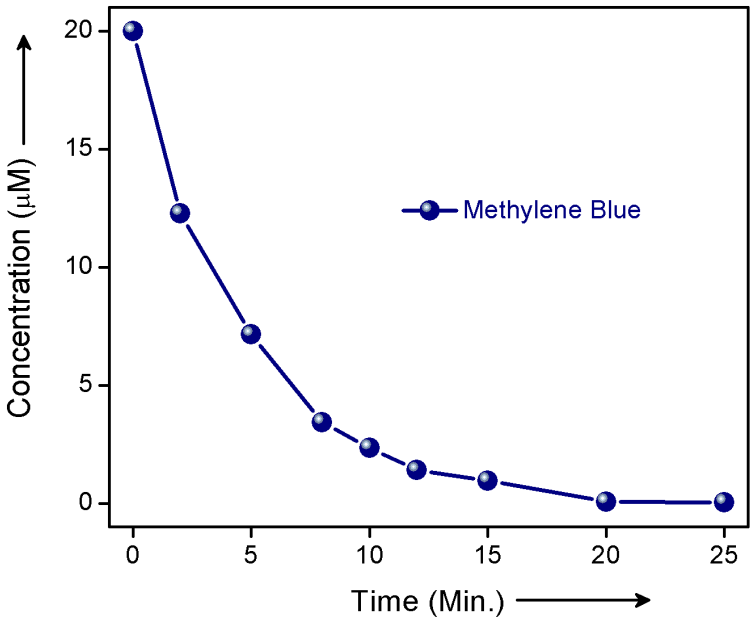

Appendix 3.14: Change in concentration of methylene blue with time in presence of HCP-91@Na.

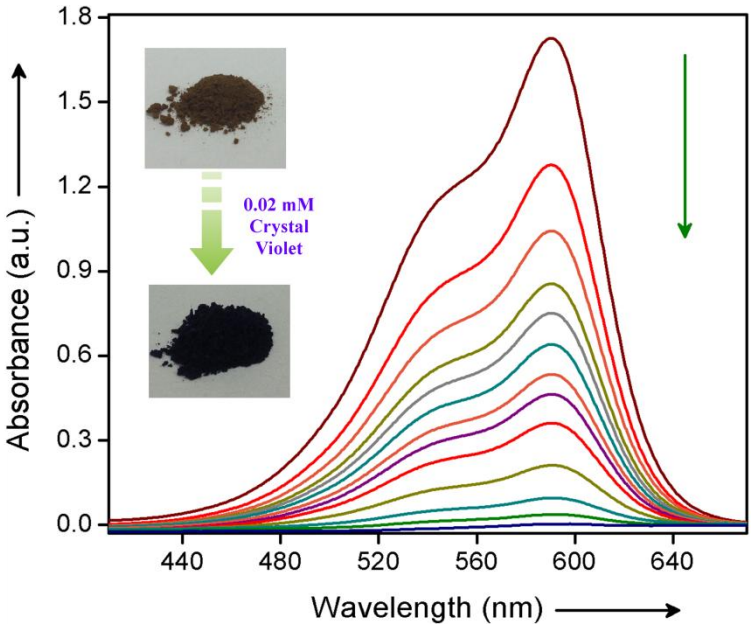

Appendix 3.15: UV-Vis spectra of 0.02 mM crystal violet solution in presence of HCP-91@Na at different time.

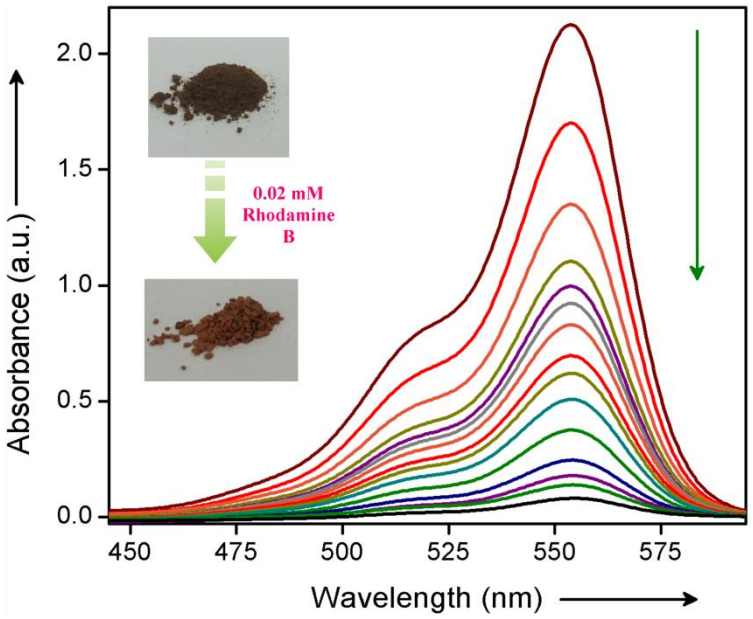

Appendix 3.16: UV-Vis spectra of 0.02 mM rhodamine B solution in presence of HCP-91@Na at different time.

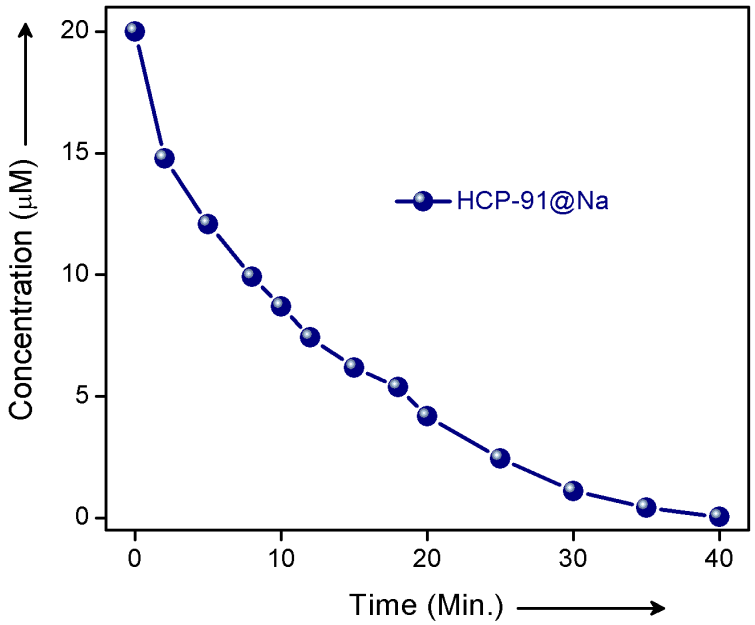

Appendix 3.17: Change in concentration of crystal violet with time in presence of HCP-91@Na.

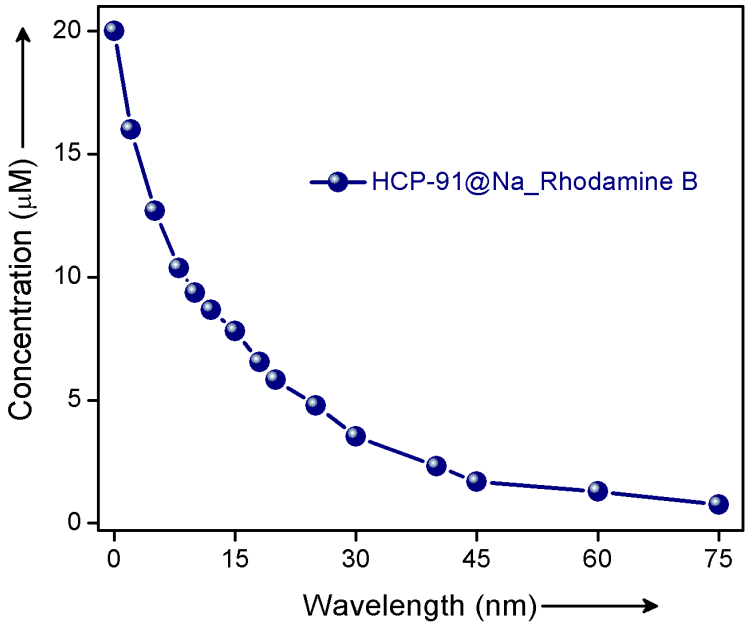

Appendix 3.18: Change in concentration of rhodamine B with time in presence of HCP-91@Na.

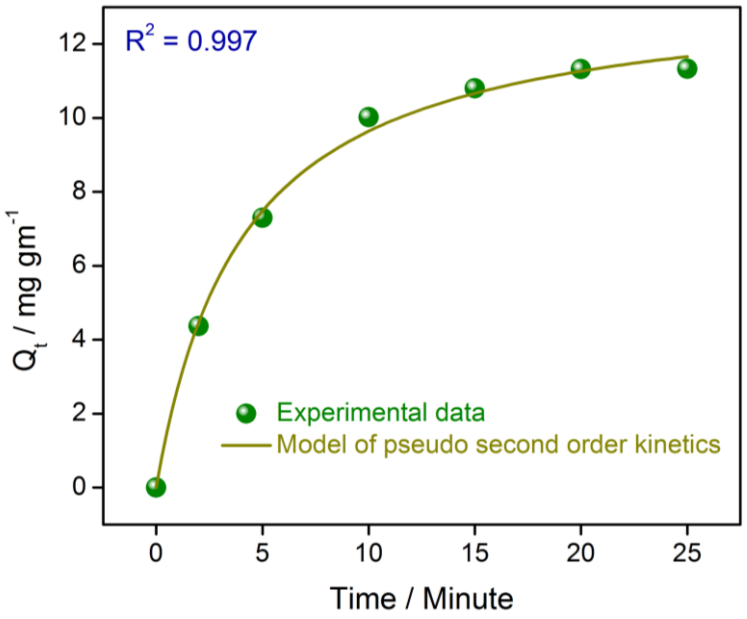

Appendix 3.19: Kinetics for the capture of methylene blue with HCP-91@Na.

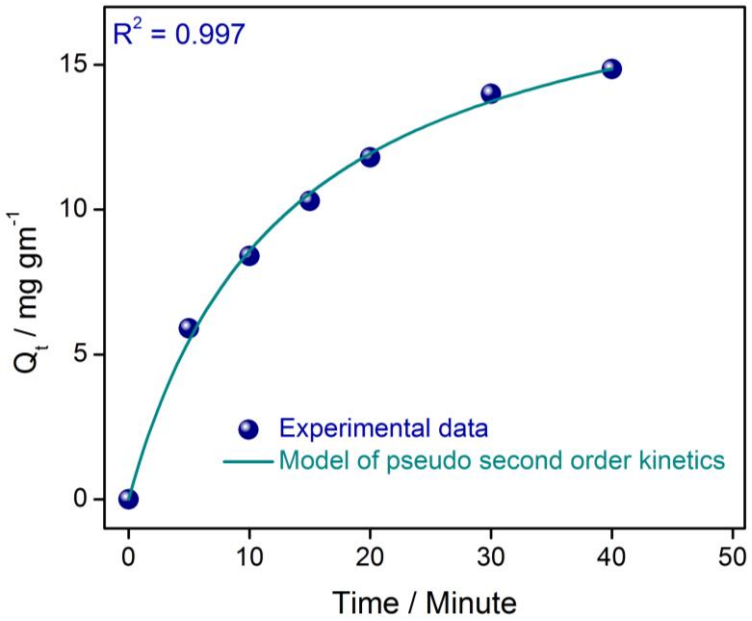

Appendix 3.20: Kinetics for the capture of crystal violet with HCP-91@Na.

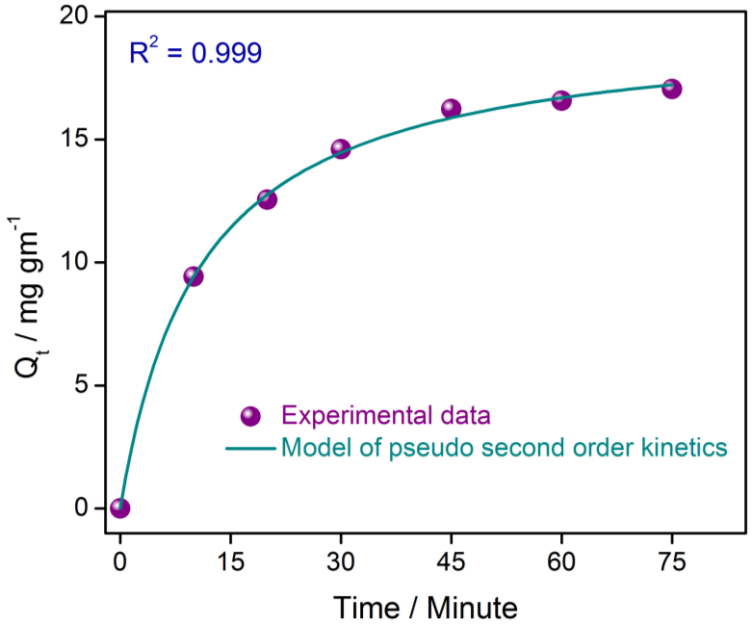

Appendix 3.21: Kinetics for the capture of rhodamine B with HCP-91@Na.

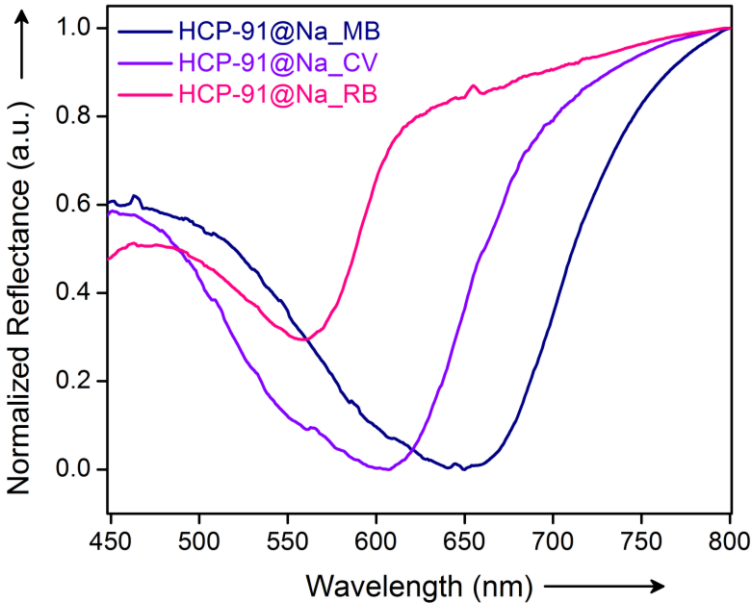

Appendix 3.22: Solid state UV-Vis spectra of methylene blue encapsulated HCP-91@Na (blue), crystal violet encapsulated HCP-91@Na (violet) and rhodamine B encapsulated HCP-91@Na (pink).

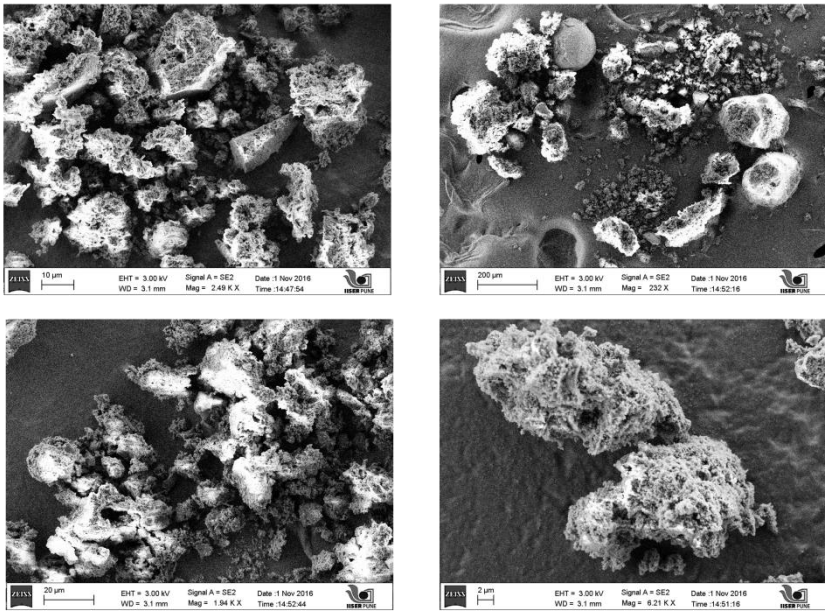

Appendix 3.23: FE-SEM images of methylene blue (MB) encapsulated HCP-91@Na.

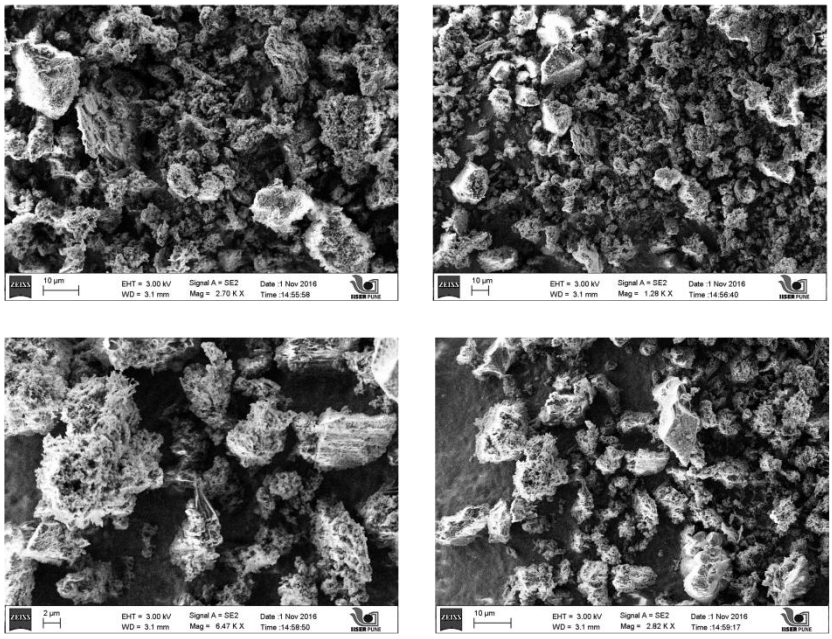

Appendix 3.24: FE-SEM images of crystal violet (CV) encapsulated HCP-91@Na.

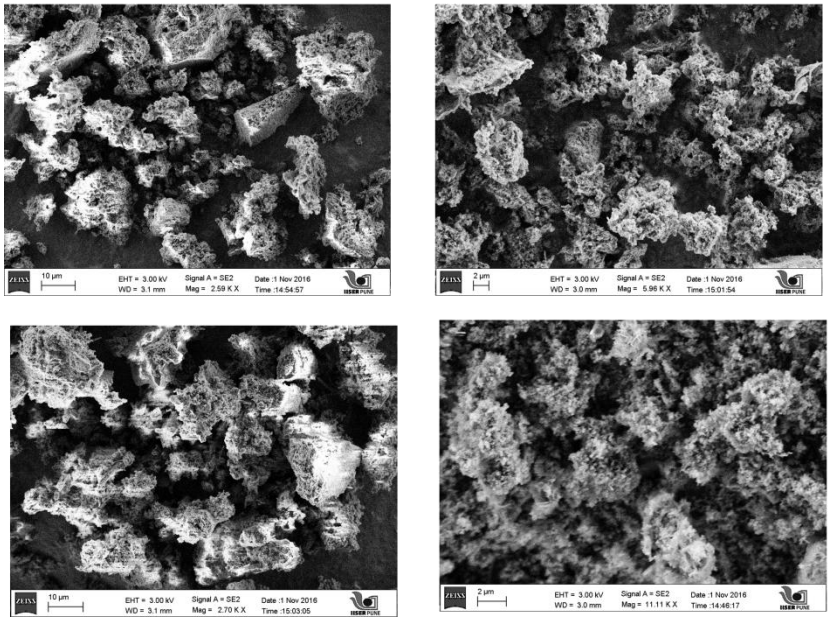

Appendix 3.25: FE-SEM images of rhodamine B (RB) encapsulated HCP-91@Na.

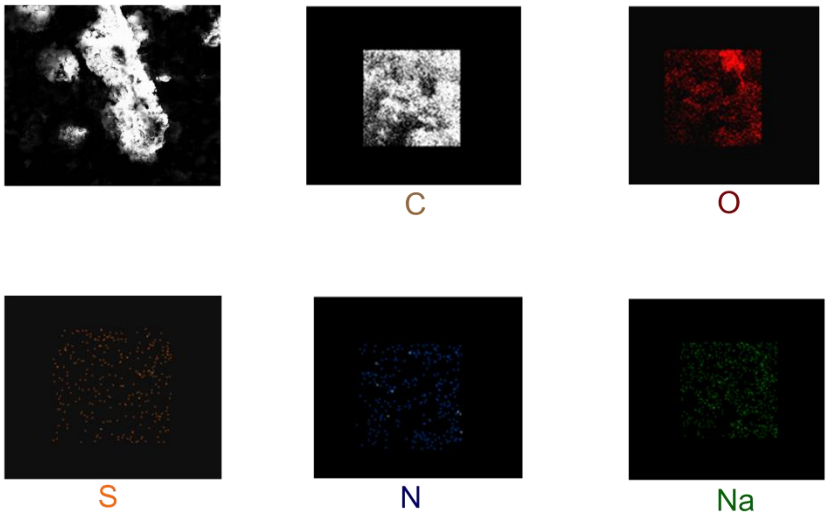

Appendix 3.26: EDX elemental imaging of methylene blue (MB) HCP-91@Na.

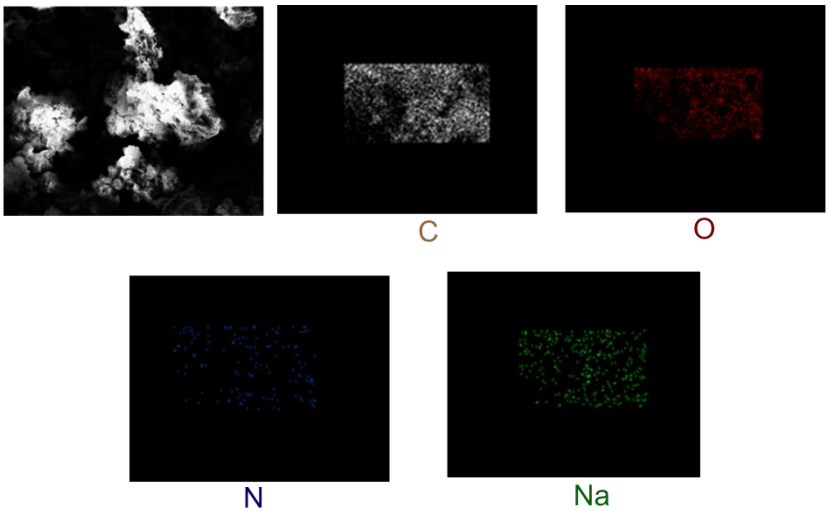

Appendix 3.27: EDX elemental imaging of crystal violet (CV) HCP-91@Na.

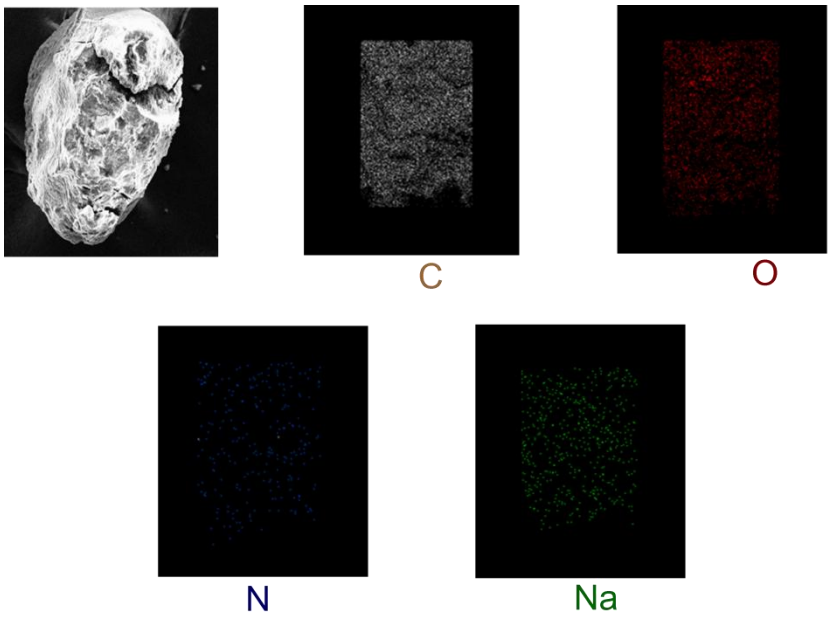

Appendix 3.28: EDX elemental imaging of rhodamine B (RB) HCP-91@Na.

Compounds	% of C	% of H	% of N	% of S
HCP-91@Na	66.05	4.475	0.0	0.0
HCP-91@Na _MB	68.47	3.228	1.01	0.399
HCP-91@Na _CV	68.93	3.775	0.89	0.0
HCP-91@Na _RB	62.15	6.25	1.45	0.0

Appendix 3.29: CHNS elemental analysis of HCP-91@Na and different cationic dye encapsulated HCP-91@Na.

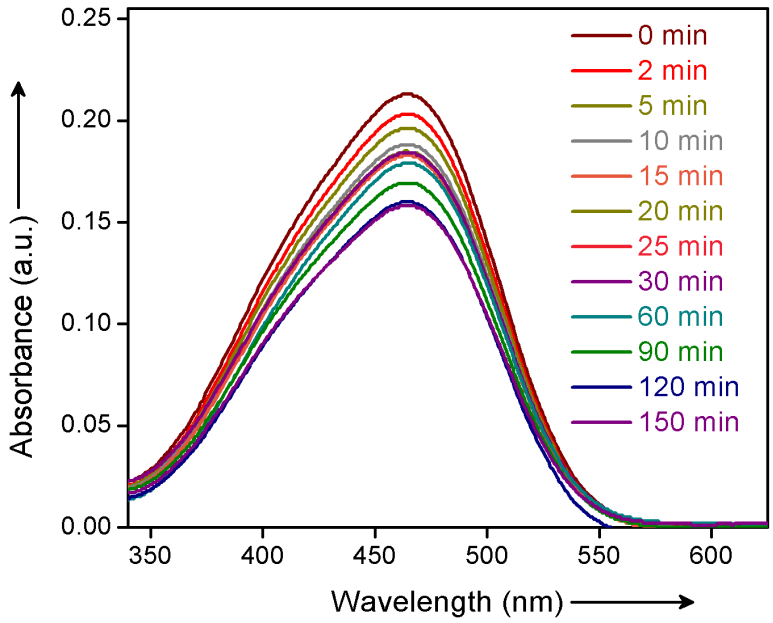

Appendix 3.30: UV-Vis spectra of 0.02 mM methyl orange solution in presence of HCP-91@Na at different time.

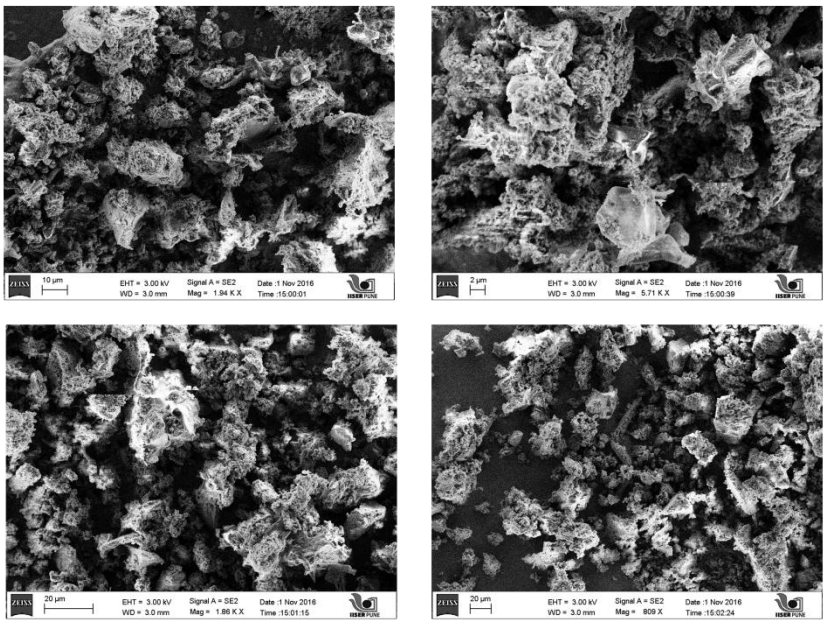

Appendix 3.31: FE-SEM images of methyl orange treated HCP-91@Na.

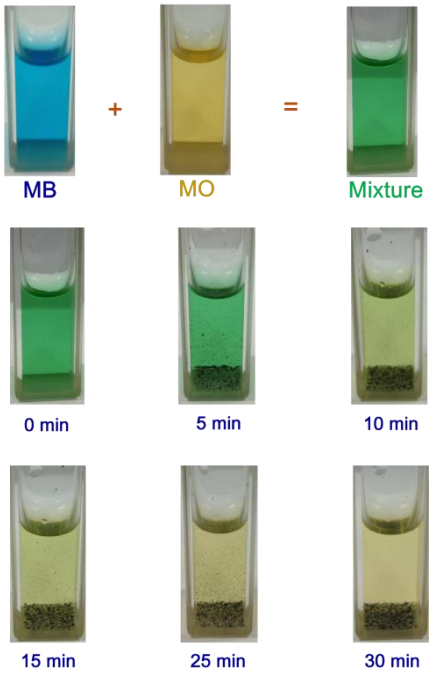

Appendix 3.32: Images at different time of equimolar mixed solution of methylene blue and methyl orange in presence of HCP-91@Na.

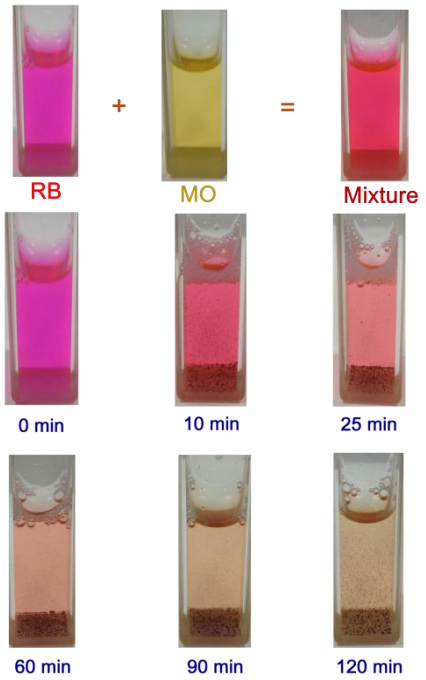

Appendix 3.33: Images at different time of equimolar mixed solution of rhodamine B and methyl orange in presence of HCP-91@Na.

3.6 References

1. (a) Y. Xu, S. Jin, H. Xu, A. Nagai and D. Jiang, *Chem. Soc. Rev.*, 2013, **42**, 8012-8031 ; (b) A. G. Slater and A. I. Cooper, *Science*,2015**, 348**, DOI: org/10.1126/science.aaa8075; (c) P. J. Waller, F. Gándara and O. M. Yaghi, *Acc. Chem. Res.*, 2015, **48**, 3053 -3063; (d) D. Yuan, W. Lu, D. Zhao and H.-C. Zhou, *Adv. Mater.*, 2011, **23**, 3723 –3725; (e) R. Dawson, E. Stöckel, J. R. Holst, D. J. Adams and A. I. Cooper, *Energy Environ. Sci.*, 2011, **4**, 4239 -4245; (f) C. R. DeBlase, K. E. Silberstein, T. –T. Truong, H. D. Abruña and W. R. Dichtel, *J. Am. Chem. Soc.*, 2013, **135**, 16821 -16824.

2. (a) M. G. Rabbani and H. M. El-Kaderi, *Chem. Mater.*, 2011, **23**, 1650 -1653; (b) B. Li, Y. Zhang, D. Ma, Z. Shi and S. Ma, *Nat. Comm.*, 2014, DOI: 10.1038/ncomms6537; (c) W. Lu, D. Yuan, D. Zhao, C. I. Schilling, O. Plietzsch, T. Muller, S. Bräse, J. Guenther, J. Blümel, R. Krishna, Z. Li, Zhou, H.-C., *Chem. Mater.*, 2010, **22**, 5964 -5972; (d) A. Karmakar, A. Kumar, A. K. Chaudhari, P. Samanta, A. V. Desai, R. Krishna and S. K. Ghosh, *Chem. Eur. J.*, 2016, **22**, 4931 –4937; (e) T. Ben, H. Ren, S. Q. Ma, D. P. Cao, J. H. Lan, X. F. Jing, W. C. Wang, J. Xu, F. Deng, J. M. Simmons, S. L. Qiu and G. S.

Zhu, *Angew. Chem., Int. Ed.*, 2009, **48**, 9457 –9460; (f) H. A. Patel, S. H. Je, J. Park, D. P. Chen, Y. Jung, C. T. Yavuz and A. Coskun, *Nat. Comm.*, 2013, DOI: 10.1038/ncomms2359; (g) S. Dalapati, E. Jin, M. Addicoat, T. Heine and D. Jiang, *J. Am. Chem. Soc.*, 2016, **138**, 5797-5800; (h) A. Karmakar, R. Illathvalappil, B. Anothumakkool, A. Sen, P. Samanta, A. V. Desai, S. Kurungot and S. K. Ghosh, *Angew.Chem. Int.Ed.*, 2016, **55**, 10667 –10671.

3. (a) Y. Luo, B. Li, W. Wang, K. Wu and B. Tan, *Adv. Mater.*, 2012, **24**, 5703 –5707; (b) R. Dawson, L. A. Stevens, T. C. Drage, C. E. Snape, M. W. Smith, D. J. Adams and A. I. Cooper, *J. Am. Chem. Soc.*, 2012, **134**, 10741 -10744.

4. (a) B. Li, R. Gong, W. Wang, X. Huang, W. Zhang, H. Li, C. Hu and B. Tan, *Macromolecules*, 2011, **44**, 2410 -2414; (b) R. Dawson, T. Ratvijitvech, M. Corker, A. Laybourn, Y. Z. Khimyak, A. I. Cooper and D. J. Adams, *Polym. Chem.*, 2012, **3**, 2034 -2038.

5. (a) S. Bhunia, B. Banerjee and A. Bhaumik, *Chem. Commun.*, 2015, **51**, 5020 -5023; (b) P. Samanta, P. Chandra and S. K. Ghosh, *Beilstein J. Org. Chem.*, 2016, **12**, 1981 –1986.

6. (a) R. T. Woodward, L. A. Stevens, R. Dawson, M. Vijayaraghavan, T. Hasell, I. P. Silverwood, A. V. Ewing, T. Ratvijitvech, J. D. Exley, S. Y. Chong, F. Blanc, D. J. Adams, S. G. Kazarian, C. E. Snape, T. C. Drage and A. I. Cooper, *J. Am. Chem. Soc.*, 2014, **136**, 9028-9035; (b) S. Mondal, J. Mondal and A. Bhaumik, *ChemCatChem*, 2015, **7**, 3570 –3578; (c) X. Jing, D. Zou, P. Cui, H. Ren and G. Zhu, *J. Mater. Chem. A*, 2013, **1**,13926 -13931; (d) J. Wang, W. Sng, G. Yi and Y. Zhang, *Chem. Commun.*,2015, **51**, 12076 -12079.

7. (a) S. J. Allen and B. Koumanova, *J. Univ. Chem. Technol. Metall.*, 2005, **40**, 175 -192; (b) C. –C. Wang, J. –R. Li, X. –L. Lv, Y. –Q. Zhang and G. Guo, *Energy Environ. Sci.*, 2014, **7**, 2831 -2867.

8. X. Liu, W. Gong, J. Luo, C. Zou, Y. Yang and S. Yang, *Appl. Surf. Sci.*, 2016, **362**, 517 -524.

9. (a) A. Ayati, M. N. Shahrak, B. Tanhaei and M. Sillanpää, *Chemosphere*, 2016, **160**, 30 -44; (b) S. –R. Zhang, J. Li, D. –Y. Du, J. –S. Qin, S. –L. Li, W. –W. He, Z. –M. Su and Y. –Q. Lan, *J. Mater. Chem. A*, 2015, 3, 23426 -23434; (c) S. Chen, J. Zhang, C. Zhang, Q. Yue, Y. Li and C. Li, *Desalination*, 2010, **252**, 149 -156; (d) A. Mittal, A. Malviya, D. Kaur, J. Mittal and L. Kurup, *J. Hazard. Mater.*, 2007, **148**, 229-240.

10. (a) E. Haque, V. Lo, A. I. Minett, A. T. Harris and T. L. Church, *J. Mater. Chem. A*, 2014, **2**, 193 -203; (b) E. Haque, J. E. Lee, I. T. Jang, Y. K. Hwang, J. –S. Chang, J. Jegal and S. H. Jhung, *J. Hazard. Mater.*, 2010, **181**, 535-542.

11. (a) G. Crini, *Bioresour. Technol.*, 2006, **97**, 1061 –1085; (b) K. K. H. Choy, G. McKay and J. F. Porter, *Resour. Conserv. Rec.*, 1999, **27**, 57-71.

12. (a) C. Zou, Z. Zhang, X. Xu, Q. Gong, J. Li and C. –D. Wu, *J. Am. Chem. Soc.*, 2012, **134**, 87 –90; (b) X. Zhao, X. Bu, T. Wu, S. –T. Zheng, L. Wang and P. Feng, *Nat. Comm.*, 2013, 10.1038/ncomms3344; (c) M. –L. Ma, J. –H. Qin, C. Ji, H. Xu, R. Wang, B. –J. Li, S. –Q. Zang, H. –W. Hou and S. R. Batten, *J. Mater. Chem. C*, 2014, **2**, 1085-1093; (d) Z. Zhu, Y. –L. Bai, L. Zhang, D. Sun, J. Fang and S. Zhu, *Chem. Commun.*,2014, **50**, 14674 -14677; (e) Y. –Q. Lan, H. –L. Jiang, S. –L. Li and Q. Xu, *Adv. Mater.*, 2011, **23**, 5015 –5020; (f) J. –S. Qin, S. –R. Zhang, D. –Y. Du, P. Shen, S. –J. Bao, Y. –Q. Lan and Z. –M. Su, *Chem. Eur. J.*, 2014, **20**, 5625 – 5630; (g) P. Li, N. A. Vermeulen, X. Gong, C. D. Malliakas, J. F. Stoddart, J. T. Hupp and O. K. Farha, *Angew. Chem., Int. Ed.*, 2016, **128**, 10514 –10518; (h) S. Kumar, G. Verma, W. –Y. Gao, Z. Niu, L. Wojtas and S. Ma, *Eur. J. Inorg. Chem.*, 2016, 4373 -4377; (i) P. Yu, Q. Li, Y. Hu, N. Liu, L. Zhang, K. Su, J. Qian, S. Huang and M. Hong, *Chem. Commun.*, 2016, **52**, 7978 -7981; (j) X. Liu, Z. Xiao, J. Xu, W. Xu, P. Sang, L. Zhao, H. Zhu, D. Sun and W. Guo, *J. Mater. Chem. A*, 2016, **4**, 13844 -13851; (k) D. Chen, W. Shi and P. Cheng, *Chem. Commun.*, 2015, **51**, 370 -372; (l) Y. Han, S. Sheng, F. Yang, Y. Xie, M. Zhaoa and J. –R. Li, *J. Mater. Chem. A*, 2015, **3**, 12804 -12809; (m) Z. Hasan and S. H. Jhung, *J. Hazard. Mater.*, 2015, **283**, 329 -339; (n) H. Hahm, S. Kim, H. Ha, S. Jung, Y. Kim, M. Yoon and M. Kim, *CrystEngComm*, 2015, **17**, 8418 -8422; (o) Y. Zhu, Y. -M. Wang, S. -Y. Zhao, P. Liu, C. Wei, Y. -L. Wu, C. -K. Xia and J. -M. Xie, Inorg. Chem. 2014, 53, 7692 –7699; (p) A. V. Desai, B. Manna, A. Karmakar, A. Sahu and S. K. Ghosh, *Angew. Chem. Int. Ed.*, 2016, 55, 7811-7815; (q) Y. -Y. Jia, Y. -H. Zhang, J. Xu, R. Feng, M. -S. Zhang and X. -H. Bu, *Chem. Commun.*, 2015, 51, 17439 -17442; (r) A. Karmakar, B. Joarder, A. Mallick, P. Samanta, A. V. Desai, S. Basu and S. K. Ghosh, *Chem. Commun.*, 2017, **53**, 1253 -1256.

13. (a) D. M. D'Alessandro, B. Smit and J. R. Long, *Angew. Chem., Int. Ed.*, 2010, **49**, 6058 -6082; (b) W. Lu, D. Yuan, J. Sculley, D. Zhao, R. Krishna and H. –C. Zhou, *J. Am. Chem. Soc.*, 2011, **133**, 18126 -18129.

14. S. –B. Yu, H. Lyu, J. Tian, H. Wang, D. –W. Zhang, Y. Liu and Z. –T. Li, *Polym. Chem.*, 2016, **7**, 3392 -3397.

Chapter 4

Hydroxy Functionalized Porous Organic Material: A Cost Effective Route to Remove Iodine from Vapor and Water Medium

4.1 Introduction

Gradual increase in the water pollution due to various toxic and hazardous chemicals has become huge threat to the living system. Among all kinds of water pollutants radioactive species have become one of the major challenge in recent years.[1] Worldwide increasing civilizations and industrializations has led to the immense crisis of electrical energy.[2] In addition to huge emission of greenhouse gasses and also diminution of the conventional sources (such as coal) of electrical energy has forced to search for alternative sources.[3] In this context, nuclear power has been found to be one of the candidate for the alternative source of electrical energy. However, nuclear wastes with different types of radioactive water pollutants has turned out to be a global concern. Such nuclear wastes are majorly composed of various radionuclides such as ^{137}Cs, ^{90}Sr, ^{99}Tc, along with some volatile radionuclides, minor actinides, lanthanides etc.[4] Among those volatile radionuclides, iodine (^{129}I and ^{131}I) is one of the main component. Radioiodine has attracted much public concern since volatile iodine spread very rapidly through air and contaminant the environment.[5] Further very high half-life of ^{129}I ($t_{1/2}$ = 15.7 million years) has been found to cause major problems. Owing to such high half-life, high mobility through air and radio-toxicity radioiodine has become a global concern which has to be addressed soon.[6] Apart from volatile iodine in air, water soluble forms of iodine in waste water has also attracted much attention.[7] Due to the pollution of groundwater and drinking water with radioiodine, the risk of thyroid cancer has been found to be increased.[8] Water pollution with radioactive iodine has been found to occur when volatile iodine reach the water streams via rainfall.[9] In addition, nuclear disasters like Chernobyl and Mayak incidents and open air nuclear bomb testing (in 1950) have also contributed hugely to the water pollution with radioiodine.[10] Recent statics has shown that the possibility of the thyroid cancer has been found to be increased from as a consequence of the Chernobyl and Mayak incidents and also recent Fukushima disaster.[11] In this regard, a lot of research has been devoted to design and synthesize of materials which can remove iodine from water as well as in vapor phase.

In this context, it has been observed that currently employed techniques for the capture of iodine have been found to be based on synthetic or natural metal-exchanged zeolite materials.[12] On the other hand, silver doped materials are also being used for the iodine capture as silver converts iodine to form AgI. Although these materials are hydrolytically and chemically stable but their low sorption capacity has often led to difficulties. In case of such silver doped materials, maximum capacity has been calculated stoichiometrically to be 1.18 g g^{-1} (per gram of silver), but often very low sorption capacity ranges from 0.1-0.31 g g^{-1} has been observed.[13] In this regard, researchers are trying to develop alternative materials with higher sorption capacity, low cost and easy synthesis. Porous materials with tuneable architectures, such as metal-organic frameworks (MOFs), porous organic materials etc. have come up as an alternate to

the conventional systems.[14] Iodine capture with porous organic materials has found to be advantageous over other congener materials because of its high stability, high capacity etc. Further, most of the research with porous organic materials has been dedicated to the vapor phase capture, on the other hand studies on capture of iodine from water have found to be very rare.[15] In this regard, search for the efficient materials for removal of iodine from both vapor phase and water medium is still in nascent stage. In the domain of porous organic materials, micro-porous hyper-cross-linked polymers (HCPs) via knitting strategy has evolved in last few years.[16] HCPs have been found to be synthesized via lewis acid catalyzed Friedel-Crafts reaction based cross linking. Owing to easy one pot synthesis, low cost, high surface area, high chemical stability etc., HCPs has attracted huge attention. This type of micro-porous cross-linked materials have already been explored for CO_2 capture, heterogeneous catalysis etc.[17] But HCPs has rarely been employed for the remediation of water pollutants. Herein, two cost-effective and chemically stable hydroxy-functionalized HCPs have been utilized for the removal of iodine from water medium and vapor phase (Scheme 4.1).

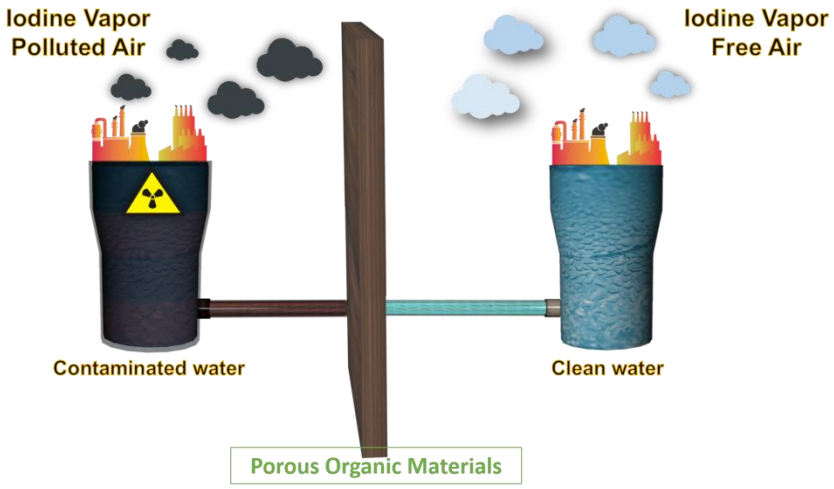

Scheme 4.1: Schematic representation of iodine capture with porous organic material.

4.2 Experimental

4.2.1 Materials:

4-phenylphenol, 4,4′-dihydroxybiphenyl, $FeCl_3$, formaldehyde dimethyl acetal (FDA) were purchased from Sigma-Aldrich. Iodine, KI and all other remaining solvents were purchased locally. All the chemicals were used without any further purification.

4.2.2 Physical measurements

All UV-Visible spectra were recorded on Shimadzu UV 2600 Spectrophotometer. Gas adsorption measurements were carried out using BelSorp-max instrument from Bel Japan. FE-SEM was done by using FEI Quanta 3D dual beam ESEM at 30KV. Solid-state ^{13}C CP-MAS NMR spectra was recorded with a Bruker Advance-III Ultrashield500WB spectrometer (probe: MAS BB 4MM, spinning rate: 5KHz).

4.2.3 Synthesis:

Synthesis of HCP-91: HCP-91 has been synthesized via Friedel-Craft reaction from cross-coupling of 4-phenylphenol by following our previous reported protocol.[16d]

Synthesis of HCP-92: HCP-92 has been synthesized from cross-coupling of 4,4′-dihydroxybiphenyl (Scheme 4.2) by following the same protocol as similar to HCP-91. To a round bottom flask 4,4′-dihydroxybiphenyl (300 mg, 1.612 mmol) has been taken and to that 20 ml of dichloroethane ($C_2H_4Cl_2$) was added. Then to the reaction mixture, formaldehyde dimethyl acetal (430 µl, 4.836 mmol) and $FeCl_3$ (820 mg, 4.836 mmol) were added respectively. Thus resulted reaction mixture was heated at 50 °C for 5 hours and then was allowed to reflux at 80 °C for 20 hours. On completion of the reaction dark brown colored precipitate was filtered off and washed with DMF, methanol, water, chloroform, dichloromethane and tetrahydrofuran (THF) repeatedly. Thus obtained dark brown colored solid material was then kept in 1:1 $CHCl_3$-THF mixture (25 ml) for 3 days to remove the high boiling solvents from the porous network of HCP-92. Then the solvent exchanged phase of HCP-92 was heated at 100 ^oC under vacuum to obtain the guest free activated material and with this phase further works have been carried out. Yield: 310 mg.

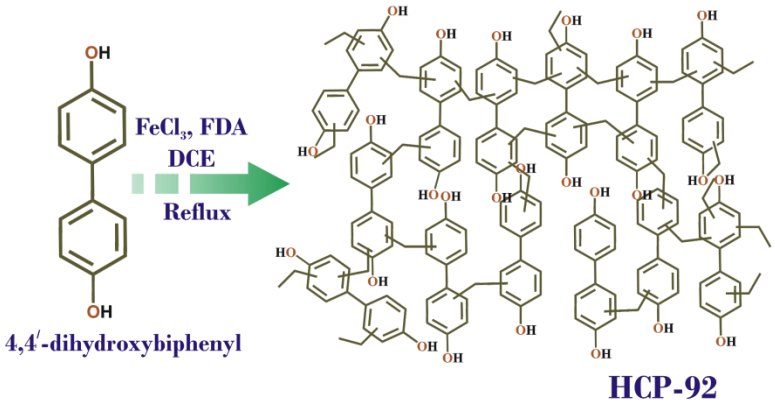

Scheme 4.2: Synthesis scheme of HCP-92.

4.2.4 Vapor phase iodine capture study:

To carry out the vapor phase iodine capture study, iodine was taken in a 15 mL vial. To the glass vial containing iodine, a smaller glass vial with respective (30 mg of HCP-91 or HCP-92) compound was kept inside (Fig. 4.1). The whole set up was heated at 75 °C to vaporize the iodine and was kept for 96 hours. After the iodine sorption, weight of the respective compounds were checked. Capacity of the respective compounds for iodine vapor was calculated further via gravimetric analysis.

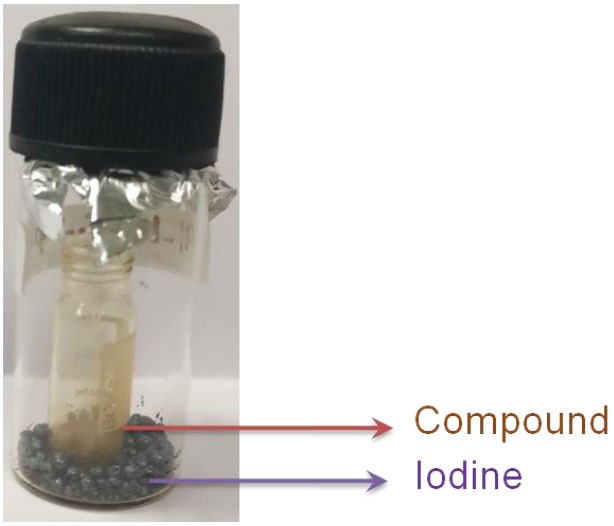

Figure 4.1: Image of the iodine vapor capture set up.

4.2.5 Time dependent capture of I_3^- ion from water:

For I_3^- ion removal study from water, 2 mL aqueous solution of 0.5 mM I_3^- ion has been taken in a cuvette and initial absorbance of the solution has been recorded with UV-Vis spectroscopy. To the solution, 2 mg of each desolvated HCP compound (HCP-91 or HCP-92) has been added and corresponding absorbance spectra of the supernatant solution has been recorded the at several time intervals. Furthermore, % removal and decrease in concentration of I_3^- ion from water with time have been calculated from this time dependent study by using the following equation,

$$D_t = \frac{C_0 - C_t}{C_0} \text{ x } 100\% = \frac{A_0 - A_t}{A_0} \text{ x } 100\%$$

$$i.e., \qquad C_t = C_0 - \frac{A_0 - A_t}{A_0} \mathbf{x}\, C_0$$

Where, D_t is exchange capacity, A_0 and C_0 are initial absorbance and concentration of the I_3^- ion solution respectively, A_t and C_t, are the absorbance and concentration of the I_3^- ion solution at time 't' respectively.

4.2.6 Anion dependent study of I_3^- ion capture:

For anion dependent studies, here Cl^-, NO_3^- and SO_4^{2-} ions have been taken as the competing anions, which have been found to be omnipresent in the common water sources and waste waters. Equimolar mixtures of (2.5 mM; 1:1) aqueous solutions of targeted I_3^- ion and the competing anion have been taken. To the aforementioned solutions 2 mg of desolvated HCPs (HCP-91 or HCP-92) have been added and kept for stirring for 24 hours. After 24 hours, respective solutions have been filtered off and characterised with UV-Vis spectroscopy. Thus obtained solutions have been diluted 5 times to measure the UV-Vis spectroscopy and further the capture efficiency of HCPs in presence of other anions has been studied by comparing with blank (Blank: only 2.5 mM of I_3^- ion has been taken instead of mixture).

4.2.7 Kinetics study for the I_3^- ion capture:

Kinetics for the capture studies were calculated from the titration plots for the respective compounds. Further, best fit model for capture with both compounds were found to be pseudo second order kinetics. The equation for the pseudo second order model as follows,

$$Q_t = \frac{k_2 {Q_e}^2 t}{1 + k_2 Q_e t}$$

where, Q_e and Q_t are the amount of adsorbate (mg gm^{-1}) onto adsorbent at equilibrium and different time intervals respectively, t is the time in minute.

4.2.8 Calculation of capacity:

To check the capacity of HCP-91 and HCP-92, 10 mg of desolvated compounds have been kept with 20 mL of 5 mM I_3^- ion solution for 1 day at stirring condition. After 24 hours dispersed compounds have been filtered out and the respective filtrate has been used for further study. UV-Vis measurement has been carried out by diluting the solution. From the initial and final absorbance value of the I_3^- ion solution we have calculated the storage capacity of HCPs in 1 day by using the following equation,

$$Q_t = \frac{(C_0 - C_t) * V}{m}$$

Where, Q_t, C_0, C_t, V and m are the capacity of adsorbent, initial concentration of I_3^- ion solution, concentration of the I_3^- ion solution at specific times, volume of the solution and mass used for the adsorbent respectively.

4.2.9 Adsorption isotherm experiment:

HCP-91 (5 mg) was immersed in 2 mL water solution of I_3^- ion having different concentration (ranges from 1 mM to 7.5 mM of I_3^- ion solution). After 10 hours UV-Visible spectroscopy was carried out with the supernatant solution and further fitted with following equation,

Freundlich Model, $$Q_e = K_F C_e^{1/n}$$

where, K_F and 1/n are the Freundlich model constants, indicating capacity and intensity of adsorption, respectively.

Similarly for HCP-92, sorption isotherm was observed by following the same protocol as compare to HCP-91.

4.2.10 Recyclability test of compound-1:

In a typical experiment, recyclability of both the compounds was checked up to three cycles for I_3^- ion capture study. 20 mg of the iodine encapsulated compounds were used for the recycling experiments, both the compounds were regenerated with methanol. Further, both the compounds were desolvated under vacuum at ~ 100 °C. Those desolvated phases of HCP-91 and HCP-92 were further employed for the second cycle of I_3^- ion capture study with 6 mL 5 mM I_3^- ion water solution as used for the first cycle. After one day the supernatant was analysed with UV-Vis spectroscopy. Further the similar protocol was employed to check the reusability of the compounds for I_3^- ion capture from water.

4.3 Results and discussion

Herein, the efficient removal of iodine from water has been demonstrated with two chemically stable cost-effective micro-porous hyper-cross-linked polymers (HCPs), viz. HCP-91 and HCP-92. Both the compounds were synthesized via knitting strategy with Friedel-Craft reaction by using $FeCl_3$ as lewis acid and formaldehyde dimethyl acetal (FDA) as cross linker. In case of HCP-91, cross-linking of 4-phenylphenol (mono hydroxy based building unit) led to the polymeric material whereas, cross-linking of 4,4′-dihydroxybiphenyl (dihydroxy based building unit) led to the formation of HCP-92. After synthesis, both the compounds were washed with various solvents (such as tetrahydrofuran (THF), methanol,

chloroform, dimethylformamide (DMF), water) to remove oligomers and starting materials. Then both the compounds were kept in 1:1 THF-$CHCl_3$ mixture for solvent exchange to remove high boiling solvents with low boiling solvents. After three days both the compounds were desolvated under vacuum at ~ 100 °C to obtain guest free phases. Thus obtained desolvated HCPs was characterized with FT-IR spectroscopy, thermo-gravimetric analysis (TGA), EDX (Energy-dispersive X-ray spectroscopy) analysis, low temperature gas adsorption, solid-state ^{13}C-NMR etc. In FT-IR spectroscopy, peaks at 2923 cm^{-1} and 2857 cm^{-1} for HCP-91 and peaks at 2919 cm^{-1} and 2850 cm^{-1} for HCP-92 were found corresponding to the C-H stretching of the -CH_2- linkages (Appendix 4.1). Further, FT-IR peaks corresponding to the C=C bond stretching of aromatic rings were found to be present at 1612 cm^{-1} and 1469 cm^{-1} for HCP-91 and at 1646 cm^{-1} and 1461 cm^{-1} for HCP-92 respectively (Appendix 4.1). TGA profile of the desolvated phase of the HCP-91 revealed negligible change up to ~ 250 °C and after that continuous loss was observed (Appendix 4.2). Similarly for HCP-92, TGA profile showed negligible change in weight up to ~ 210 °C followed by a sharp decrease with increasing heating of the compound (Appendix 4.3). In addition, EDX elemental mapping showed the homogeneous distribution of carbon and oxygen throughout the samples for both HCP-91 and HCP-92 (Appendix 4.4-4.7). Solid state ^{13}C-NMR study of HCP-91 revealed the presence of the aromatic building block (broad peak at 116-154 ppm), i.e., 4-phenylphenol, along with cross linker -CH_2- group (broad peak at 20-40 ppm) (Appendix 4.8). As similar to the HCP-91, broad peak in the region of 110-160 ppm corresponding to the aromatic carbons of 4,4´-dihydroxybiphenyl affirmed the presence of the respective building unit and another broad peak at 22-40 ppm was found to corresponding to the methylene linkages (Appendix 4.9). Furthermore, low temperature (195 K) CO_2 adsorption study was carried out to check porosity of HCP-92. CO_2 uptake for HCP-92 was found to be 142 mLg^{-1} which was relatively less as compare to the HCP-91 (Appendix 4.10). This might be attributed to the pore blocking effect of more functionality in HCP-92. Furthermore, chemical stability of such compounds already been demonstrated in previous chapter with HCP-91.

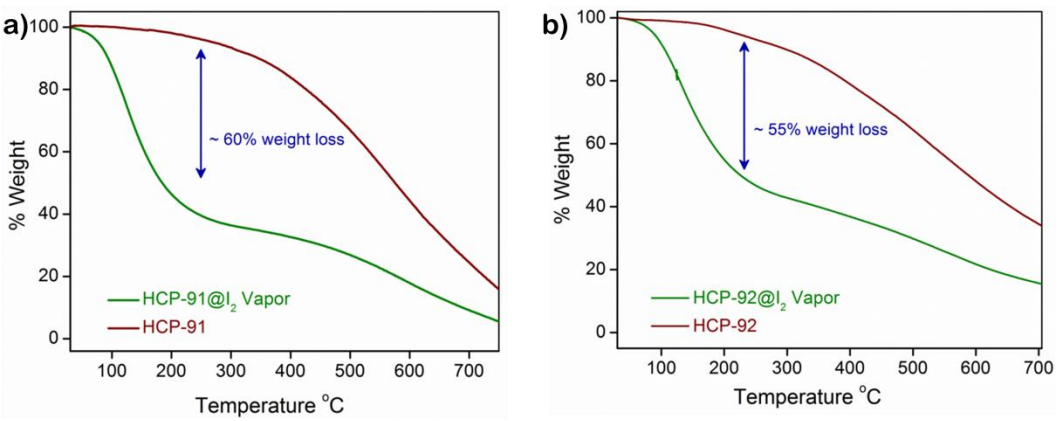

Figure 4.2: Thermo-gravimetric analysis profile of (a) HCP-91⊃I_2 and (b) HCP-92⊃I_2.

Thereafter, we sought to check the performance of both HCPs towards vapor phase iodine capture. For this we have taken ~ 2 gm of iodine in a 15 mL vial and 30 mg HCP was taken in another small vial and placed inside the 15 mL vial containing I_2 molecules (Fig. 4.1). This set up was kept at 75 °C for 96 hours. After that final weight of the compound has been taken. In case of HCP-91 ~ 41.9 mg iodine was taken by the 30 mg of porous materials while ~ 27.4 mg of I_2 uptake was found for HCP-92. Capacity for the both materials have been calculated from this study and it was found to be 2.4 g g^{-1} and 1.9 g g^{-1} for HCP-91 and HCP-92 respectively. Higher capacity for HCP-91 may be attributed to the higher porosity of the compound as compare to HCP-92. Iodine encapsulated phases were characterized with TGA, EDX analysis, etc. TGA profile for both the I_2 loaded compounds demonstrated ~ 60% and ~ 55% loss for the I_2 molecules inside the network for HCP-91 and HCP-92 respectively (Fig. 4.2). In addition, EDX elemental mapping also revealed the presence of iodine along with carbon and oxygen in both compounds (Appendix 4.11-4.12). This result showed that both HCP-91 and HCP-92 able to capture iodine in vapor phase.

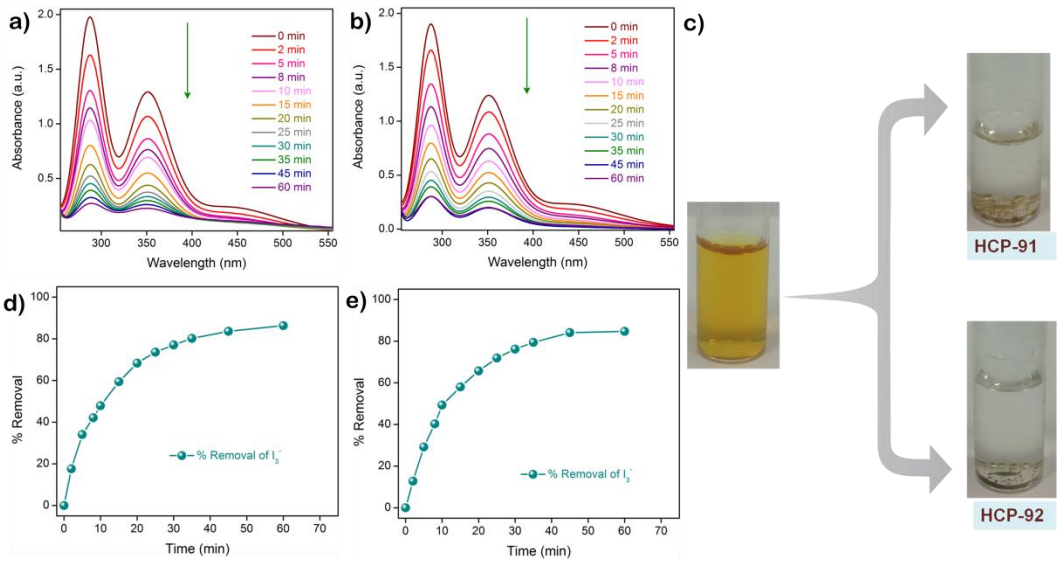

Figure 4.3: Titration curve of I_3^- ion water solution for (a) HCP-91 and (b) HCP-92; (c) Images of decolorization of I_3^- ion solution on treatment with HCP-91 and HCP-92; % removal profile with time of I_3^- ion for (d) HCP-91 and (e) HCP-92.

Enthused from this result we further sought to explore the I_3^- ion removal study from water with HCP-91 and HCP-92. Already, it has been stated that although iodine capture has been explored extensively in vapor phase, but iodine capture from water medium has been studied rarely in the domain of porous materials. For this study, 0.5 mM of I_3^- ion solution in water medium was taken and then absorbance of the solution was measured with the help of UV-Vis spectroscopy. The UV-Vis profile showed three absorbance peaks at 288 nm, 350 nm and 460 nm. To the solution, 2 mg of HCP-91 was then added and absorbance of the supernatant solution was monitored at different time intervals (Fig. 4.3a-4.3b). With increasing time decrease in the absorbance peaks was observed due to the removal of iodine from water with HCP-91. After 60 minutes almost colorless solution was found whereas the initial solution was dark straw yellow in color (Fig. 4.3c). After 60 min ~ 87% of I_3^- ion was removed with only 2 mg of HCP-91 (Fig. 4.3d and Appendix 4.13). In a similar way, iodine removal from water study was performed with HCP-92 (Appendix 4.14). In case of HCP-92, almost ~ 85% of I_3^- ion was found to get captured within 60 minutes (Fig. 4.3e). Further, capacity of HCP-91 and HCP-92 for I_3^- ion have been checked and it was found the both the compounds are efficient in terms of capacities also (HCP-91: 2.9 g gm^{-1} HCP-92: 2.49 g gm^{-1}) (Appendix 4.15-4.16). Iodine encapsulated phases were further characterized with solid state UV-Vis study and EDX analysis (Appendix 4.17-4.20). EDX data showed the presence of iodine in both the samples after capture study (Appendix 4.17-4.18). Elemental mapping from EDX study revealed the

homogeneous distribution of carbon, oxygen and iodine throughout the iodine encapsulated HCP-91 and HCP-92. In addition, peak around 350 nm in solid state UV-Vis study was clearly observed for iodine entrapped phase of both HCP-91 and HCP-92 (Appendix 4.19-4.20). On the other hand, in UV-Vis study I_3^- ion in water showed two peaks at 288 nm and 350 nm. Consequently, from solid state UV-Vis study the presence of I_3^- ion in the iodine entrapped phases of HCPs was affirmed. Moreover, kinetics for the iodine removal study with HCP-91 and HCP-92 was found to be well fitted with pseudo second order kinetics (Fig. 4.4a-4.4b). Rate constants were for this capture studies were found to be 4.89 x 10^{-4} g $mg^{-1}min^{-1}$ and 4.16 x 10^{-4} g $mg^{-1}min^{-1}$ for HCP-91 and HCP-92 respectively. In each cases adsorption isotherm was fitted in Freundlich isotherm model (Appendix 4.21-4.22). In addition, post I_3^- ion capture phases of the respective HCPs was checked for any leaching of volatile iodine via gravimetric analysis. Even after seven days no change in weight was observed which was corresponding to the no leaching of iodine from post I_3^- ion capture phases of the compounds (Appendix 4.23-4.24).

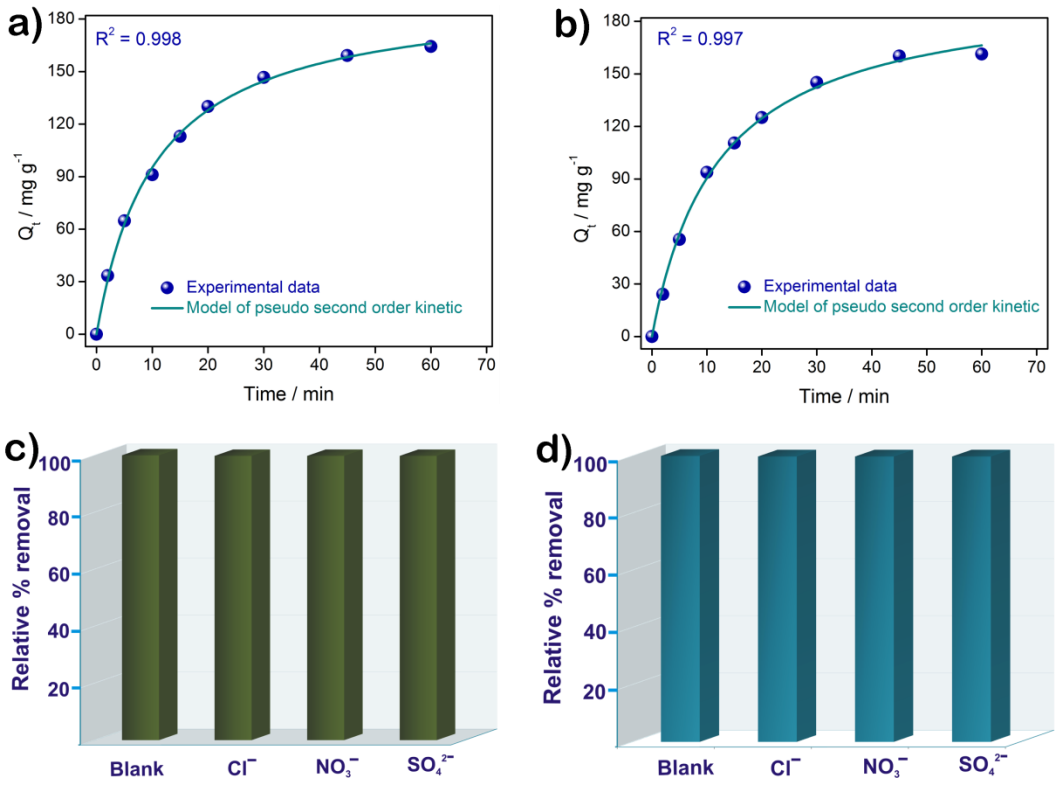

Figure 4.4: Kinetics profile of I_3^- ion capture study with (a) HCP-91 and (b) HCP-92; Bar diagram represents anion dependent removal of I_3^- ion from water with (c) HCP-91 and (d) HCP-92.

Since waste water contain soluble iodine along with other concurrent anions such as Cl^- ion, NO_3^- ion and SO_4^{2-} ion, we checked the performance of HCP-91 and HCP-92 in real time aspect. For this study, 1:1 mixture of I_3^- ion and other anions was taken and treated the mixed solution with HCPs. After 1 day UV-Vis spectroscopy was performed and it was observed that both the HCPs are capable enough to remove I_3^- ion from water even in presence omnipresent anions like Cl^- ion, NO_3^- ion and SO_4^{2-} ion (Fig. 4.4c-4.4d). Further, for both HCP-91 and HCP-92 recyclability was checked and even after three cycles both the compounds were found to be performed well (Appendix 4.25-4.26).

4.4 Conclusions

In conclusion, two chemically stable and cost-effective microporous hyper-cross-linked polymers (HCPs) were synthesized, namely, HCP-91 and HCP-92. Both the HCPs (HCP-91 and HCP-92) showed vapor phase capture of iodine at 75 °C. In addition, I_3^- ion capture was studied from water with HCP-91 and HCP-92 which is very rarely explored in the domain of porous materials. Due to the presence of -OH functionality inside the HCPs, efficient and rapid removal of I_3^- ion have been observed in both cases. Capacity of both the compounds for I_3^- ion were found to be very high and also kinetics (pseudo second order kinetics) also were found to be very fast. Since waste water may contain other anions like Cl^- ion, NO_3^- ion and SO_4^{2-} ion, we have performed the I_3^- ion capture study in presence of those omnipresent anions. Both the HCPs have shown considerable amount of I_3^- ion capture even in presence of those concurrent competing anions. We believe that this work will propel the research in the area of radioactive and hazardous iodine capture from water and vapor phase with such robust and cost-effective porous materials.

4.5 Appendix Section

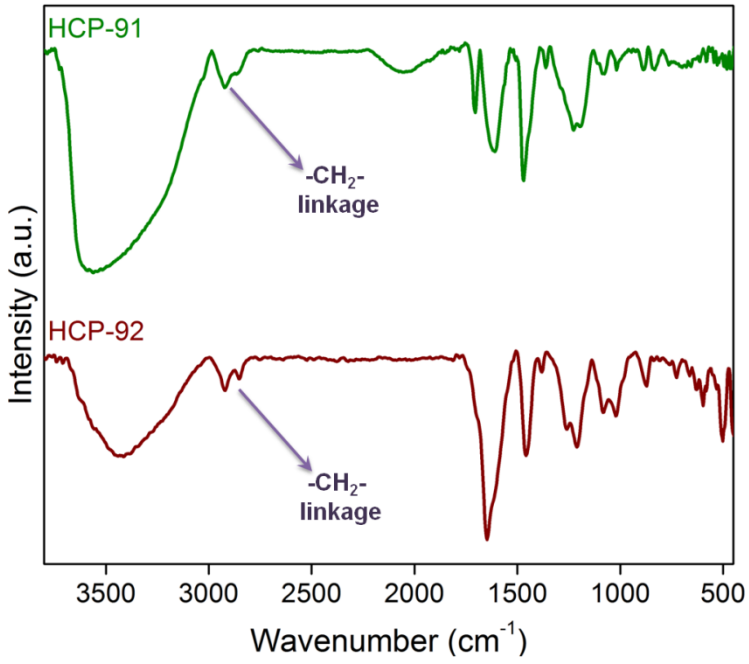

Appendix 4.1: FT-IR spectra of HCP-91 and HCP-92.

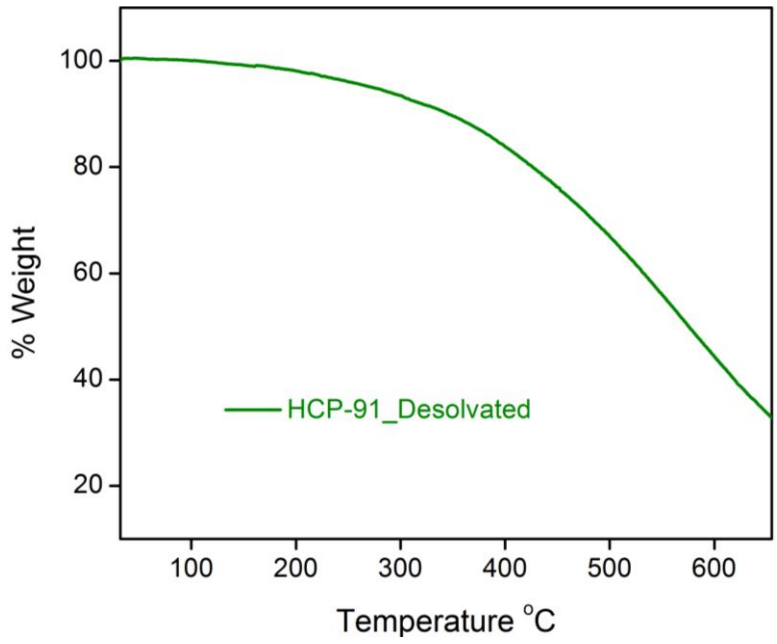

Appendix 4.2: Thermo-gravimetric analysis (TGA) profiles of desolvated HCP-91.

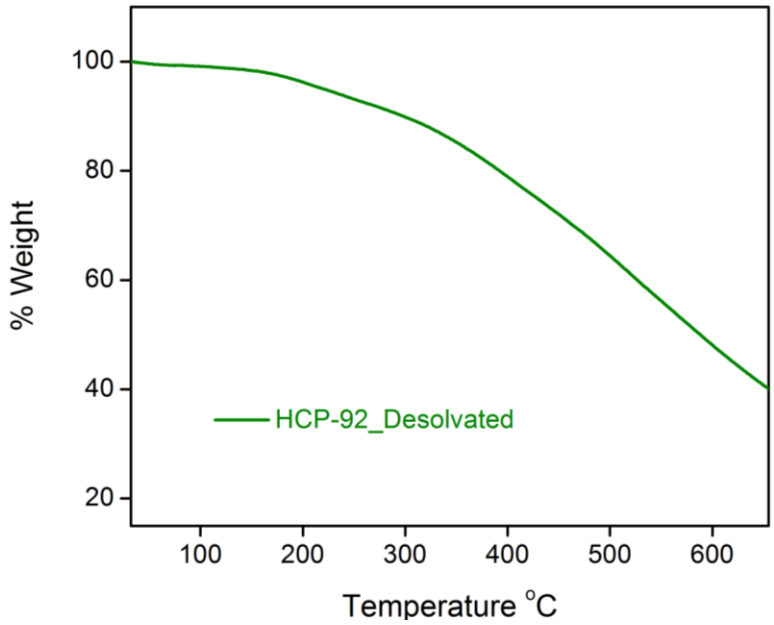

Appendix 4.3: Thermo-gravimetric analysis (TGA) profiles of desolvated HCP-92.

Element	Weight %
C	78.3
O	21.6

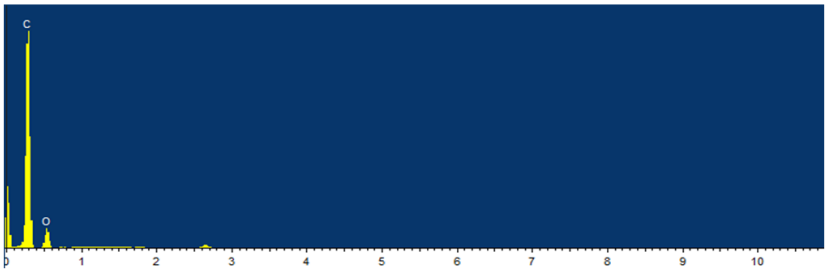

Appendix 4.4: EDX analysis of HCP-91.

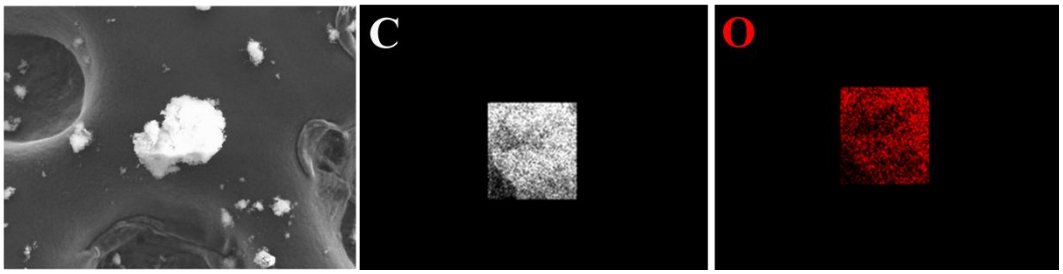

Appendix 4.5: Elemental mapping of HCP-91.

Element	Weight %
C	73.7
O	26.2

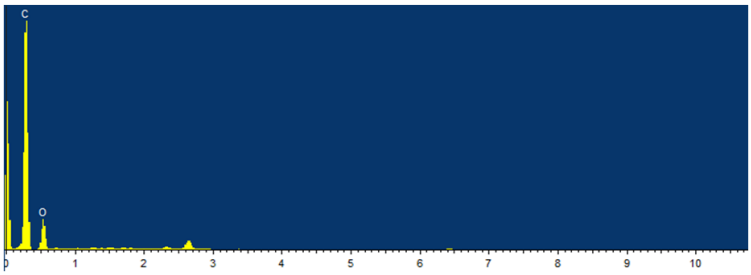

Appendix 4.6: EDX analysis of HCP-92.

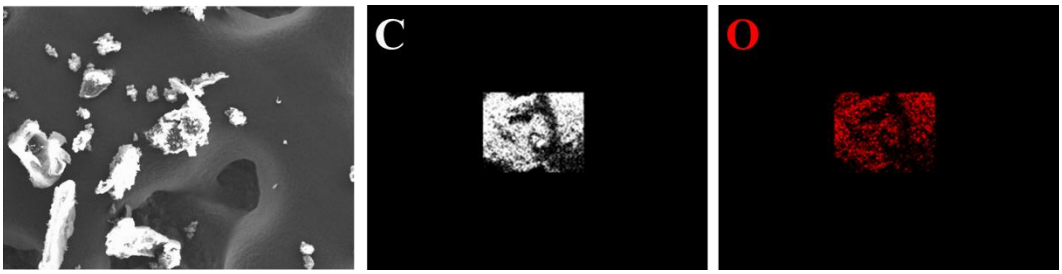

Appendix 4.7: Elemental mapping of HCP-92.

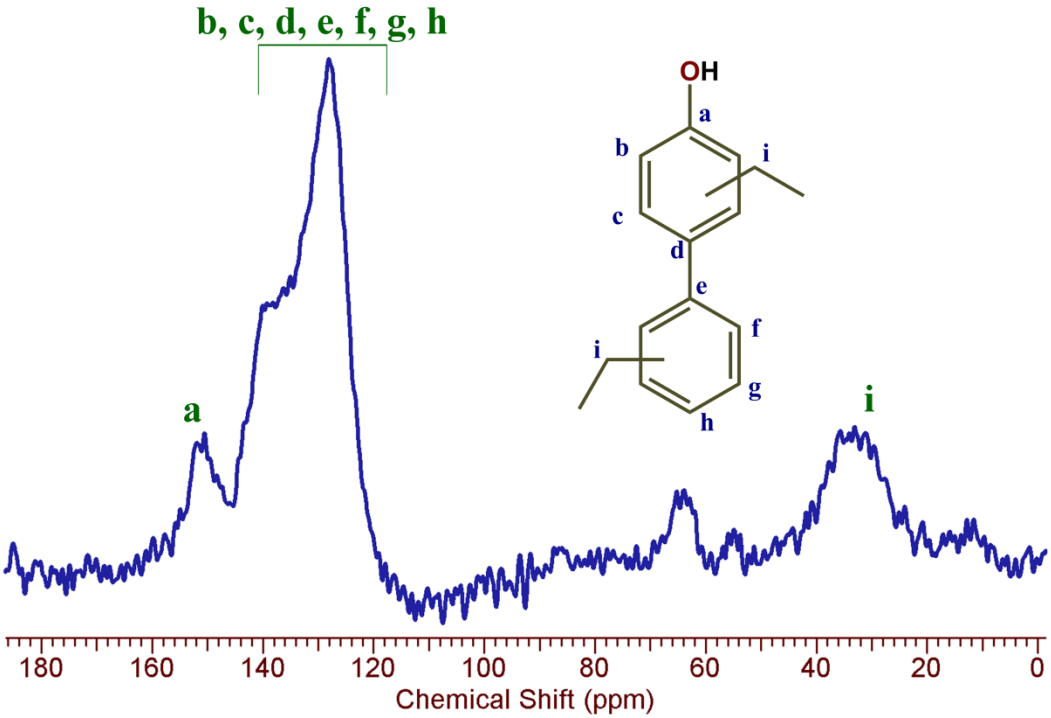

Appendix 4.8: Solid state ^{13}C-NMR of HCP-91.

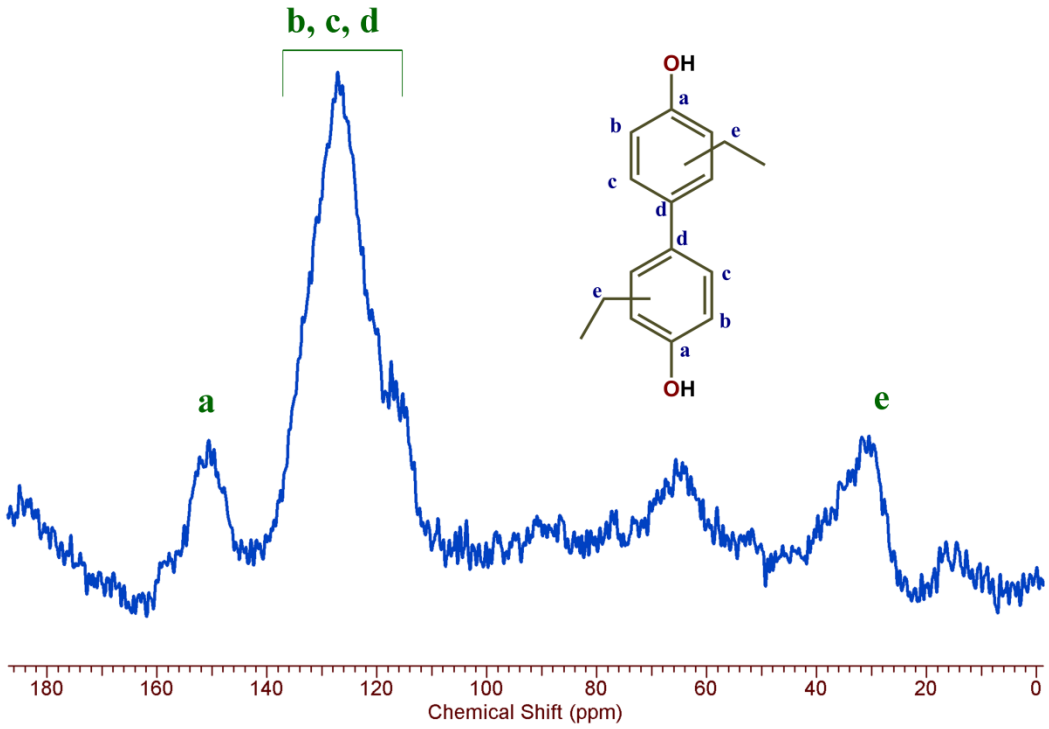

Appendix 4.9: Solid state ^{13}C-NMR of HCP-92.

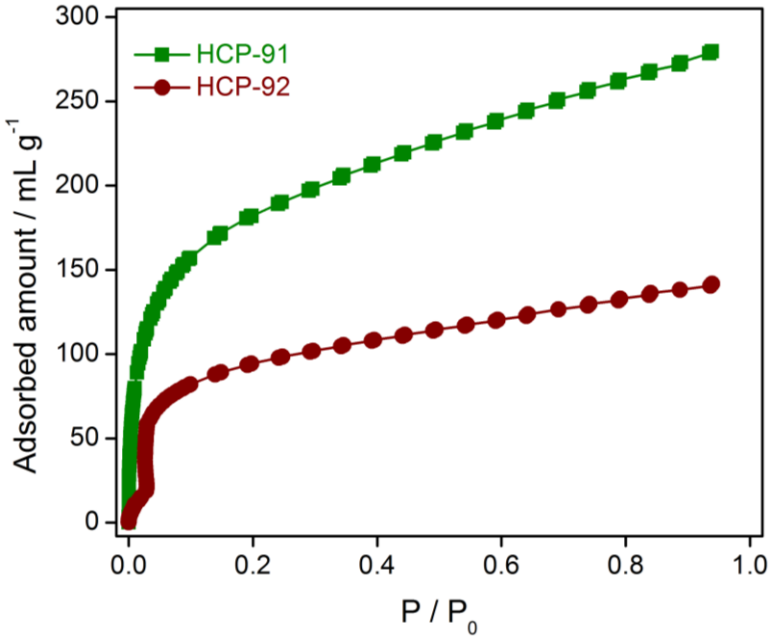

Appendix 4.10: Low temperature (195 K) CO_2 adsorption of HCP-91 (green) and HCP-92 (wine red).

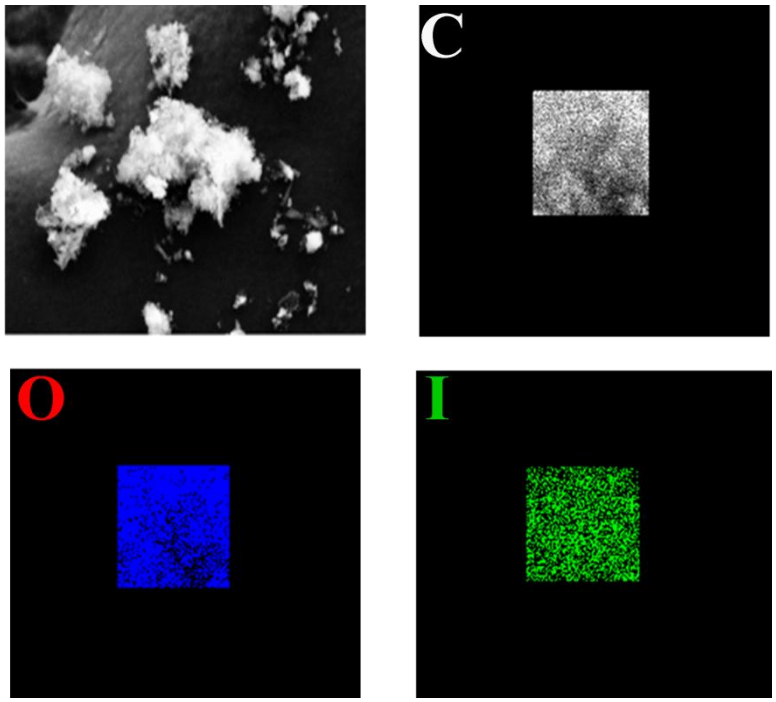

Appendix 4.11: Elemental mapping of HCP-91 after vapor phase iodine capture.

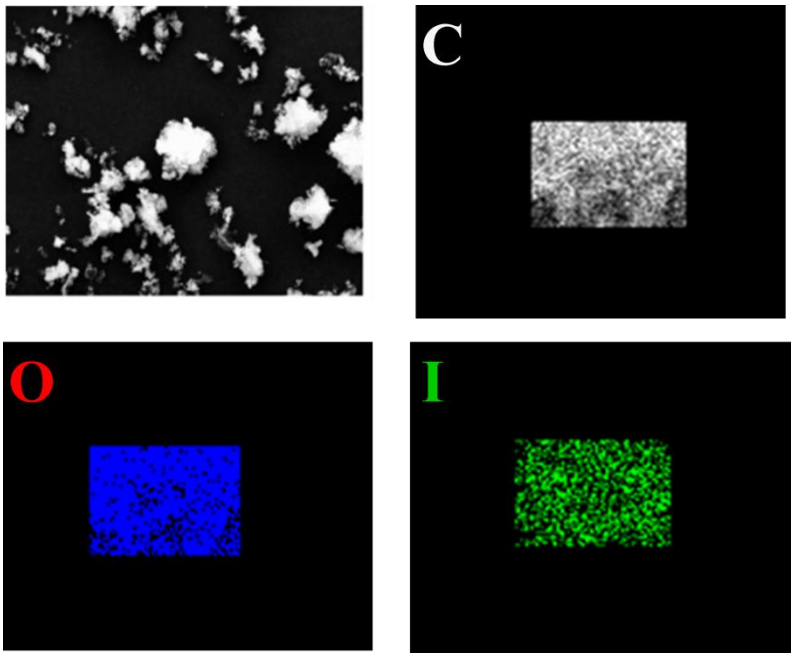

Appendix 4.12: Elemental mapping of HCP-92 after vapor phase iodine capture.

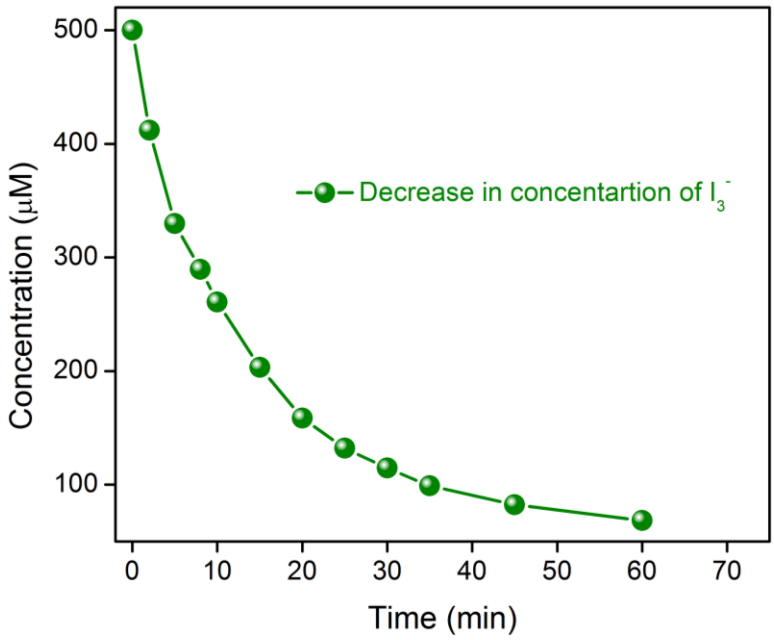

Appendix 4.13: Decrease in the concentration of I_3^- ion from water with HCP-91.

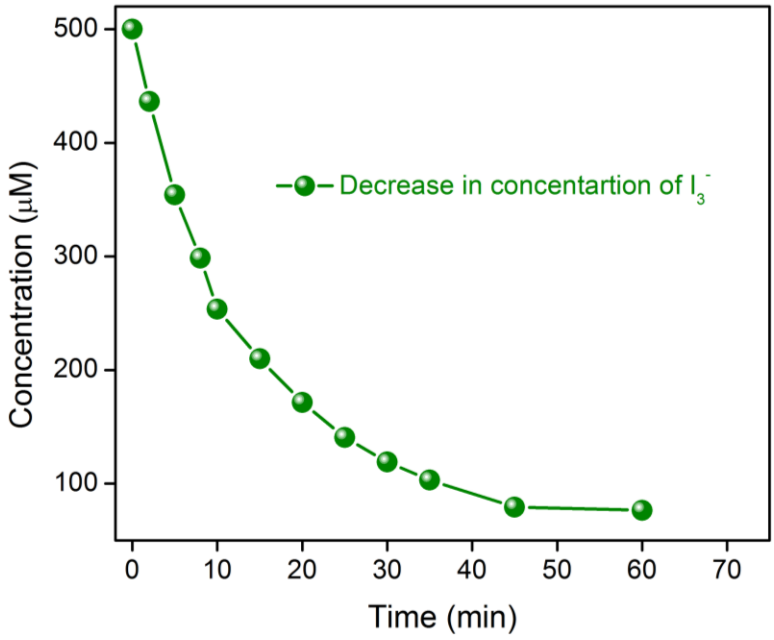

Appendix 4.14: Decrease in the concentration of I_3^- ion from water with HCP-92.

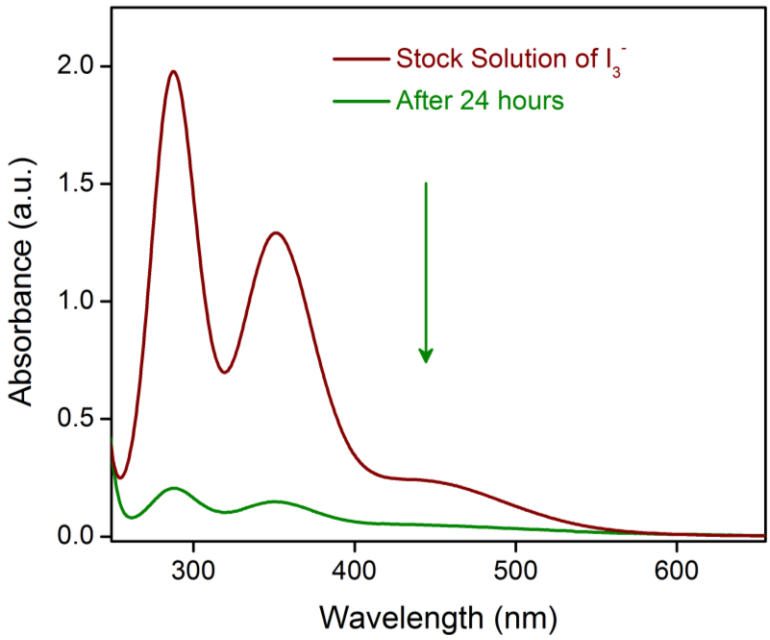

Appendix 4.15: UV-Vis spectra for the calculation of capacity for HCP-91.

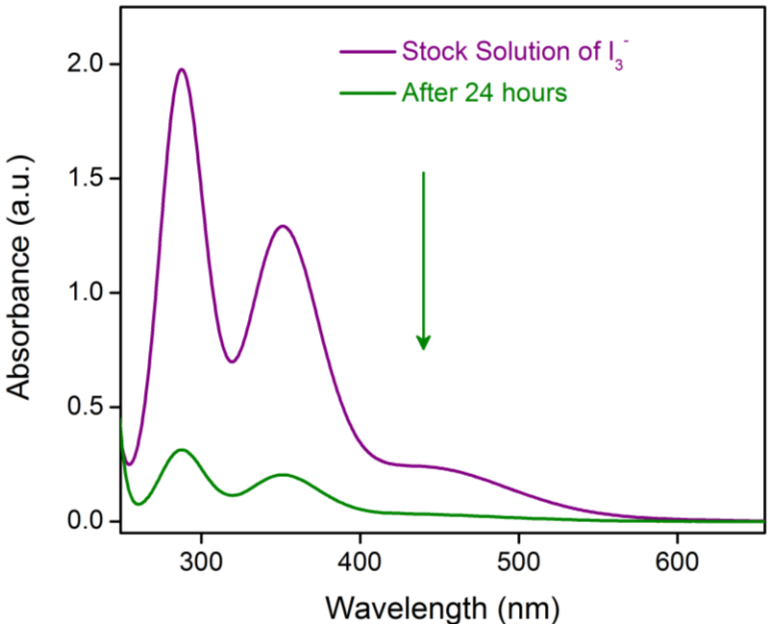

Appendix 4.16: UV-Vis spectra for the calculation of capacity for HCP-92.

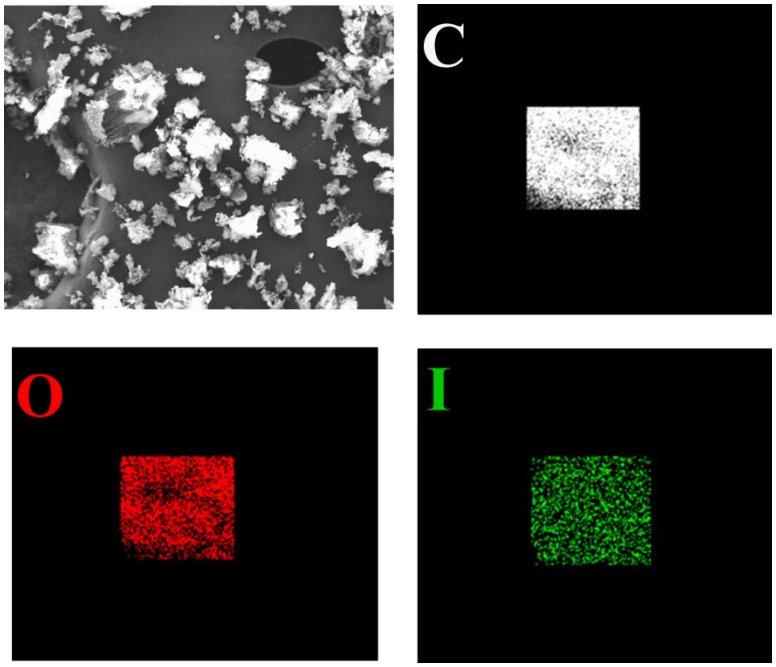

Appendix 4.17: Elemental mapping of I_3^- ion treated HCP-91.

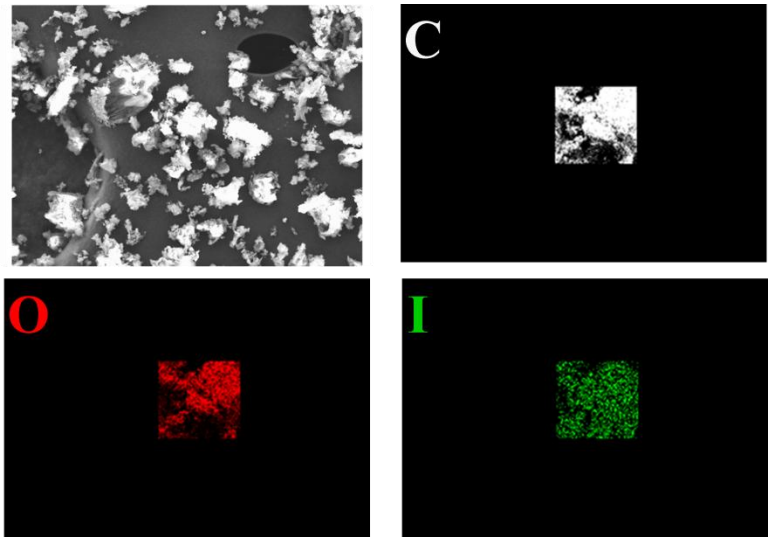

Appendix 4.18: Elemental mapping of I_3^- ion treated HCP-92.

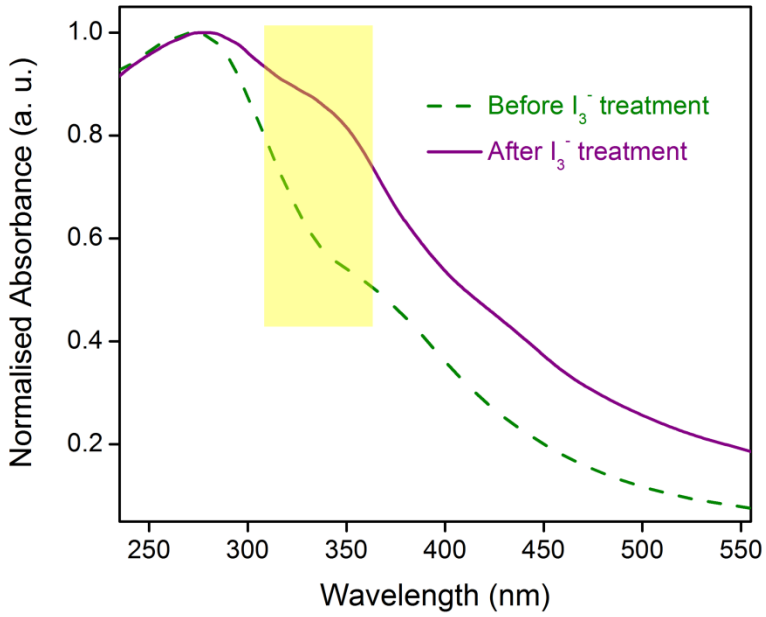

Appendix 4.19: Solid state UV-Vis spectra of HCP-91 after I_3^- ion capture study.

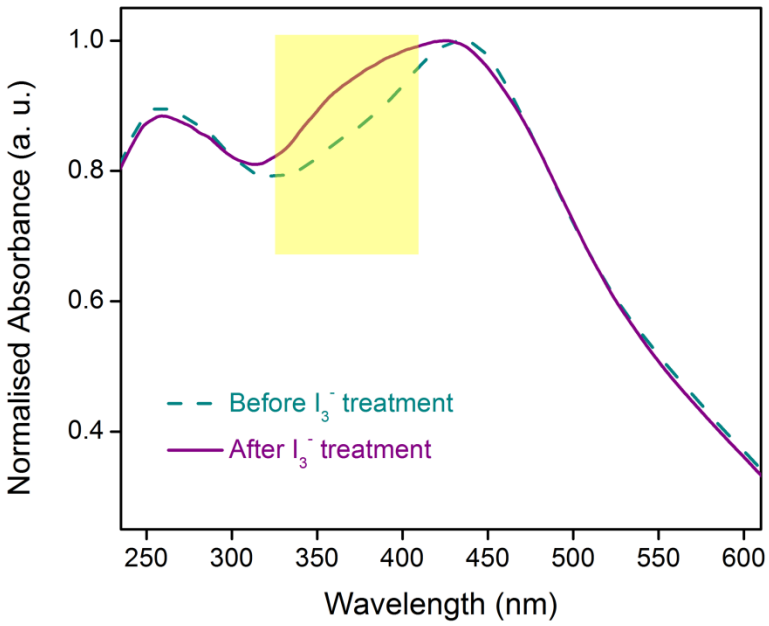

Appendix 4.20: Solid state UV-Vis spectra of HCP-92 after I_3^- ion capture study.

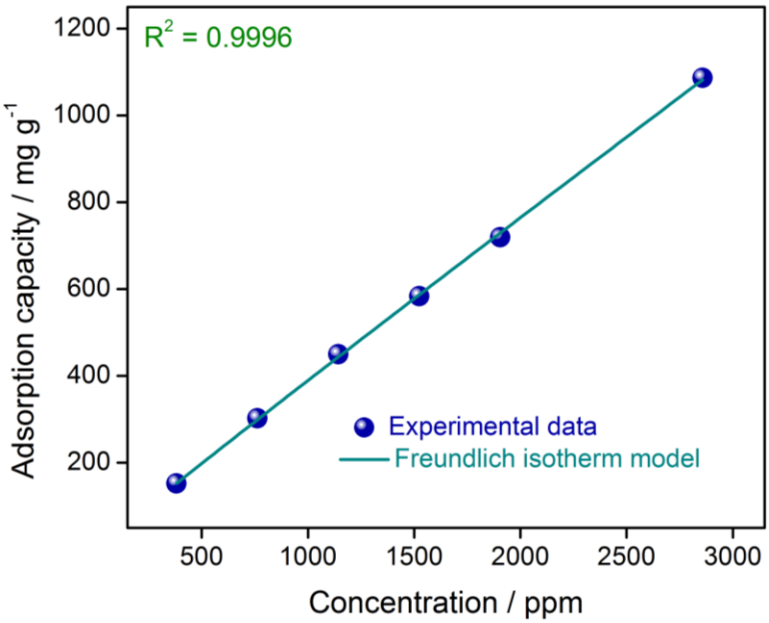

Appendix 4.21: Sorption isotherm of I_3^- ion capture study with HCP-91.

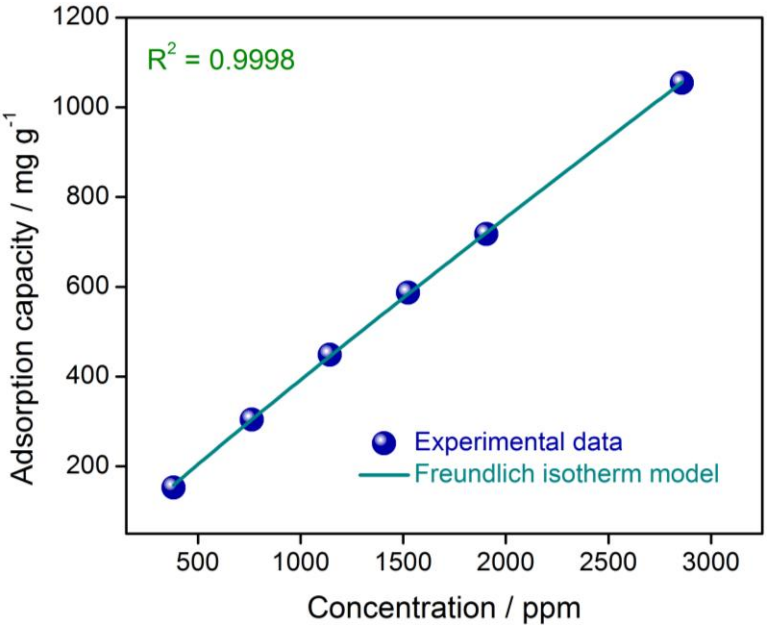

Appendix 4.22: Sorption isotherm of I_3^- ion capture study with HCP-92.

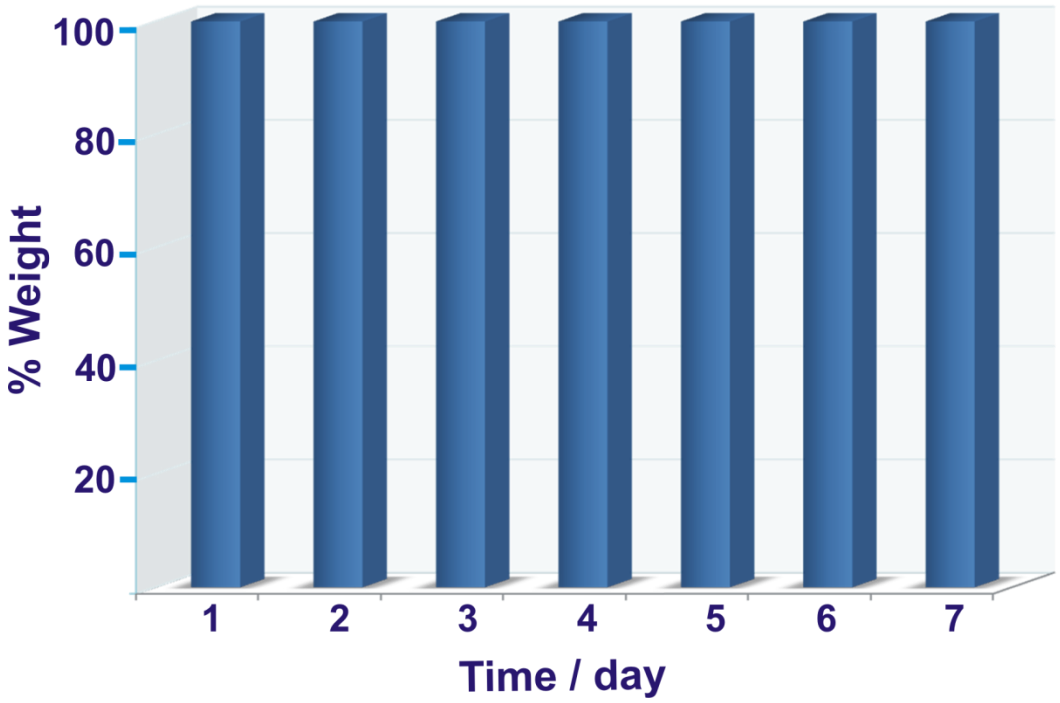

Appendix 4.23: Iodine leaching test of iodine encapsulated HCP-91 after I_3^- ion capture study via gravimetric analysis.

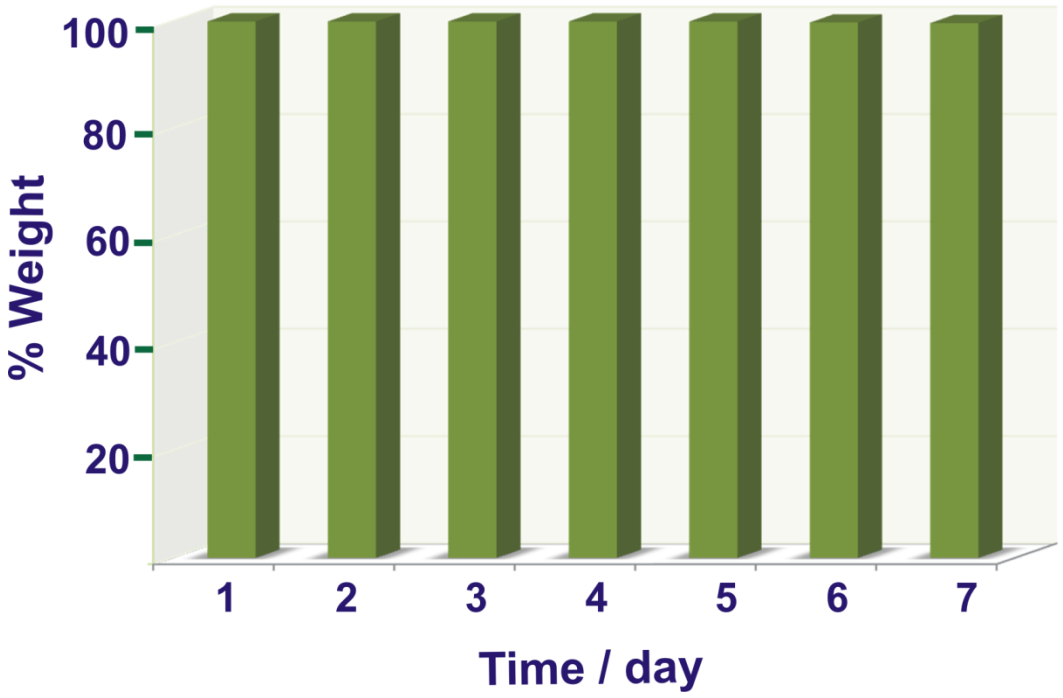

Appendix 4.24: Iodine leaching test of iodine encapsulated HCP-92 after I_3^- ion capture study via gravimetric analysis.

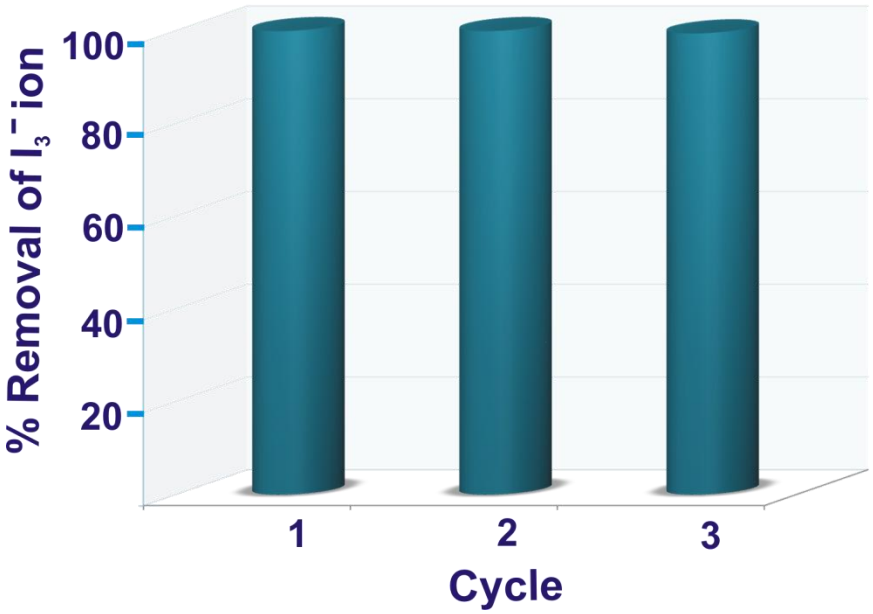

Appendix 4.25: Recyclability test of HCP-91 for I_3^- ion capture study.

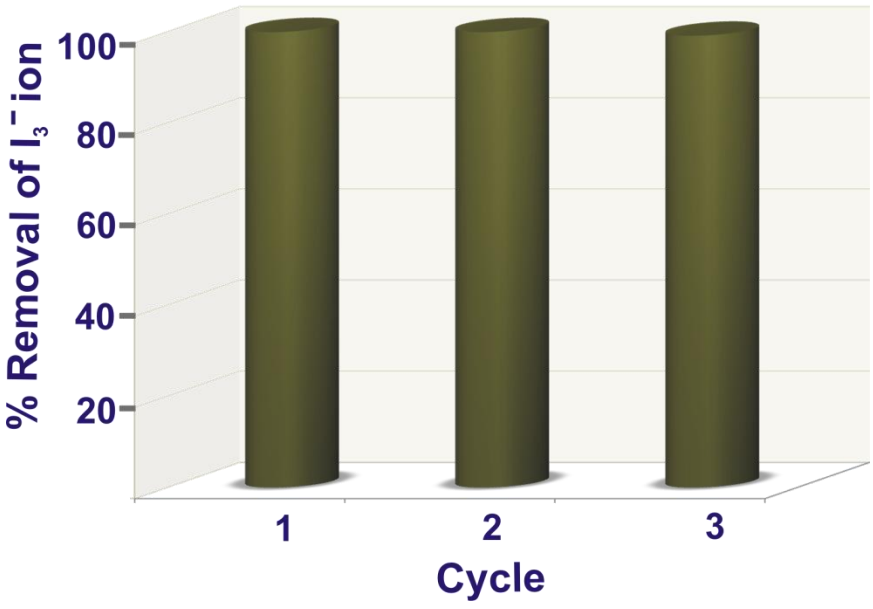

Appendix 4.26: Recyclability test of HCP-92 for I_3^- ion capture study.

4.6 References

1. (a) G. M. Naja and B. Volesky, *Heavy Met. Environ.*, 2009, **8**, 16–18. (b) C. Xiao, M. A. Silver and S. Wang, *Dalton Trans.*, 2017,**46**, 16381–16386.

2. (a) A. J. Howarth, Y. Liu, J. T. Hupp and O. K. Farha, *CrystEngComm*, 2015, **17**, 7245–7253. (b) N. Middleton, The Global Casino: An Introduction to Environmental Issues, Routledge New York, 2013.

3. (a) E. Kintisch, *Science*, 2005, **310**, 1406–1406. (b) R. C. Ewing and F. N. von Hippel, *Science*, 2009, **325**, 151–152. (c) J. D. Vienna, *Int. J. Appl. Glass Sci.*, 2010, **1**, 309–321.

4. D. F. Sava, M. A. Rodriguez, K. W. Chapman, P. J. Chupas, J. A. Greathouse, P. S. Crozier and T. M. Nenoff, *J. Am. Chem. Soc.*, 2011, **133**, 12398–12401.

5. (a) X. Guo, Y. Tian, M. Zhang, Y. Li, R. Wen, X. Li, X. Li, Y. Xue, L. Ma, C. Xia and S. Li, *Chem. Mater.*, 2018, **30**, 2299−2308. (b) W. J. Weber and F. P. Roberts, *Nucl. Technol.*, 1983, **60**, 178−198. (c) D. R. Haefner, and T. J. Tranter, Methods of Gas Phase Capture of Iodine from Fuel Reprocessing Off-Gas: A Literature Survey; Idaho National Laboratory: 2007. (d) F. C. Kuepper, M. C. Feiters, B. Olofsson, T. Kaiho, S. Yanagida, M. B. Zimmermann, L. J. Carpenter, G. W. Luther, Z. Lu, M. Jonsson, Angew. Chem., Int. Ed. 2011, 50, 11598-11620. (e) A. Saiz-Lopez, J. M. C. Plane, A. R. Baker, L. J. Carpenter, R. von Glasow, J, C. G. Martin, G. McFiggans and R. W. Saunders, Chem. Rev. 2012, 112, 1773-1804.

6. (a) G. Steinhauser, *Environ. Sci. Technol.*, 2014, **48**, 4649–4663. (b) M. I. Ojovan and W. E. Lee, An Introduction to Nuclear Waste Immobilisation, Elsevier Science, Amsterdam, 2005.

7. C. E. Strickland, C. D. Johnson, B. D. Lee, N. P. Qafoku, J. E. Szecsody, M. J. Truex and V. R. Vermeul, Identification of Promising Remediation Technologies for Iodine in the UP-1 Operable Unit. *Pacific Northwest National Laboratory*, 2017.

8. G. Mushkacheva, E. Rabinovich, V. Privalov, S. Povolotskaya, V. Shorokhova, S. Sokolova, V. Turdakova, E. Ryzhova, P. Hall, A. B. Schneider, D. L. Preston and E. Ron, *Radiat. Res.*, 2006, **166**, 715-722.

9. C. Neal, M. Neal, H. Wickham, L. Hill and S. Harman, *Hydrol. Earth Syst. Sci.*, 2007, **11**, 283-293.

10. (a) Z. Jaworowski, *Science*, 2001, **293**, 605−606. (b) A. Zonenberg, M. Leoniak and W. Zarzycki, *Endokrynol. Polym.*, 2006, **57**, 38−44. (c) M. Hosoda, S. Tokonami, H. Tazoe, A. Sorimachi, S. Monzen, M. Osanai, N. Akata, H. Kakiuchi, Y. Omori, T. Ishikawa, S. T. Sahoo, T. Kovács, M. Yamada, A. Nakata, M. Yoshida, H. Yoshino, Y. Mariya and I. Kashiwakura, *Sci. Rep.*, 2013, **3**, 2283−2288.

11. (a) UN Scientifi c Committee on the Effects of Atomic Radiation (UNSCEAR). UNSCEAR 2008 report volume II. Report to the general assembly with scientifi c annexes: sources and effects of ionizing radiation. 2011. http://www.unscear.org/docs/reports/2008/11-80076_Report_2008_Annex_D.pdf (accessed May 20, 2016). (b) S. Suzuki, Childhood and adolescent thyroid cancer in Fukushima after the Fukushima Daiichi nuclear power plant accident: 5 years on. *Clin Oncol (R Coll Radiol)*, 2016, **28**, 263–271. (c) Health effects of the Chernobyl accident: an overview, Report by World Health Organization, April 2006.

12. (a) "Developments in the Removal of Airborne Iodine Species with Metal Substituted Zeolites": D. T. Pence, F. A. Duce, W. J. Maeck in Proceedings of the 12th AEC Air Cleaning Conference, August 1972, Paper No. CONF-720823. (b) R. T. Jubin, Organic Iodine Removal from Simulated Dissolver Off-Gas Streams Using Silver Exchanged Mordenite, In Proceedings of the 16th DOE Nuclear Air Cleaning Conference, 1981, Paper No. CONF-8208322.

13. (a) K. W. Chapman, P. J. Chupas and T. M. Nenoff, *J. Am. Chem. Soc.*, 2010, **132**, 8897-8899. (b) B. J. Riley, J. D. Vienna, D. M. Strachan, J. S. McCloy and J. L. Jerden, *J. Nucl. Mater.*, 2016, **470**, 307-326.

14. (a) L. Mohanambe and S. Vasudevan, *Inorg. Chem.*, 2004, **43**, 6421–6425. (b) T. Hertzsch, F. Budde, E. Weber and J. Hîlliger, *Angew. Chem. Int. Ed.*, 2002, **41**, 2281–2284. (c) Z. M. Wang, B. Zhang, H. Fujiwara, H. Kobayashi and M. Kurmoo, *Chem. Commun.*, 2004, 416–417. (d) H. J. Choi and M. P. Suh, *J. Am. Chem. Soc.*, 2004, **126**, 15844-15844. (e) C. E. Willans, S. French, K. M. Anderson, L. J. Barbour, J. -A. Gertenbach, G. O. Lloyd, R. J. Dyer, P. C. Junk and J. W. Steed, *Dalton Trans.*, 2011, **40**, 573–582. (f) D. F. Sava, M. A. Rodriguez, K. W. Chapman, P. J. Chupas, J. A. Greathouse, P. S. Crozier and T. M. Nenoff, J. Am. Chem. Soc., 2011, 133, 12398-12401. (g) D. F. Sava, K. W. Chapman, M. A. Rodriguez, J. A. Greathouse, P. S. Crozier, H. Zhao, P. J. Chupas and T. M. Nenoff, Chem. Mater.

2013, 25, 2591-2596. (h) B. F. Abrahams, M. Moylan, S. D. Orchard, R. Robson, Angew. Chem. Int. Ed. 2003, 42, 1848–1851. (i) T. J. Garino, T. M. Nenoff, J. L. Krumhansl and D. X. Rademacher, *J. Am. Ceram. Soc.*, 2011, **94**, 2412–2419. (j) D. Shetty, J. Raya, D. S. Han, Z. Asfari, J. -C. Olsen, and A. Trabolsi, *Chem. Mater.*, 2017, **29**, 8968−8972. (k) F. Ren, Z. Zhu, X. Qian, W. Liang, P. Mu, H. Sun, J. Liu and A. Li, *Chem. Comm.*, 2016, **52**, 9797-9800. (l) X. Guo, Y. Tian, M. Zhang, Y. Li, R. Wen, X. Li, X. Li, Y. Xue, L. Ma, C. Xia, and S. Li, *Chem. Mater.*, 2018, **30**, 2299−2308. (m) Z. Yan, Y. Yuan, Y. Tian, D. Zhang, and G. Zhu, *Angew. Chem. Int. Ed.*, 2015, **54**, 12733–12737. (n) P. Wang, Q. Xu, Z. Li, W. Jiang, Q. Jiang, and D. Jiang, *Adv. Mater.*, 2018, DOI: 10.1002/adma.201801991. (o) K. Jie, Y. Zhou, E. Li, Z. Li, R. Zhao and F. Huang, *J. Am. Chem. Soc.*, 2017, **139**, 15320−15323. (p) K. S. Subrahmanyam, C. D. Malliakas, D. Sarma, G. S. Armatas, J. Wu and M. G. Kanatzidis, *J. Am. Chem. Soc.*, 2015, **137**, 13943−13948. (q) S. Ma, S. M. Islam, Y. Shim, Q. Gu, P. Wang, H. Li, G. Sun, X. Yang and M. G. Kanatzidis, *Chem. Mater.*, 2014, **26**, 7114−7123. (r) Z. M. Wang, Y. J. Zhang, T. Liu, M. Kurmoo and S. Gao, *Adv. Funct. Mater.*, 2007, **17**, 1523–1536. (s) M. H. Zeng, Q. X. Wang, Y. X. Tan, S. Hu, H. X. Zhao, L. S. Long and M. Kurmoo, *J. Am. Chem. Soc.*, 2010, **132**, 2561–2563. (t) G. Das, T. Skorjanc, S. K. Sharma, F. Gándara, M. Lusi, D. S. S. Rao, S. Vimala, S. K. Prasad, J. Raya, D. S. Han, R. Jagannathan, J. -C. Olsen and A. Trabolsi, *J. Am. Chem. Soc.*, 2017, **139**, 9558–9565. (u) L. Dobrzan´ska, G. O. Lioyd, H. G. Raubenheimer and L. J. Barbour, *J. Am. Chem. Soc.*, 2006, **128**, 698–699. (v) G. Das, T. Prakasam, S. Nuryyeva, D. S. Han, A. Abdel-Wahab, J. -C. Olsen, K. Polychronopoulou, C. Platas-Iglesias, F. Ravaux, M. Jouiad, A. Trabolsi, *J. Mater. Chem. A*, 2016, **4**, 15361−15369. (w) Y. Zhu, Y. -J. Ji, D. -G. Wang, Y. Zhang, H. Tang, X. -R. Jia, M. Song, G. Yu and G. -C. Kuang, *J. Mater. Chem. A*, 2017, **5**, 6622–6629.

15. (a) Y. Lin, X. Jiang, S. T. Kim, S. B. Alahakoon, X. Hou, Z. Zhang, C. M. Thompson, R. A. Smaldone and C. Ke, *J. Am. Chem. Soc.*, 2017, **139**, 7172−7175. (b) J. Chen, Q. Gao, X. Zhang, Y. Liu, P. Wang, Y. Jiao and Y. Yang, *Sci. of the Total Environ.*, 2019, **646**, 634–644. (c) X. Zhao, H. Xiao, Z. Li, H. Huang, D. Liu and C. Zhong, *Appl. Surf. Sci.*, 2015, **351**, 760–764.

16. (a) L. Tan and B. Tan, *Chem. Soc. Rev.*, 2017, DOI: 10.1039/c6cs00851h. (b) B. Li, R. Gong, W. Wang, X. Huang, W. Zhang, H. Li, C. Hu, and B. Tan, *Macromolecules*, 2011, **44**, 2410–2414. (c) R. Dawson, T. Ratvijitvech, M. Corker, A. Laybourn, Y. Z. Khimyak, A. I. Cooper and D. J. Adams, *Polym. Chem.*, 2012, **3**, 2034–2038. (d) P. Samanta, P. Chandra and S. K. Ghosh, *Beilstein J. Org. Chem.*, 2016, **12**, 1981.

17. (a) R. Dawson, E. St€ockel, J. R. Holst, D. J. Adams and A. I. Cooper, *Energy Environ. Sci.*, 2011, **4**, 4239–4245. (b) Y. Luo, B. Li ,W. Wang, K. Wu and B. Tan, *Adv. Mater.*, 2012, **24**, 5703–5707. (c) R. Dawson, L. A. Stevens, T. C. Drage, C. E. Snape, M. W. Smith, D. J. Adams, and A. I. Cooper, *J. Am. Chem. Soc.*, 2012, **134**, 10741−10744. (d) X. Jing, D. Zou, P. Cui, H. Ren and G. Zhu, *J. Mater. Chem. A*, 2013, **1**, 13926–13931. (e) S. Bhunia, B. Banerjee and A. Bhaumik, *Chem. Commun.*, 2015, **51**, 5020-5023. (f) J. Wang, W. Sng, G. Yi and Y. Zhang, *Chem. Commun.*, 2015, **51**, 12076-12079. (f) R. T. Woodward, L. A. Stevens, R. Dawson, M. Vijayaraghavan, T. Hasell, I. P. Silverwood, A. V. Ewing, T. Ratvijitvech, J. D. Exley, S. Y. Chong, F. Blanc, D. J. Adams, S. G. Kazarian, C. E. Snape, T. C. Drage and A. I. Cooper, *J. Am. Chem. Soc.*, 2014, **136**, 9028−9035.

Chapter 5

Chemically Stable Viologen-based Organic Network for Efficient Removal of Hazardous Oxo-anions from Water

5.1 Introduction

Increasing water pollution has become a global concern in recent years and remediation of such toxic pollutants has drawn much attention worldwide. Pollution due to metal derived oxo-anions (CrO_4^{2-}, TcO_4^-, SeO_3^{2-}, AsO_4^{3-} etc.) has become one of the pressing challenges as most of them are omnipresent in environment.[1] Especially, Cr(VI) based oxo-anions are found to be very carcinogenic and mutagenic to living system.[2] Understanding the importance, the EPA (Environmental Protection Agency, U.S.) has included such oxo-anions in the priority pollutant list.[3] Chromate has been found in wide range of applications in various industries like leather tanning, textile dyes and pigments, steel manufacturing, wood preservation, electroplating etc., where only tanning industries discharge ~30-35 liters of Cr(VI) contaminated water for each kilogram of leather.[4] It also affects the vitrification of low activity radioactive waste as it forms spinels and resulted into weakening the integrity of waste glass.[5] Further, Hinkley groundwater contamination is one of the well known disaster caused by dumped Cr(VI) in California.[6] Other than this case, several more incidents was found and moreover, the problems are still continued, which has led researchers to design affordable and efficient techniques to capture Cr(VI) based oxo-anions.[7] Apart from chromate, another oxo-anion pertechnetate (TcO_4^-) ion has also appealed much concern as one isotope of technetium (^{99}Tc) is radioactive element with very high half-life time (2.1×10^5 years). ^{99}Tc has been found to be formed as nuclear fission product of ^{235}U or ^{239}Pu with a high fission yield. Upto 2010 it has been estimated that ~305 metric tons of ^{99}Tc has been produced from weapons testing and nuclear reactors.[8] Further, Tc exists mostly as TcO_4^- in environment, which is highly soluble in water with high mobility. As a consequence of this, TcO_4^- may exist in the low level waste also. Till date different techniques have been employed for removal of oxo-anions, like ion exchange, chemical precipitation, adsorpion, electrodialysis, photocatalysis etc.[9] Ion exchange method has been considered as efficient technique over other owing to low cost, comparatively simple and safe, efficient performance even for waste having low concentration of pollutants etc.[10] Although several anion exchange resins have been reported, but poor selectivity, poor exchange kinetics and lack of stability has led researchers on rendering new materials for efficient oxo-anions capture from water.[11] As an alternative, porous cationic framework based materials, such as layered double hydroxides (LDHs), metal-organic frameworks (MOFs) etc., have emerged in recent years.[12] Recent reports has shown that both MOFs and LDHs materials can be a useful for the removal of toxic and hazardous anionic pollutants from waste water.[13]

Progress in the domain of porous materials has skyrocketed over the past few decades due to their wide range of applications. Among them metal-organic frameworks (MOFs) and lately evolved porous organic materials have seen much progress in recent years over congener materials, because of features like

amenability in the design, high surface area and tuneable pore surface as per requirements.[14] Although MOFs have been employed to captue oxo-anions from water, but lack of sufficient physiochemical stability of most of the MOFs and difficulties in the bulk scale synthesis have hindered their applications.[15] In contrast, porous organic materials are constructed from strong covalent bonds which resulted into high physiochemical stability. Such stability have made them one of the frontrunner in the domain of porous materials and it has been witnessed that for real time applications stability has gained much priority over direct structure property correlation.[16] These compounds have already acquired much attention in the field of gas adsorption, catalysis, drug delivery, fuel cell applications etc.; but very rarely employed to capture hazardous oxo-anions from water.[17] To execute anion capture via ion exchange, cationic network with exchangeable anions is primary requirement. But direct synthesis of such cationic organic frameworks has rarely been explored.[18] In the literature very few reports are present on direct synthesis of ionic organic frameworks and viologen based organic frameworks are one of them, which have been synthesized via Schiff base reaction, Sonogashira−Hagihara coupling, Menshutkin reaction and trimerisation of -CN groups.[19] Zincke's reaction is one of the effective tool to synthesize viologen based compounds in a single step, but this reaction has not been used much to synthesize extended porous organic networks.[20] Trabolsi & co-workers have shown that the morphologies of compounds can be different depending on the polarity of solvents used during synthesis, which can directly influence the properties of those compounds.[20a] Owing to such structural diversity and chemical stability, cationic frameworks can be well suited for capture of hazardous anionic pollutants from water. Herein, we have demonstrated efficient capture of toxic oxo-anions with a viologen based organic network (compound-1) owing to its chemical stability and free exchangeable anions (Fig. 5.1).

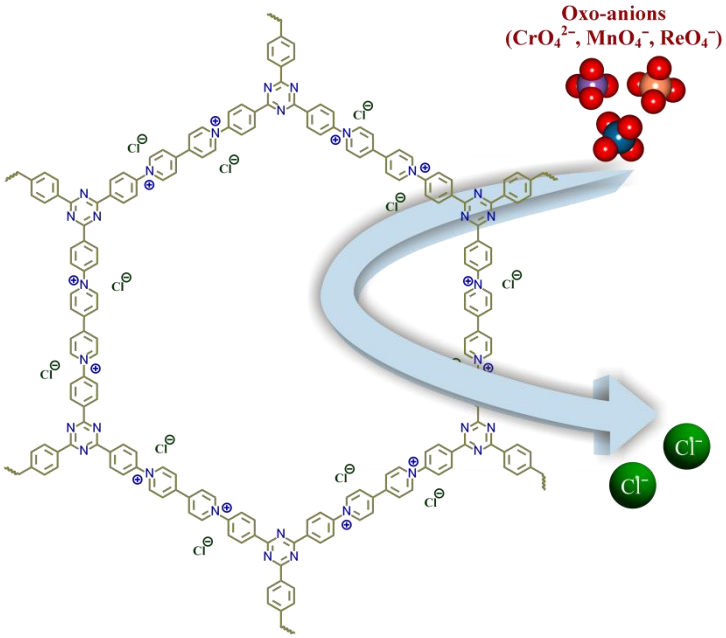

Figure 5.1: Schematic representation of the oxo-anions capture with compound-1.

5.2 Experimental

5.2.1 Materials:

4,4´-dipyridyl, 1-chloro-2,4-dinitrobenzene and 4-aminobenzonitrile were purchased from Sigma-Aldrich, $KReO_4$ was purchased from Alfa-Aesar; triflic acid, $KMnO_4$ and K_2CrO_4 and all other solvents were purchased locally. Thus obtained chemicals were used without any further purification.

5.2.2 Physical Measurements:

All Infra-red (IR) Spectra were recorded by using NICOLET 6700 FT-IR spectrophotometer and by using KBr pellet in the range of 400-4000 cm^{-1}. Thermo-gravimetric analysis (TGA) was recorded on Perkin-Elmer STA 6000 TGA analyser under N_2 atmosphere with heating rate of 10 °C/min. Gas adsorption measurements were carried out by using BelSorp-max instrument from Bel Japan. FESEM was done by using FEI Quanta 3D dual beam ESEM at 30KV. UV spectra were acquired on Shimadzu UV 2600 Spectrophotometer.

5.2.3 Synthesis:

Synthesis of 4,4',4''-(1,3,5-triazine-2,4,6-triyl)trianiline (Precursor 1): Precursor 1 has been synthesised from 4-aminobenzonitrile via acid catalyzed trimerisation reaction by following a previously reported protocol.[21]

Synthesis of 1,1'-bis(2,4-dinitrophenyl)-4,4'-bipyridinium dichloride (Precursor 2): Precursor 2 has also been synthesised by following previously reported protocol.[22]

Synthesis of compound-1: Compound-1 has been synthesized via Zincke reaction of precursor 1 and 2 (Scheme 5.1). First, a schlenk tube was charged with 560 mg precursor 2 (1 mmol) and 177 mg of precursor 1 (0.5 mmol); then 20 mL ethanol (EtOH), 20 mL 1,4-dioxane and 20 mL of Cl-benzene were added respectively to the reaction mixture. After that the reaction mixture was purged with N_2 gas and allowed to reflux for 2 days at that condition. After completion of the reaction the reaction mixture was filtered and washed with different solvents like dimethylformamide (DMF), water, tetrahydrofuran (THF), MeCN, acetone, methanol (MeOH) and dichloromethane (DCM) to remove unreacted materials and small polymers (oligomers). A brown colored solid material was obtained, which further has been kept in a 1:1 mixture of chloroform and THF to exchange guest molecules (with high boiling point) with low boiling solvent molecules. After 4 days compound was filtered off and heated at ~ 100 °C under vacuum to remove the occluded guest molecules. Yield: 240 mg.

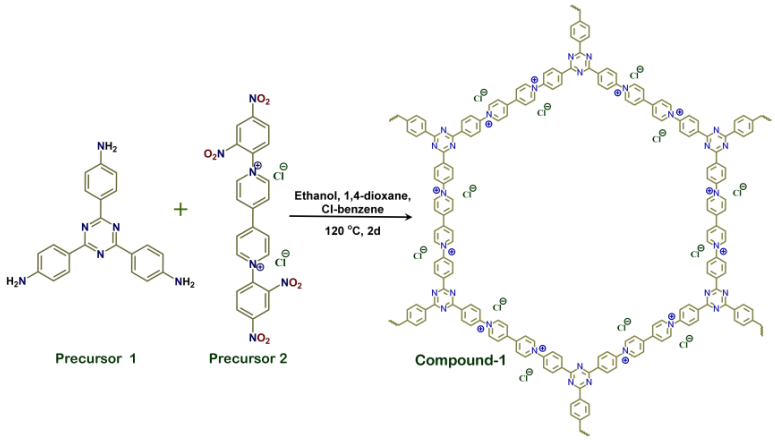

Scheme 5.1: Synthesis scheme of compound-1.

5.2.4 Time dependent study of oxo-anion removal:

First, In case of CrO_4^{2-} removal study, we have taken 2 mL aqueous solution of 0.25 mM CrO_4^{2-} ion in a cuvette and recorded the initial absorbance with UV-Vis spectroscopy. To the cuvette, 1 mg of desolvated compound-1 has been added and after several time intervals we have recorded the corresponding

absorbance spectra of the supernatant solution. In a similar way, we have carried out the UV-Vis spectroscopy for MnO_4^- and ReO_4^- ions. But in this case, we have taken an aqueous solution of 0.5 mM for each MnO_4^- and ReO_4^- ion. Further from this time dependent study we have calculated % removal and decrease in concentration of oxo-anions vs time by using the following equation,[17j]

$$D_t = \frac{C_0 - C_t}{C_0} \text{ x } 100\% = \frac{A_0 - A_t}{A_0} \text{ x } 100\%$$

$$i.e., \qquad C_t = C_0 - \frac{A_0 - A_t}{A_0} \text{x } C_0$$

Where, D_t is the exchange capacity, C_0 and A_0 are initial concentration and absorbance of the oxo-anion solution respectively, C_t and A_t, are concentration and absorbance of the oxo-anion solution at specific times respectively.

Further, kinetic data for CrO_4^{2-} and ReO_4^- ions were fitted in pseudo second-order model with the help of following equation,[12i]

$$Q_t = \frac{k_2 Q_e^{\,2} t}{1 + k_2 Q_e t}$$

where, t is the time in minute, Q_t and Q_e are the amount of adsorbate (mg gm^{-1}) onto adsorbent at the different time intervals and equilibrium respectively.

5.2.5 Study of oxo-anion trapping in presence of competing anions:

In this study, we have taken Cl^-, Br^-, NO_3^- and SO_4^{2-} ions as the competing anions, which are omnipresent in the common water sources and waste waters. We have taken equimolar (2.5 mM; 1:1) aqueous solution of targeted oxo-anion and the competing anion. To the mixture 2 mg of desolvated compound-1 has been added and stirred for 18 hours. After 18 hours, solution was filtered off to separate the compound-1 and the solution was characterised with UV-Vis spectroscopy. Thus obtained solution was diluted 10 times to measure the UV-Vis spectroscopy and further the capture efficiency of compound-1 in presence of other anions has been studied by comparing with blank (Blank: only 2.5 mM of oxo-anion has been taken instead of mixture). Along with UV-Vis spectroscopy, this study has been affirmed also from ICP-AES analyses.

5.2.6 Calculation of capacity:

5 mg of desolvated compound-1 has been kept with 2.5 mL of 5 mM oxo-anion solution for 24 hours at stirring condition. After 1 day compound-1 has been filtered out and the filtrate has been used for further

characterisation. UV-Vis measurement has been carried out by diluting the solution. From the initial and final absorbance value of the oxo-anion solution we have calculated the storage capacity of compound-1 in 1 day by using the following equation, [17j]

$$\boldsymbol{Q_t = \frac{(C_0 - C_t) * V}{m}}$$

Where, Q_t, C_0, C_t, V and m are the capacity of adsorbent, initial concentration of oxo-anion solution, concentration of the oxo-anion solution at specific times, volume of the solution and mass used for the adsorbent respectively. Further, the capacity for compound-1 has been rechecked with ICP-AES analyses.

5.2.7 Recyclability test of compound-1:

Compound-1⊃oxo-anion (10 mg) has been regenerated with 3M HCl solution (2 mL) by keeping for ~20 hours.[35] Reusability of the regenerated material has been checked with 5 mL of 1 mM oxo-anion (CrO_4^{2-} and ReO_4^-) solutions. After ~20 hours, concentration of the oxo-anion solution was measured with UV-Vis spectroscopy. This study has been repeated upto four cycles for each cases (CrO_4^{2-} and ReO_4^- ions). Further, similar method has been employed for the column where 3M HCl has been passed through the column to regenerated the material. And then CrO_4^{2-} ion solution was passed through the column to check the performance.

5.2.8 Adsorption isotherm experiment:

Compound-1 (5 mg) was immersed in 2 mL water solution of oxo-anion having different concentration (in case of CrO_4^{2-} ion concentration was taken in the range of 29-580 ppm and for ReO_4^- ion the range of concentration is 62.5-1251 ppm). After 2 hours UV-Visible spectroscopy was carried out with the supernatant solution and further fitted with following equation,

Langmuir model, $$Q_e = \frac{Q_m C_e}{K_d + C_e}$$

where, C_e (ppm) and Q_e (mg gm^{-1}) are the oxo-anion concentration at equilibrium and amount of oxo-anion adsorbed at equilibrium respectively. Q_m (mg gm^{-1}) is the maximum amount of oxo-anion per unit mass of adsorbent to form a complete monolayer. K_d (mg/L) is a constant related to the affinity of the binding sites.

Freundlich Model, $$Q_e = K_F C_e^{1/n}$$

where, K_F and 1/n are the Freundlich model constants, indicating capacity and intensity of adsorption, respectively.

5.2.9 pH-dependent capture study:

Compound-1 (2 mg) was immersed in 2 mL solution of 2.5 mM oxo-anion (in case of CrO_4^{2-} ion pH-1.7, pH-4, pH-9, pH-10 and pH-12.4 were used, whereas for ReO_4^- ion pH-9, pH-10 and pH-12.4 were used) and stirred for 24 hours. After 1 day UV-Vis study was carried out to check the removal efficiency of compound-1. Following equation has been used for calculation and compared with the data at pH-7 for relative performance, [17j]

$$\boldsymbol{D_t = \frac{C_0 - C_t}{C_0} \text{ x } 100\% = \frac{A_0 - A_t}{A_0} \text{ x } 100\%}$$

Where, D_t is the exchange capacity, C_0 and A_0 are initial concentration and absorbance of the oxo-anion solution respectively, C_t and A_t, are concentration and absorbance of the oxo-anion solution at specific times respectively.

5.3 Results and discussion

Compound-1 has been synthesized from precursor 1 and 2 via Zincke's reaction and found to be insoluble in various solvents which indicated the formation of extended network (Scheme 5.1). Coskun & co-workers recently reported the structure of compound-1, synthesized via trimerisation of -CN groups in an ionothermal method.[19b] Very recently Wen & co-workers reported the compound via Zincke's reaction with same precursors, but different reaction condition resulted into different morphology of material and further employed for electrosynthesis of H_2O_2.[20c] Further, to remove occluded solvent molecules, compound-1 was kept in $CHCl_3$-THF (1:1) for 4 days and then desolvated under vacuum at ~100 °C. Desolvated phase was characterized with fourier transform infra-red (FT-IR) spectroscopy, thermo-gravimetric analysis (TGA), solid state ^{13}C-NMR, gas adsorption, field emission scanning electron microscope (FE-SEM) and EDX analysis. Almost negligible change in weight upto ~ 250 °C in TGA profile revealed the desolvation of compound-1 (Appendix 5.1). Replacement of the 2,4-dinitroaniline via Zincke's reaction from precursor-2 has been confirmed by the FT-IR, as peak at ~1550 cm^{-1} (for -NO_2 groups) disappeared in compound-1 (Appendix 5.2). The amount of N_2 uptake (at 77 K) was found to be 34.2 mLg^{-1}, such low uptake corroborated to the presence of Cl^- ions in compound-1 (Appendix 5.3). Further, CO_2 adsorption at 195 K has showed strong hysteresis in desorption profile due to interaction between Cl^- ions and CO_2 molecules (Appendix 5.4). Solid state ^{13}C-NMR study supported the presence

of triazine core along with the viologen moiety in compound-1 (Appendix 5.5). The presence of Cl^- ions was verified by EDX analysis (Appendix 5.6-5.8). Further, to check chemical stability, we kept compound-1 (25 mg) in 2 M HCl and 2 M KOH solution respectively for 7 days. After 1 week we found negligible change in the weight for each and further characterized with FT-IR, TGA, FE-SEM and EDX analysis. No change in the FT-IR peak positions affirmed no changes in functional groups (Appendix 5.9). Morphologies of acid-base treated phases of compound-1 were also found to be unaltered in FE-SEM study (Appendix 5.10). The decomposition temperatures for each compounds were also found at similar position as that of compound-1, which indicated that the networks remained similar (Appendix 5.13).

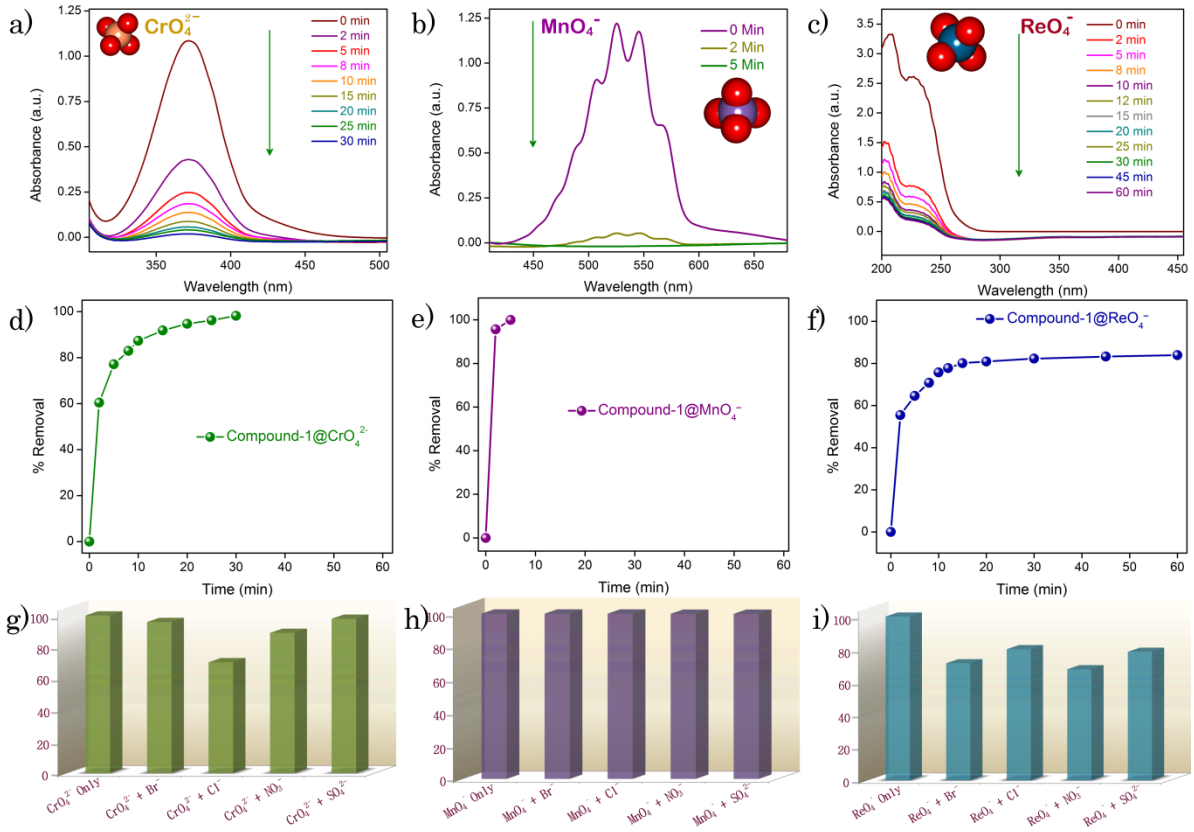

Figure 5.2: UV-Vis spectroscopy in presence of compound-1 at different time intervals for the water solution of (a) CrO_4^{2-} ion, (b) MnO_4^- ion and (c) ReO_4^- ion; Removal (in %) of (d) CrO_4^{2-} ion, (e) MnO_4^- ion and (f) ReO_4^- ion with compound-1 at different time intervals; Bar diagram represents the removal efficiency of compound-1 in presence of anions like Cl^-, Br^-, NO_3^- and SO_4^{2-} for (g) CrO_4^{2-} ion, (h) MnO_4^- ion and (i) ReO_4^- ion.

Enthused from such physiochemical stability and presence of the free Cl^- ions inside compound-1, we sought to check anion exchange study in water medium. Due to ionic nature of compound-1, it was well

dispersed in water which can be an advantage for anion exchange studies. Further, yellow color of CrO_4^{2-} solution turned colorless with time when compound-1 was added to it. Encouraged from this observation, we thought to perform the CrO_4^{2-} ion capture study from water with compound-1 and monitored with UV-Visible spectroscopy. In situ titration was carried out with 0.25 mM of CrO_4^{2-} ion (2 mL) in water with 1 mg of compound-1 by monitoring absorption peak at 372 nm (λ_{max} for CrO_4^{2-}) in UV-Vis spectrum (Fig. 5.2a). UV-Vis spectra of the supernatant at different time intervals revealed continuous decrease of the peak at 372 nm due to removal of CrO_4^{2-} ion. Almost 77% removal of CrO_4^{2-} ion was observed by compound-1 in only 5 min and reached ~98.25% with saturation in 30 min with the decolorization of the solution (Appendix 5.14-5.15). The % removal vs time plot showed rapid capture of CrO_4^{2-} ion with compound-1 (Fig. 5.2d). Further, capacity of compound-1 for CrO_4^{2-} ion was calculated (133 mg g^{-1}) from UV-Vis study and further verified with ICP-AES analysis (Appendix 5.16). Notably, capacity of compound-1 for CrO_4^{2-} can be counted as one of the highest values in the regime of porous material (Appendix Table 1). Peak at 894 cm^{-1} in FT-IR spectra revealed the presence of CrO_4^{2-} in compound-1⊃CrO_4^{2-} (Appendix 5.17). Also, appearance of Cr in EDX analysis affirmed capture of CrO_4^{2-} in compound-1, whereas FE-SEM study showed no change in morphology (Appendix 5.18-5.20).

Apart from CrO_4^{2-}, TcO_4^- ion also accounted as hazardous water pollutant due to radioactive nature of ^{99}Tc. As handling such radioactive species is not convenient in common laboratory, we have taken MnO_4^- and ReO_4^- as model ions which are non-radioactive surrogate for TcO_4^-. Further, MnO_4^- and ReO_4^- ions are close chemical analogue of TcO_4^- ion (Mn, Tc and Re belong to same group in periodic table) and also size of TcO_4^- ion is in between of MnO_4^- and ReO_4^- ions which will help to mimic real time scenario. Detailed studies of removal of MnO_4^- and ReO_4^- ions from water has been performed as similar to CrO_4^{2-} ion capture. Here, 2 mL of 0.5 mM solutions of each oxo-anion have been used to perform the study with 1 mg of compound-1. For MnO_4^- ion, the capture study was monitored at 525 nm (λ_{max}) while for ReO_4^- ion at 208 nm (λ_{max}) (Fig. 5.2b-5.2c). For MnO_4^- ion a rapid decrease in the absorption spectra was observed and within 5 minutes the solution got decolorized from purple (Appendix 5.21). As the size of ReO_4^- ion is much bigger, a relatively slow kinetic was observed as compared to both MnO_4^- and CrO_4^{2-} ion. The presence of MnO_4^- and ReO_4^- ion in compound-1⊃MnO_4^- and compound-1⊃ReO_4^- were affirmed by FT-IR and EDX analysis. The peaks at ~902 cm^{-1} and ~918 cm^{-1} have been observed in FT-IR spectra for MnO_4^- and ReO_4^- ions respectively (Appendix 5.22-5.23). EDX analysis revealed the presence of Mn and Re corresponding to their oxo-anions; whereas the absence of Cl^- also confirmed the anion exchange phenomenon (Appendix 5.24-5.27). FESEM revealed the morphology of compound-1⊃MnO_4^- and compound-1⊃ReO_4^- remained similar as that of compound-1 (Appendix 5.28-5.29). Further, time dependent decrease in concentration as well as % removal of oxo-anions from water have

been calculated from UV-Vis profiles (Fig. 5.2e-5.2f, Appendix 5.30-5.31). Almost 99.9% of MnO_4^- ion has been removed within 5 min, while for bulky ReO_4^- ion >80% has been achieved with 1 mg of compound-1 within only 60 minutes (Fig. 5.2e-5.2f). Enthused from this, we checked the capacity of compound-1 for each oxo-anions from UV-Vis studies (Appendix 5.32-5.33) and further verified from ICP-AES analyses. Notably, high capacities of each oxo-anions (MnO_4^-: 297.3 mg g^{-1} ReO_4^-: 517 mg g^{-1}) are again one of the highest values in the domain of porous materials (Table S2). Further, it has been found that removal of both CrO_4^{2-} and ReO_4^- ions with compound-1 follows the pseudo second order kinetics (Appendix 5.37-5.38).

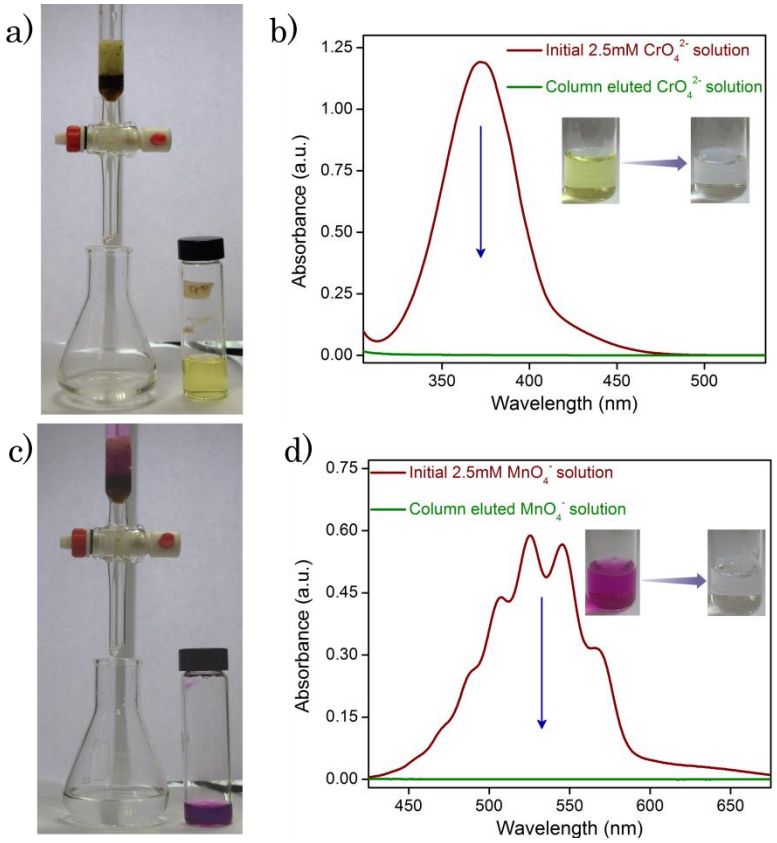

Figure 5.3: (a) Image and (b) UV-Vis spectra of the 2.5 mM CrO_4^{2-} solution before and after passing through the compound-1 loaded packed column; (c) Image and (d) UV-Vis spectra of the 2.5 mM MnO_4^- ion solution before and after passing through the compound-1 loaded packed column.

By virtue of such high capacity, we thought to explore the oxo-anion capture by mimicking real time situation. Waste water contains other competing anions (Cl^-, NO_3^-, SO_4^{2-} etc.) along with the targeted oxo-anions. In this regard, we have performed binary mixture studies for all oxo-anions with different

competing anions (Cl^-, Br^-, NO_3^- and SO_4^{2-}). Considerable amount of capture of respective oxo-anions have been observed even in presence of competing anions (Fig. 5.2g-5.2i). Removal of MnO_4^- ion remains undisturbed even in presence of other anions, while ≥80% ReO_4^- has been captured by compound-1 from mixture (Fig. 5.2h-5.2i). In case of CrO_4^{2-} ion, efficient removal was observed in presence of Br^-, NO_3^- and SO_4^{2-} ions (Fig. 5.2g). Only mixture of Cl^-:CrO_4^{2-} ions exhibited a relatively less efficiency (~70%) which may be due to the presence of Cl^- ions in both compound-1 and solution. This binary mixture study showed the efficiency of compound-1 to capture oxo-anions even in presence of competing anions. In addition, since pH of the waste water can vary in different ranges, we have performed removal of CrO_4^{2-} ion in both acidic and alkaline medium (Appendix 5.39). While as TcO_4^- ion is mostly found in alkaline medium, we have demonstrated the removal of ReO_4^- ion in alkaline medium (Appendix 5.40). Again, reusability of compound-1 has been tested with 3M HCl solution. In case of both CrO_4^{2-} and ReO_4^- ions, compound-1 was found to be maintaining its efficiency without any significant changes upto four cycles (Appendix 5.41-5.42). This study has shown that compound-1 is also stable even after the capture of respective oxo-anions and regeneration with 3M HCl, and has been further useful for the capture of those anions over a period of cycles. Moreover, a chromatographic column has been prepared embedded with compound-1 and employed for removal of oxo-anion from water (Appendix 5.43). 2.5 mM stock solution of each oxo-anions has been passed through the column. For MnO_4^- and CrO_4^{2-} ions, distinct color change of the eluent has been noticed, as a consequence of getting captured by compound-1 (Fig. 5.3a and 5.3c). Further, UV-Vis studies revealed the absence of oxo-anions in the eluted water, which ascertained such compound-1 based column can be useful for removal of toxic oxo-anions (Fig. 5.3b, 5.3d and Appendix 5.44). To validate whether the process is anion exchange or surface adsorption in the column, water was passed through the compound-1⊃oxo-anion loaded column. Colorless eluent affirmed the anion exchange process discarding any option of surface adsorption. In addition, as the compound-1 can be regenerated after treating with 3M HCl solution, we have tried reuse the column in a similar way. When 3M HCl has been passed through the column yellow colored solution has come out corresponding to the Cr(VI) oxo-anion (Appendix 5.45). And the column has been used further for second cycle of CrO_4^{2-} ion capture study (Appendix 5.46).

5.4 Conclusions

In conclusion, rapid capture of oxo-anions from water have been demonstrated with an ionic viologen based covalently linked organic network (compound-1) owing to its chemical stability of and presence of free exchangeable Cl^- ions inside the network. Rapid decolorization of the yellow colored CrO_4^{2-} solution

was observed due to the removal of CrO_4^{2-} ions from water in presence of compound-1. Further, to study the capture of radioactive ^{99}Tc based oxo-anion (TcO_4^-), close analogue MnO_4^- and ReO_4^- have been used as surrogate of TcO_4^-. Capacities for each oxo-anions were found to be high and comparable with some of well studied materials known for their highest capacities. As waste water contains competing anions like Cl^-, NO_3^-, SO_4^{2-} etc. along with toxic oxo-anions, we have demonstrated efficient capture of oxo-anions with compound-1 even in concurrent presence of competing anions. This result demonstrate a unique class of feature where dual capture of toxic oxo-anions has been well performed by a porous organic material which is not common in this domain. We believe, this result can open up a new avenue for the capture of toxic anions based on the ionic porous covalently linked organic materials.

5.5 Appendix Section

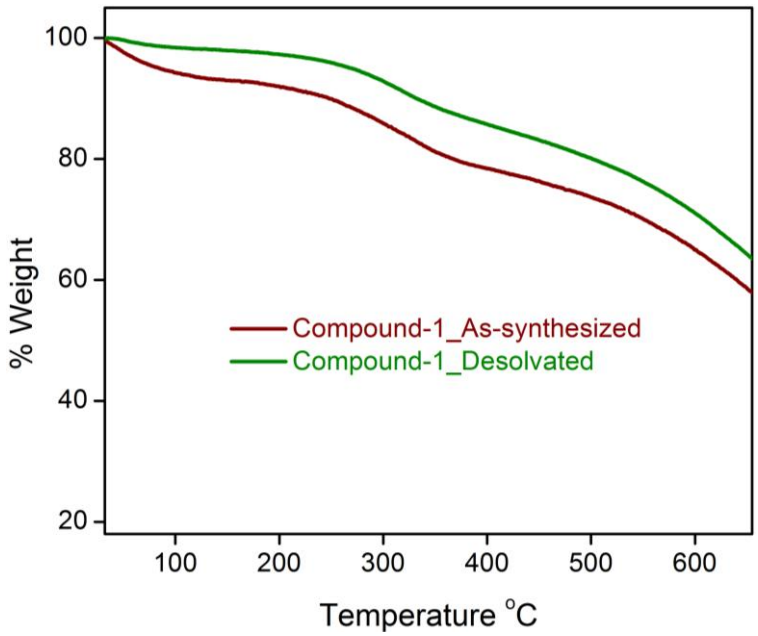

Appendix 5.1: Thermogravimetric analysis (TGA) of as-synthesized compound-1 (wine red) and desolvated phase of compound-1 (green).

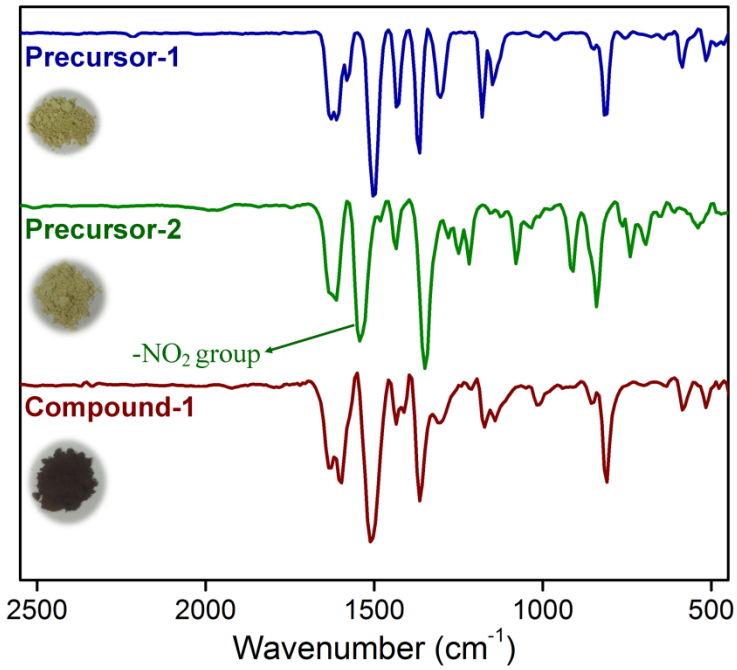

Appendix 5.2: Infra-red (IR) spectroscopy of starting materials [precursor 1 (blue) and precursor 2 (green)] and compound-1 (wine red).

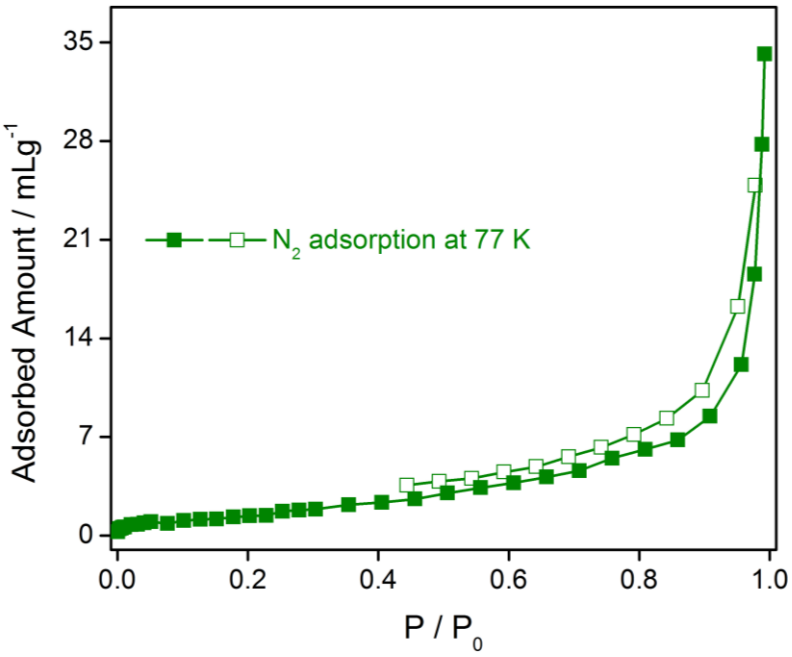

Appendix 5.3: Low temperature (77 K) N_2 adsorption profile of compound-1.

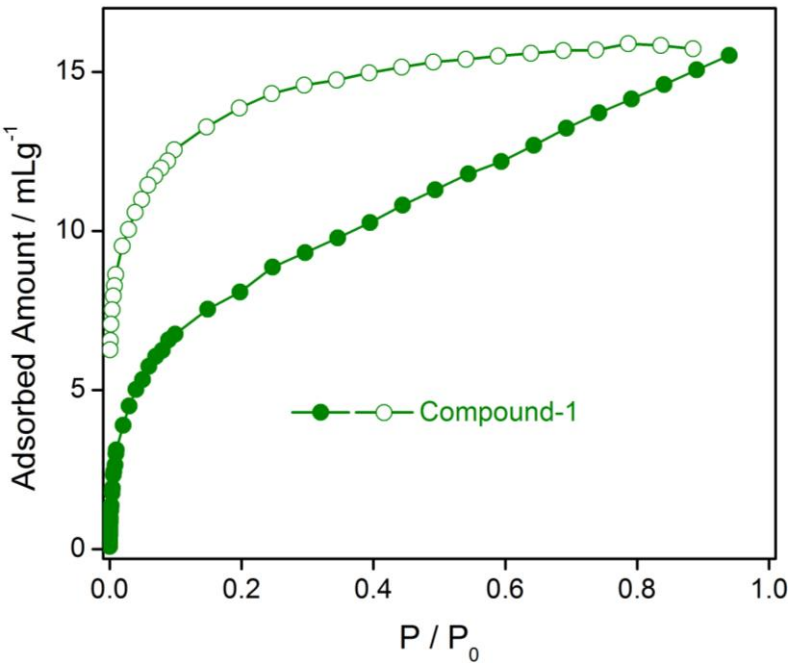

Appendix 5.4: Low temperature (195 K) CO_2 adsorption profile of compound-1.

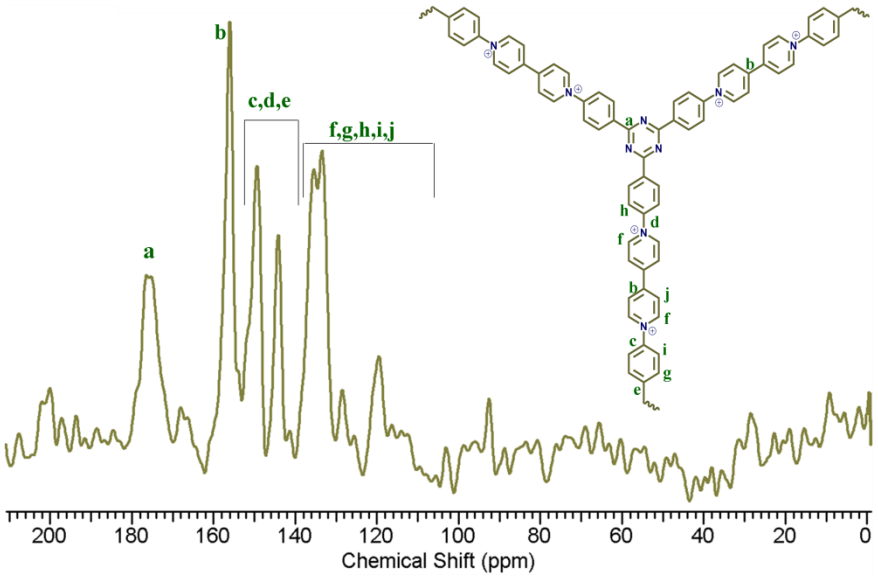

Appendix 5.5: Solid state ^{13}C-NMR of compound-1.

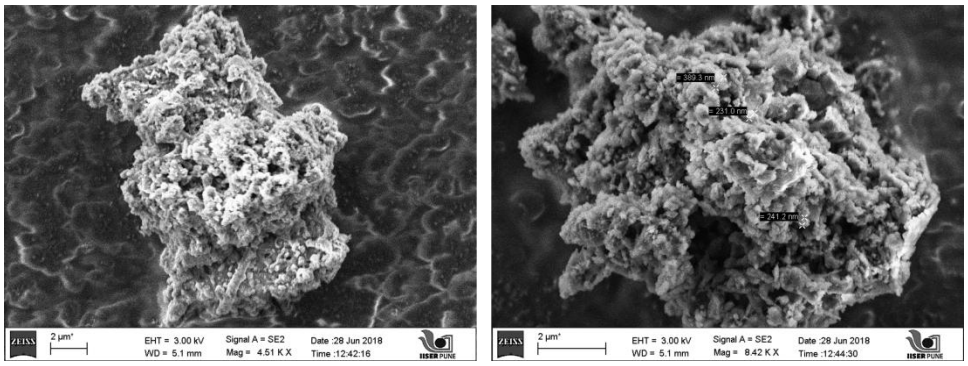

Appendix 5.6: FE-SEM images of compound-1.

Element	Weight %
C	73.08
N	6.46
O	17.61
Cl	2.85
Total	100

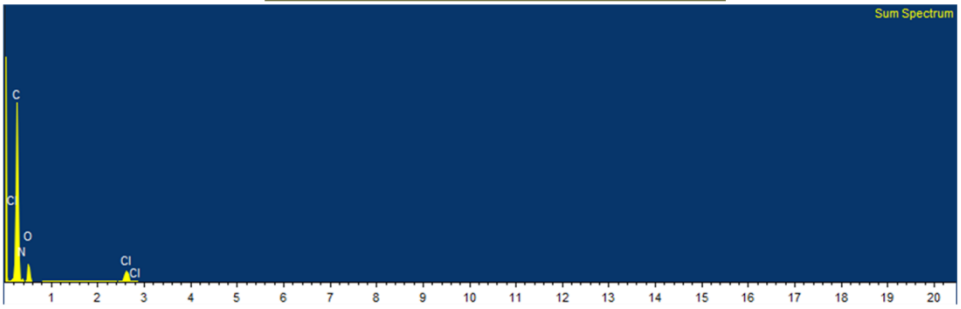

Appendix 5.7: EDX analysis of compound-1.

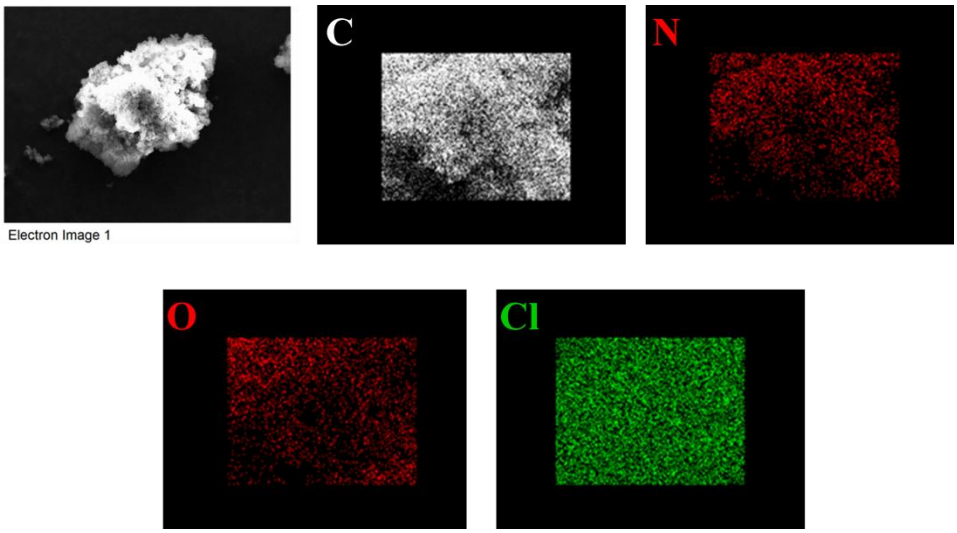

Appendix 5.8: Elemental mapping of compound-1.

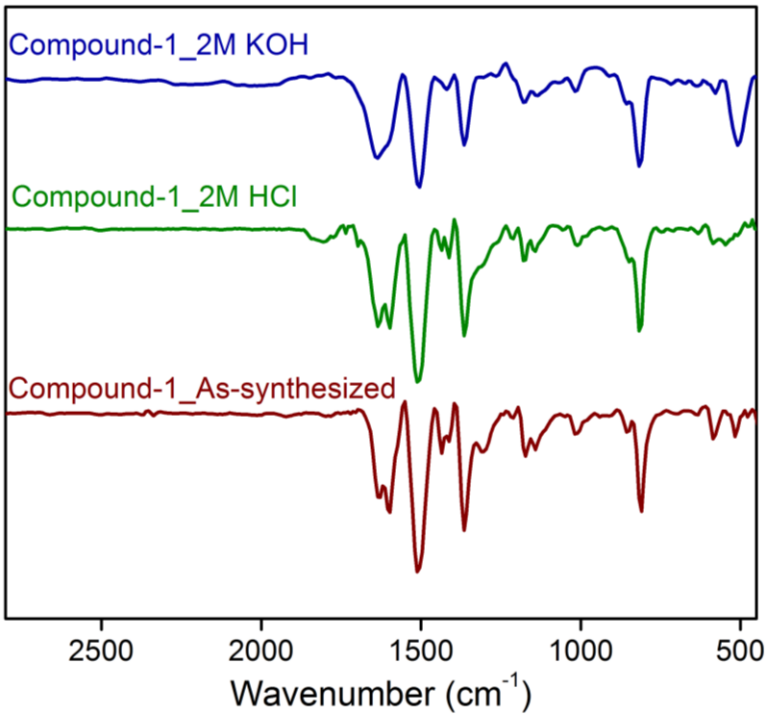

Appendix 5.9: Infra-red (IR) spectroscopy of compound-1 (wine red), 2 M HCl treated compound-1 (green) and 2 M KOH treated compound-1 (blue).

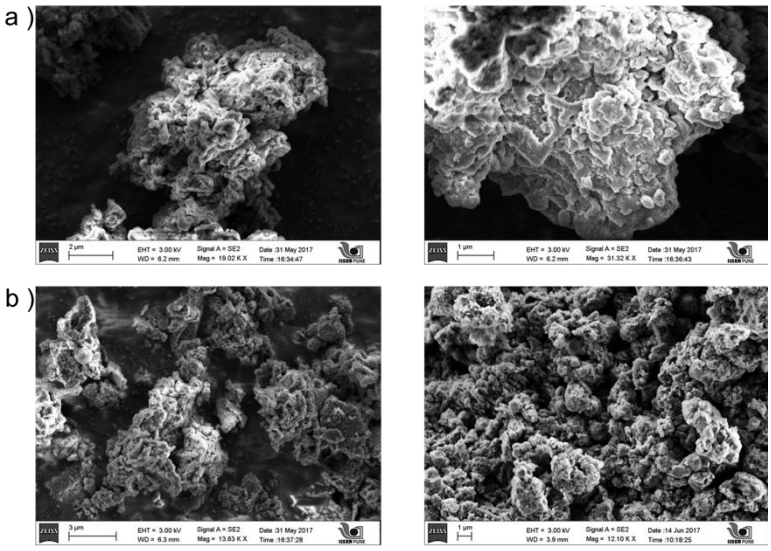

Appendix 5.10: FE-SEM images of a) 2 M HCl treated compound-1 and b) 2 M KOH treated compound-1.

Element	Weight %
C	71.60
N	7.60
O	14.58
Cl	6.22
Total	100

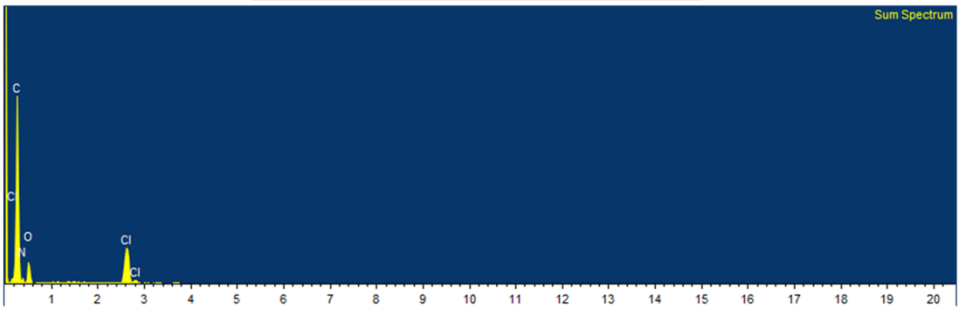

Appendix 5.11: EDX analysis of 2 M HCl treated compound-1.

Element	Weight %
C	71.45
N	8.24
O	17.93
Cl	2.38
Total	100

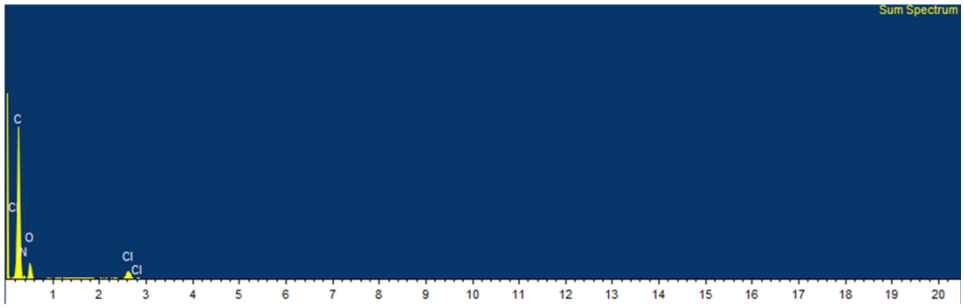

Appendix 5.12: EDX analysis of 2 M KOH treated compound-1.

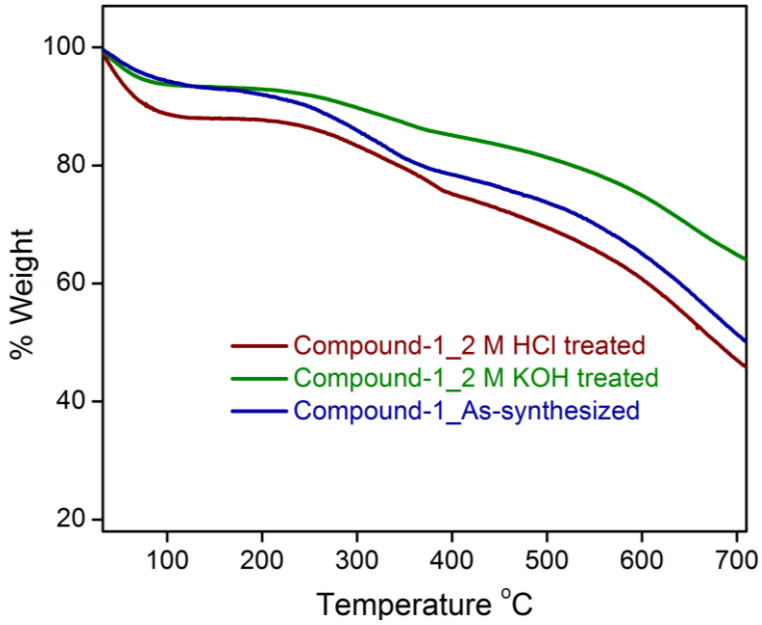

Appendix 5.13: Thermogravimetric analysis (TGA) of compound-1 (blue), 2 M HCl treated compound-1 (wine red) and 2 M KOH treated compound-1 (green).

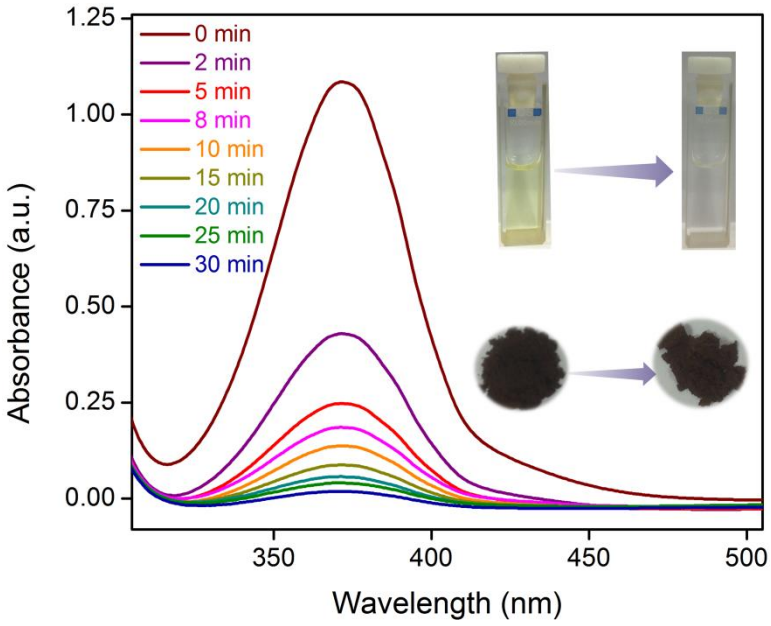

Appendix 5.14: UV-Vis spectroscopy of CrO_4^{2-} ion solution in water in presence of compound-1 at different time intervals (Inset: images of CrO_4^{2-} ion solution and solid compound-1 before and after of capture study).

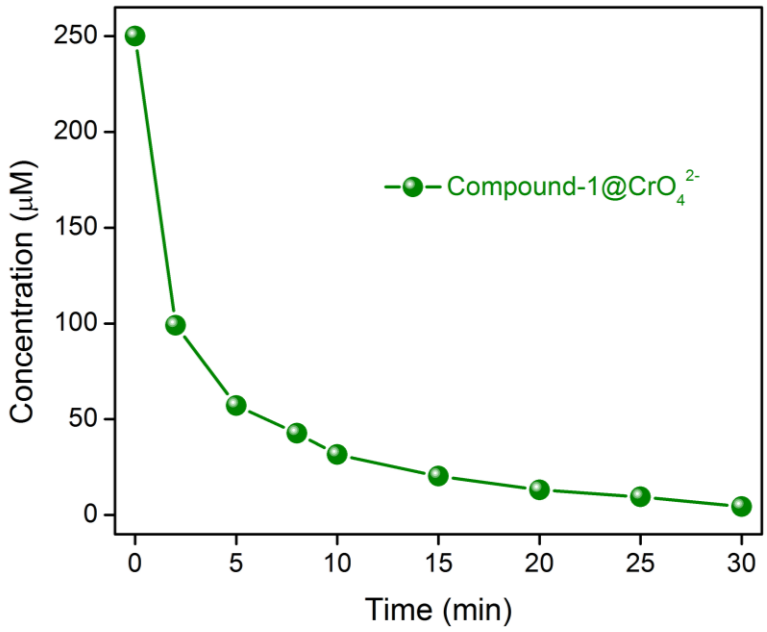

Appendix 5.15: Decrease in the concentration of the CrO_4^{2-} ion from water after addition of compound-1.

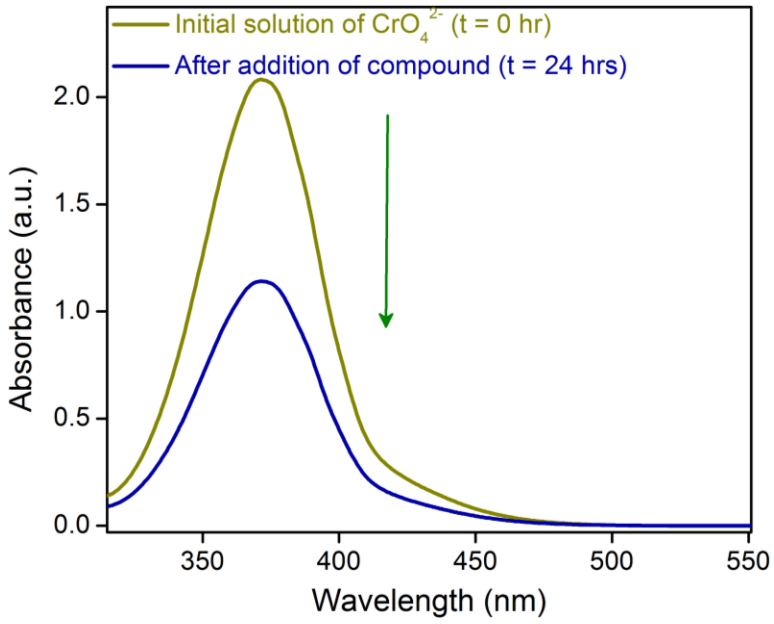

Appendix 5.16: UV-Vis spectra of only CrO_4^{2-} before (dark yellow) and after (blue) addition of compound-1 (time duration: 24hrs); capacity of compound-1 for CrO_4^{2-} ion has been calculated from this data.

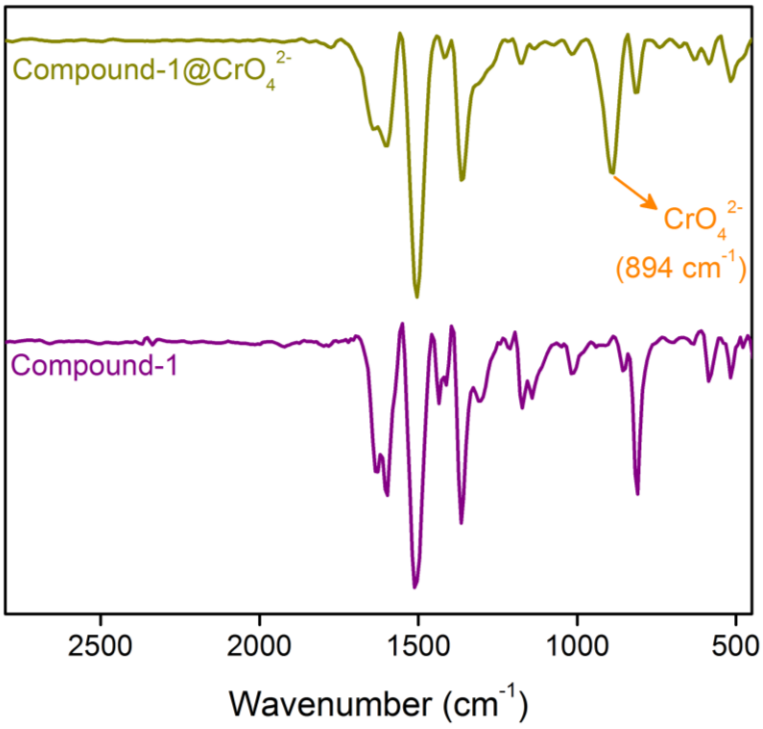

Appendix 5.17: Infra-red (IR) spectroscopy of compound-1 (purple) and compound-1⊃CrO_4^{2-} (dark yellow).

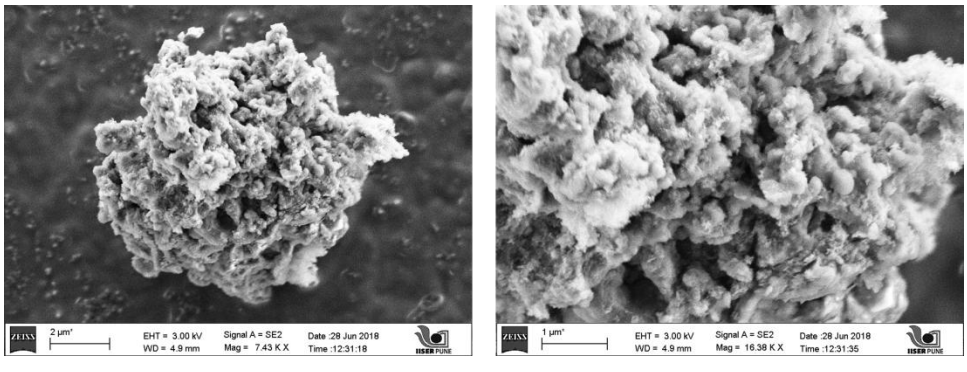

Appendix 5.18: SEM images of CrO_4^{2-} encapsulated compound-1 (compound-1⊃CrO_4^{2-}).

Element	Weight %
C	58.10
N	15.96
O	19.33
Cr	6.61
Total	100

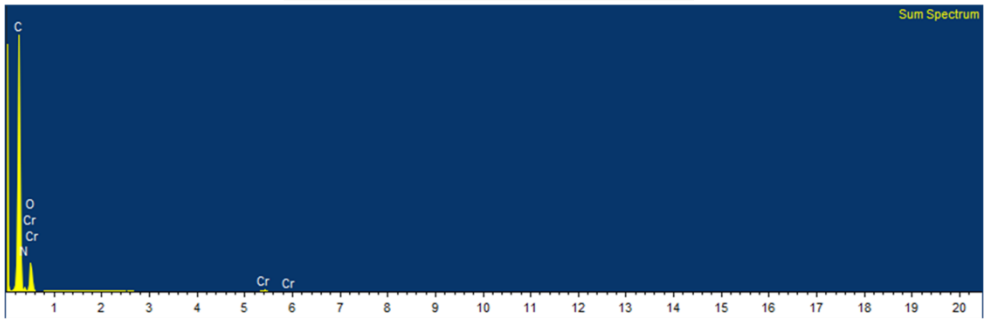

Appendix 5.19: Infra-red (IR) spectroscopy of compound-1 (purple) and compound-1⊃CrO_4^{2-} (dark yellow).

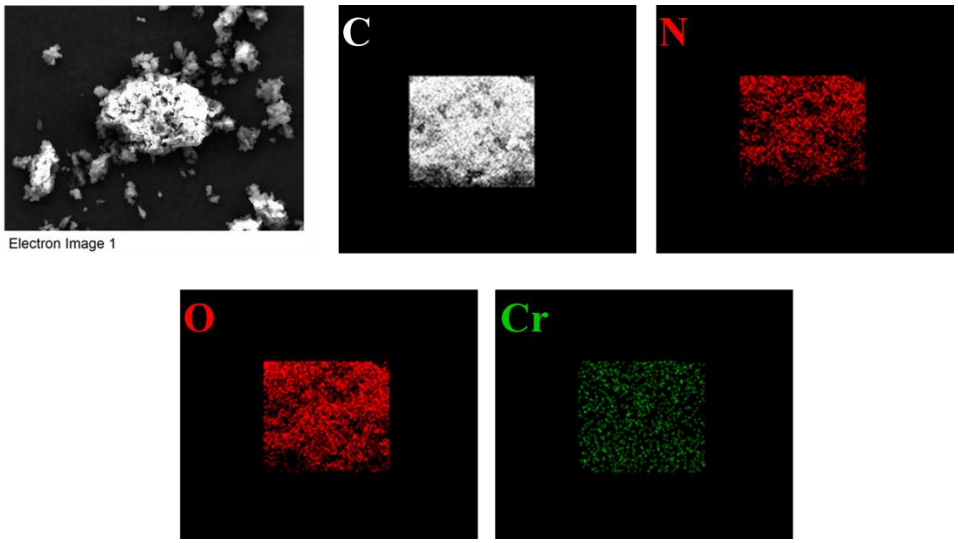

Appendix 5.20: Infra-red (IR) spectroscopy of compound-1 (purple) and compound-1⊃CrO_4^{2-} (dark yellow).

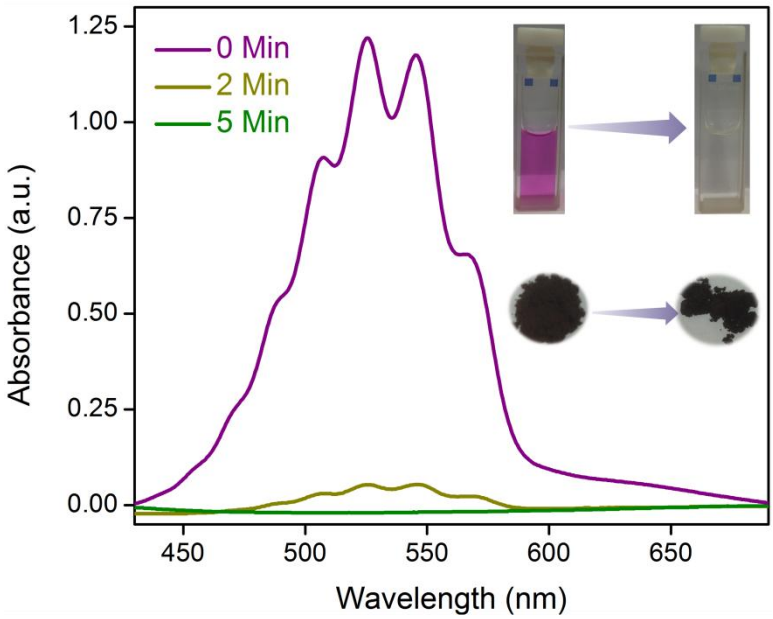

Appendix 5.21: UV-Vis spectroscopy of MnO_4^- ion solution in water in presence of compound-1 at different time intervals (Inset: images of MnO_4^- ion solution and solid compound-1 before and after of capture study).

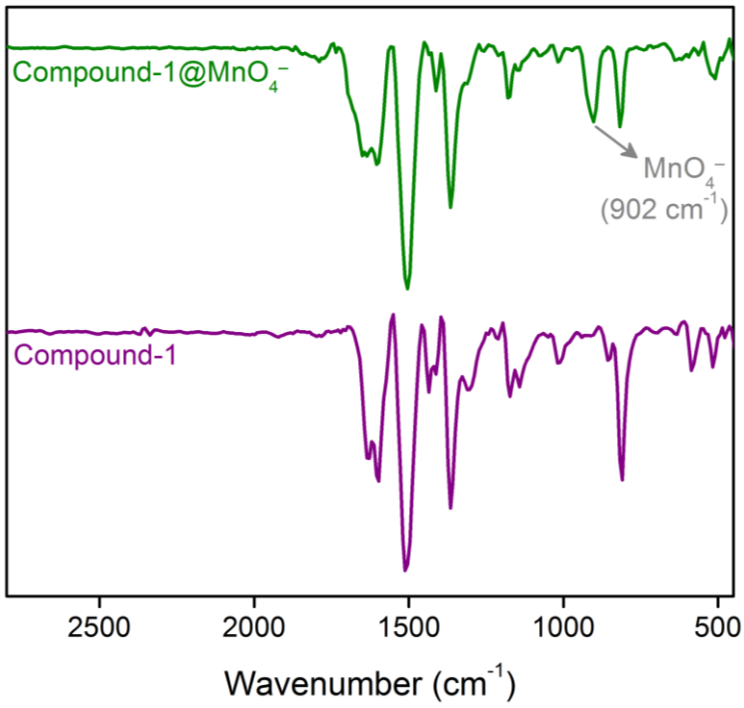

Appendix 5.22: Infra-red (IR) spectroscopy of compound-1 (purple) and compound-1⊃MnO_4^- (green).

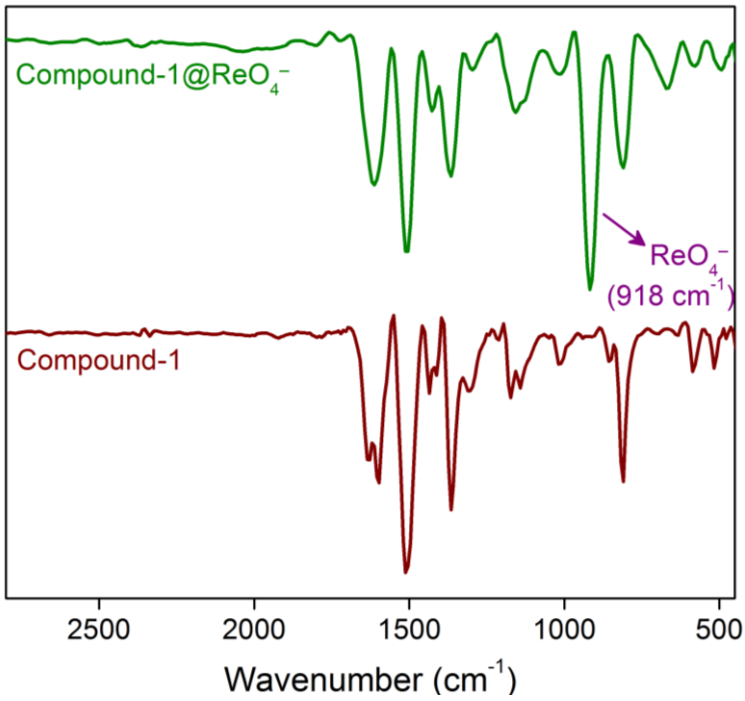

Appendix 5.23: IR spectra of compound-1 (wine red) and ReO_4^- treated compound-1 (green).

Element	Weight %
C	61.01
N	13.87
O	15.22
Mn	9.90
Total	100

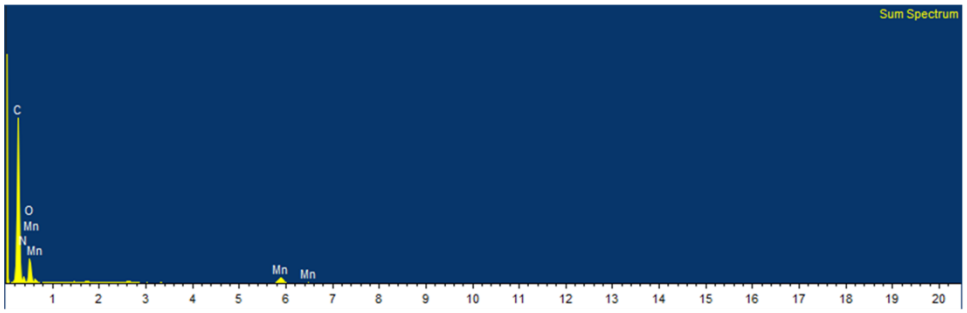

Appendix 5.24: EDX analysis of MnO_4^- encapsulated compound-1 (compound-1⊃MnO_4^-).

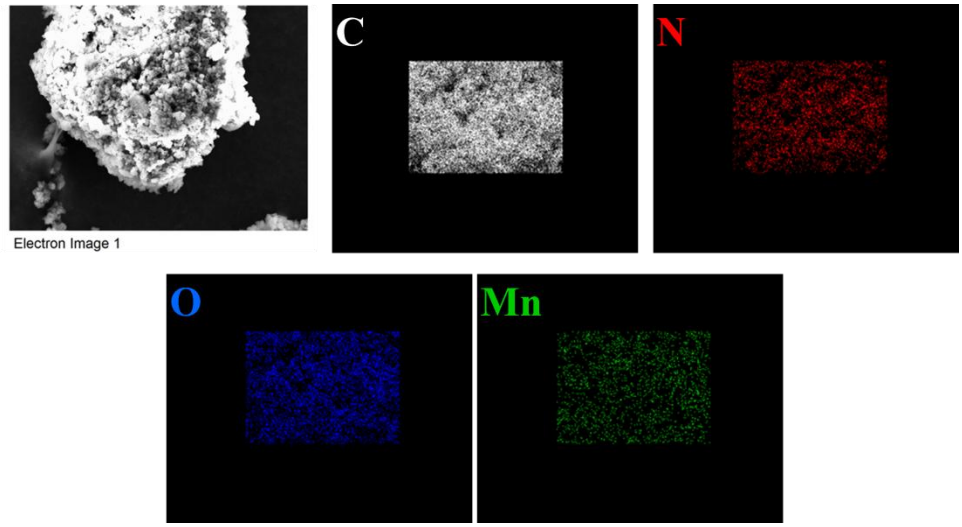

Appendix 5.25: Elemental mapping of MnO_4^- encapsulated compound-1 (compound-1⊃MnO_4^-).

Element	Weight %
C	69.23
N	3.63
O	21.82
Re	5.32
Total	100

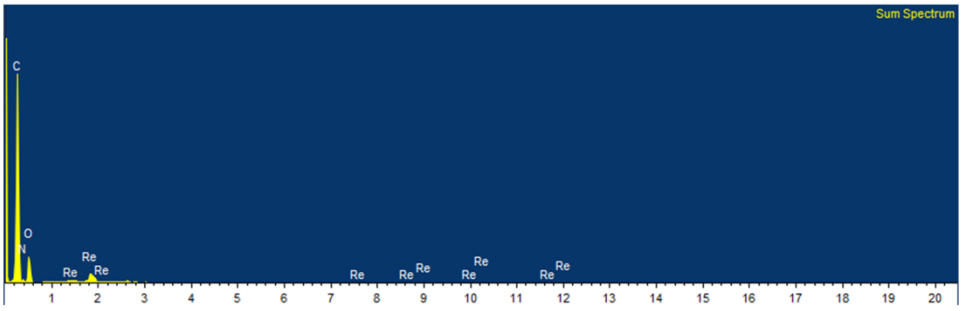

Appendix 5.26: EDX analysis of compound-1 after the capture of ReO_4^-.

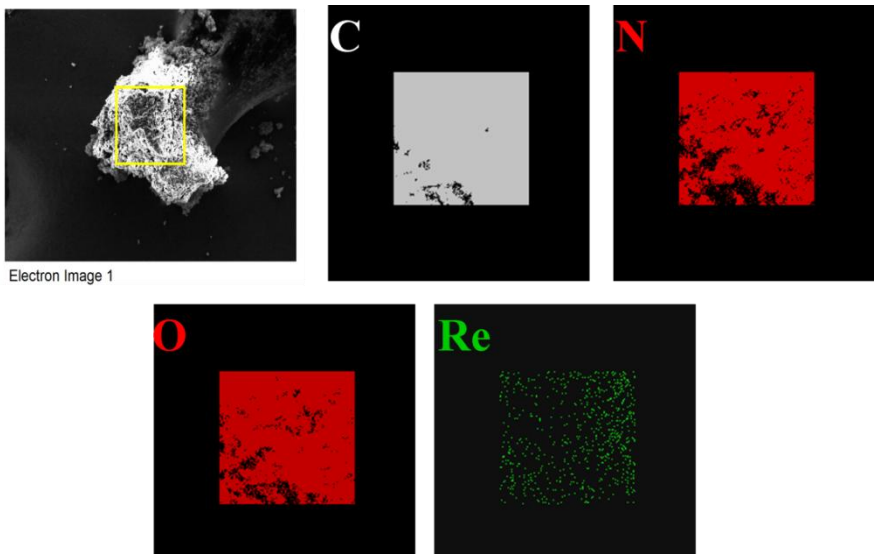

Appendix 5.27: Elemental mapping of compound-1 after the capture of ReO_4^-.

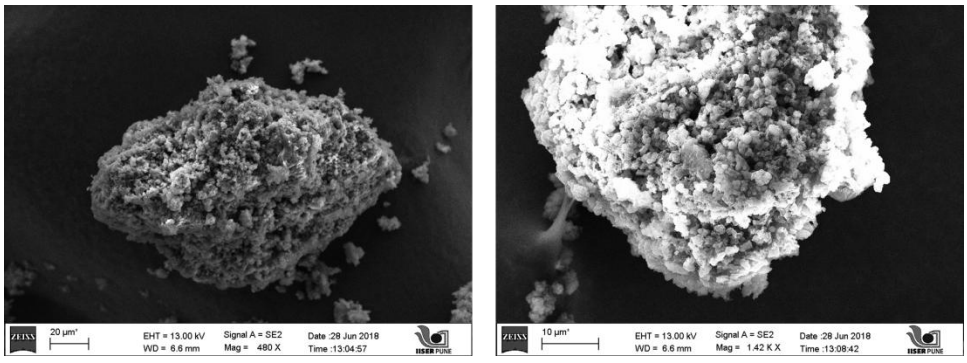

Appendix 5.28: SEM images of MnO_4^- encapsulated compound-1 (compound-1⊃ MnO_4^-).

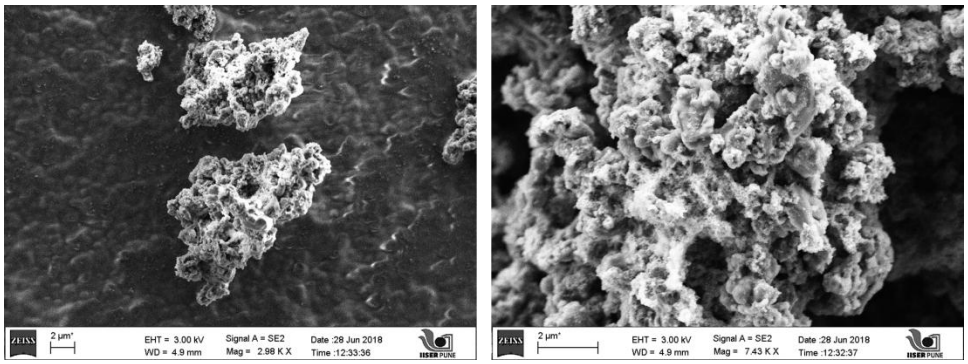

Appendix 5.29: SEM images of compound-1 after the treatment of ReO_4^- in water medium.

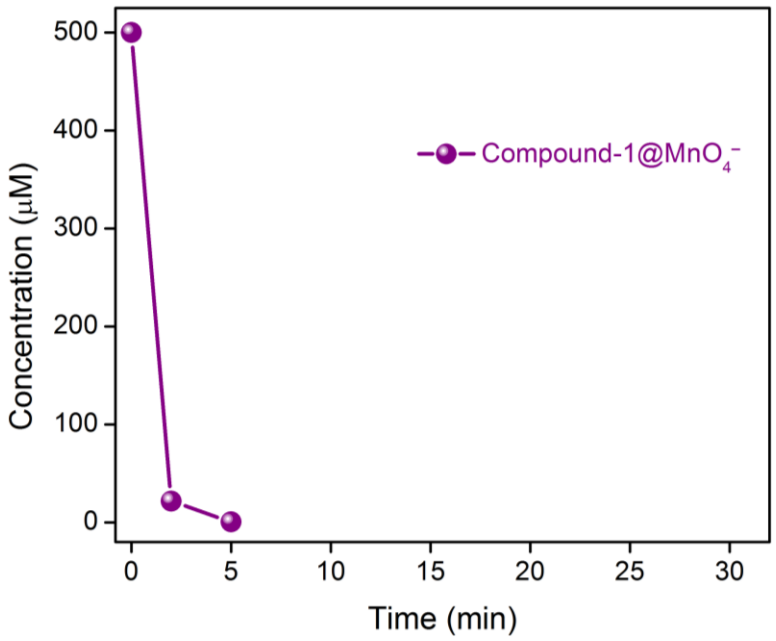

Appendix 5.30: Decrease in the concentration of the MnO_4^- ion from water after addition of compound-1.

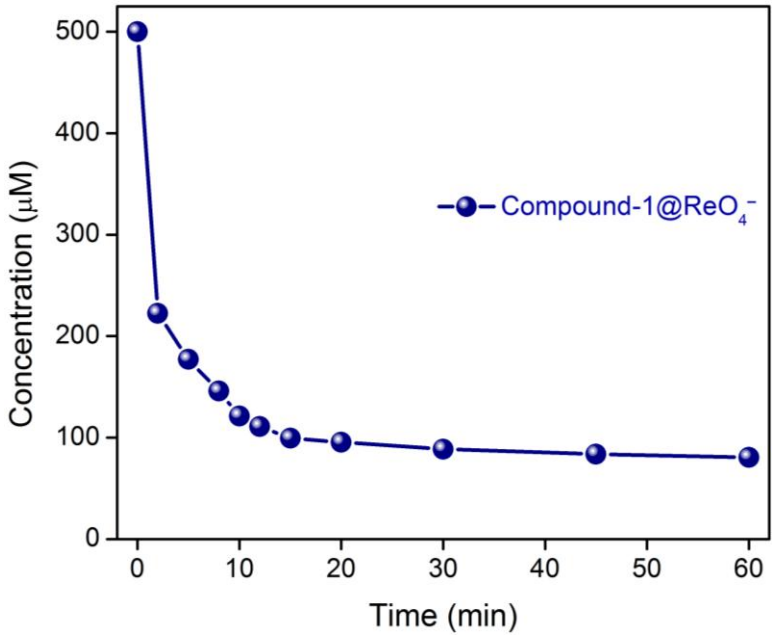

Appendix 5.31: Decrease in the concentration of the ReO_4^- ion from water solution on addition of compound-1.

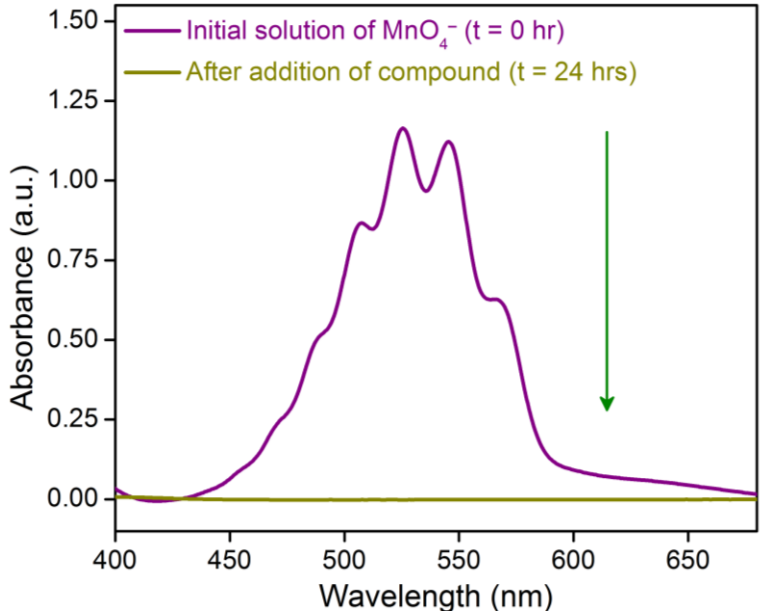

Appendix 5.32: UV-Vis spectra of only MnO_4^- before (purple) and after (dark yellow) addition of compound-1 (time duration = 24hrs); capacity of compound-1 for MnO_4^- ion has been calculated from this data.

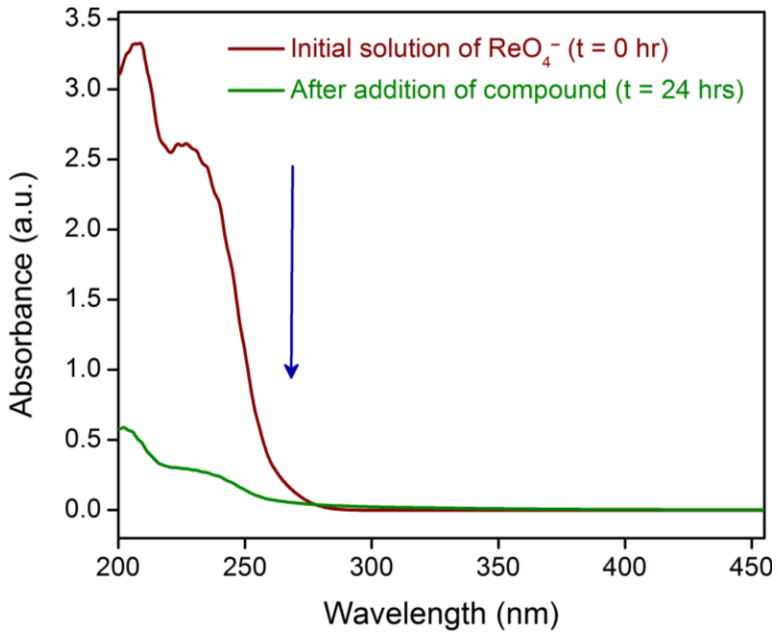

Appendix 5.33: UV-Vis spectra of only ReO_4^- before (wine red) and after (green) the addition of compound-1 (time duration = 24hrs); capacity of compound-1 for ReO_4^- ion has been calculated from this data.

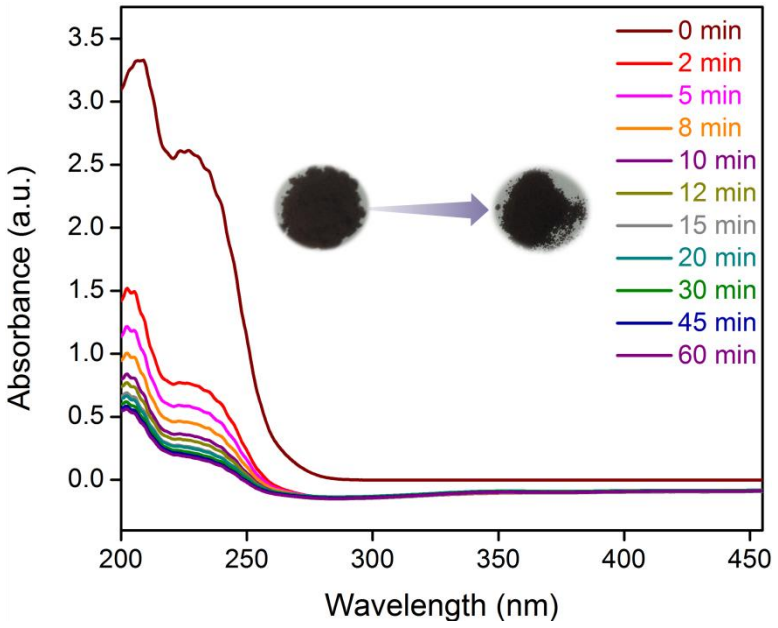

Appendix 5.34: UV-Vis spectroscopy of ReO_4^- ion solution in water in presence of compound-1 at different time intervals (Inset: images of ReO_4^- ion solution and solid compound-1 before and after of capture study).

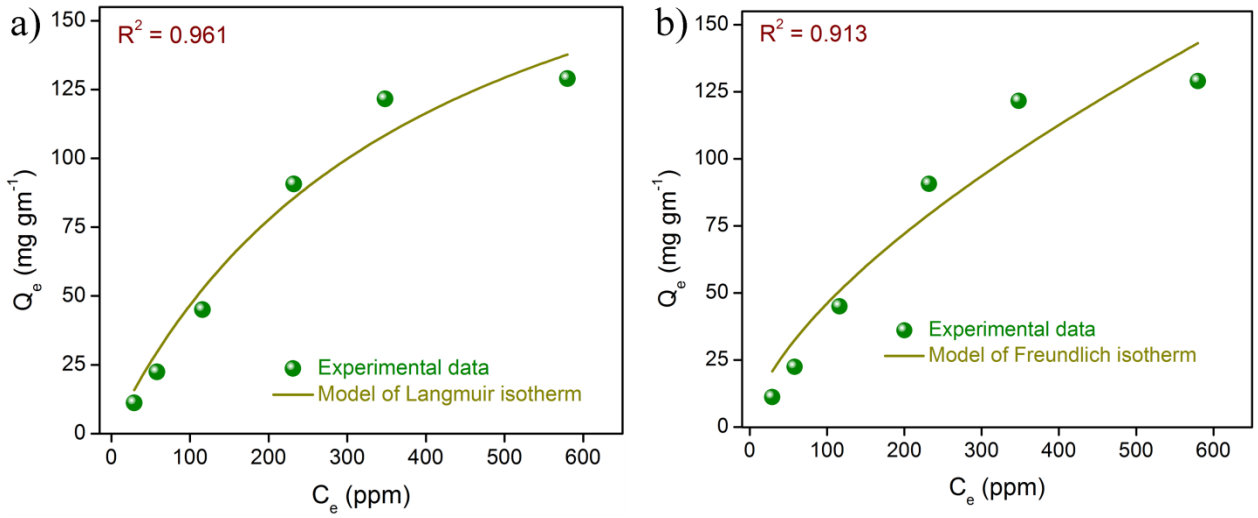

Appendix 5.35: (a) Langmuir model and (b) Freundlich model of CrO_4^{2-} ion capture study with compound-1.

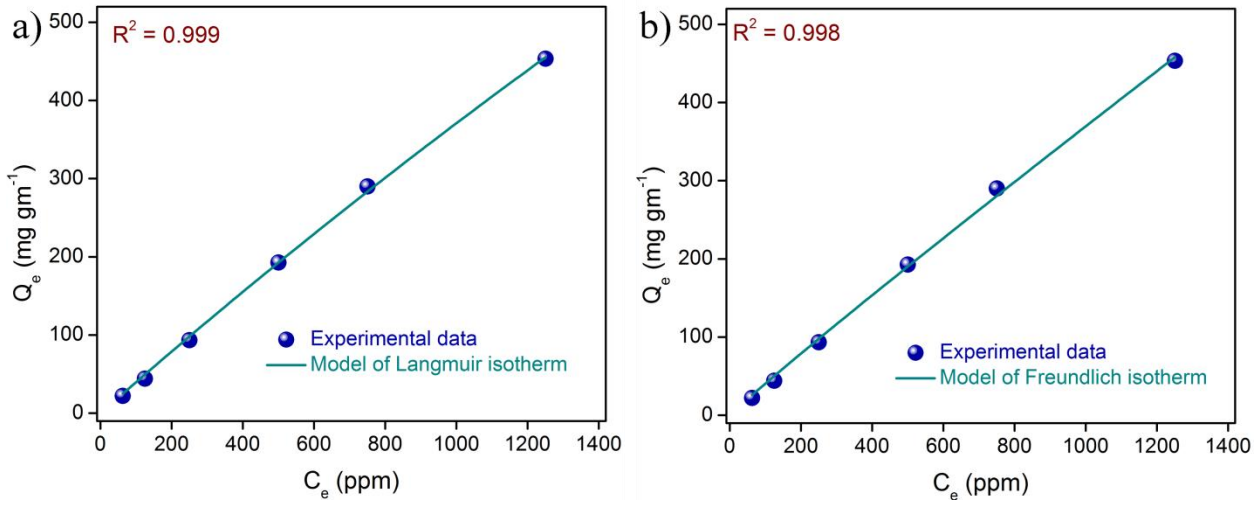

Appendix 5.36: (a) Langmuir model and (b) Freundlich model of ReO_4^- ion capture study with compound-1.

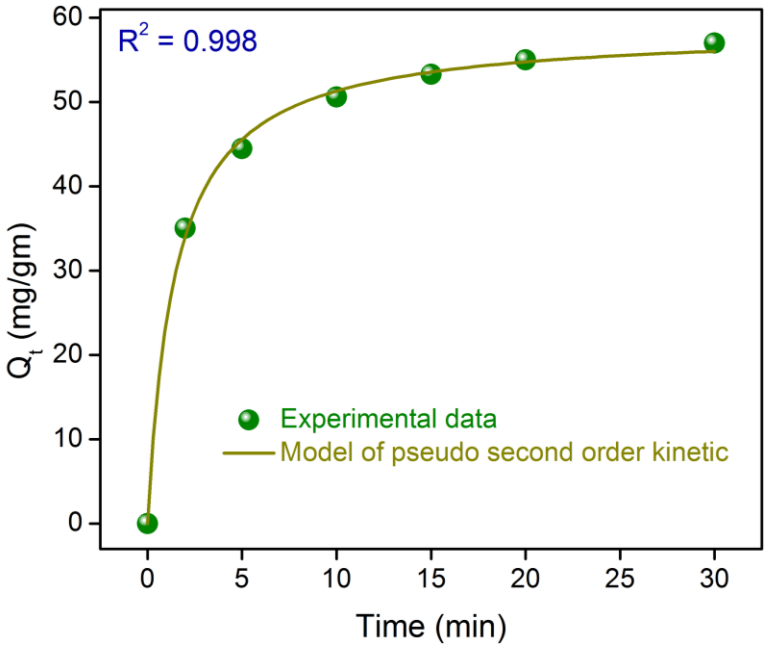

Appendix 5.37: Kinetic study of CrO_4^{2-} ion capture with compound-1.

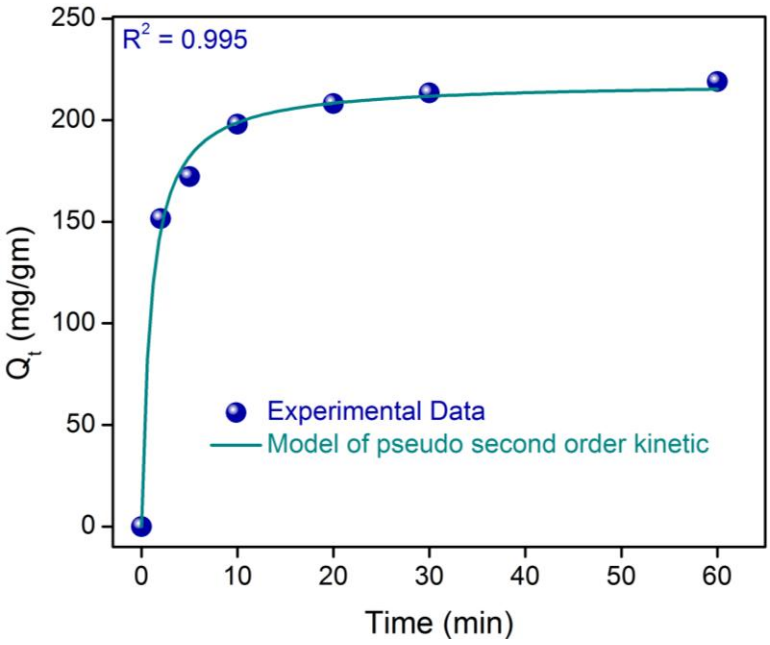

Appendix 5.38: Kinetic study of ReO_4^- ion capture with compound-1.

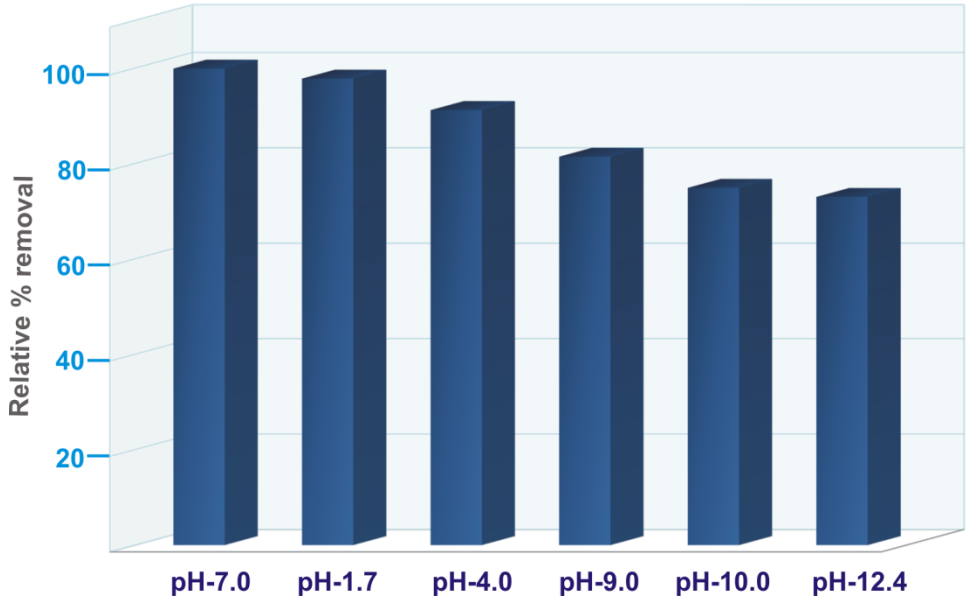

Appendix 5.39: Bar diagram representing relative % removal of CrO_4^{2-} ion from water by compound-1 at different pH-medium.

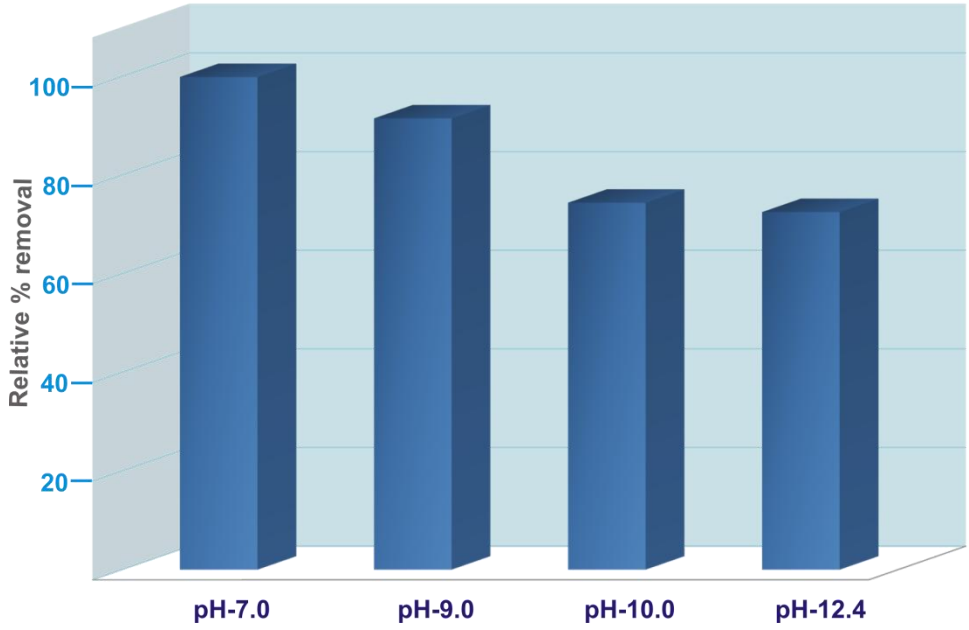

Appendix 5.40: Bar diagram representing relative % removal of ReO_4^- ion from water by compound-1 at different alkaline pH-medium.

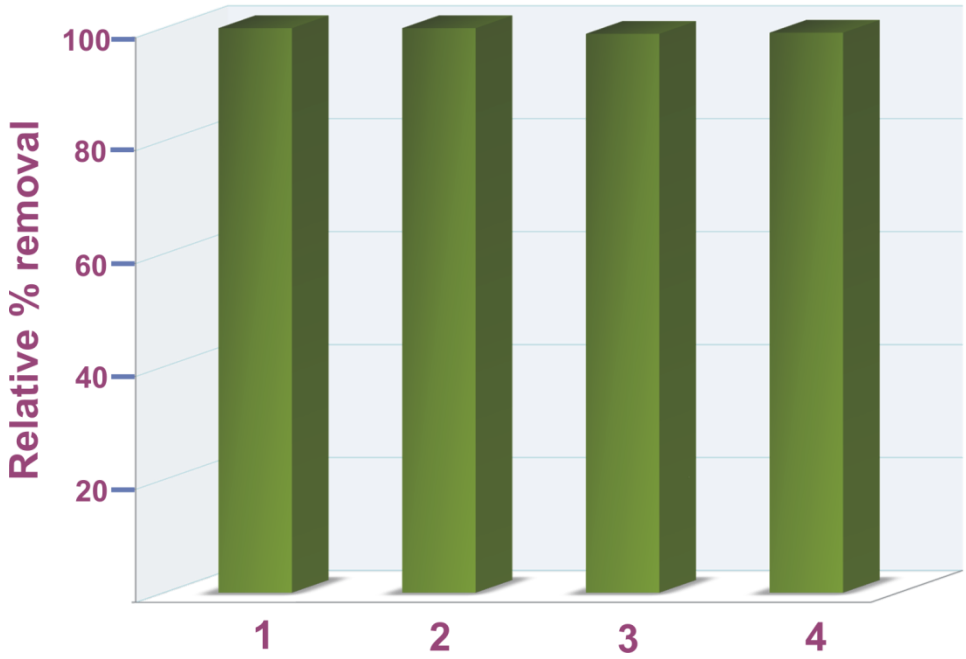

Appendix 5.41: Recyclability test of compound-1 for CrO_4^{2-} ion.

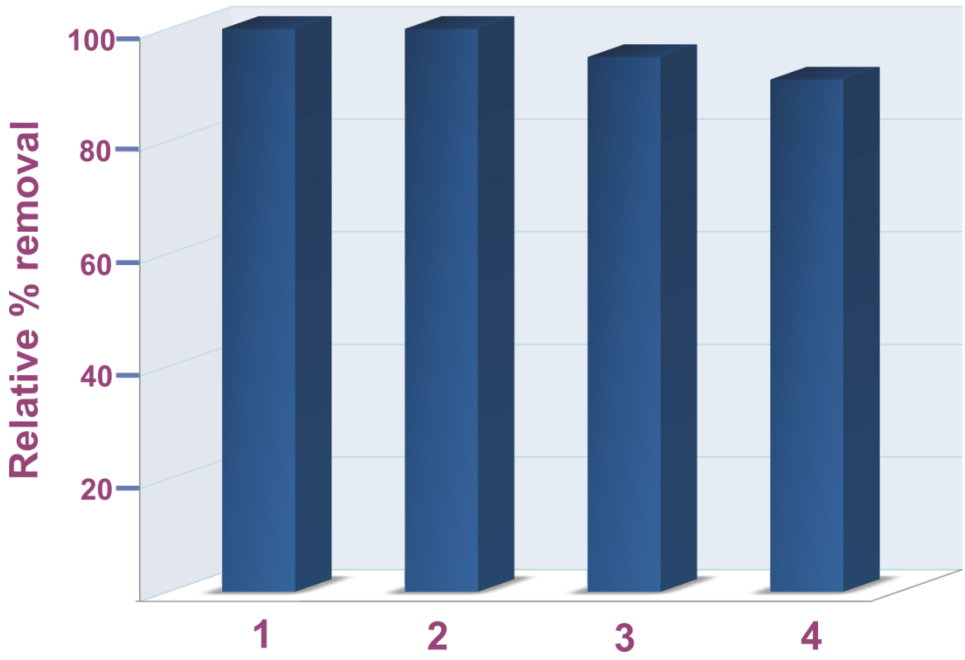

Appendix 5.42: Recycle test of compound-1 for ReO_4^- ion.

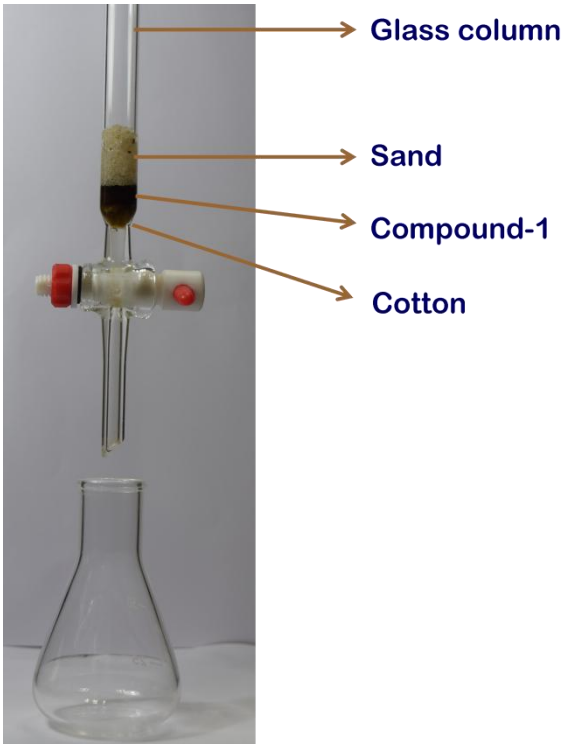

Appendix 5.43: Representation of the compound-1 loaded column used for column chromatographic separation of oxo-anion from water.

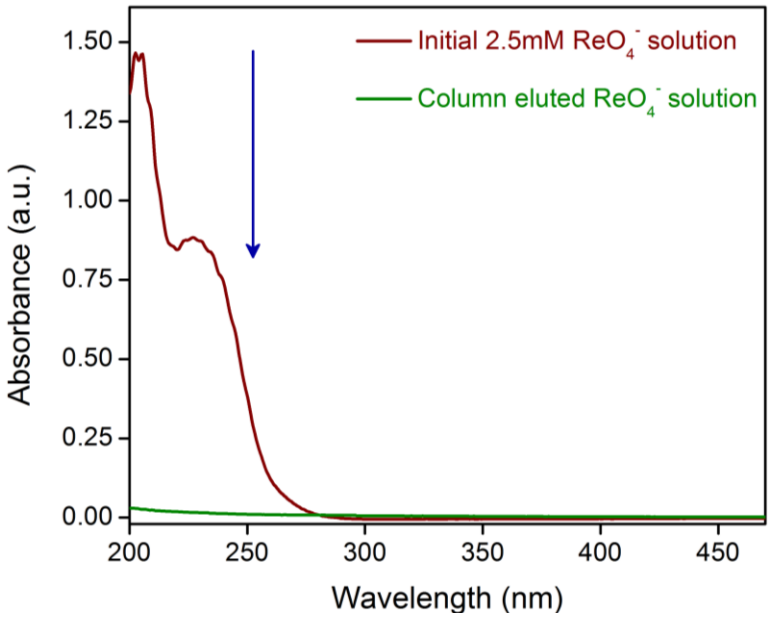

Appendix 5.44: UV-Vis spectra of the 2.5 mM ReO_4^- solution before (wine red) and after (green) passing through the compound-1 loaded column.

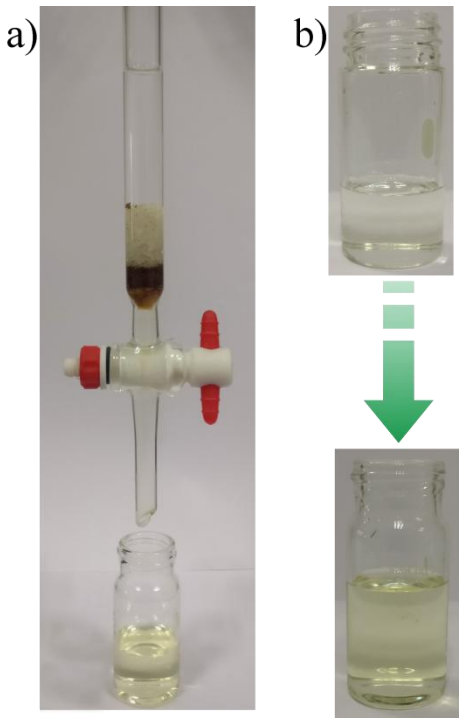

Appendix 5.45: (a) Regeneration of the column with 3 M HCl solution; (b) images of HCl solution before (top) and after (bottom) passing through the column.

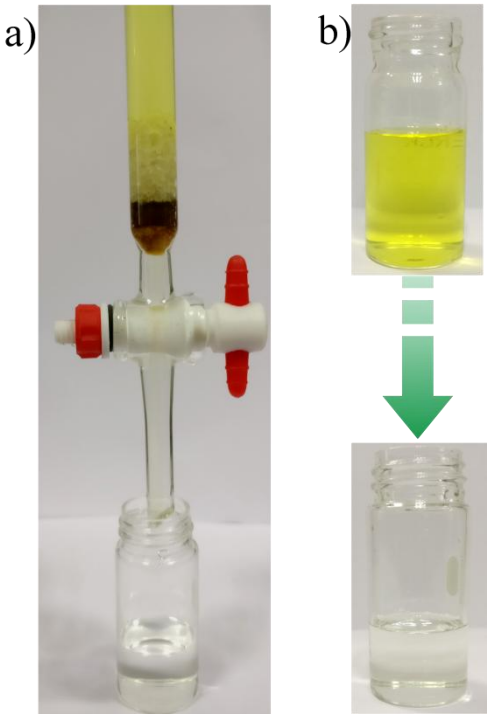

Appendix 5.46: (a) Recyclability test with the regenerated column; (b) images of CrO_4^{2-} solution (top) and after (bottom) passing through the column.

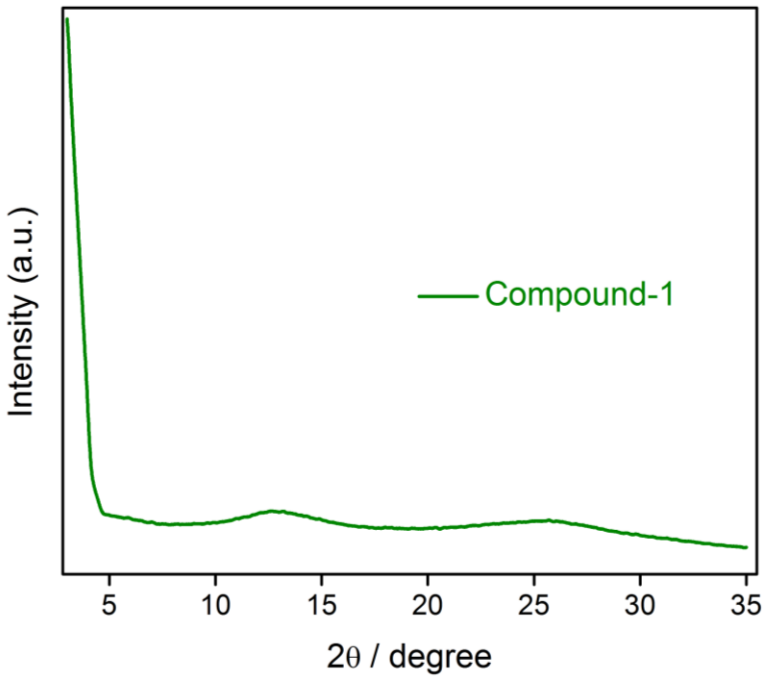

Appendix 5.47: Powder X-ray diffraction (PXRD) pattern of compound-1.

Appendix Table 1: A comparison table of CrO_4^{2-} capture (CrO_4^{2-} mg/gm) with some well-studied examples in the literature (N.D.: Not done)

Compound	Capacity (mg/gm)	Selectivity	Reference
Compound-1	133	Cl^-, NO_3^-, Br^-, SO_4^{2-}	This work
Carbon nanocomposites	3.74	N.D.	23
Polyaniline	18.1	N.D.	24
MOR-2	263	Cl^-, NO_3^-, HCO_3^-, etc.	12o
SLUG-21	60	NO_3^-, CO_3^{2-}	12d
1-ClO_4	62.9	halide anions	12b
1-NO_3	82.5	NO_3^-, CO_3^{2-}	25
Fe nanoparticles	109	N.D.	26
Zn–Co-SLUG-35	68.5	NO_3^-, SO_4^{2-}	12e
TJU-1	279	Cl^-, HCO_3^-, NO_3^-, SO_4^{2-}	12n
MgAl-LDHs	112	N.D.	27
ED-rGO	100	N.D.	28
ZIF-67	5.88-13.34	N.D.	29

Appendix Table 2: A comparison table of ReO_4^- and MnO_4^- capture (mg/gm) with some well-studied examples in the literature

Element	Compound	Capacity (mg/gm)	Selectivity	Reference
ReO_4^-	Compound-1	517	Cl^-, NO_3^-, Br^-, SO_4^{2-}	This Work
MnO_4^-	Compound-1	297.3	Cl^-, NO_3^-, Br^-, SO_4^{2-}	This Work
ReO_4^-	D318 resin	351	-	30
ReO_4^-	PAF-1-F	420	SO_4^{2-}, PO_4^{3-}	17k
ReO_4^-	Dowex1x8	98.1	-	17k
ReO_4^-	Purolite 530E	96	-	17k
ReO_4^-	SLUG-21	602	-	3a
ReO_4^-	UiO-66-NH_3^+	159	NO_3^-, SO_4^{2-}, PO_4^{3-}	12f
ReO_4^-	SCU-100	541	CO_3^{2-}, SO_4^{2-}, PO_4^{3-}	10a
ReO_4^-	SCU-101	217	various anions	12a
ReO_4^-	PolyDMAEMA hydrogels	30.5	-	31
ReO_4^-	4-ATR resin	354		32
ReO_4^-	SBN	786	-	33
ReO_4^-	LDHs	130	-	33
MnO_4^-	SLUG-21	283	NO_3^-, CO_3^{2-}	3a

2.6 References

1. L. H. Keith and W. A. Teillard, *Environ. Sci. Technol.*, 1979, **13**, 416–423.

2. (a) *Toxicological Profile for Chromium*; Public Health Service Agency for Toxic Substances and Diseases Registry, U.S. Department of Health and Human Services: Atlanta, GA, 2012. (b) R. Vonburg and D. Liu, *J. Appl. Toxicol.*, 1993, **13**, 225−230.

3. (a) H. Fei, D. L. Rogow and S. R. J. Oliver, *J. Am. Chem. Soc.*, 2010, **132**, 7202–7209. (b) R. Cao, B. D. McCarthy and S. J. Lippard, *Inorg. Chem.*, 2011, **50**, 9499–9507.

4. (a) L. Khezami and R. Capart, *J. Hazard. Mater.*, 2005, **123**, 223−231. (b) M. B. Luo, Y. Y. Xiong, H. Q. Wu, X. F. Feng, J. Q. Li and F. Luo, *Angew. Chem. Int. Ed.*, 2017, **56**, 16376–16379.

5. (a) W. Liu, Y. Wang, Z. Bai, Y. Li, Y. Wang, L. Chen, L. Xu, J. Diwu, Z. Chai and S. Wang, *ACS Appl. Mater. Interfaces*, 2017, **9**, 16448−16457. (b) S. R. J. Oliver, *Chem. Soc. Rev.*, 2009, **38**, 1868−1881.

6. S. Banks, *Environs*., 2003, **26**, 219–251.

7. (a) H. Yoshitake, T. Yokoi and T. Tatsumi, *Chem. Mater.*, 2002**, 14**, 4603–4610. (b) The World's Worst Pollution Problems 2016: The Toxics Beneath Our Feet, *Pure Earth and Green Cross Switzerland*, 2016, http://www.worstpolluted.org/docs/WorldsWorst2016.pdf.

8. S. Wang, P. Yu, B. A. Purse, M. J. Orta, J. Diwu, W. H. Casey, B. L. Phillips, E. V. Alekseev, W. Depmeier, D. T. Hobbs and T. E. Albrecht-Schmitt, *Adv. Funct. Mater.*, 2012, **22**, 2241–2250.

9. (a) T. H. Boyer and P. C. Singer, *Environ. Sci. Technol.*, 2008, **42**, 608–613. (b) B. Gammelgaard, Y. P. Liao and O. Jons, *Anal. Chim. Acta*, 1997, **354**, 107−113. (c) B. Wen, X. Q. Shan and J. Lian, *Talanta*, 2002, **56**, 681−687. (d) A. Syty, R. G. Christensen and T. C. Rains, *J. Anal. At. Spectrom.*, 1988, **3**, 193−197.

10. (a) D. Sheng, L. Zhu, C. Xu, C. Xiao, Y. Wang, Y. Wang, L. Chen, J. Diwu, J. Chen, Z. Chai, T. E. Albrecht-Schmitt and S. Wang, *Environ. Sci. Technol.*, 2017, **51**, 3471−3479. (b) D. Banerjee, D. Kim, M. J. Schweiger, A. A. Kruger and P. K. Thallapally, *Chem. Soc. Rev.*, 2016, **45**, 2724−2739.

11. A. V. Desai, B. Manna, A. Karmakar, A. Sahu and S. K. Ghosh, *Angew. Chem. Int. Ed.*, 2016, **55**, 7811–7815.

12. (a) L. Zhu, D. Sheng, C. Xu, X. Dai, M. A. Silver, J. Li, P. Li, Y. Wang, Y. Wang, L. Chen, C. Xiao, J. Chen, R. Zhou, C. Zhang, O. K. Farha, Z. Chai, T. E. Albrecht-Schmitt and S. Wang, *J. Am. Chem. Soc*., 2017, **139**, 14873−14876. (b) P. -F. Shi, B. Zhao, G. Xiong, Y. -L. Hou and P. Cheng, *Chem. Commun.*, 2012, **48**, 8231–8233. (c) A. J. Howarth, Y. Liu, J. T. Hupp and O. K. Farha, *CrystEngComm*, 2015, **17**, 7245–7253. (d) H. Fei, M. R. Bresler and S. R. J. Oliver, *J. Am. Chem. Soc.*, 2011, **133**, 11110–11113. (e) H. Fei, C. S. Han, J. C. Robins and S. R. J. Oliver, *Chem. Mater.*, 2013, **25**, 647−652. (f) D. Banerjee, W. Xu, Z. Nie, L. E. V. Johnson, C. Coghlan, M. L. Sushko, D. Kim, M. J. Schweiger, A. A. Kruger, C. J. Doonan and P. K. Thallapally, *Inorg. Chem.*, 2016, **55**, 8241−8243. (g) X. Li, H. Xu, F. Kong and R. Wang, *Angew. Chem. Int. Ed.*, 2013, **52**, 13769–13773. (h) H.-R. Fu, Z.-X. Xu and J. Zhang, *Chem. Mater.*, 2015, **27**, 205–210. (i) Q. Zhang, J. Yu, J. Cai, L. Zhang, Y. Cui, Y. Yang, B. Chen and G. Qian, *Chem. Commun.*, 2015, **51**, 14732–14734. (j) H. Fei and S. R. J. Oliver, *Angew. Chem. Int. Ed.*, 2011, **50**, 9066–9070. (k) J. J. Neeway, R. M. Asmussen, A. R. Lawter, M. E. Bowden, W. W. Lukens, D. Sarma, B. J. Riley, M. G. Kanatzidis and N. P. Qafoku, *Chem. Mater.*, 2016, **28**, 3976−3983. (l) S. Rapti, A. Pournara, D. Sarma, I. T. Papadas, G. S. Armatas, A. C. Tsipis, T. Lazarides, M. G. Kanatzidis and M. J. Manos, *Chem. Sci.*, 2016, **7**, 2427–2436. (m) C. -P. Li, B. -L. Liu, L. Wang, Y. Liu, J. -Y. Tian, C. -S. Liu and M. Du, *ACS Appl. Mater. Interfaces*, 2017, **9**, 7202−7208. (n) H. Yang and H. Fei, *Chem. Commun.*, 2017, **53**, 7064−7067. (o) S. Rapti, D. Sarma, S. A. Diamantis, E. Skliri, G. S. Armatas, A. C. Tsipis, Y. S. Hassan, M. Alkordi, C. D. Malliakas, M. G. Kanatzidis, T. Lazarides, J. C. Plakatouras and M. J. Manos, *J. Mater. Chem. A*, 2017, **5**, 14707–14719.

13. (a) L. Zhu, L. Zhang, J. Li, D. Zhang, L. Chen, D. Sheng, S. Yang, C. Xiao, J. Wang, Z. Chai, T. E. Albrecht-Schmitt and S. Wang, *Environ. Sci. Technol.*, 2017, **51**, 8606−8615. (b) X. Zhao, X. Bu, T. Wu, S. -T. Zheng, L. Wang and P. Feng, *Nat. Commun.*, 2013, DOI: 10.1038/ncomms3344. (c) A. V. Desai, A. Roy, P. Samanta, B. Manna and S. K. Ghosh, *iScience*, 2018, **3**, 21-30. (d) Y. Li, Z. Yang, Y. Wang, Z. Bai, T. Zheng, X. Dai, S. Liu, D. Gui, W. Liu, M. Chen, L. Chen, J. Diwu, L. Zhu, R. Zhou, Z. Chai, T. E. Albrecht-Schmitt and S. Wang, *Nat. Commun.*, 2017, DOI: 10.1038/s41467-017-01208-w.

14. (a) X. Feng, X. Ding and D. Jiang, *Chem. Soc. Rev.*, 2012, **41**, 6010–6022. (b) A. G. Slater and A. I. Cooper, *Science*, 2017, **348**, DOI: 10.1126/science.aaa8075. (c) H. M. El-Kaderi, J. R. Hunt, J. L. Mendoza-Cortés, A. P. Côté, R. E. Taylor, M. O'Keeffe and O. M. Yaghi, *Science*, 2007, **316**, 268–272. (d) A. Karmakar, A. V. Desai and S. K. Ghosh, *Coord. Chem. Rev.*, 2016, **307**, 313–341. (e) S. Furukawa, J. Reboul, S. Diring, K. Sumida and S. Kitagawa, *Chem. Soc. Rev.*, 2014, **43**, 5700–5734. (f) A. J. Howarth, M. J. Katz, T. C. Wang, A. E. Platero-Prats, K. W. Chapman, J. T. Hupp and O. K. Farha, *J. Am. Chem. Soc.*, 2015, **137**, 7488−7494. (g) T. Kitao, Y. Zhang, S. Kitagawa, B. Wang and T. Uemura, *Chem. Soc. Rev.*, 2017, **46**, 3108–3133. (h) Z. Hu, B. J. Deibert and J. Li, *Chem. Soc. Rev.*, 2014, **43**, 5815–5840.

15. (a) W. Lu, D. Yuan, J. Sculley, D. Zhao, R. Krishna and H. –C. Zhou, *J. Am. Chem. Soc.*, 2011, **133**, 18126–18129. (b) S. Keskin, T. M. van Heest and D. S. Sholl, *ChemSusChem*, 2010, **3**, 879–891.

16. (a) W. Lu, D. Yuan, D. Zhao, C. I. Schilling, O. Plietzsch, T. Muller, S. Bräse, J. Guenther, J. Blümel, R. Krishna, Z. Li and H. -C. Zhou, *Chem. Mater.*, 2010, **22**, 5964–5972. (b) M. G. Rabbani and H. M. El-Kaderi, *Chem. Mater.*, 2011, **23**, 1650–1653.

17. (a) S. Das, P. Heasman, T. Ben and S. Qiu, *Chem. Rev.*, 2017, **117**, 1515−1563. (b) P. J. Waller, F. Gándara and O. M. Yaghi, *Acc. Chem. Res.*, 2015, **48**, 3053−3063. (c) L. Zou, Y. Sun, S. Che, X. Yang, X. Wang, M. Bosch, Q. Wang, H. Li, M. Smith, S. Yuan, Z. Perry and H. -C. Zhou, *Adv. Mater.*, 2017, **29**, 1700229. (d) Y. Xu, S. Jin, H. Xu, A. Nagai and D. Jiang, *Chem. Soc. Rev.*, 2013, **42**, 8012–8031. (e) U. Diaza and A. Corma, *Coord. Chem. Rev.*, 2016, **311**, 85–124. (f) P. Samanta, A. V. Desai, B. Anothumakkool, M. M. Shirolkar, A. Karmakar, S. Kurungot and S. K. Ghosh, *J. Mater. Chem. A*, 2017, **5**, 13659–13664. (g) R. P. Bisbey and W. R. Dichtel, *ACS Cent. Sci.*, 2017, **3**, 533−543. (h) B. Aguila, Q. Sun, J. A. Perman, L. D. Earl, C. W. Abney, R. Elzein, R. Schlaf and S. Ma, *Adv. Mater.*, 2017, **29**, DOI: 10.1002/adma.201700665. (i) P. Samanta, P. Chandra, A. V. Desai and S. K. Ghosh, *Mater. Chem. Front.*, 2017, **1**, 1384–1388. (j) Y. Su, Y. Wang, X. Li, X. Li and R. Wang, *ACS Appl. Mater. Interfaces*, 2016, **8**, 18904−18911. (k) D. Banerjee, S. K. Elsaidi, B. Aguila, B. Li, D. Kim, M. J. Schweiger, A. A. Kruger, C. J. Doonan, S. Ma and P. K. Thallapally, *Chem. Eur. J.*, 2016, **22**, 17581–17584. (l) B. Li, Y. Zhang, D. Ma, Z. Xing, T. Ma, Z. Shi, X. Ji and S. Ma, *Chem. Sci.*, 2016, **7**, 2138–2144.

18. (a) N. Huang, P. Wang, M. A. Addicoat, T. Heine and D. Jiang, *Angew. Chem. Int. Ed.*, 2017, **56**, 4982–4986. (b) H. Ma, B. Liu, B. Li, L. Zhang, Y. -G. Li, H. -Q. Tan, H. -Y. Zang and G. Zhu, *J. Am. Chem. Soc.*, 2016, **138**, 5897−5903. (c) S. Fischer, A. Schimanowitz, R. Dawson, I. Senkovska, S. Kaskel

and A. Thomas, *J. Mater. Chem. A*, 2014, **2**, 11825–11829. (d) S. Mitra, S. Kandambeth, B. P. Biswal, A. Khayum M., C. K. Choudhury, M. Mehta, G. Kaur, S. Banerjee, A. Prabhune, S. Verma, S. Roy, U. K. Kharul, R. Banerjee, *J. Am. Chem. Soc.*, 2016, **138**, 2823−2828. (e) Z. Li, H. Li,; X. Guan, J. Tang, Y. Yusran, Z. Li, M. Xue, Q. Fang, Y. Yan, V. Valtchev and S. Qiu, *J. Am. Chem. Soc.*, 2017, **139**, 17771−17774.

19. (a) S. -B. Yu, H. Lyu, J. Tian, H. Wang, D. -W. Zhang, Y. Liu and Z. -T. Li, *Polym. Chem.*, 2016, **7**, 3392–3397. (b) O. Buyukcakir, S. H. Je, S. N. Talapaneni, D. Kim and A. Coskun, *ACS Appl. Mater. Interfaces*, 2017, **9**, 7209−7216. (c) C. Hua, B. Chan, A. Rawal, F. Tuna, D. Collison, J. M. Hook and D. M. D'Alessandro, *J. Mater. Chem. C*, 2016, **4**, 2535−2544. (d) O. Buyukcakir, S. H. Je, D. S. Choi, S. N. Talapaneni, Y. Seo, Y. Jung, K. Polychronopoulou and A. Coskun, *Chem. Commun.*, 2016, **52**, 934−937. (e) G. Chen, Y. Zhou, X. Wang, J. Li, S. Xue, Y. Liu, Q. Wang and J. Wang, *Sci. Rep.*, 2015, **5**, 11236-1−11236-14.

20. (a) G. Das, T. Skorjanc, S. K. Sharma, F. Gándara, M. Lusi, D. S. S. Rao, S. Vimala, S. K. Prasad, J. Raya, D. S. Han, R. Jagannathan, J. -C. Olsen and A. Trabolsi, *J. Am. Chem. Soc.*, 2017, **139**, 9558–9565. (b) G. Das, T. Prakasam, S. Nuryyeva, D. S. Han, A. Abdel-Wahab, J.-C. Olsen, K. Polychronopoulou, C. Platas-Iglesias, F. Ravaux, M. Jouiad, A. Trabolsi, *J. Mater. Chem. A*, 2016, **4**, 15361−15369. (c) L. -Z. Peng, P. Liu, Q. -Q. Cheng, W. -J. Hu, Y. A. Liu, J. -S. Li, B. Jiang, X. -S. Jia, H. Yang and K. Wen, *Chem. Commun.*, 2018, **54**, 4433−4436.

21. R. Gomes, P. Bhanja and A. Bhaumik, *Chem. Commun.*, 2015, **51**, 10050−10053.

22. S. Asaftei, D. Huskens and D. Schols, *J. Med. Chem.*, 2012, **55**, 10405−10413.

23. J. Zhu, S. Wei, H. Gu, S. B. Rapole, Q. Wang, Z. Luo, N. Haldolaarachchige, D. P. Young, Z. Guo, *Environ. Sci. Technol.*, 2012, **46**, 977–985.

24. B. Qiu, C. Xu, D. Sun, H. Wei, X. Zhang, J. Guo, Q. Wang, D. Rutman, Z. Guo, S. Wei, *RSC Adv.*, 2014, **4**, 29855‑29865.

25. L. Li, X. Feng, R. Han, S. Zang, G. Yang, *J. Hazard. Mater.*, 2017, **321**, 622−628.

26. J. Cao, W. -X. Zhang, *J. Hazard. Mater.*, 2006, **132**, 213−219.

27. Y. Li, B. Gao, T. Wu, D. Sun, X. Li, B. Wang, F. Lu, *Water Res.*, 2009, **43**, 3067−3075.

28. H. -L. Ma, Y. Zhang, Q. -H. Hu, D. Yan, Z. -Z. Yu, M. Zhai, *J. Mater. Chem.*, 2012, **22**, 5914−5916.

29. X. Li, X. Gao, L. Ai, J. Jiang, *Chem. Eng. J.*, 2015, **274**, 238−246.

30. Z. Shu, M. Yang, *Chinese. J. Chem. Eng.* 2010, **18**, 372−376.

31. Y. Yan, M. Yi, M. L. Zhai, H. F. Ha, Z. F. Luo, X. Q. Xiang, *React. Funct. Polym.*, 2004, **59**, 149-154.

32. C. Xiong, C. Yao, X. Wu, *Hydrometallurgy*, 2008, **90**, 221-226.

33. L. Zhu, C. Xiao, X. Dai, J. Li, D. Gui, D. Sheng, L. Chen, R. Zhou, Z. Chai, T. E. Albrecht-Schmitt, S. Wang, *Environ. Sci. Technol. Lett.*, 2017, **4**, 316−322.

Chapter 6

Summary and Perspectives

6.1 Summary and Perspectives

In summary, target specific porous materials (metal-organic frameworks or porous organic materials) were designed and synthesized for environmental applications in this thesis. The main objective of the works included in this thesis was to synthesize functional water stable (or chemically stable) porous materials which can be further employed for the remediation of water pollutants. In this regard, a task specific butyne-group functionalized water stable MOF (UiO-series MOF), namely, UiO-66@Butyne was synthesized and thoroughly characterized. Further, UiO-66@Butyne was employed for the selective sensing of toxic Hg(II)-ion in water medium via oxymercuration reaction owing to the presence of butyne-functionality. Since only sensing is not enough to tackle water pollution, further removal of highly toxic and hazardous pollutants from water were studied with porous materials. Moreover, MOFs are often found to be unstable in water medium as well as at varied pH-ranges, but on the other hand capture of hazardous pollutants from aquatic systems requires higher chemical stability of the adsorbent materials. Owing to the high chemical stability of covalently linked porous organic materials, these kind of materials were utilized for the removal of various types of water pollutants (cationic organic dyes, water soluble iodine, oxo-anions etc.). Removal of organic and inorganic pollutants from water medium were performed with hyper-cross-linked polymers (HCPs) and viologen based extended organic network. Chemically stable, cost-effective hyper-cross-linked polymer was employed for the capture of organic dyes from water. Selective removal of cationic dyes over anionic dyes was achieved with post synthetic modification in a hydroxy functionalized HCP by incorporating free exchangeable Na^+ ions via alkaline treatment. Apart from cationic water pollutants, several anionic toxic and hazardous pollutants have been found to cause huge pollution worldwide. Hydroxy functionalized HCPs were employed for the capture of radioactive iodine (^{131}I and ^{129}I) from water via surrogating ^{127}I species as I_3^- ion. The capture studies were found to be unperturbed even in presence of other concurrent anions like Cl^-, NO_3^- and SO_4^{2-} ion. High capacities and reusability of aforementioned hydroxy functionalized HCPs made them suitable candidate for the removal of iodine from waste water. Further, capture of hazardous oxo-anions has appealed huge attention because of its carcinogenicity and toxicity towards the environment. Capture of chromate (CrO_4^{2-}) ion was demonstrated with a viologen based organic cationic network with exchangeable free chloride ions. In addition, removal of TcO_4^- ion (by using surrogating MnO_4^- and ReO_4^- ions) was also carried out with this compound. This cationic network showed efficient capture of aforementioned oxo-anions even presence of concurrent anions like Cl^-, Br^-, NO_3^- and SO_4^{2-} ion. These works demonstrated porous materials with tuneable architecture can be well suited for such remediation of environmental pollutants. Amenability in design, high surface, high chemical stability of such porous organic materials have facilitated their applicability for the removal of environmentally toxic and

hazardous species. Although porous organic materials have not been employed much for this type of applications till now, but such materials can be well suited for remediation of water pollutants in near future.

Inorganic Chemistry
Cite This: Inorg. Chem. 2018, 57, 2360−2364
Communication
pubs.acs.org/IC

Selective Recognition of Hg^{2+} ion in Water by a Functionalized Metal−Organic Framework (MOF) Based Chemodosimeter

Partha Samanta,[†] Aamod V. Desai,[†] Shivani Sharma,[†] Priyanshu Chandra,[†] and Sujit K. Ghosh*[,†,‡]

[†]Indian Institute of Science Education and Research (IISER), Dr. Homi Bhabha Road, Pashan, Pune 411 008, India
[‡]Centre for Research in Energy & Sustainable Materials, IISER Pune, India

Supporting Information

ABSTRACT: A metal−organic framework (MOF)-based highly selective and sensitive probe (UiO-66@Butyne) for the detection of Hg(II) ion has been developed. To the best our knowledge, this is the foremost example of a chemodosimeter-based approach to sense Hg(II) ion using a MOF-based probe. The chemical stability of UiO-66@Butyne renders the sensitive detection of Hg^{2+} ion in an aqueous phase. UiO-66@Butyne has been found to be selective for Hg(II) ions even in the presence of other metal ions.

Environmental pollution due to heavy-metal (mercury, lead, arsenic, and cadmium) ions is becoming a huge threat to human life and other biological species because of their high toxicity and carcinogenicity.[1] Among these heavy metals, mercury ion (Hg^{2+}) is one of the most poisonous and widespread environment pollutants because it easily reacts with various biomolecules, causing several deadly diseases like acrodynia (pink disease), minamata, and Hunter−Russell syndrome, even at very low concentration.[2] Extensive use of Hg^{2+} across different fields (batteries, dental amalgams, electrical apparatuses, etc.) has led to remarkable disposal and contamination of the environment. According to the U.S. Environmental Protection Agency (EPA), the estimated release of Hg^{2+} into the environment has reached ∼7500 tons per year.[3] Contamination of Hg^{2+} in natural water resources, especially in drinking water, is one of the most threatening issues. Considering the deleterious consequences of mercury, it has become imperative to urgently design efficient sensors that can detect Hg^{2+} ion at very low concentration in an aqueous medium.

Until now, numerous efforts have been made to develop efficient sensors for Hg^{2+} ion. Different kinds of techniques such as liquid chromatography, chemiluminescence, colorimetric detection, inductively coupled plasma mass spectrometry, X-ray absorption spectroscopy, and anodic stripping voltammetry have been employed for the detection of toxic mercury ion.[4] Among these techniques, chemiluminescence has attracted considerable attention over the others because of its operational simplicity, instant response, cost effectiveness, and high sensitivity.[5] Prompted by the efficacy of this technique, various types of fluorescent probes have been developed based on organic small molecules, DNA, quantum dots, inorganic−organic hybrid materials, organic polymers, etc.[6] However, low water solubility of organic-molecule-based sensors and low water stability of the organic−inorganic hybrid materials hinder their suitability for real-time application. These shortcomings have necessitated the urgent development of new efficient Hg^{2+} sensors.

In recent years, metal−organic frameworks (MOFs) have emerged as a promising and unique class of materials with extended crystalline and porous architecture.[7] MOFs have been synthesized from metal nodes and organic struts, wherein the organic linker can be functionalized in accordance with the targeted applications. Because of their large surface area, tunable porosity, and functionality, MOFs have emerged as front-runners as target-specific guest-accessible host systems. On the basis of such host−guest chemistry, MOFs have been employed in the field of gas and solvent separation, drug delivery, catalysis, sensing application, etc.[8] Detection of Hg^{2+} ion using MOFs has recently been investigated with plenty of room for improvement in terms of both control over selectivity/sensitivity and applicability under real-time conditions.[9] Most of the MOFs for Hg^{2+} sensing and trapping that have been reported to date are based on chemosensors, and they can be classified as two types: (1) having nitrogen centers or amine groups, which can coordinate to Hg^{2+}, and (2) sulfur-rich probes, where Hg^{2+} can bind strongly to the sulfur center due to soft−soft interaction between them (Hg···S interaction) to produce the signal. Despite having reasonable sensitivity, the aforementioned probes have certain inherent drawbacks: (1) both amines and sulfides can undergo aerial oxidation during long-time storage; (2) on the other hand, sulfur-based probes cannot provide a suitable response in a sulfur-rich environment because of the presence of mercury in great quantity.[10] To overcome these difficulties, we have adopted the chemodosimeter-based approach, which is devoid of the presence of any amine or sulfur functionality. In the case of the chemodosimeter, the target analyte reacts with dosimeter molecules (probes) in an irreversible fashion (unlike chemosensors) to provide permanent signals.[11] As a consequence, it has been observed that both the sensitivity and selectivity of chemodosimeters toward the analyte are high in comparison to those of chemosensors. Consequently, we sought to develop an alkyne-functionalized MOF-based chemodosimeter for the detection of Hg^{2+} ion (Scheme 1), based on the knowledge that Hg^{2+} ions react with alkyne groups via oxymercuration reaction in the presence of water.[10,12] To the best of our knowledge, reaction-based detection of Hg(II) in an aqueous medium has not been reported in the regime of MOF to date.

Received: September 22, 2017
Published: February 20, 2018

DOI: 10.1021/acs.inorgchem.7b02426
Inorg. Chem. 2018, 57, 2360−2364

MATERIALS CHEMISTRY
FRONTIERS

RESEARCH ARTICLE

View Article Online
View Journal | View Issue

Cite this: *Mater. Chem. Front.*, 2017, **1**, 1384

Chemically stable microporous hyper-cross-linked polymer (HCP): an efficient selective cationic dye scavenger from an aqueous medium†

Partha Samanta, Priyanshu Chandra, Aamod V. Desai and Sujit K. Ghosh*

Received 15th December 2016,
Accepted 17th February 2017

DOI: 10.1039/c6qm00362a

rsc.li/frontiers-materials

A cost-effective and robust microporous hyper-cross-linked organic material (**HCP-91**) has been post-synthetically modified for the rational incorporation of sodium cations *via* alkali treatment (**HCP-91@Na**). The presence of free cations has been tapped for the selective capture of cationic dyes *via* rapid ion-exchange. For this study we have used three cationic dye molecules [namely, methylene blue (MB), crystal violet (CV) and rhodamine B (RB)] and one anionic dye (methyl orange). The performance of **HCP-91@Na** in an aqueous medium for size and charge-selective dye entrapment has been comprehensively investigated with monocomponent dye solution studies, as well as binary mixtures of cationic and anionic dye molecules.

Introduction

Last decade has witnessed the evolution of microporous organic polymers (MOPs) in the domain of materials chemistry. The high surface area, tuneable porosity and high physiochemical stability of such materials have stimulated much interest among researchers.[1] A wide range of microporous organic materials have been explored in recent times, such as covalent organic frameworks (COFs), porous organic frameworks (POFs), porous aromatic frameworks (PAFs), covalent triazine frameworks (CTFs), porous organic polymer (POPs), porous polymer networks (PPNs) *etc.*[2] Hyper-cross-linked polymers (HCPs) have emerged as a relatively new subclass in the field of MOPs.[3] Single step Friedel–Crafts reaction provides a key tool to build a network of aromatic molecules *via* extensive hyper-cross-linked polymerization in the presence of anhydrous $FeCl_3$ and formaldehyde dimethyl acetal (FDA) as external cross-linking agents.[4] In such cases small organic aromatic building units have been connected and held together by methylene ($-CH_2-$) groups. Such extensive cross-linking among several organic building blocks results in permanent porosity and high stability of such materials. In addition to the simple one-step easy synthesis of HCPs and high physiochemical stability, tunable porosity by varying the organic unit and low cost synthesis have attracted great attention from researchers.[5] It is noteworthy to mention that HCPs are a much less-explored class of materials in the regime of microporous organic materials. To date, microporous HCPs have often been used for carbon capture and catalysis applications; but to the best of our knowledge, pollutant removal from an aqueous medium has not been investigated yet.[6]

Dye molecules are widely used in many industries including pharmaceuticals, paper, printing, ceramics, paints, textile, cosmetics, plastics *etc.* The removal of such pollutant dye molecules from colored wastewater has emerged as a big challenge for researchers, as a consequence of heavy usage of dyes in the growing industries. It has been found that there are over 100 000 dyes available in the market with a production rate of over 7×10^5 tons per year; among which 2% of dyes are released into different water bodies.[7] Water pollution because of dye molecules hinders growth of bacteria which are responsible for degradation of water impurities and also affects photosynthesis of aquatic plants.[8] Apart from this, a few dyes can result into aesthetic problem as well as chronic effects on exposure to organisms.[9] Furthermore, organic dye molecules are very much chemically stable (even stable to oxidation and light), so the chances of biodegradation for such water pollutants are much lower.[10] Several techniques based on physical, chemical and biological methods have been introduced to remove dye pollutants from wastewater. Among them adsorption based dye removal has attracted much attention, because it can produce high quality water and function at ambient temperature, is cost-effective and can feasibly remove multiple dyes simultaneously.[11] Although several adsorbents have been reported in the literature for the removal of dye molecules, materials with high capacity and separation by virtue of both size and ionic selectivity are still a challenge to be addressed. With advantages like tunable porosity and separation based on

Indian Institute of Science Education and Research (IISER), Dr Homi Bhabha Road, Pashan, Pune, 411008, India. E-mail: sghosh@iiserpune.ac.in; Web: http://www.iiserpune.ac.in/~sghosh/; Fax: +91 20 2589 8022; Tel: +91 20 2590 8076

† Electronic supplementary information (ESI) available. See DOI: 10.1039/c6qm00362a

Chemical Science

EDGE ARTICLE

View Article Online
View Journal | View Issue

Cite this: *Chem. Sci.*, 2018, **9**, 7874

All publication charges for this article have been paid for by the Royal Society of Chemistry

Chemically stable ionic viologen-organic network: an efficient scavenger of toxic oxo-anions from water†

Partha Samanta,[a] Priyanshu Chandra,‡[a] Subhajit Dutta,‡[a] Aamod V. Desai[a] and Sujit K. Ghosh*[ab]

Received 4th June 2018
Accepted 20th August 2018

DOI: 10.1039/c8sc02456a

rsc.li/chemical-science

Detoxification of water has been demonstrated with a viologen-based cationic organic network (compound-**1**), which was stable not only in water, but also in acidic and basic media. The presence of free exchangeable Cl^- ions inside the network of compound-**1** and a high physiochemical stability of the materials offered a suitable scope for the capture of hazardous anionic pollutants from water. Rapid removal of the toxic water pollutant and carcinogenic chromate (CrO_4^{2-}) from water was shown with compound-**1**. Furthermore, the oxo-anion of the radioactive isotope of technetium (^{99}Tc), *i.e.* the TcO_4^- ion, also counts as a toxic water pollutant and by using surrogate anions (MnO_4^- and ReO_4^-), a model capture study was performed. Notably, compound-**1** showed high capacity values for each of the oxo-anions and these were comparable to some of the well-performing compounds reported in the literature. Furthermore, to check the real time aspect, removal of all of the aforementioned anions from water was demonstrated, even in the presence of other concurrent anions.

Introduction

Increasing water pollution has become a global concern in recent years, and remediation of such toxic pollutants has drawn much attention worldwide. Pollution due to metal derived oxo-anions (CrO_4^{2-}, TcO_4^-, SeO_3^{2-}, AsO_4^{3-} *etc.*) has become a pressing challenge, as most of them are omnipresent in the environment.[1] Especially, Cr(VI) based oxo-anions are found to be very carcinogenic and mutagenic to living systems.[2,3] Understanding the importance of this, the EPA (Environmental Protection Agency, U.S.) has included such oxo-anions in the priority pollutant list.[4,5] Chromate has been found in a wide range of applications in various industries like leather tanning, textile dyes and pigments, steel manufacturing, wood preservation, electroplating *etc.*, where tanning industries alone discharge ~30–35 liters of Cr(VI) contaminated water for each kilogram of leather.[6,7] It also affects the vitrification of low activity radioactive waste, as it forms spinels and has resulted in weakening the integrity of waste glass.[8,9] Furthermore, the Hinkley groundwater contamination is one of the well known disasters caused by dumped Cr(VI) in California.[10] Apart from this case, several more incidents were found, and moreover the problems are still continuing, which has led researchers to design affordable and efficient techniques to capture Cr(VI) based oxo-anions.[11,12] Apart from chromate, another oxo-anion, the pertechnetate (TcO_4^-) ion, has caused much concern as one isotope of technetium (^{99}Tc) is a radioactive element with a very high half-life time (2.1×10^5 years). ^{99}Tc has been found to be formed as a nuclear fission product of ^{235}U or ^{239}Pu with a high fission yield. Up to 2010 it was estimated that ~305 metric tons of ^{99}Tc was produced from weapons testing and nuclear reactors.[13] Furthermore, Tc exists mostly as TcO_4^- in the environment, which is highly soluble in water with high mobility. As a consequence of this, TcO_4^- may also exist in low level waste. To date, many different techniques have been employed for the removal of oxo-anions, like ion exchange, chemical precipitation, adsorption, electrodialysis, photocatalysis *etc.*[14–17] The ion exchange method has been considered as a more efficient technique over the others owing to its low cost, being comparatively simple and safe, and its efficient performance even for waste which has a low concentration of pollutants *etc.*[18,19] Although several anion exchange resins have been reported, their poor selectivity, poor exchange kinetics and lack of stability have led researchers to render new materials for efficient oxo-anion capture from water.[20] As an alternative, porous cationic framework based materials, such as layered double hydroxides (LDHs), metal–organic frameworks (MOFs) *etc.*, have emerged in recent years.[21–35] Recent reports have shown

[a]*Department of Chemistry, Indian Institute of Science Education and Research, Dr. Homi Bhabha Road, Pashan, Pune 411008, India. E-mail: sghosh@iiserpune.ac.in; Tel: +91 20 2590 8076*

[b]*Centre for Energy Science, IISER Pune, Dr. Homi Bhabha Road, Pashan, Pune 411008, India*

† Electronic supplementary information (ESI) available. See DOI: 10.1039/c8sc02456a

‡ These authors contributed equally.